Green Chemistry

Cutting-edge research for a greener sustainable future

Aggregation

Activity

RSCPublishing

Methods in Organic Synthesis:
Cover Competition

18060752

Are you creative?

Highly subscribed database *Methods in Organic Synthesis* is now holding a cover competition, for all those involved or interested in organic chemistry.

With a large readership and diverse array of abstracts in every issue, the winner of the competition can be sure that their cover will be seen by readers across the globe. The image will feature on the RSC website and on the front of *Methods in Organic Synthesis* throughout 2008, making it highly visible to our extensive international audience. In addition, the winner will recieve a free subscription for one year (print and online).

Methods in Organic Synthesis highlights the most novel, current and topical research from the organic chemistry field, and as such the winning image should reflect these values. Can you bring organic chemistry to life visually?

Deadline for submissions: Monday 22nd October 2007

Go online and submit your image today

RSC Publishing

www.rsc.org/mos/covercomp

Registered Charity Number 207890

Green Chemistry

Cutting-edge research for a greener sustainable future

www.rsc.org/greenchem

RSC Publishing is a not-for-profit publisher and a division of the Royal Society of Chemistry. Any surplus made is used to support charitable activities aimed at advancing the chemical sciences. Full details are available from www.rsc.org

IN THIS ISSUE

Cover
The image is a schematic description of the fate of Candida Antarctica Lipase B (CALB) in terms of structure and function when dissolved in water and the ionic liquid $[C_2mim][N(CN)_2]$. Image reproduced with permission from Daniel J. P. Sate, *Green Chem.*, **9**(8), 859.

CHEMICAL TECHNOLOGY

T57

Chemical Technology highlights the latest applications and technological aspects of research across the chemical sciences.

Chemical Technology
August 2007/Volume 4/Issue 8
www.rsc.org/chemicaltechnology

NEWS

822

Green chemistry in Ethiopia: the Third Annual Workshop

Yonas Chebude, Debebe Yilma, Peter Licence and Martyn Poliakoff report on the Third Ethiopian Workshop on Green Chemistry, held on the 18–19th May 2007 at Jimma University, Jimma, Ethiopia.

Green Chemistry

Cutting-edge research for a greener sustainable future

www.rsc.org/greenchem

Green Chemistry focuses on cutting-edge research that attempts to reduce the
environmental impact of the chemical enterprise by developing a technology base that is
inherently non-toxic to living things and the environment.

INFORMATION FOR AUTHORS

Full details of how to submit material for publication
in Green Chemistry are given in the Instructions for
Authors (available from http://www.rsc.org/authors).
Submissions should be sent *via* ReSourCe: http://
www.rsc.org/resource.

CRITICAL REVIEW

823

Recent developments on the chemistry of aliphatic nitro compounds under aqueous medium

Roberto Ballini,* Luciano Barboni, Francesco Fringuelli, Alessandro Palmieri, Ferdinando Pizzo* and Luigi Vaccaro

Aliphatic nitro derivatives represent an important class of useful molecules in organic synthesis and, only recently, it has been shown that these reactions are also very efficient using water as reaction medium.
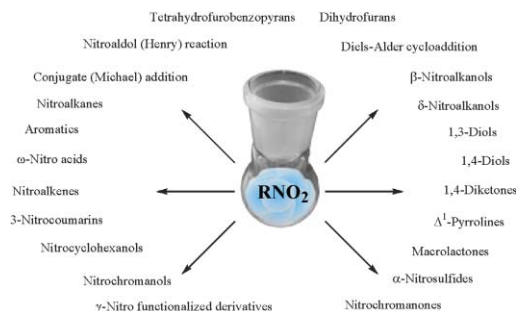
COMMUNICATIONS

839

The synthesis of diphenolic acid using the periodic mesoporous $H_3PW_{12}O_{40}$-silica composite catalysed reaction of levulinic acid

Yihang Guo, Kexin Li and James H. Clark*

The periodic mesoporous $H_3PW_{12}O_{40}$-silica composite has been prepared by a direct sol-gel co-condensation technique. The composite is an efficient and reusable solid catalyst for the condensation of phenol with levulinic acid to produce diphenolic acid.
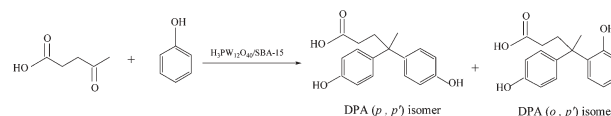
842

New chitosan/CEG (compressed expanded graphite) composites—preparation and physical properties

M. Krzesińska,* A. Tórz, J. Zachariasz, J. Muszyński, J. Socha and A. Marcinkowski

The new group of high porous, rigid bio-composite materials based on compressed expanded graphite impregnated by a chitosan were prepared and examined by means of adequate physical methods.
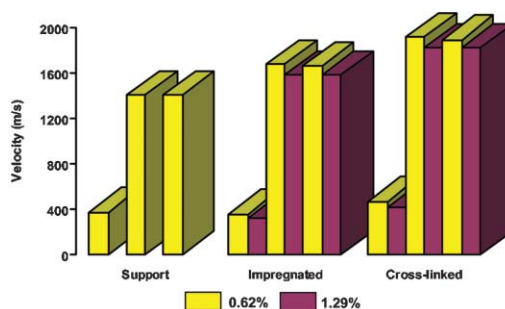
845

Enhanced selectivity in green catalytic epoxidation using a supported cobalt complex

Rajesh Chakrabarty, Birinchi K. Das* and James H. Clark

A supported reagent made by immobilising a tetrameric cobalt(III) cubane cluster on mesoporous silica catalyses the aerobic oxidation of α-pinene with enhanced epoxidation selectivity compared with other systems.
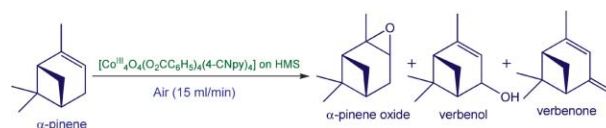
COMMUNICATIONS

849

Synthesis of chloroanilines: selective hydrogenation of the nitro in chloronitrobenzenes over zirconia-supported gold catalyst

Daiping He, Hui Shi, Yu Wu and Bo-Qing Xu*

Selective production of chloroanilines from chloronitrobenzenes without any dechlorination was found feasible by catalytic hydrogenation over zirconia-supported gold catalyst, which uncovers a clean synthetic approach for useful chloroanilines.

PAPERS

852
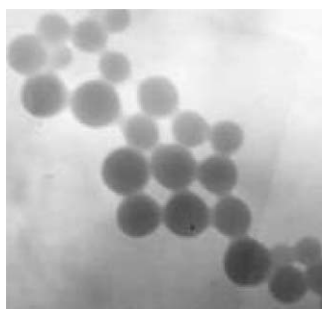
Green synthesis of silver nanoparticles using *Capsicum annuum* L. extract

Shikuo Li, Yuhua Shen,* Anjian Xie,* Xuerong Yu, Lingguang Qiu, Li Zhang and Qingfeng Zhang

Silver nanoparticles were rapidly synthesized using a *Capsicum annuum* L. extract. The reaction process was simple and convenient to handle; the practical reaction suggested this green synthesis method could be widely used to prepare nanomaterials.

859
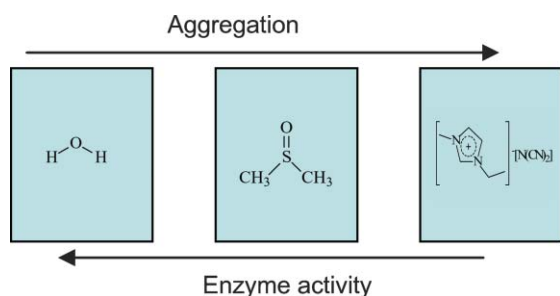
Enzyme aggregation in ionic liquids studied by dynamic light scattering and small angle neutron scattering

Daniel Sate, Michiel H. A. Janssen, Gill Stephens, Roger A. Sheldon, Kenneth R. Seddon and Jian R. Lu*

Aggregation of *Candida antarctica* Lipase B (CALB) in water, DMSO and three ionic liquids, [C$_2$mim]X ([C$_2$mim] = 1-ethyl-3-methylimidazolium; X = [N(CN)$_2$]$^-$, [NO$_3$]$^-$ or [EtOSO$_3$]$^-$) was studied by dynamic light scattering and small angle neutron scattering: CALB formed micellar aggregates in DMSO and all three ionic liquids, correlated with loss of enzymatic activity.

868
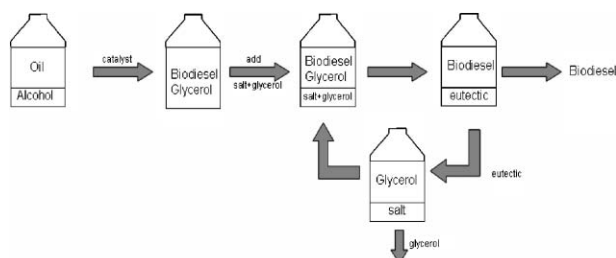
Extraction of glycerol from biodiesel into a eutectic based ionic liquid

Andrew P. Abbott,* Paul M. Cullis, Manda J. Gibson, Robert C. Harris and Emma Raven

The use of a simple quaternary ammonium–glycerol eutectic is shown to be an effective way of removing glycerol from biodiesel.

PAPERS

873

Effect of ionic liquids on human colon carcinoma HT-29 and CaCo-2 cell lines

Raquel F. M. Frade, Ana Matias, Luis C. Branco, Carlos A. M. Afonso and Catarina M. M. Duarte*

The toxicity of ionic liquids, involving different classes of cations and different types of anions, was evaluated by a colorimetric assay with 3-(4,5-dimethylthiazolyl-2)-2,5-diphenyltetrazolium bromide (MTT) in two colon carcinoma HT-29 and CaCo-2 cell lines.
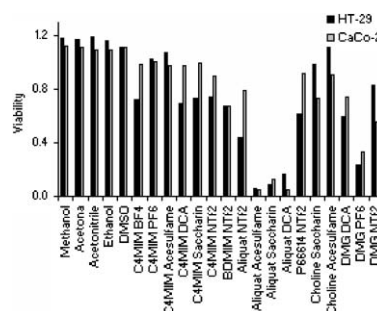
878

A green process for *O*-heterocyclization of cyclooctane-1,5-diene by peroxotungstic species with aqueous H_2O_2

Ruihua Gao, Wei-Lin Dai,* Yingyi Le, Xinli Yang, Yong Cao, Hexing Li and Kangnian Fan

The hydroxy- and carbonyl-derivatives of 9-oxabicyclo[3.3.1]nonane have been synthesized (98% yields) through an economic and green catalytic reaction between cyclooctane-1,5-diene (COD) and aqueous H_2O_2 with tungstic acid as the catalyst.
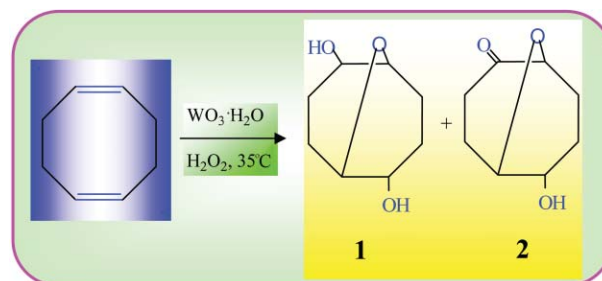
882

Supercritical carbon dioxide and poly(ethylene glycol): an environmentally benign biphasic solvent system for aerobic oxidation of styrene

Jin-Quan Wang, Fei Cai, Er Wang and Liang-Nian He*

The PdCl$_2$-catalyzed aerobic oxidation of styrene in a biphasic PEG/scCO$_2$ system leads to two possible products, the Wacker reaction product acetophenone and benzaldehyde, switching by the co-catalyst CuCl, from 92% in favor of acetophenone in the presence of CuCl to 85% favoring benzaldehyde without any co-catalyst.
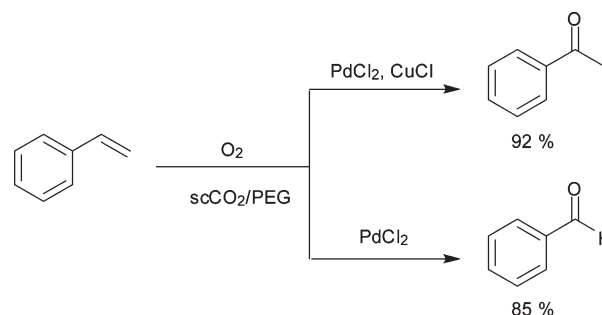
888

Coupling chiral homogeneous biocatalytic reactions with benign heterogeneous separation

Elizabeth M. Hill, James M. Broering, Jason P. Hallett, Andreas S. Bommarius, Charles L. Liotta and Charles A. Eckert

Organic aqueous tunable solvent (OATS) systems facilitate asymmetric homogeneous enzymatic transformations of hydrophobic substrates with a built in heterogeneous separation. Excellent enantiomeric excess (ee) values in OATS are shown for the chiral resolution of 1-phenylethyl acetate.

PAPERS

AUTHOR INDEX

FREE E-MAIL ALERTS AND RSS FEEDS

Contents lists in advance of publication are available on the web via www.rsc.org/greenchem - or take advantage of our free e-mail alerting service (www.rsc.org/ej_alert) to receive notification each time a new list becomes available.

Try our RSS feeds for up-to-the-minute news of the latest research. By setting up RSS feeds, preferably using feed reader software, you can be alerted to the latest Advance Articles published on the RSC web site. Visit www.rsc.org/ publishing/technology/rss.asp for details.

ADVANCE ARTICLES AND ELECTRONIC JOURNAL

Free site-wide access to Advance Articles and the electronic form of this journal is provided with a full-rate institutional subscription. See www.rsc.org/ejs for more information.

* Indicates the author for correspondence: see article for details.

Electronic supplementary information (ESI) is available via the online article (see http://www.rsc.org/esi for general information about ESI).

View Online

Chemical Technology

Polymer changes its glass transition temperature on contact with water

Keeping your powder dry

Ever wondered why there is a little packet marked 'Do not eat' inside the box for your new DVD player? It's there to absorb moisture that could potentially damage the equipment, but how do you tell if it has been exposed? Chemists from the US think they have the answer with a humidity sensor that irreversibly changes colour on contact with water.

Many coloured dye molecules exhibit different properties when isolated from, or associated with, one another. This effect has been known for many years, but now Christoph Weder and colleagues from Case Western Reserve University have used this property to develop a moisture sensor.

Dye molecules within a polymer matrix can be effectively isolated from one another by rapidly cooling the polymer–dye mixture below its glass transition temperature (think of how inflexible a piece of rubber tubing becomes if you freeze it in liquid nitrogen). If the polymer is heated above its glass transition temperature, then the dye
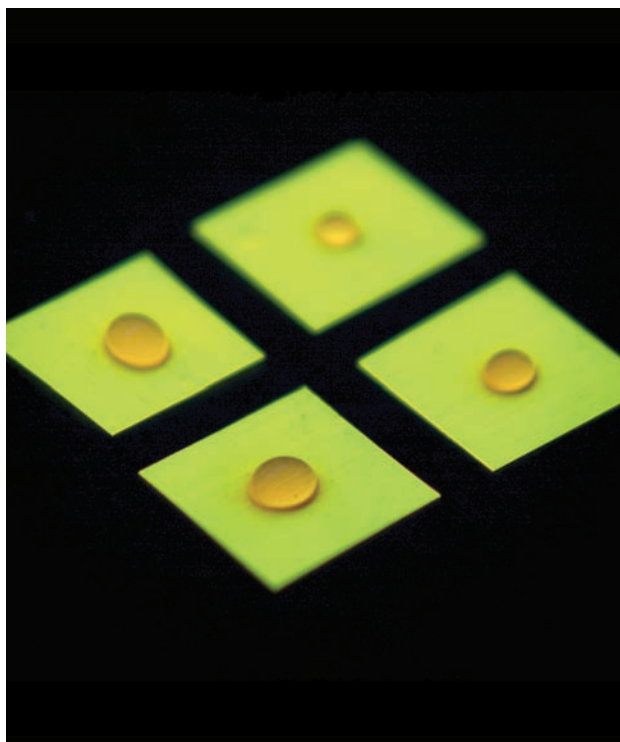
The polymer's colour changes irreversibly when it gets wet

molecules can aggregate and cause a colour change – an effect used in the past for temperature sensors.

The trick to making this sense water was to design a polymer system that changes its glass transition temperature on contact with water. Exposure of the team's polyamide to a humid atmosphere causes a change in the glass transition temperature from ~50°C to well below 0°C, and a corresponding irreversible colour change from green to orange.

'What we'd like to do next is investigate whether we can change the properties to create specificity for other analytes,' said Jill Kunzelman, one of Weder's team. This seems to be a very realistic goal: Qinetiq research fellow Ian Sage said 'The new sensor shows good potential for a low cost device whose properties can be tuned to a particular purpose.'

Stephen Davey

Reference

J Kunzelman, B R Crenshaw and C Weder, *J. Mater. Chem.,* 2007, **17**, 2989 (DOI: 10.1039/b705880b)

In this issue

Clearing a path to cancer detection
Optical illusions create anomalies in IR mapping of cells

Ionic liquids on tap
Continuous process gives yields greatly in excess of batch reactor

Interview: Molecular electronics
Nicolas Weibel, Sergio Grunder and Marcel Mayor, University of Basel, Switzerland, look at functional molecules in circuits

Instant insight: Transport on a chip
Microfluidics meets analytical chemistry. Paul Bohn talks to Jenna Wilson about molecular transport in small channels
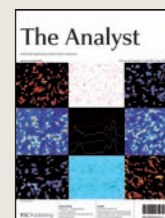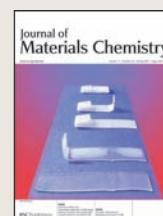
The latest applications and technological aspects of research across the chemical sciences

Application highlights

Optical illusions create anomalies in IR mapping of cells

Clearing a path to cancer detection

Improved imaging of prostate cancer proteins in single cells is possible thanks to scientists at the University of Manchester. The UK researchers identified and investigated an optical illusion in the imaging of single cells that gave inconsistent results.

'Developing the use of infrared spectroscopy in cancer diagnosis' is the aim of the UK team led by Peter Gardner. 'Prostate cancer, if it remains localised, is a manageable condition and patients can survive for many years,' Gardner said. 'However, the cancer can spread, particularly to the bone, and this is almost always fatal.' Gardner's team, in collaboration with Noel Clark, a consultant urologist at the Christie Hospital and Paterson Institute for Cancer Research, have therefore been studying how cancer cells move through tissue.

They study cancer cells by sending a beam of infrared (IR) radiation through the cancer
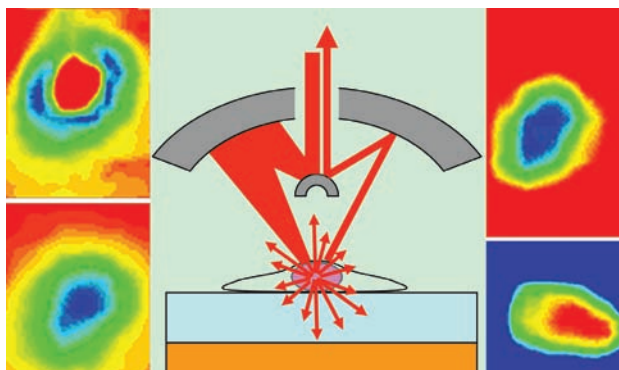
Some protein substrates gave negative images of cancer cells

cell and what it is growing on (its biological support generally called the substrate). The beam then bounces off an IR reflective surface and reflects back into the detector, measuring how much is absorbed. A map of the absorption creates an image of the cancer cell proteins.

The problem seen by Gardner's team was that, with some high protein substrates, they sometimes saw negative images of the cells.

This illusion was caused by the IR radiation being scattered by the nucleus of the cancer cell. As it scatters in all directions, some goes directly into the detector resulting in more radiation being recorded, indicating that less has been absorbed. This gives the illusion of a negative image of the cancer cell.

Deducing the origin of these optical illusions 'contributes significantly to the debate concerning "anomalies" observed in infrared-microscopy mapping of single cells,' according to John Chalmers of VS Consulting, Stokesley, UK. The Manchester researchers cautioned that 'people using infrared spectroscopy to study cells on biological supports must be careful how they interpret their results'.

Wendy Crocker

Reference
J L Lee *et al, Analyst,* 2007, **132**, 750 (DOI: 10.1039/b702064c)

Continuous process gives yields greatly in excess of batch reactor

Ionic liquids on tap
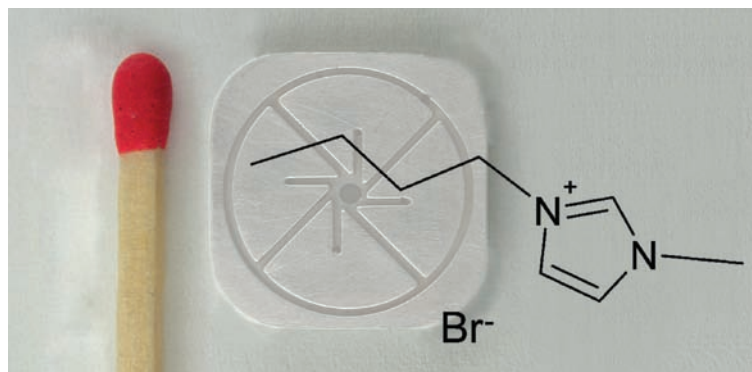
No solvent required: the system effectively removes heat itself

Researchers in Germany have developed an intensive process for preparing ionic liquids using a continuously operating micro-reactor system. Previously their manufacture on a large scale has been limited by the use of batch procedures.

Daniel Waterkamp and colleagues at the Centre for Environmental Research and Technology UFT, University of Bremen, prepared 1-butyl-3-methylimidazolium bromide that was more than 99% pure at a rate of nine kilograms per day. They achieved a space–time yield 24 times that achieved using a conventional batch reactor.

'In the field of ionic liquid production ineffective procedures

still dominate. Many researchers, including members of our working group, have already demonstrated the advantages of unit operations at the micro-scale,' said Waterkamp.

'The next logical step was to combine our experience in chemistry and engineering and prove the applicability of micro-reaction technology for ionic liquid synthesis at the production scale,' he said.

Another advantage of the process is that the addition of solvent to control the reaction is unnecessary, as the high specific surface area of the reaction system carries away any heat generated during the process.

A theoretical model of the reaction showed that further optimisation of the process could potentially lead to space–time yields a hundred times those of a batch reactor.

Joanna Stevens

Reference
D A Waterkamp *et al, Green Chem.,* 2007, DOI: 10.1039/b616882e

View Online

Fast and cheap PCR on a microchip
Magnetic force drives device

A magnet-driven microchip can rapidly and reliably replicate DNA, for many uses including forensic investigation at crime scenes.

The polymerase chain reaction (PCR) is a tool for replicating DNA. Copies are made by passing DNA fragments through three different temperature zones; each cycle doubling the amount of DNA.

The miniature PCR device designed by Nam-Trung Nguyen and colleagues at Nanyang Technological University, Singapore, is simpler and more reliable than existing methods because magnetic force is used to drive the DNA sample around the microchip rather than a pump mechanism. Pumps are expensive and put high mechanical requirements on the microchip as the channels have to withstand high pressures.

The speed and number of replication cycles can be altered
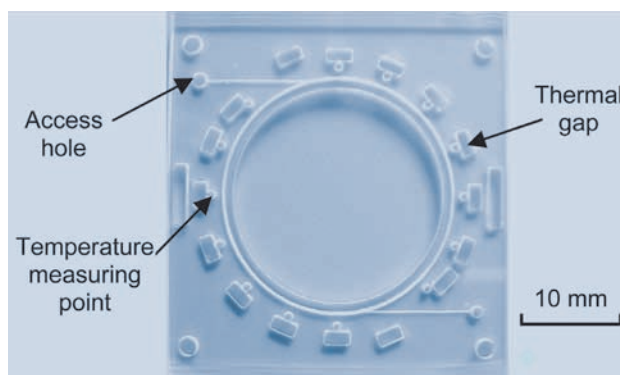
In Nguyen's system, the DNA sample flows continually through a circular closed loop, driven by a plug controlled by an external permanent magnet. As the sample goes around the microchannel loop it passes through the three temperature zones. 'Successful PCR was achieved in less than four minutes,' said Nguyen.

The time taken for the fluid to cycle around the zones can be adjusted by changing the speed of the external magnet. According to Nguyen, the magnet is a good way to drive the system as it is low cost, has small power consumption and a flexible number of PCR cycles.

'Other similar designs face problems of temperature control, high driving pressures and leakage,' said Nguyen, 'but the implementation of this chip in a complex lab-on-a-chip system should not have these issues.

'Our aim is to develop an integrated system for fast screening of DNA samples at a crime scene,' said Nguyen.

Alison Stoddart

Reference
Y Sun et al, Lab Chip, 2007, **7**, 1012 (DOI: 10.1039/b700575j)

Alkanes produced in two simple processes
From glycerol to gas

Liquid alkane fuel can be produced from a by-product of biomass processing, thanks to researchers from the University of Wisconsin, Madison, US.

As the world's reserves of petroleum dwindle, finding alternative sources of fuel is becoming increasingly important. Producing liquid alkanes from biomass is attractive because its use produces less carbon dioxide, and so it impacts less on global warming. Liquid alkanes have advantages over other biofuels, such as ethanol, for use as transportation fuels because they can be used in existing engines and distributed using infrastructure already in place.

James Dumesic and co-workers devised a system that involves the integration of two processes. The first process is the production of synthesis gas, a mixture of carbon monoxide and hydrogen, from glycerol. The second is a Fischer–Tropsch synthesis, where
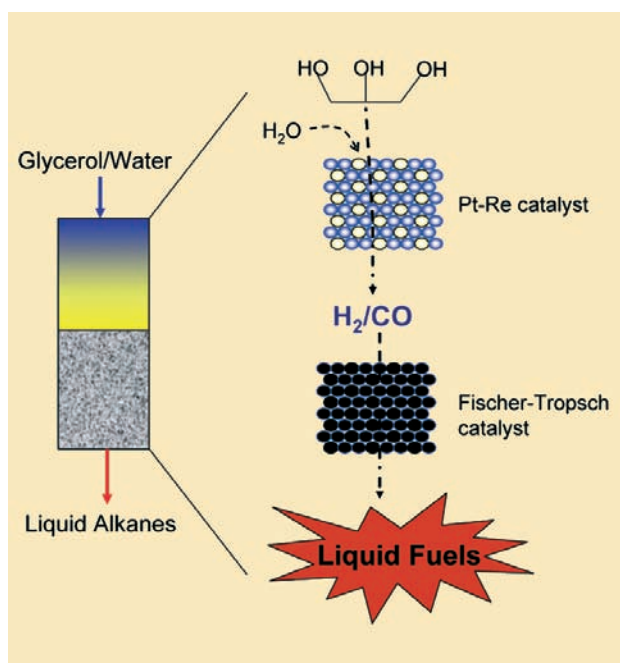
Synthesis gas is made from glycerol, and then converted to alkanes

the synthesis gas is converted to hydrocarbons. Both processes are catalytic, with the first being endothermic and the second exothermic, and the system operates at low temperature and moderate pressure. In integrating the two processes Dumesic's team found that they could feed the synthesis gas produced in the first process directly into the second without purification.

They also found that in addition to the liquid alkanes produced, the gaseous and aqueous phase by-products include methanol and ethanol, useful in their own right. Dumesic said that this gives 'the potential to improve the economics of green Fischer–Tropsch synthesis by reducing capital costs and increasing thermal efficiency'.

Madelaine Chapman

Reference
D A Simonetti et al, Green Chem., 2007, DOI: 10.1039/b704476c

Family of perovskite materials allow fuel cells to perform at lower temperature

Cool fuel

Materials scientists from Spain and the UK have made a cathode material that allows solid oxide fuel cells (SOFCs) to be used at lower temperatures.

Albert Tarancón and colleagues at the University of Barcelona, and Imperial College London found that the oxide $GdBaCo_2O_{5+\delta}$ performed very well in the temperature range 500–700°C.

SOFCs consist of three main components: an anode, cathode and electrolyte. The cathode catalyses the reduction of oxygen at its surface and allows ions to be transported to the electrolyte. At the anode, the fuel (for example, hydrogen) is oxidised.

Lowering the temperature at which SOFCs operate reduces costs and improves durability. However, the cathode performance is the limiting factor when lowering the temperature. New
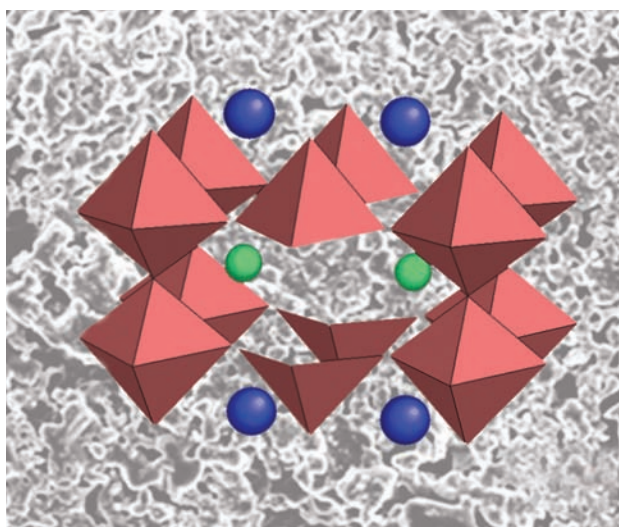
cathode materials with higher catalytic activities are needed, in which the oxide ions are able to diffuse easily.

Lower temperatures mean cheaper cells

According to Tarancón, the oxygen transport properties and electrical performance of the perovskite-structured oxide were comparable to other excellent cathodes. He also suggested that 'its structural characteristics suggest a new family of SOFCs cathode materials based on layered perovskites'.

Peter Slater, a materials chemist at the University of Surrey, Guildford, UK, praised Tarancón's research, saying 'they elegantly demonstrate high oxygen surface exchange properties, along with low activation energies for both surface exchange and oxide ion diffusion' and agreed that the family has great promise as cathode materials.

Susan Batten

Reference

A Tarancón *et al*, *J. Mater. Chem.*, 2007, **17**, 3175 (DOI: 10.1039/b704320a)

Replacing a laser with an LED makes for miniaturised screening

Exciting changes for cancer detection
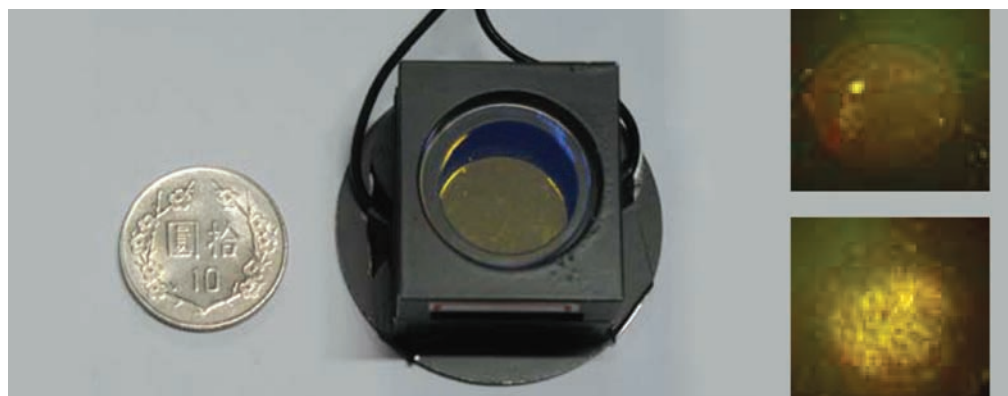
A new development from scientists in Taiwan could simplify the detection and monitoring of various cancers. The group lead by Ta-Chau Chang at the National Taiwan University Hospital in Taipei have developed a small portable system that can be used for routine cancer screening.

Using an existing fluorescent dye that binds to the G-quadruplex

structure of human telomeric structure, a common feature of several different cancers, the group manufactured a microarray for detecting cancerous cells. The miniaturisation means that an LED can be used as the light source to excite the fluorescent dye, which makes the device much cheaper than if a laser is used. Chang hopes that the low cost and portability

The device is designed for non-specialists to use

will allow diagnosis to take place in small health centres in the developing world, where otherwise patients would have to wait for a long time for test results.

The team studied cells from several different types of cancer to show that the technique was robust in distinguishing cancer cells from non-cancerous tissue. Chang explained that 'the device is designed not only for specialists but also for non-specialists'. He added, 'Considering the low cost for each test, this method will be available for routine screening of cancer. In addition, the test can be done within 20 minutes of sample collection.'

Chang's group now hope for an easy method of sample collection to be developed to allow home screening.

Laura Howes

Reference

C-C Kang *et al*, *Analyst*, 2007, **132**, 745 (DOI: 10.1039/b617733f)

View Online

Instant insight

Molecular memory

Nicolas Weibel, Sergio Grunder and Marcel Mayor, University of Basel, Switzerland look at functional molecules in electronic circuits

The miniaturization trend known as Moore's law is only driven by the prospect of reducing the price per unit – more chips per silicon wafer reduces production costs. The exponential increase in the cost of semiconductor production will most likely stop this miniaturization trend before its physical limits are reached. The growing interest in alternative concepts, like the integration of molecules as carriers of an electronic function, is not surprising in view of the expected restrictions. Mainly driven by the greed for fundamental knowledge, the increasing availability of investigative tools and the hope for appealing solutions at lower cost, molecular electronics has developed to a mature research area in the past few years. Alongside central contributions from physics, electronic engineering, nanotechnology and other applied sciences, only physical and synthetic chemistry provide the desired feedback mechanisms required for a successful development of molecular structures for electronic devices. Together, they can judiciously correlate molecular structure with physical properties, and design and synthesize tailor-made functional molecules.

With numerous examples of molecules integrated into electronic circuits, our recent Perspective article[1] illustrates the promising potential of the concept but also the remaining challenges and limitations. From the point of view of a synthetic chemist, the focus is set on molecular structure as the origin of electronic function. Particularly, examples of systems providing rectification and switching are considered, as the combination of rectification with hysteretic switching paves the way to future molecule-based memory devices.
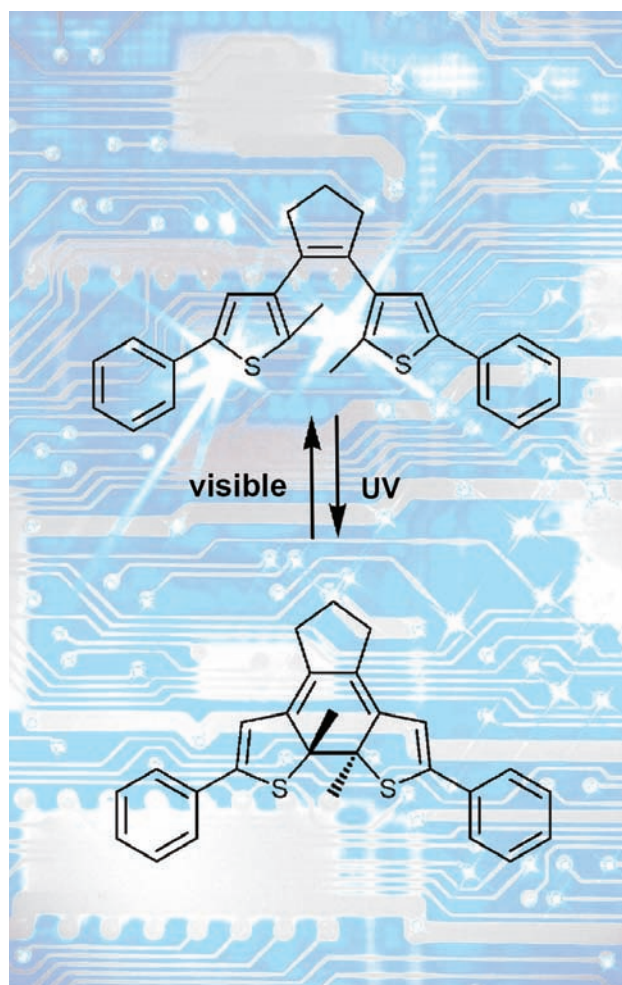
Rectification, the very first electronic function suggested to be provided by a single molecule, has meanwhile been achieved in devices comprising different numbers of molecules, ranging from large self-assembled monolayers down to individual molecules. While the integrated molecules were confirmed to be the origin of the observed current rectification, the present performances of these molecular rectifiers can barely compete with those of their semiconductor fellows.

Switching between two current levels, triggered by an external stimulus such as light or an electrochemical potential, has been realized in several prototype set-ups consisting of integrated molecules. While these studies are of fundamental interest to investigate the underlying mechanisms and the potential of molecules as switches, the integration of neither a light source nor an electrolyte into an integrated circuit of the future is very likely to happen. However, a few examples of hysteretic switches, which are of particular interest as potential memory devices, have been achieved. Interestingly, these switches are triggered by an applied potential. However, the underlying mechanisms are still under investigation.

In summary, the future of molecular electronics is not to supplant but rather to complement and enrich existing electronic circuits. The advent of hybrid devices profiting from molecules as functional units integrated into pre-existing platforms will most likely permit fundamental scientific advances and technological achievements. Overcoming the size gap between electrodes and molecules as well as bringing in new concepts for massive parallel contacting of molecular devices are still major challenges in the field of nanotechnology. We are convinced that numerous unpredicted solutions and applications will arise from the fascinating and challenging interdisciplinary research in the area of molecular electronics.

Molecular switches like this one are triggered by light

Reference
1 N Weibel, S Grunder and M Mayor, *Org. Biomol. Chem.*, 2007, **5**, 2343 (DOI: 10.1039/b703287k)

Read the full Perspective article 'Functional molecules in electronic circuits' in issue 15 of Organic and Biomolecular Chemistry.

Interview

Transport on a chip

Microfluidics meets analytical chemistry. Paul Bohn talks to Jenna Wilson about molecular transport in small channels

Paul Bohn

Paul Bohn is the Schmitt professor of chemical and biomolecular engineering at the University of Notre Dame, US, and associate editor of *The Analyst*. His research focuses on understanding and controlling molecular transport on the nanometre length scale.

How did you become interested in microfluidics?
It has been a bit of a random walk. However, I have always been fascinated with the notion of molecular transport and the movement of molecules on the supramolecular level but on relatively short timescales. I am interested in how to control the placement of molecules in space and time and potential applications of this.

What projects are you working on at the moment?
We work on integrated microfluidics – three dimensional structures capable of performing successively linked chemical analysis tasks. It is a way of performing complicated processing to obtain valuable information. We concentrate on three dimensional ways to do this, using electrokinetically actuated fluid transfer in different microfluidic layers so we can achieve multidimensional chemical analysis directly on the chip.

We are also interested in optoelectronic materials and devices for chemical sensing, especially the Group 13 nitrides. These materials are extremely robust so can be used in harsh chemical environments, as well as, as the name implies, having useful optical and electronic properties. In particular, the aluminium nitride and gallium nitride end of the family are solar blind so they are useful for applications where other semiconductors are not.

The final area we work in is chemical mapping, which is a way of mapping chemical reactions onto surfaces of arbitrary geometry. This is done by using electrochemical potentials that are anisotropic in the plane, allowing us to create materials that are directly or spatially anisotropic.

What do you hope your next breakthrough will be?
We are on the cusp of demonstrating the first powerful two-dimensional separation in a three-dimensional integrated microfluidic circuit – this is based on electrophoresis separation followed by chiral separation. The idea is to take a complex mixture of biological molecules, separate them by chemical identity, and then take the racemic mixture that is represented by the particular component we are interested in and separate the enantiomers in a chiral column.

Ultimately, we want to be able to pick out a particular component from a mixture and move it into a different region of the channel, and then operate on that. If we can achieve that once, then the opportunity to do it in parallel presents itself and it could become a powerful technique.

You could imagine replacing two-dimensional gels used for proteomic experiments, with an integrated microfluidic format that would be simpler and able to handle smaller volumes, and hopefully lower the number of repetitions required for the assay.

What do you think is the biggest challenge faced by people working in your area?
The Holy Grail is to take a complex mixture and provide a chemical catalogue of its components, and to do this in a way which preserves both spatial and temporal information. I have just described probably the next 500 years of analytical chemistry, but perhaps a smaller goal for the immediate future in chemical sensing is to provide a complete inventory of a complex chemical mixture, and to do that with single molecule sensitivity.

If you went back into the lab, what experiment would you do?
Our most exciting current project involves incorporating optoelectronic materials into traditional microfluidic formats. I would like to do experiments that use these exciting advances in electrokinetic transport in order to further develop microfluidics. Unfortunately, I have given that project to a student so he would be mad if I showed up and did the experiments myself!

What message do you have for young scientists?
Chemistry continues to be an endlessly fascinating part of contemporary science because so much of what happens in science is tied up in the way in which molecules organise themselves and interact with each other. You only have to look below the surface a little bit to see that chemistry has been an enduring and very broad substructure to advances in science as a whole. If I have any advice, I would encourage people to look for the problems at the interface between traditional subject areas, where a good chemical knowledge can have an impact.

Finally, if you weren't a chemist, what would you be?
That's easy...I would be a professional golfer. The only thing that gets in my way is lack of talent!

Essential elements

RSC journals – even more impact!

RSC Publishing is celebrating the continued success of its journals following the release of the 2006 impact factors calculated by ISI®. Journals from across the collection have recorded significant rises, while new interdisciplinary titles have received their first official ranking of the internationally recognised publishing industry metric.

Among the headline success stories, *Green Chemistry*, the only journal publishing both primary and secondary research in the field, sees a staggering 29% rise in impact factor to 4.19. The already impressive impact factor for *Lab on a Chip* has increased by a further 10% to 5.82, ensuring it remains one of the leading journals in micro and nano-research.

The RSC materials science journals further strengthen and grow. For the second year running, weekly *Journal of Materials Chemistry*'s impact factor rose significantly, to 4.29. Meanwhile, new interdisciplinary journal *Soft Matter* (launched June 2005) received an impressive first (partial) impact factor of 4.39, positioning it ahead of its competitors and achieving the journal's aim of bringing together interdisciplinary research in this field.

RSC journals at the interface with biology have also been bolstered by increasing impact factors, with *Organic & Biomolecular Chemistry*

and *Natural Product Reports* achieving 2.87 and 8.89 (rises of 13% and 21%) respectively. Newcomer *Molecular BioSystems* (launched May 2005) celebrates its first (partial) impact factor of 2.45.

These successes come after a year of innovative developments to the presentation and linking of research in RSC Journals, particularly those containing biological content, through the industry-leading Project Prospect.

Topical research ...

It's official! Work published in RSC journals is also amongst the most topical. The immediacy indices for a number of RSC journals are now leading the way. When it comes to topical and urgent research, JAAS (*Journal of Analytical Atomic Spectrometry*) and *The Analyst* top the charts for analytical chemistry journals, with figures of 0.94 and 0.93 respectively. *Dalton Transactions* becomes the

leading general inorganic journal, with an immediacy index of 0.89 (an increase of 22% on its 2005 figure).

These impressive new figures, coupled with the RSC's position as the fastest publisher of chemical science research, reinforce RSC Publishing's reputation as the home of exciting new research.

RSC Publishing would like to thank all our authors, referees and readers for their continued support.

Footnote: The annual ISI® impact factors provide an indication of the average number of citations per paper. The impact factor for 2006 is calculated from the total number of citations given in 2006 to citeable articles published in 2004 and 2005, divided by the number of citeable articles published in 2004 and 2005.

The immediacy index measures how topical and urgent the papers published in a journal are. The 2006 immediacy index is the total number of citations given in 2006 to citeable articles published in 2006 divided by the number of citeable articles published in 2006.

Data based on 2006 impact factors, calculated by ISI®, released June 2007.

Cover it up!

Methods in Organic Synthesis is holding a cover competition, for all those involved or interested in organic chemistry.

With a large readership and diverse array of abstracts in every issue, the winner of the competition can be sure that their cover will be seen by readers across the globe. The winning image will feature on the RSC website as well as on the front of *Methods in Organic Synthesis* throughout 2008, making it highly visible to our extensive international audience.

Methods in Organic Synthesis presents the most novel, current and topical research in organic chemistry and the winning image should reflect this.

The existing MOS cover image – could you do better?

Can you bring organic chemistry to life visually? Then why not visit *www.rsc.org/mos/covercomp* and submit your image today!

DREAMSTIME

RSC Publishing

©The Royal Society of Chemistry 2007

Future Energy: Chemical Solutions

12 - 14 September 2007
University of Nottingham, UK

This unique three-day conference recognises the importance of the chemical sciences in the field of sustainable energy, a priority of the RSC.

The scientific programme is representative of the key energy areas, including sessions on energy materials, energy innovation and policy, fuel cells, nuclear waste management, carbon capture and storage, bio-energy and catalysts for energy.

Invited speakers include:

- Steve Koonin (*BP plc*)
- Sir Richard Friend FRS (*Cambridge*)
- Peter Edwards FRS (*Oxford*)
- John Griffiths (*Leeds*)
- Keith Shine (*Reading*)
- Bernard Boullis (*CEA, France*)
- David Carslaw (*Leeds*)
- David Vincent (*Carbon Trust*)

Register now – see the website for full programme and registration information

RSC | Advancing the Chemical Sciences

www.rsc.org/Energy07

Registered Charity Number 207890

Green chemistry in Ethiopia: the Third Annual Workshop

Yonas Chebude, Debebe Yilma, Peter Licence and Martyn Poliakoff report on the Third Ethiopian Workshop on Green Chemistry, held on the 18–19th May 2007 at Jimma University, Jimma, Ethiopia.

The third Ethiopian workshop on Green Chemistry was held on 18–19th May 2007 at Jimma University. It was organised jointly by Jimma University, Hawassa University, Addis Ababa University and the University of Nottingham, with the support of the British Council DelPHE programme, the GCI and RSC. The workshop was attended by 75 scientists and students from 9 universities and 2 research centres from across Ethiopia, as well as Pete Licence and Martyn Poliakoff from the UK. The meeting had two main focuses, (i) dissemination and implementation of green chemistry practices in Ethiopia and (ii) the use of renewables for the manufacture of chemicals and biofuels. There was lively discussion on both topics and several interesting points emerged.

The first challenge is how to promote green chemistry and encourage industries and other stakeholders to adopt the principles of green chemistry in a country where there is little enforcement of existing environmental legislation. There was general agreement that the most effective route was *via* case studies which could persuade stakeholders of the financial benefit associated with the cleaner production and handling of chemicals. Particular target industries include leather processing, textiles, brewing and other food industries, including sugar production. A start has been made in promoting ISO 14001 and associated ISO protocols (www.ecpc.org.et) which can provide organisations with a proven mechanism for the implementation and maintenance of cleaner technologies. One poster at the workshop described how this approach has already "greened" the production of beer in both an environmentally and economically beneficial way.

The question of biofuels is currently a topic of discussion in Ethiopia, primarily for reasons of security of supply, but also for climate change and sustainability. Already, several foreign countries are planting Jatropha (*Jatropha curcas*), an oil bearing tree, to obtain raw materials for biodiesel production but it does not grow at the altitudes found in much of Ethiopia. An interesting and indeed promising suggestion is the planting of endemic oil bearing trees, *e.g.* birbra (*Millettia ferruginea*) and korch (*Erythrina brucei*) for reforestation of neglected areas that cannot be used for the growing of arable crops. This process could have twin benefits apart from the reforestation itself; firstly the planting of the trees will halt potentially disastrous soil erosion, a problem that is common throughout Ethiopia; secondly, the oil produced will make the forests economically sustainable.

The main outcome of the workshop was the decision by delegates from the different universities to organise regional workshops to disseminate the important messages from Jimma to their own students, local industries and high schools in each area. This way, the impact of the Jimma workshop can be multiplied many times and a start can be made on introducing cleaner technologies right across this very large African country. The whole event was characterised by great enthusiasm and a desire to learn which, perhaps, can form a role model for other African countries. The Federation of African Societies of Chemistry (www.faschem.org) are organising their first annual congress in Addis Ababa in September this year, and green chemistry will be the principal theme of the congress. The Jimma meeting ended with each university receiving two copies of a green chemistry book, Green Chemistry, An Introductory Text, as a gift from the RSC and a vote of thanks to the principal organisers, *Ato Tefera Entele* (JU) and *Dr Nigist Asfaw* (AAU).

Yonas Chebude, Department of Chemistry, Addis Ababa University, Addis Ababa, Ethiopia, **Debebe Yilma**, Ethiopian Cleaner Production Centre (ECPC), PO-Box 2482, Addis Ababa, Ethiopia, **Peter Licence**, Department of Chemistry, Addis Ababa University, Addis Ababa, Ethiopia and School of Chemistry, The University of Nottingham, Nottingham, NG7 2RD, UK and **Martyn Poliakoff**, School of Chemistry, The University of Nottingham, Nottingham, NG7 2RD, UK, E-mail: Martyn.Poliakoff@nottingham.ac.uk

Recent developments on the chemistry of aliphatic nitro compounds under aqueous medium

Roberto Ballini,*[a] Luciano Barboni,[a] Francesco Fringuelli,[b] Alessandro Palmieri,[a] Ferdinando Pizzo*[b] and Luigi Vaccaro[b]

Aliphatic nitro derivatives represent an important class of useful molecules in organic synthesis. The versatility of these compounds is largely due to their easy availability and transformation into a variety of diverse functionalities. Moreover, aliphatic nitro compounds are very important building blocks (both as nucleophiles or as electrophiles) for the generation of new carbon–carbon bonds, mainly *via* nitroaldol-Henry reactions, Michael reactions and Diels–Alder cycloadditions. Usually, organic solvents are believed to be necessary for achieving the best efficiency in the reactions of aliphatic nitro compounds and, only recently, it has been shown that these reactions are also very efficient using water as reaction medium. Such progress in the chemistry of aliphatic nitro compounds is particularly attractive to industry since the replacement of toxic solvents still remains a crucial (and expensive) challenge. Thus, this report is focused on the chemistry of aliphatic nitro derivatives performed in aqueous media.

1. Introduction

It is still common feeling that most organic reactions should be performed in organic solvents and generally under dry conditions. Actually, this scenario is changing and, according to the urgent needs for a more environmentally responsible chemistry, alternative reaction media are taking a leading role in the development of efficient and cleaner organic chemistry.

Fifteen years ago, the number of scientific publications concerning the use of ionic liquids, supercritical fluids, water or solvent-free conditions was very little.

Today, we are participating in rapidly growing attention towards this research field with a concomitant development of green chemistry.

Among the alternative reaction media, water is one of the most intriguing due to its peculiar properties. Water is the most abundant and available molecule on the planet and many biochemical processes occur in aqueous medium. Nevertheless, for a long time it has been rarely used as reaction medium by organic chemists, because its presence has always been associated with the ''decomposition'' of the reagents normally believed to be usable only in dry organic solvents. In fact, water has been generally used to work-up organic reactions and therefore it has been associated to a ''waste-production step'' and to the consequent obvious problems of cleaning-up water from reactants' residues.

In 1980, Breslow's observations on the acceleration of some Diels–Alder reactions when carried out in water with respect to

organic solvent[1] undoubtedly played a special role in the development of organic synthesis in aqueous media, but it must be mentioned that much earlier Diels–Alder reactions had been performed in water.[2] In 1931, Diels and Alder themselves[2a] used water as reaction medium in the cyclo-addition of furan with maleic anhydride. In 1948, Woodward and Baer[2b] employed aqueous maleic acid as dienophile, and in 1973 the beneficial effect of aqueous medium on the reaction was successfully investigated also by Koning and Carlson.[2c] However, Breslow's kinetic work was the first that quantitatively showed the beneficial effects of water on the reactivity and selectivity of an organic reaction (for example the reaction of cyclopentadiene with butenone in water was accelerated by 740 times compared to that performed in isooctane). This paper had the important role of stimulating further research in this area.

Many excellent reviews dealing with different aspects on this field have appeared, witnessing the large number of scientists nowadays involved in the study of water as reaction medium and its implications in different research areas.[3]

There are many advantages in the use of aqueous reaction media. Among them, we wish to mention the possibility of recovery and re-use of the aqueous medium and all the soluble species dissolved in it (catalysts and reactants), and the possibility of controlling the pH. This is of particular interest because it makes possible to influence the reactivity and solubility of the reactants, often allowing unique chemical behaviours to be displayed and isolation procedures to be simplified.[4] For example, it has been shown that salts such as $AlCl_3$, $TiCl_4$, $SnCl_4$ and $ZnCl_2$, believed to be decomposed by water, are on the contrary very effective catalysts provided that they are used under controlled pH conditions.[5]

Aliphatic nitro compounds are a very important class of molecules in modern organic chemistry; the remarkable synthetic importance of these compounds has ensured long-standing

[a]''Green Chemistry Group'', Dipartimento di Scienze Chimiche dell'Università and Consorzio Interuniversitario ''La Chimica per l'Ambiente'' (INCA) UDR di Camerino1, Via S. Agostino 1, 62032, Camerino (MC), Italy. E-mail: roberto.ballini@unicam.it
[b]CEMIN – Centro di Eccellenza Materiali Innovativi Nanostrutturati, Dipartimento di Chimica, Università di Perugia, Via Elce di Sotto, 8, 06123, Perugia, Italia. E-mail: pizzo@unipg.it; Fax: +39 075 5855560; Tel: +39 075 5855558

studies on their utilization in organic procedures.[6] The versatility of nitro compounds in synthesis is largely due to their easy availability and to the simple transformation of the nitro group into a variety of diverse functionalities.[7] Moreover, aliphatic nitro compounds are very important building blocks (both as nucleophiles or as electrophiles) for the generation of new carbon–carbon single and double bonds.

Nitronate anions, that can be generated from nitroalkanes[8] using a wide range of bases, act as carbon nucleophiles with common electrophiles including aldehydes (nitroaldol-Henry reaction),[9] and electron-poor alkenes (Michael addition),[10] leading to carbon–carbon bond formation.

On the other hand, conjugated nitroalkenes are very useful electron-poor alkenes, prone to act as nucleophilic acceptors mainly in the Michael reaction[11] or in the Diels–Alder cycloaddition.[12]

Anyway, all these methodologies of employment of aliphatic nitro compounds give valuable accesses to polyfunctionalized molecules, and these reactions are typically carried out under homogeneous conditions by using an organic solvent and a soluble catalyst.[7–12]

In recent years, aliphatic nitro compounds have displayed a high reactivity in aqueous reaction medium, mainly in the formation of new carbon–carbon bonds.

2. Preparation of nitroalkanes from haloderivatives

Due to the increasing importance of nitroalkanes in organic synthesis,[6–10] their easy and convenient availability is crucial. The conversion of alkyl halides to nitro compounds by metal nitrites is one of the most used methods for the preparation of primary nitroalkanes. However, long reaction times, the use of toxic solvents (dimethyl sulfoxide, N,N-dimethylformamide, etc.), and tedious work-up procedures are necessary and/or low yields are generally obtained.[13] Moreover, a further and serious drawback is that the isolated products are usually a mixture, difficult to purify, of the desired nitroalkanes **2** together with the undesired alkyl nitrites.

A more efficient and eco-friendly procedure for the conversion of **1** to **2**, uses water as reaction medium. By treating primary alkyl halides **1** with 4 equiv. of silver nitrite at room temperature or 60 °C, in water, a variety of primary nitroalkanes, **2**, have been isolated in satisfactory to good yields (53–93%, Table 1), generally in very short reaction times (0.5–1.25 h) and with minimal formation of the undesired alkyl nitrites (<4–5%).
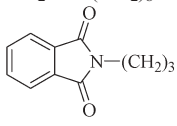
The reason for using 4 equiv. of silver nitrite is that in these conditions the reaction is fast enough to minimize the competitive formation of the corresponding alcohol.

Although the method works well with both alkyl bromides and iodides, the latter generally show a higher reactivity. Functionalities such as carbon–carbon double bonds, esters, imides, and ketones are preserved under the needed reaction conditions.

Of particular interest is the possibility to perform the one-pot transformation of α,ω-diiodo compounds **3** to the corresponding dinitroalkanes **4** (Scheme 1).

Moreover, this procedure avoids the use of high toxic solvents and the formation of undesired by products.

Table 1 Primary nitroalkanes **2** prepared from haloderivates **1**

Entry	R	X	$T/°C$	t/h	Yield (%)
1	p-NO$_2$C$_6$H$_4$CH$_2$	Br	60	24	53
2	Ph	Br	r.t.	2	55
3	CH$_3$(CH$_2$)$_8$	Br	r.t.	2.5	85
4	CH$_2$=CH(CH$_2$)$_8$	Br	60	5	64
5	p-NO$_2$C$_6$H$_4$CH$_2$	I	60	1	65
6	Ph	I	r.t.	0.5	56
7	CH$_3$(CH$_2$)$_8$	I	r.t.	0.5	93
8	CH$_3$(CH$_2$)$_6$	I	r.t.	1	83
9	CH$_3$(CH$_2$)$_9$	I	r.t.	0.75	84
10	CH$_2$=CH(CH$_2$)$_8$	I	r.t.	1.25	83
11	(phthalimido)—(CH$_2$)$_3$	I	60	1	84

n = 3 (62%), 6 (64%), 8 (61%)
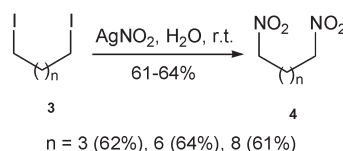
Scheme 1 Conversion of α,ω-diiodo structures to α,ω-dinitroalkanes.

3. The Henry reaction

Carbon–carbon bond formation is the essence of organic synthesis. The Henry reaction, an aldol-type condensation between a nitroalkane and a carbonyl compound, represents one of the classical C–C bond-forming processes,[9] and it has been used extensively in many important syntheses.[6]

The classical nitroaldol reaction is routinely performed in presence of a base in an organic solvent (Scheme 2).

Since basic reagents are also catalysts for the aldol condensation and for the Cannizzaro reaction when aldehydes are used as carbonyl sources, it is necessary to adopt experimental conditions to suppress these competitive reactions. To obtain better yields of 2-nitro alcohols, a careful control of the basicity of the reaction medium is necessary, and long reaction times are required. Furthermore, the formed β-nitroalkanols may undergo base-catalyzed water elimination
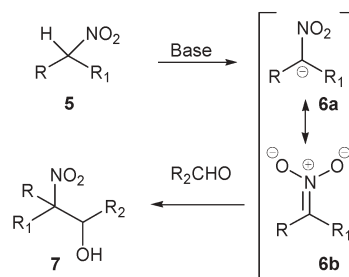
Scheme 2 The Henry reaction.

to give nitroalkenes that readily polymerize.[14] This elimination is difficult to avoid when aryl aldehydes are employed.
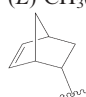
3.1. Nitroaldol reaction for the synthesis of β-nitroalcohols

It is well known that aqueous medium is less expensive and less dangerous with respect to organic solvents, while it allows the control of the pH and the use of microaggregates such as surfactants. Generally, the low solubility of most reagents in water is not an obstacle to the reactivity,[3c,3e,15] which, on the contrary, is reduced with the use of co-solvents. The nitroaldol reaction can be efficiently performed in aqueous media, under very mild conditions, using a stoichiometric amount of nitroalkanes **5** with an aldehyde, in 0.025 M NaOH and in the presence of cetyltrimethylammonium chloride (CTACl) as a cationic surfactant. As shown in Table 2, the yields of the nitroalkanols **7** range from good to excellent when the nitroalkanes react with aliphatic aldehydes, while yields slightly decrease with the aromatic ones. Short reaction times (2–6 h) are required, and both primary and secondary nitroalkanes give good results.

Contrary to other methods, the success of this approach is independent of the catalyst/substrate ratio and it doesn't need long reaction times, tedious preparation of the catalyst, large excess of the nitroalkane, or severe reaction conditions that are too cumbersome, especially for large scale preparations. In addition, the very mild reaction conditions prevent the typical side reactions, such as retro-aldol reaction or dehydration of 2-nitroalcohols into nitroalkenes even if aromatic aldehydes are used. High chemoselectivity is observed since several functionalities such as hydroxyl groups, esters, acetals, tetrahydropyranyls, (Z)-C,C double bonds, and furyls are preserved. Compared to conventional methods, this procedure provides the formation of the nitroalkanols **7** under inexpensive and green conditions, with evident environmental advantages for widespread industrial use.

A new aqueous catalytic approach for the Henry reaction has been defined by using cetyltrimethylammonium hydroxide

Table 2 Selected examples of the nitroalkanols **7** prepared in 0.025 M NaOH/CTACl

Entry	R	R_1	R_2	t/h	Yield (%)^a
1	H	H	Ph	2	70
2	H	Et	Ph	2	71
3	H	Me	2-Furyl	3	70
4	H	Me	p-$NO_2C_6H_4$	4	72
5	H	$CH_3(CH_2)_3$	$Ph(CH_2)_2$	5	85
6	H	$THPOCH_2$	$Ph(CH_2)_2$	3	85
7	H	[dioxolane]—$(CH_2)_2$	$Ph(CH_2)_2$	3	90
8	H	$CH_3(CH_2)_4$	c-C_6H_{11}	2	85
9	Me	Me	$Ph(CH_2)_2$	6	88
10	H	Me	Me—[furan]—$(CH_2)_2$	6	90
11	H	$HO(CH_2)_6$	(Z)-$EtCH=CH(CH_2)_2$	3	75
12	H	$CH_3CO(CH_2)_2$	$CH_3(CH_2)_2CH(CH_3)$	2	85
13	H	$MeO_2C(CH_2)_6$	Et	3	80
14	H	–$(CH_2)_5$–	Et	3	85

^{a} Isolated yield of **7**

Table 3 Selected examples of the nitroalkanols **7** prepared by using CTAOH

Entry	R	R_1	R_2	t/h	Yield (%)^a
1	H	Et	$CH_3(CH_2)_8$	3	82
2	H	$CH_3(CH_2)_4$	$CH_3(CH_2)_4$	3	81
3	H	$CH_3(CH_2)_4$	p-$NO_2C_6H_4$	4	76
4	H	$MeOCO(CH_2)_4$	$CH_3(CH_2)_4$	3	77
5	–$(CH_2)_4$–		n-Pr	4	83
6	H	$PhCH_2$	(E)-$CH_3(CH_2)_4CH=CH(CH_2)_2$	3	86
7	H	$CH_3(CH_2)_3$	[norbornene]	3	85

^{a} Isolated yield of **7**

(CTAOH, 10% water solution).[16] In fact, treatment of nitroalkane **5** (1 mmol) with aldehydes (1 mmol), at room temperature and in a 10% water solution of CTAOH (0.3 ml), produces β-nitroalkanols **7** in good yields (68–86%). Thus, all the reactions were carried out in the presence of a minimum amount of water and work well with a series of linear and cyclic nitroalkanes and with an array of both aliphatic and aromatic aldehydes (Table 3).

The very mild reaction conditions prevent both the retro-aldol reactions and the dehydration of **7**, and allow the survival of other functionalities.

3.2. Nitroaldol reaction for the synthesis of polyfunctionalized 1,3-diols
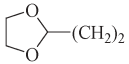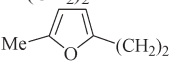
α-Nitro ketones have proven to be useful synthetic intermediates in organic synthesis.[18] 2-Nitrocycloalkanones are able to produce a consistent array of functionalized molecules through the nucleophilic retro-Claisen condensation.[18a] In this context, α-nitro cycloalkanones **8** can be used as precursors of 2-nitro-1,3-diol-ω-alkanoic acids **11**, via a tandem double nitroaldol reaction-ring cleavage, performed in aqueous medium.[19] As reported in Table 4, the reaction of **8** with an excess of 30% aqueous solution of formaldehyde proceeds at room temperature, in the presence of potassium carbonate as base.

A possible pathway begins with the Henry reaction of the starting nitro ketone **8** with formaldehyde, catalyzed by potassium carbonate. The intermediate **9** undergoes ring cleavage by water, which acts as the nucleophile. The obtained open-chain nitroalkanol **10** is prone to give a further nitroaldol reaction, with the one-pot formation of **11** in satisfactory overall yields (48–75%, Table 4).[17]

The method, in which water acts both as solvent and as reagent, seems to be independent from the ring size of the cycloalkanone.

The 1,3-diols **11** can also be considered as ω-hydroxyacids, which are the immediate precursors of lactones. Moreover, these compounds possess two other important functionalities which offer valuable opportunities for further elaboration due to the high versatility of carboxylic and nitro groups. An application of this procedure is the preparation of 2-amino-1,3-diols **12** (Scheme 3), a class of molecules[20] with a remarkable value in the field of cosmetics,[21] by ammonium formate/Pd–C reduction.

Table 4 Synthesis of 2-nitro-1,3-diols **11**

Entry	R	R_1	n	Yield (%)[a]
1	H	H	0	60
2	H	H	1	75
3	H	H	2	60
4	H	H	7	50
5	H	H	10	48
6	H	Me	1	65
7	H	t-Bu	1	63
8	Me	H	1	54

[a] Isolated yield of **11**

R = H;
R_1 = H, Me, t-Bu
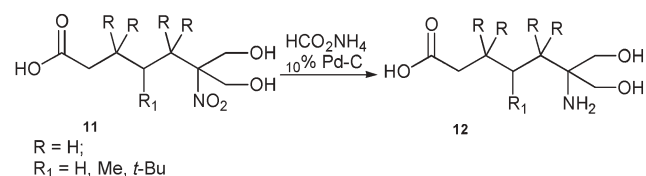
Scheme 3 Preparation of 2-amino-1,3-diols.

4. Michael addition of nitroalkanes to electron-poor alkenes

Conjugate addition of nucleophiles to electron-deficient alkenes, the so-called Michael addition, is an important tool for the creation of carbon–carbon bonds.[22]

Because the nitro group is a strong electron-withdrawing group, nitronate anions can be easily obtained and are of great utility in Michael additions because the formed nitroderivative adducts offer a variety of possible transformations.[7] As for the nitroaldol reaction, the conjugate addition of nitroalkanes to electron-poor alkenes is routinely conducted in a homogeneous solution of a base in an organic solvent, and several bases have been used for this purpose. In general, bases used in the Henry reactions are also effective for Michael additions. Anyhow, some drawbacks are often observed, such as the use of toxic solvent, the formation of by-products due to multiple additions, low yields and/or tedious work up.

4.1. Conjugate addition of nitroalkanes to electron-poor alkenes in aqueous medium

The first example of the Michael addition of nitroalkanes in water was reported by Lubineau and Augé, by using sugars as surfactants.[23] However, this method seems to be effective only when nitromethane or nitroethane are used as nucleophiles and methylvinylketone (MVK) as the electrophilic alkene. Moreover, long reaction times are required, especially when nitroethane is employed. Later, the reaction has been

Table 5 Michael reaction of nitroalkanes with conjugated enones **13**

Entry	R	R_1	R_2	R_3	t/h	Yield (%)[a]
1	Me	H	H	Me	1	85
2	Et	H	H	Me	1	78
3	n-Bu	H	H	Me	1	83
4	Me	Me	H	Me	1	75
5	Me	H	H	Et	2	76
6	Et	H	H	Et	1	64
7	n-Bu	H	H	Et	1	70
8	Me	Me	H	Et	1	71
9	Me	H	H	n-Pr	1	68
10	Et	H	H	n-Pr	1	82
11	n-Bu	H	H	n-Pr	2	68
12	Me	Me	H	n-Pr	2	77
13	Me(CH_2)_9	H	H	Me	2	74
14	Me(CH_2)_9	H	H	Et	2	70
15	Me	H	Me	Et	15	60
16	–(CH_2)_5–		H	Me	1	72
17	n-Bu	H	–(CH_2)_3–		2	79
18	Me	H	–(CH_2)_2–		2	72
19	n-Bu	H	–(CH_2)_2–		1	93

[a] Isolated yield of **14**

dramatically improved in aqueous medium by using a diluted solution of sodium hydroxide 0.025 M in the presence of a catalytic amount of cetyltrimethylammonium chloride (CTACl) as a cationic surfactant (Table 5).[24]

Under these conditions both primary and secondary nitroalkanes **5** easily react with a variety of conjugated enones **13**, even those substituted at the β-position (Table 5). Very short reaction times are sufficient to obtain γ-nitro ketones **14**.
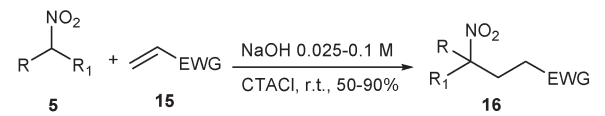
Electron-deficient alkenes,[22] such as α,β-unsaturated esters, nitriles and sulfones are less reactive than the corresponding ketones in the Michael reaction with nitroalkanes. In fact, strongly basic conditions,[25] long reaction times,[26] a large excess of nitroalkanes,[27] or the help of ultrasound[28] are required. The need to accomplish these important transformations under milder conditions and with less toxic and environmentally compatible materials has led to the development of an original aqueous procedure (Table 6) for the conjugate addition to α,β-unsaturated nitriles, esters and sulfones. Primary and secondary nitroalkanes **5** easily react with a collection of electrophilic alkenes[15,29] on diluted sodium hydroxide (0.025–0.1 M) and in the presence or in the absence (Table 6, entries 1–3, 12, 13 and 16) of a catalytic amount of CTACl to give the corresponding Michael adducts **16**.

The aqueous medium and the right control of the pH prevent the polymerisations or the polyadditions often observed during this reaction. Satisfactory to good yields were obtained in short reaction times (Table 6), additionally, the very mild reaction conditions tolerate several functionalities.

An important extension of this procedure is the efficient tandem conjugate addition–elimination (HBr) observed when nitroalkanes **5** react with ethyl 2-(bromomethyl)acrylate **17** (Scheme 4). The aqueous medium plays a key role in the one-pot formation of α,β-unsaturated esters **19**, since the

Table 6 Michael reaction of nitroalkanes **5** with different electron-poor alkenes **15**

Entry	R	R_1	EWG	NaOH/ M	Presence of CTACl	t/h	Yield $(\%)^a$
1	H	Me	CO_2Me	0.1	No	1	80
2	H	Et	CO_2Me	0.1	No	1	80
3	H	$CH_3(CH_2)_3$	CO_2Me	0.025	No	2	58
4	Me	Me	CO_2Me	0.1	Yes	8	54
5	H	Ph	CO_2Me	0.025	Yes	2	59
6	H	$CH_3CHOH(CH_2)_2$	CO_2Me	0.025	Yes	3	55
7	H	Me	CN	0.025	Yes	1	50
8	H	Et	CN	0.025	Yes	1	57
9	Me	Me	CN	0.025	Yes	2	74
10	H	$CH_3(CH_2)_4$	CN	0.025	Yes	1	61
11	$-(CH_2)_5-$		CN	0.025	Yes	4	78
12	H	Me	SO_2Ph	0.025	No	2	70
13	H	Et	SO_2Ph	0.025	No	2	58
14	H	$CH_3(CH_2)_4$	SO_2Ph	0.025	Yes	1	61
15	Me	Me	SO_2Ph	0.025	Yes	1	56
16	H	Ph	SO_2Ph	0.025	No	2	90
17	H	$CH_3CO(CH_2)_2$	SO_2Ph	0.025	Yes	2	50
18	H	$MeO_2C(CH_2)_2$	SO_2Ph	0.025	Yes	1	51

^{a} Isolated yield of **16**

appropriate choice of the pH provides the (i) generation of the nitro-carbanion, (ii) elimination of bromhidric acid from **18**, and (iii) prevention of the hydrolysis of the ester functionality. Compounds **19** are of special interest since they can be simultaneously employed as electrophiles (Michael acceptor) and/or as nucleophiles at carbons bearing the nitro group (R = H).

Nitroacetic acid derivatives **20** are valuable intermediates for the synthesis of many nitro and amino containing compounds. Michael addition of **20** to enones **21** opens a very attractive route towards γ-oxo-functionalized (α-alkylated) α-amino acids. However, Michael reactions of α-nitro esters under basic conditions often suffer from low yields.[30] Similarly, rather drastic conditions (refluxing dioxane and six days of reaction time) were required when this reaction was catalyzed by copper(II) acetate.[30]

Keller and Feringa[31] investigated the use of lanthanide triflates as reusable Lewis acids in Michael reactions of **20** with α,β-enones **21** in water, at room temperature and in the presence of a catalytic amount of ytterbium triflate [Yb(OTf)$_3$] (Scheme 5).
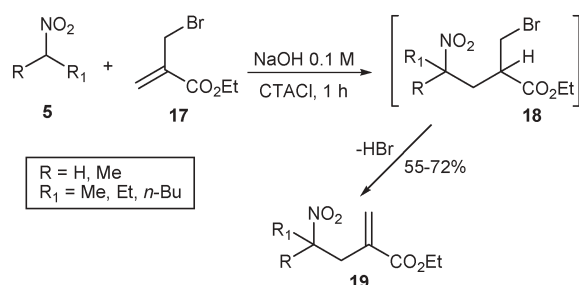
Scheme 4 Tandem Michael reaction–HBr elimination.
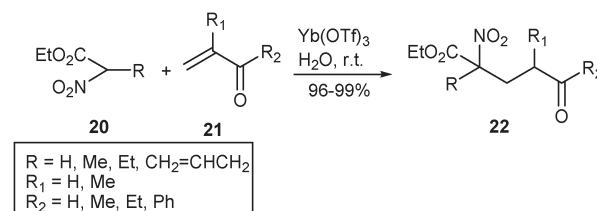
Scheme 5 Michael reaction of nitroacetic acid derivatives.
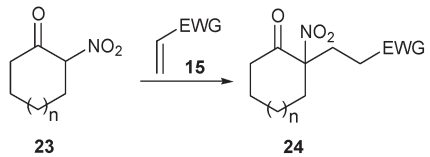
The Michael adducts **22** were obtained in nearly quantitative yields in the presence of 10 mol% of Yb(OTf)$_3$, while in the absence of the catalyst the reaction was much slower, giving a low conversion of the desired Michael adduct even after prolonged reaction times. It should be emphasized that single products were obtained using this simple procedure and in most cases no further purification was necessary, since the conjugate addition was not accompanied by unwanted O-alkylation or hydrolysis of the ester functionality. When aliphatic α,β-unsaturated enones bearing various substituents at the α′-position were employed, again quantitative yields of the 1,4-adducts were found. However, when cyclic or β-substituted α,β-unsaturated enones were used no reaction was observed even after prolonged reaction times. With the Michael acceptors bearing various electron withdrawing groups, only acrolein or conjugated enones gave the desired 1,4-adduct, whereas α,β-unsaturated esters or nitriles were not reactive under these conditions.

The addition is proposed to proceed via a twofold coordination of the α-nitro esters by ytterbium triflate as well as by activation of the Michael acceptor as depicted in Scheme 6.

α-Nitro ketones are the source of important building blocks,[18] but, in spite of this interest, some aspects of their chemistry, in particular their Michael reactions, have received little attention. The traditional basic catalysts used for promoting Michael reactions make α-nitro ketones and their Michael adducts unstable in the reaction conditions, since they tend to be opened by external nucleophiles, such as water.[18a,19] For this reason, the conjugate addition of these substrates have been conventionally carried out in organic solvents, using
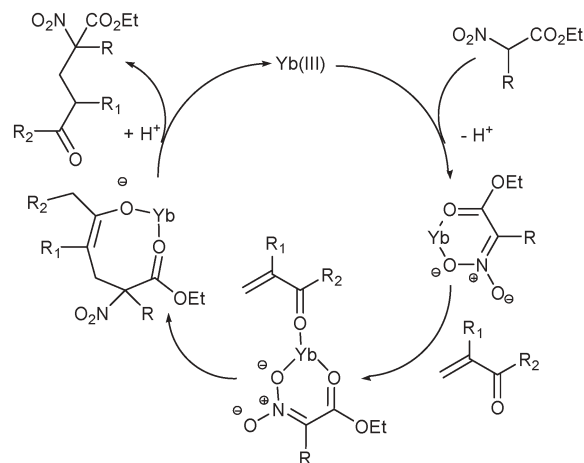
Scheme 6 Proposed mechanism for the Michael addition of **20** (counterions omitted for clarity).

Table 7 Michael reaction of α-nitrocycloalkanones **23** with **15**

Entry	EWG	n	Conditions	Yield (%)[a]
1	CHO	1	H_2O, r.t., 14 h	98
2	CHO	2	H_2O, r.t., 8 h	85
3	COMe	2	H_2O, r.t., 4 h	93
4	COEt	2	H_2O, r.t., 4 h	85
5	CHO	3	H_2O, r.t., 14 h	99
6	COMe	3	H_2O, r.t., 4 h	98
7	CHO	5	H_2O, r.t., 37 h	99
8	CHO	7	H_2O, r.t., CTAB (10%) 5 d	99
9	CO_2Me	2	H_2O, r.t., 7 d	30
10	CO_2Me	2	H_2O, reflux, 1d	40
11	COMe	2	$KHCO_3$ (0.07 M in H_2O), r.t., 3 h	76
12	COMe	2	$KHCO_3$ (0.035 M in H_2O), r.t., 4 h	65
13	COMe	2	$KHCO_3$ (0.07 M in H_2O), r.t., 0.5 h	92
14	COEt	2	$KHCO_3$ (0.07 M in H_2O), r.t., 1 h	80
15	CO_2Me	2	$KHCO_3$ (0.07 M in H_2O), r.t., 45 min	49
16	CHO	2	$KHCO_3$ (0.07 M in H_2O), r.t., 0.5 h	55
17	CN	2	$KHCO_3$ (0.07 M in H_2O), r.t., CTAB (10%) 3 h	60
18	SO_2Ph	2	$KHCO_3$ (0.07 M in H_2O), r.t., CTAB (10%) 3 h	77

[a] Isolated yield of **24**

Table 8 Selected examples of Michael reaction under CTAOH

Entry	Nitroalkane	α,β-Unsaturated compound	t/h	Yield (%)[a]
1	$EtNO_2$	methyl acrylate	1	78
2	n-$PrNO_2$	2-cyclohexenone	1	80
3	$CH_3(CH_2)_4NO_2$	2-cyclohexenone	2	90
4	n-$PrNO_2$	ethyl vinyl ketone	1	75
5	$CH_3(CH_2)_5NO_2$	methyl acrylate	1	87
6	$CH_3(CH_2)_5NO_2$	acrylonitrile (CN)	1	70
7	$CH_3CH(OH)(CH_2)_3 NO_2$	acrylonitrile (CN)	1	72
8	$CH_3(CH_2)_5NO_2$	vinyl sulfone (SO_2Ph)	1	70
9	$MeOCO(CH_2)_5 NO_2$	vinyl sulfone (SO_2Ph)	2	73
10	$CH_3(CH_2)_5NO_2$	methyl acrylate	1	87

[a] Isolated yield of the Michael adduct.

amine or phosphine as catalysts.[32] Within this context, Menéndez et al. recently published[33] the preparation of **24** by the Michael reaction, in water, of several α-nitrocyclo-akanones **23** with structurally varied Michael acceptors **15** using neutral or very mild basic conditions (Table 7).

The authors decided to use water as reaction medium, with no additional catalyst, believing that the acidity[34] of the α-nitrocarbonyl group would be enough to promote the reaction. These conditions allowed the Michael addition of compounds **23** to acrolein, methyl vinyl ketone and ethyl vinyl ketone in excellent yields (Table 7), and without formation of open-chain derivatives. The method seems to be independent of the ring size of the starting nitrocyclo-alkanones **23**; anyway, larger nitro ketones (n = 7), because of their lower water solubility, required the presence of the cationic surfactant cetyltrimethylammonium bromide (CTABr) in the reaction medium.

Attempts to extend these conditions to less reactive Michael acceptors, such as methyl acrylate, were not similarly successful; however, the use of diluted solution of potassium carbonate (0.07 M) contributes to improve the yields of the Michael adducts (Table 7).

A 10% water solution of cetyltrimethylammonium hydroxide (CTAOH) also works well for the Michael addition at room temperature of nitroalkanes to a variety of electron-poor alkenes.[16]

As reported in Table 8, even hindered electrophilic alkenes, such as 2-cyclohexen-1-one, that usually need long reaction times and gives low yields, in these conditions allow excellent yields of the nitro adduct (entry 2 and 3) in only 1–2 h. Moreover, with this protocol, simple and functionalized nitroalkanes easily react with different electrophilic alkenes, and the yields seem to be fairly independent of the degree of electron-deficiency of the alkene and of the steric hindrance.

The above described procedure, was extended to the conjugate addition of nitroalkanes to optically active acrylates,[35] considering that derivatives of α,β-unsaturated carboxylic acids bearing a chiral auxiliary on the acyl moiety have found a widespread utilisation in synthesis, mainly as dienophiles in cycloaddition reactions. Intermolecular conjugate addition of nitronate anions to these chiral electron-poor alkenes had not been previously reported, and would have hopefully produced the corresponding nitro derivative in a diastereoselective fashion. As a test reaction, the addition of 1-nitropentane to the acrylate **25** has been carried out in a series of base–solvent combinations in homogeneous and heterogeneous conditions, and, as reported in Table 9, the best results could be obtained using CTAOH in water.

A number of simple and functionalised nitrocompounds have been made to react with optically active acrylates, and, although only modest levels of diastereoselectivity can be observed (Table 10), probably because the chiral auxiliary is located too far from the reaction centre, the Michael adducts **26** can be easily transformed into interesting building blocks as γ-amino acids and cyclic hydroxycarbamates.

Table 9 Trend of Michael addition (R = *i*-Pr) with different bases

Entry	Base	Solvent	t/h	Yield (%)^a
1	DBU	THF	5	55
2	TMG	CH$_3$CN	6	68
3	*t*-BuOK	THF	5.5	5
4	Amberlyst A-21	Et$_2$O	22	41
5	CTAOH	H$_2$O	6.5	77

^{a} Isolated yield of **26**

Table 10 Selected examples of the Michael addition of nitroalkanes to chiral acrylates leading to compounds **26**

Entry	Nitroalkane	Aux.	d.r.	t/h	Yield (%)^a
1	CH$_3$(CH$_2$)$_4$NO$_2$		6 : 4	6.5	71
2	(CH$_3$)$_2$CH$_2$CH$_2$NO$_2$		6 : 4	6.5	77
3	MeOCO(CH$_2$)$_2$NO$_2$		6 : 4	7	57
4	Ph(CH$_2$)$_2$NO$_2$		6 : 4	6	76
5	CH$_3$CO(CH$_2$)$_3$NO$_2$		6 : 4	7	52
6			6 : 4	7.5	61
7			6 : 4	6.5	40
8	CH$_3$(CH$_2$)$_4$NO$_2$		7 : 3	6	72
9	Ph(CH$_2$)$_2$NO$_2$		7 : 3	6	82

^{a} Isolated yield of **26**
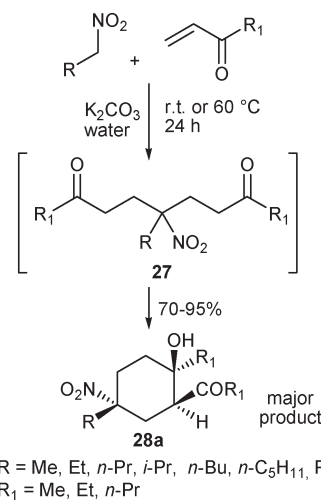
Scheme 7 One-pot synthesis of nitrocyclohexanol derivatives.

4.2. Synthesis of nitrocyclohexanol and aromatic derivatives

Nitrocyclohexanol derivatives are an interesting class of polyfunctionalized molecules, prone to give many other transformations into a variety of different molecular structures. These compounds have been recently obtained in a one-pot way, under aqueous medium,[36] by reaction of primary nitroalkanes with two equivalents of α,β-unsaturated ketones, and in the presence of potassium carbonate as base (Scheme 7).

The first step of the reaction is the double Michael addition of the nitroalkane to the enone, followed by, *in situ*, intramolecular aldol reaction of the adduct **27**. Cyclohexanols **28** are obtained in 70–95% yields and with excellent stereochemical selectivity, stereisomer **28a** being largely predominant (Scheme 7).

The one-pot formation of **28** is strongly favoured by the use of water as solvent, since the employment of the conventional procedures give only moderate yields of the intermediate **27**.

If the diastereomeric mixture of **28** is dissolved in toluene, in the presence of a stoichiometric amount of TsOH, and refluxed with a Dean–Stark apparatus, with the simultaneous injection of air, the aromatic compounds **31** were directly obtained (Scheme 8).[37]

The conversion of **28** to **31** proceeds initially through the elimination of both water (compound **29**) and nitrous acid, leading to the compounds **30**, which convert, by air oxidation, to the aromatic systems **31**. This means that **31** can be obtained from simple nitroalkanes, in only two steps with moderate use of chemicals and reduced production of waste.
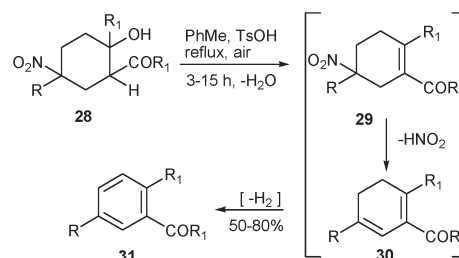
Scheme 8 One-pot aromatization of **28**.

4.3. One-pot synthesis of 1,4-diketone, 1,4-diol, γ-nitroalkanol and tetrahydrofuran derivatives

The reaction of complex molecules is traditionally performed by a sequence of separate reaction steps, each one requiring its own conditions, reagents, solvent, catalyst, and purification steps. Now, environmental and economic pressure are forcing the search for more efficient ways of performing chemical transformations, such as the possibility of achieving more synthetic steps in a one-pot procedure.

In this context, nitroalkanes and aqueous medium contribute in efficient synergy for the one-pot synthesis of γ-nitroalkanol, tetrahydronfuran, 1,4-diketone and 1,4-diol derivatives, with evident reduction of wastes.[38] The common key step for these synthesis is the conjugate addition of primary nitroalkanes to enones in aqueous medium, using K_2CO_3 as catalyst.

Thus, the one-pot synthesis of γ-nitroalkanols **32**, which have proven to be the key building blocks of tetrahydrofurans and spiroketals,[39] was achieved in good yields (78–94%, Scheme 9) by Michael reaction of nitroalkanes and unsaturated ketones, followed by *in situ* reduction with $NaBH_4$. The latter was chosen both because it can be used in water and because it does not reduce the nitro group. Nitroalkanols **32** were obtained as a 1 : 1 diastereoisomeric mixture.

Hydroxytetrahydrofurans (lactols) **33** (useful intermediates in the synthesis of cyclic ethers, dihydrofurans, zoapatanol derivatives and nonactic acid)[40] were prepared (Scheme 10) by *in situ* Nef reaction of the corresponding γ-nitroalkanones, by using a 30% water solution of H_2O_2.

The conversion of a nitro group into a carbonyl (Nef reaction) can be accomplished by several alternative methods[7e] although the use of H_2O_2–K_2CO_3[41] appears to be the most compatible with the aqueous medium and the most chemoselective. The expected hydroxyketones could not be isolated, since they spontaneously cyclized to the corresponding lactols **33** in 48–58% overall yields.

1,4-Diketones **34**, an important intermediates for the synthesis of several cycles and heterocycles,[42] can be prepared by Michael addition of the nitroalkanes to the enones, followed by *in situ* Nef conversion of the nitro-Michael adduct with 30% H_2O_2 (Scheme 11).
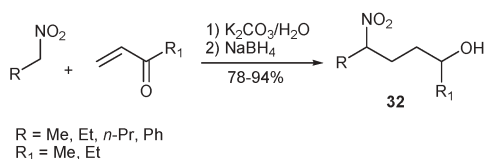
Scheme 9 One-pot synthesis of γ-nitroalkanols.
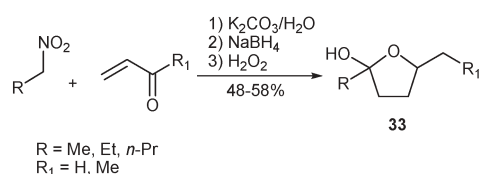
Scheme 10 One-pot synthesis of lactols.
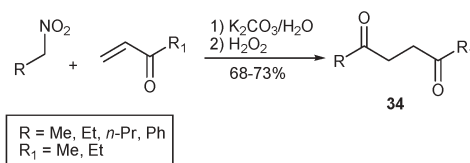
Scheme 11 One-pot synthesis of 1,4-diketones.
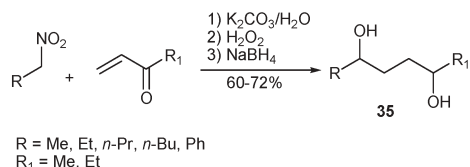
Scheme 12 One-pot synthesis of 1,4-diols.

Finally, 1,4-diols **35** (widely used molecules for the preparation of lactones, pyrroles and tetrahydrofurans)[43] were synthesized (Scheme 12) by *in situ* reduction of the obtained 1,4-diketones, using an excess of $NaBH_4$ as reducing agent.

Thus, all the one-pot synthesis of compounds **32–35** start with the Michael addition of primary nitroalkanes to conjugated enones, in which the aqueous medium plays a key role offering the advantage to perform many other transformations *in situ*.

4.4. One-pot synthesis of substituted Δ¹-pyrrolines starting from chalcones

Recently,[44] Liu reported the Michael addition of nitroalkanes to chalcones in various organic solvent–H_2O mixtures and in the presence of different bases at room temperature. The best results, in terms of reaction time and yield, were obtained by using a mixture of DMF–1 M aq. NaOH (1/1 v/v) as reaction medium.

When the reaction mixture containing **36** was treated with Zn/HCl the corresponding Δ¹-pyrrolines **37** was formed, in generally good yields, by intramolecular cyclization. The one-pot protocol is simple and has been satisfactorily used for the synthesis of variously substituted Δ¹-pyrrolines (Scheme 13).

5. Cleavage of α-nitrocycloalkanones

Given the well-known chemical differences between of the carbonyl and the carbon–nitro group moiety, their juxtaposition on two adjacent carbons offers an important reactivity pattern, peculiar to α-nitro ketones. In fact, the C–C bond between the carbonyl group and the nitro-substituted atom of cyclic α-nitro ketones undergoes cleavage by nucleophilic agents and this retro-Claisen reaction is useful for the synthesis of open-chained α,ω-disubstitued compounds.[18a]
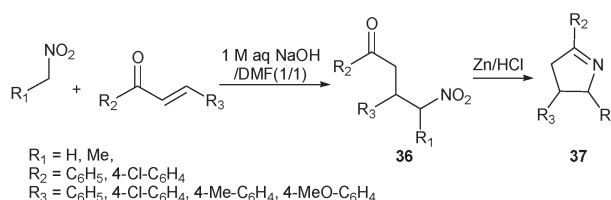
Scheme 13 One-pot synthesis of Δ¹-pyrrolines.

5.1. Synthesis of ω-nitro acids by cleavage of α-nitrocycloalkanones

ω-Nitro acids **39** are an important class of functionalized carboxylic acids that, due to the great versatility of the nitro group, can be employed as building blocks for many other targets. These acids have been prepared by ring cleavage of alkylated 2-nitrocycloalkanones **38**, using water both as solvent and as reagent.[45] In fact, by heating an aqueous solution of the nitrocycloalkanones in the presence of NaOH (0.05 M) and a catalytic amount of CTACl, as surfactant, the nucleophilic attack of water to the carbonyl moiety was observed, with the consequent ring cleavage of **38** to the open chain compounds **39** (Table 11).

By this C–C bond fission a variety of cyclic nitro ketones are efficiently cleaved in high yields (Table 11), regardless the ring size or the alkyl-substituent. Only α-nitrocyclooctanone produces a mixture of unidentified products.

5.2. Macrolactones from α-nitrocycloalkanones
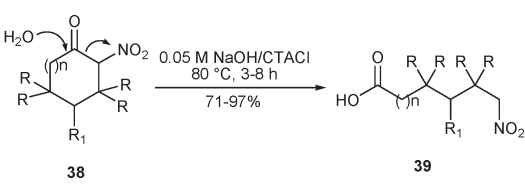
Medium- and large-sized lactones have attracted much attention due to their wide range of biological activities.

A unique domino reaction of α-nitrocycloalkanones **23** with α-alkyl α,β-unsaturated aldehydes, in aqueous base, leads to one-pot synthesis of hitherto unknown functionalized, bridged, bicyclic lactones containing 10-, 11-, 13-, and 15-membered rings **40** (Table 12).[46]

As shown in Table 12, the reaction is very versatile in terms of the size of the staring material, and therefore it could be applied to the fast preparation of functionalized macrolactones of various ring size. However, depending on the ring size, compounds **40** were isolated as a mixture of diastereomers or as a single isomer.
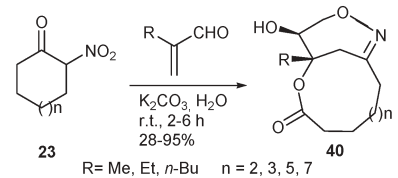
A mechanism that accounts for the formation of macrolactone **40** (*n* = 2) is summarized in Scheme 14 and involves a unique anionic domino transformation including up to six different reactions in a one-pot process. The anion **II** from the

Table 11 Preparation of ω-nitro acids

Entry	*n*	R	R₁	*t*/h	Yield (%)[a]
1	0	H	H	3	90
2	1	H	H	4	97
3	2	H	H	8	84
4	3	H	H	8	mix of prod.
5	4	H	H	8	84
6	6	H	H	8	75
7	7	H	H	8	84
8	10	H	H	8	79
9	1	H	Me	6	78
10	1	H	*t*-Bu	6	71
11	1	H	Ph	6	93
12	1	Me	H	8	75

[a] Isolated yield of **39**

Table 12 Preparation of bicyclic lactones **40** from α-nitro ketones

Entry	*n*	R	*t*/h	d.r.	Yield (%)[a]
1	2	Me	1	4 : 1	95
2	2	Et	1	3 : 1	89
3	2	*n*-Bu	1	2.5 : 1	30
4	3	Me	1.5	3 : 1	51
5	3	Et	1.5	4 : 1	57
6	3	*n*-Bu	2.5	single diastereomer	85
7	5	Me	2.5	single diastereomer	57
8	5	Et	4	single diastereomer	66
9	5	*n*-Bu	6	single diastereomer	31
10	7	Me	5	single diastereomer	52
11	7	Et	5	single diastereomer	53
12	7	*n*-Bu	5	single diastereomer	28

[a] Isolated yield of **40**

initial Michael addition evolves to **III** through a retro-Claisen-type reaction. Cyclization of **III** by attack of the nitronate oxygen onto the aldehydes group requires the existence of conformation **IV**, which would be favoured by repulsive interaction between the nitronate and alkyl group in **III** and would lead to the nitronate *N*-oxide **V**. Elimination of water
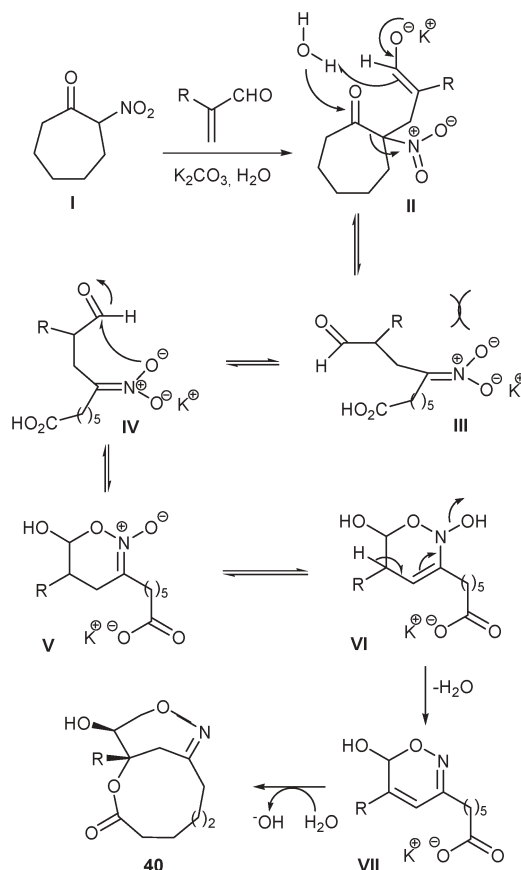
Scheme 14 Proposed mechanism for the formation of **40** (*n* = 2).
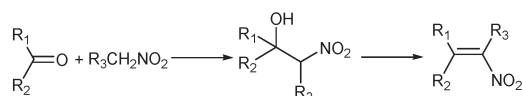
Scheme 15 Two-step synthesis of α,β-nitroalkenes.

and final intramolecular conjugate addition of the carboxylate group allow the macrolactone **40** (*n* = 2).

6. α,β-Unsaturated nitroalkenes

α,β-Unsaturated nitroalkenes are molecules of great interest owing to their biological and pharmacological properties,[47] and also because the straightforward conversion of the nitro functionality to the amino or carbonyl group gives access to a large variety of building-blocks, exploitable for the synthesis of target molecules.[48]

6.1. Preparation of α,β-unsaturated nitroalkenes

The most common method for the synthesis of conjugated nitroalkenes involves a two-step procedure: (i) an aldol-type reaction of a monosubstituted nitromethane with an aldehyde or a ketone (Henry's Reaction) and (ii) a dehydration reaction of the β-nitroalcohol adduct (Scheme 15).

The nitroaldol reaction is usually performed in organic media in the presence of a base.[49] The basicity of the reaction medium must be controlled to avoid aldol and Cannizzaro reactions.[49a] These side-reactions have been suppressed by carrying out the Henry's reaction in aqueous NaOH in the presence of cetyltrimetylammonium chloride (CTACl); the β-nitroalcohol was the sole reaction product.[50]

The dehydration step has been carried out in organic solvents, sometimes at a high temperature in the presence of dicyclo-hexylcarbodiimide,[51] methansulfonyl chloride,[52] pivaloyl chloride,[53] phtalic anhydride,[54] basic alumina,[55] triphenylphosphine,[56] ammonium acetate–acetic acid[57] or amines.[57a,58]

By a one-pot procedure, (*E*)-1-cyano-1-arylnitroethenes were prepared, in high yields at room temperature by reaction of arylaldehydes with nitroacetonitrile **41** in heterogeneous aqueous medium (Table 13).[59] The intermediate

Table 13 One-pot synthesis of (*E*)-1-cyano-1-arylnitroalkenes in water

Ar	Yield (%)[a]
Ph	90
p-ClC$_6$H$_4$	95
p-OMeC$_6$H$_4$	89
m-OMeC$_6$H$_4$	93
o-OMeC$_6$H$_4$	91
p-OHC$_6$H$_4$	94
p-MeC$_6$H$_4$	90
m-MeSC$_6$H$_4$	90
3,4-(OCH$_2$O)C$_6$H$_3$	90
2-Furyl	93
2-Thienyl	88

[a] Yield of isolated pure product

R = H (**a**), 6-OH (**b**), 7-OH (**c**), 8-OH (**d**), 6-Cl (**e**), 6,7-(OH)$_2$ (**f**), 6-OMe (**g**), 7-OMe (**h**), 8-*t*-Bu (**i**), 7-Et$_2$N (**j**), 6,7-(CH=CH)$_2$ (**k**)
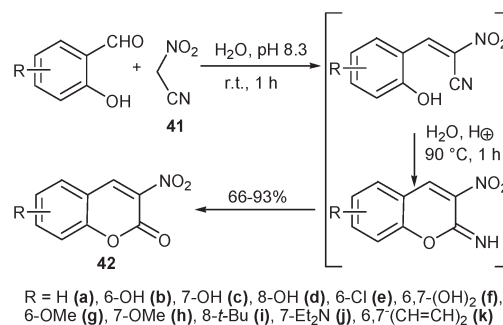
Scheme 16 Synthesis of 3-nitrocoumarins **42**.

β-nitroalcohols were not observed and the reactions were highly diastereoselective giving only *E* diastereoisomers as products. The process does not require the use of a catalyst or an organic solvent and the α-cyano-β-arylnitroethenes were isolated in practically pure form by simple Büchner filtration of the final aqueous mixture. The aqueous phase was recovered and re-used in four subsequent runs in which excellent yields were always obtained.

3-Substituted coumarins are of prominent importance among natural and synthetic coumarins because of their range of activities.[60] In the course of a wide study on the synthesis of 3-substituted coumarins in aqueous medium,[61] the 3-nitrocoumarins **42** were prepared by a one-pot procedure in water by a Knoevenagel reaction of *o*-hydroxybenzaldehyde with nitroacetonitrile followed by intramolecular Pinner reaction and hydrolysis of imidate derivative (Scheme 16).

The condensation step that produces the intermediate *o*-hydroxybenzylidene derivative was carried out at pH 8.3 and room temperature, while the Pinner and the hydrolysis reactions require acidic conditions and heating. The 3-nitro-coumarin **42a** was isolated in pure form by simple filtration of the aqueous mixture with 66% overall yield. The preparation of **42a** was also carried out in ethanol to evaluate the effect of the aqueous medium. The process is slower in ethanolic homogenous medium than in heterogeneous aqueous medium: after 2 h only 35% of 3-nitrocoumarin **42a** was produced. A practical one-pot preparation of conjugated nitroalkenes from alkenes in aqueous-organic media (ethyl acetate–water and diethyl ether–water 7.5 : 1) using sodium nitrite and iodine in the presence of ethylene glycol, was reported by Jew *et al.* (Table 14).[12,62]

The procedure is efficient and does not involve treatment with a base. In the absence of glycol, iodohydrins were obtained as the main products. It was suggested that the nitroalkenes were generated *via* iodonitroalkanes. The glycol strongly interacts with water, which is nearly saturated with sodium nitrite, thereby inhibiting the generation of hypoiodous acid and accelerating that of nitryl iodide.

6.2. α,β-unsaturated nitroalkenes as 4π or 2π components

Conjugated nitroalkenes are used as 4π or 2π components in [4 + 2] cycloadditions and as Michael acceptors for the addition of carbon nucleophiles such as enamines and enolates.[48,49,54,63,64] Processes carried out in aqueous medium

Table 14 One-pot synthesis of conjugated nitroethenes in organic-aqueous medium

Alkene	Medium	t h	Product	Yield (%)
cyclohexene	EtOAc–H$_2$O	96	cyclohexenyl-NO$_2$	72
1-phenylcyclohexene	EtOAc–H$_2$O	72	Ph/NO$_2$ product	49
styrene	EtOAc–H$_2$O	48	PhCH=CH-NO$_2$	81
	Et$_2$O–H$_2$O	48		79
benzyl acrylate	Et$_2$O–H$_2$O	72	benzyl 3-nitroacrylate	82
dihydronaphthalene	EtOAc–H$_2$O	48	2-nitro-dihydronaphthalene	78

that meet the green chemistry philosophy have recently appeared.

Cyclic six-membered nitronates are interesting synthetic intermediates that can be easily prepared by a [4 + 2] cycloaddition reaction of conjugated nitroalkenes with electron-rich alkenes.[48d,63b,65,66] The reactions are usually carried out in CH$_2$Cl$_2$, PhMe, and PhH, at −78 °C and in the presence of a Lewis acid such as TiCl$_4$, TiBr$_3$(O-i-Pr), SnCl$_4$, MAD, MAPh and ATPh.[63,64a,b] Without a catalyst, the reactions require a large excess of dienophile,[64b,67] long reaction times or the use of activated nitroalkenes.[68] In some cases, the use of high pressure conditions allows some of these difficulties to be overcome.[69]

It was discovered that the aqueous medium strongly favors the reactivity and selectivity of [4 + 2] cycloadditions of nitroalkenes working either as 4π or 2π components.[65,70,71] The cycloaddition reactions of (E)-2-aryl-1-cyano-1-nitro-alkenes **43** with ethyl vinyl ether **44** (Scheme 17, Table 15) occur rapidly in heterogeneous aqueous medium and are totally regio- and $endo$-selective.[70] The $trans$ nitronates **46**, which, in principle, can be originated from exo-type additions, in our opinion, are the result of the epimerization at C-6 of the kinetically favored cis-$endo$ adducts **45**. The $endo$ diasteroselectivity of the reaction is justified on the basis of strong secondary orbital interactions between the oxygen of the electron-rich vinyl ether **44** and the positively-charged nitrogen atom of nitroalkenes **43** which are present in the $endo$ transition state and absent in the exo-mode orientation.

The asymmetric cycloadditions of **43** in pure water were explored by using enantiopure vinyl ethers (+)-**47x**, (+)-**47y** and (−)-**47z**. The results are illustrated in Table 16. Excellent results were obtained by using ethyl vinyl ether (−)-**47z** derived
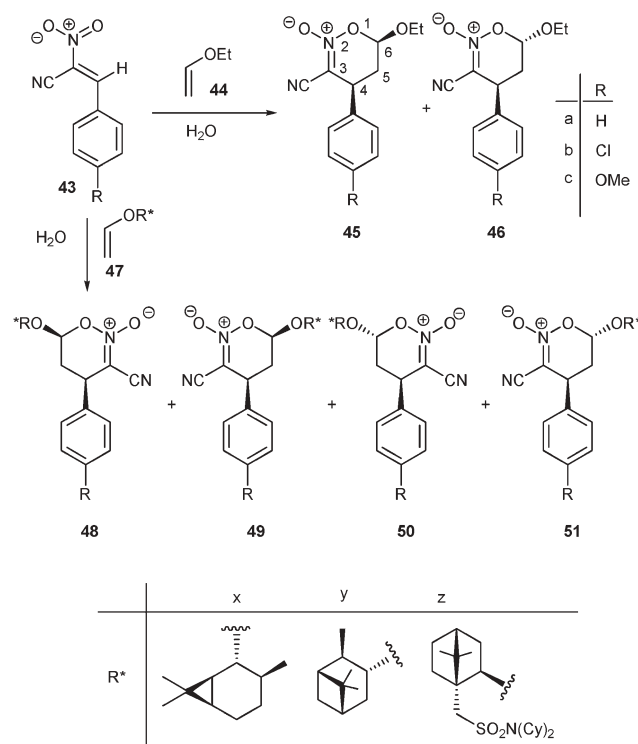
Scheme 17 Cycloaddition reactions of (E)-2-aryl-1-cyano-1-nitro-alkenes **43** with vinyl ethers **44** and **47**.

from (−)-N,N-dicyclohexyl-(1S)-isoborneol-10-sulfonamide. Only optically active **48** and **50** cycloadducts were obtained which reflects a 100% asymmetric generation of 4R diastero-isomers. The facial selectivity in the cycloadditions of nitroalkenes **43** with optically active vinyl ethers **47** are dictated by the shape of the chiral auxiliary, as well as by the s-cis or s-$trans$ reactive conformation of vinyl ether.

Cycloaddition reaction between 3-nitrocoumarin **42a** and ethyl vinyl ether **44** in water at 20 °C and pH 8.3 gives the nitrochromanols **54** and **55** in a 56 : 44 ratio with 56% of overall yield (Scheme 18).[65]

The reaction proceeds through the $endo$ selective formation of nitronate **52** (Scheme 18) which promptly hydrolyzes to give

Table 15 [4 + 2] cycloadditions of nitroalkenes **42** with ethyl vinyl ether **43** in water

Nitroalkene	T/°C	t/min	**45** (%)	**46** (%)	Yield (%)
43a	0	3	80	20	75
43b	0	20	96	4	90
43c	r.t.	10	98	2	85

Table 16 [4 + 2] cycloadditions of nitroalkenes **43** with vinyl ethers **47** in water

Reactants	T/°C	t/min	**48/49/50/51**[a]	$endo/exo$	d.e. (4R) (%)
43b + **47x**	0	30	54/35/5/6	89 : 11	18
43b + **47y**	0	30	60/30/5/5	90 : 10	30
43a + **47z**	r.t.	60	85/—/15/—	85 : 15	100
43b + **47z**	0	60	85/—/15/—	85 : 15	100
43c + **47z**	r.t.	60	83/—/17/—	83 : 17	100

[a] Percentage of the corresponding product
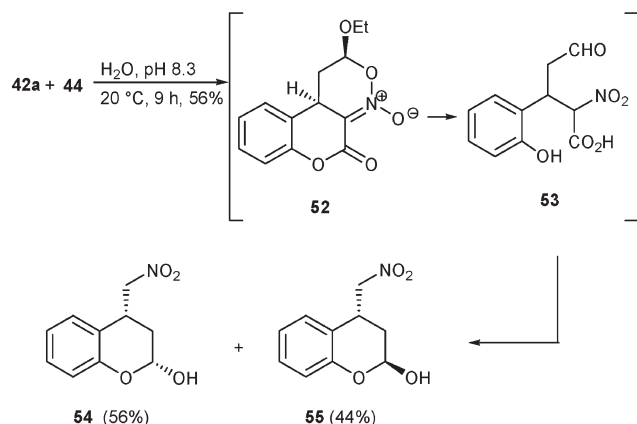
Scheme 18 Cycloaddition of 3-nitrocoumarin **42a** and ethyl vinyl ether **44** in water.

53; decarboxylation and intramolecular hemiacetalation of this intermediate gives the final products **54** and **55**.

By using dihydrofuran **56** and dihydropyran **57**, tetrahydro-furobenzopyrans **60** and **62**, and tetrahydropiranobenzopyrans **61** and **63** were obtained, respectively (Scheme 19).

If the nitronates **58** and **59** are generated under solvent-free conditions and the hydrolysis and subsequent reactions are performed by adding water *in situ*, the process allows only the *cis–cis* adducts **60** and **61**. By using this one-pot procedure, a number of tetrahydrofurobenzopyrans **64** can be prepared (Scheme 20).

A Knoevenagel–[4 + 2] cycloaddition domino process, involving an intramolecular formation of a cyclic nitronate, was performed in water at room temperature between the allyloxybenzaldehyde **65** and nitroacetonitrile **41** (Scheme 21).[59] The intermediate nitroalkene **66** immediately gives the nitronates **67** and **68** in a 16 : 1 ratio by an *endo* and an *exo* intramolecular inverse demand Diels–Alder reaction, respectively. Pure **67** was isolated in 60% overall yield and the aqueous phase was re-used for four subsequent runs with excellent results.

3-Nitrocoumarin **42a** behaves like a 2π component in the cycloadditions performed in water with 2,3-dimethyl-1,3-butadiene **69**, isoprene **70**, (*E*)-piperylene **71** and cyclopentadiene **73** (Scheme 22, Table 17).[72] The reactions occur in the
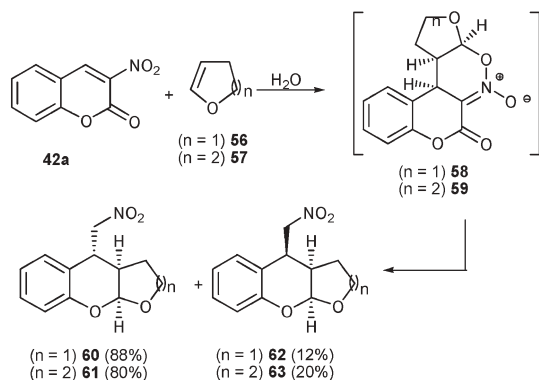
Scheme 19 Cycloaddition of 3-nitrocoumarin **42a** and dihydrofuran **56** and dihydropyran **57** in water.
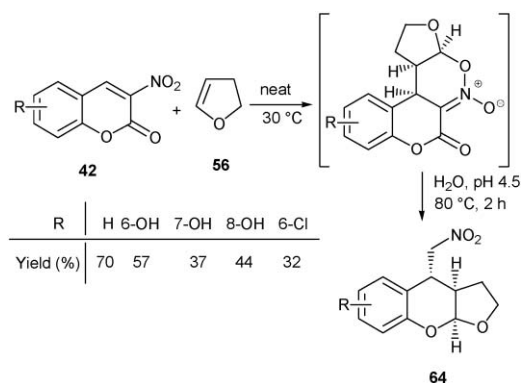
Scheme 20 Cycloaddition of 3-nitrocoumarins **42** and dihydrofuran **56** in water.
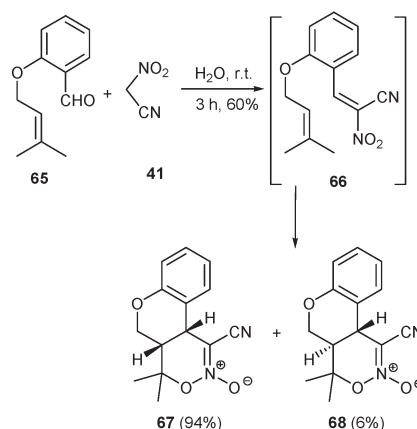
Scheme 21 A Knoevenagel–[4 + 2] cycloaddition domino process.
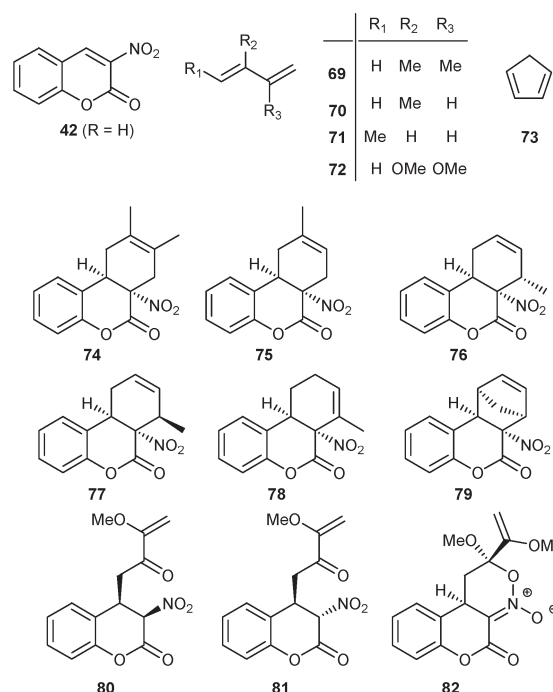
Scheme 22 [4 + 2] Cycloadditions in water of 3-nitrocoumarin **42a** with dienes **69–73**.

Table 17 [4 + 2] Cycloadditions in water of 3-nitrocoumarin **42a** with dienes **69–73**

Reactants	$T/°C$	t/h	Products (%)	Yield (%)[a]
42a + 69	90	3	**74** (100)	90
42a + 70	90	3	**75** (100)	86
42a + 71	90	3	**76** (71); **77** (23); **78** (6)	90
42a + 72	20	1	**80** (85); **81** (15)	85
42a + 73	30	3	**79** (100)	95

[a] Overall yield

Table 18 [4 + 2] Cycloadditions in water of 3-nitrocoumarin **42a** with (*E*)-piperylene **71** at 90 °C

Catalyst	t/h	76/77 (*exo/endo*)	Yield (%)
none	3	75 : 25	90
Sc(OTf)$_3$	1	80 : 20	85
Yb(OTf)$_3$	3	75 : 25	89
InCl$_3$	2	75 : 25	88

heterogeneous phase and are faster than those executed in toluene. *Exo* adducts were preferentially produced and this can be explained on the basis of the NO$_2$ group secondary orbital interactions that increase the stabilization of the *exo* transition state. The use of Lewis acids slightly accelerates the cycloaddition of **42** (R = H) with **71** and does not affect the *exo/endo* diastereoselectivity or the reaction yield (Table 18).[49e]

Surprisingly 3-nitrocoumarin **42a** behaves as 4π component in the cycloaddition with 2,3-dimethoxy-1,3-butadiene **72**. In aqueous NaHCO$_3$ and in the presence of 0.2 mol per eq. of sodium lauryl sulfate (SLS), the reaction is very fast at 20 °C, and an 85% yield of the nitrochromanones **80** and **81** in an 85 : 15 ratio were obtained (Table 17 and Scheme 22).[67] SLS has the sole effect of accelerating the reaction and the nitrochromanones **80** and **81** come from the hydrolysis of nitronate **82**. The cycloadducts **74–77** were converted by a one-pot procedure to dihydro[*b,d*]furans **83–85** (Scheme 23 and 24) under basic conditions followed by Nef and cyclization reactions at 0 °C in acidic medium. The processes are highly selective and the overall yields are good considering that they involve three main consecutive reactions.

Conjugated nitroalkenes were converted to ketones by the NaBH$_4$–H$_2$O$_2$ system in aqueous methanol.[73] The reaction occurs at room temperature and is chemoselective with respect to C=C double bond, ketal, ester and aromatic nitro group (Table 19).
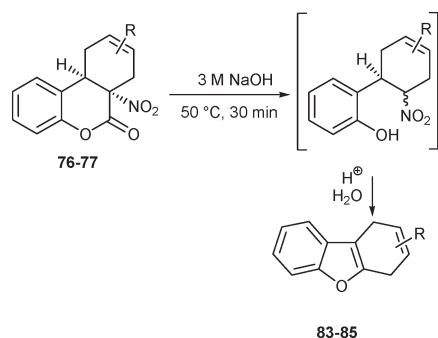
Scheme 23 One-pot synthesis of dihydro[*b,d*]furans **83–85**.
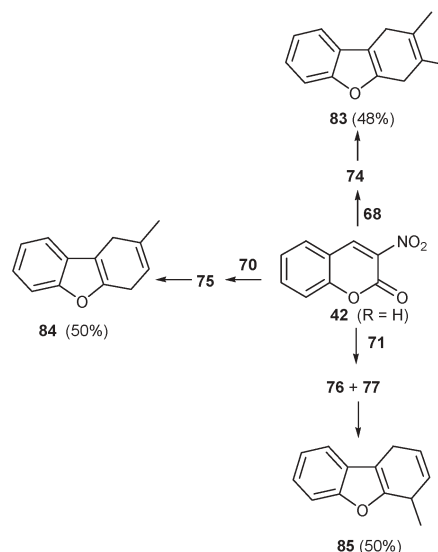
Scheme 24 One-pot synthesis of dihydro[*b,d*]furans **83–85**.

Brazilian researchers[72] found that thiophenol reacts with (*E*)-1-methyl-1-nitrostyrene in aqueous medium at room temperature to give prevalently the *syn*-α-nitrosulfide in 85% yield (Table 20). *Anti* products are prevalent when the protocol that uses thiolates followed by protonation with acetic acid at −78 °C in THF as solvent is applied,[73] contrary to what happens with the traditional method using triethylamine as base and acetonitrile as solvent.[74] With cyclic nitroalkenes the

Table 19 Chemoselective conversion of conjugated nitroalkenes to ketones in aqueous medium

R	R$_1$	Yield (%)
CH=CH(CH$_2$)$_2$	Me(CH$_2$)$_3$	58
MeCH$_2$CH=(CH$_2$)$_2$	Me(CH$_2$)$_2$	70
–(CH$_2$)$_4$–		73
–(CH$_2$)$_{13}$–		80
Ph(CH$_2$)$_2$	MeC(OCH$_2$)$_2$CH$_2$	48
Cy	Me(CH$_2$)$_3$	69
p-NO$_2$C$_6$H$_4$	Me	53
p-PhC$_6$H$_4$	Me	50
Me(CH$_2$)$_8$	Me(CH$_2$)$_3$	56
Me(CH$_2$)$_9$	(CH$_2$)$_2$CO$_2$Me	70
Me(CH$_2$)$_5$	(CH$_2$)$_2$CO$_2$Me	68
Ph(CH$_2$)$_2$	(CH$_2$)$_2$CO$_2$Me	60

Table 20 Thia-Michael addition of thiophenol to (*E*)-1-methyl-1-nitrostyrene

Reaction Conditions	$T/°C$	t/min	*anti/syn*	Yield (%)
H$_2$O, Na$_2$CO$_3$ (pH 10)	r.t.	30	69 : 31	85
THF, AcOH, BuLi	r.t. to −78	120	75 : 25	70
MeCN, Et$_3$N	r.t.	60	34 : 66	90
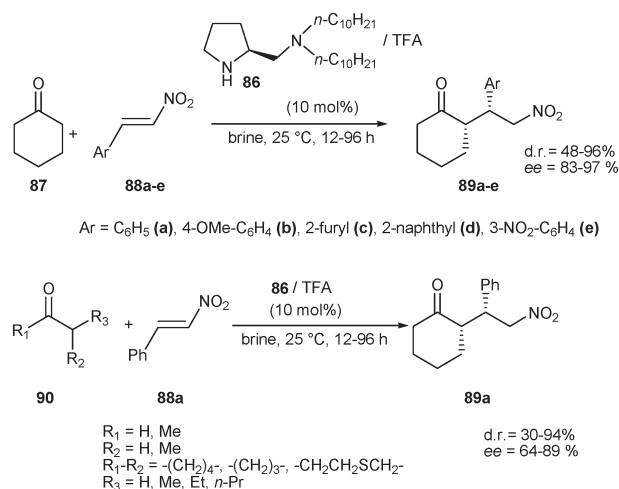
Scheme 25 Organocatalytic Michael addition of ketones and aldehydes to β-nitrostyrenes.

addition of thiophenol is more diastereoselective; the 1-nitro-cyclohexene gives exclusively the *cis*-1-nitro-2-(phenylthio)-cyclohexane.

Recently, Takabe *et al.* reported the organocatalytic Michael addition of ketones or aldehydes to β-nitrostyrenes in NaCl-saturated water (brine) (Scheme 25).[75]

Various pyrrolidine-based catalysts were tested and the best results in terms of yields and stereoselectivity of the process were obtained by using the diamine **86**/TFA bifunctional catalytic system.

Brine proved to be a more efficient reaction medium than water or DMSO. The transformation proceeds with the formation of an enamine species, for instance formed between ketone **87** and diamine catalyst **86**. The water-elimination step, which allows the formation of the active enamine intermediate, is promoted by the aggregation of the organic reactants and the hydrophobic diamine **86** which tend to exclude water from the organic phase. In brine, this is further promoted by salting out effects.

A remarkable effect of water on the reaction rate of the Ag(I)/PPh₃-catalyzed Michael additions of β-ketoesters to nitroalkenes has been recently reported by Kobayashi *et al.* The reaction of β-ketoester **91** and β-nitrostyrene **88a** has been reported in Scheme 26 as an example.[76]

The use of an optically active phosphine allowed the preparation of the major diastereoisomer of **92** in 78% *ee*.

solvent	Isolated Yield of **92** (%)
CH₂Cl₂	9
THF	3
THF-H₂O	10
Solvent-free	5
H₂O	90
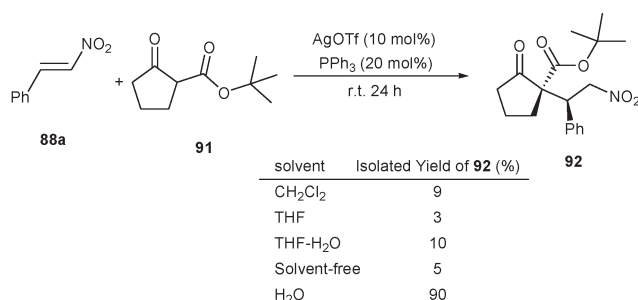
Scheme 26 Effect of solvent in the Ag(I)-catalyzed Micahel addition of β-keto ester **91** to β-nitrostyrene **88a**.

7. Conclusion

Aliphatic nitrocompounds and aqueous medium have demonstrated to be a very useful green alliance by which many synthetic opportunities are offered, including the possibility to perform, in a one-pot way, under mild and safety conditions, the preparations of important targets under eco-friendly conditions. In fact, the reactions are usually performed using cheap chemicals, avoiding the need of toxic solvents and/or severe reaction conditions.

Although this promising marriage between nitro derivatives and aqueous medium represents a pioneering field of research on organic synthesis, we hope that this account will provide an incentive for further studies in this area.

References

1 (*a*) D. C. Rideout and R. Breslow, *J. Am. Chem. Soc.*, 1980, **102**, 7816–7817; (*b*) R. Breslow, U. Maitra and D. Rideout, *Tetrahedron Lett.*, 1983, **24**, 1901–1904.
2 (*a*) O. Diels and K. Alder, *Ann. Chem.*, 1931, **490**, 243–257; (*b*) W. B. Woodward and H. Baer, *J. Am. Chem. Soc.*, 1948, **70**, 1161–1166; (*c*) B. A. Carlson, W. A. Sheppard and O. W. Webster, *J. Am. Chem. Soc.*, 1975, **97**, 5291–5293.
3 (*a*) *Aqueous-Phase Organometallic Catalysis*, ed. B. Cornils and W. A: Hermann, Wiley-VCH, Weinheim, Germany, 1998; (*b*) C. J. Li and T. H. Chang, *Organic Reactions in Aqueous Media*, Wiley, New York, 1997; (*c*) *Organic Synthesis in Water*, ed. P. A. Grieco, Blackie Academic and Professional, London, 1998; (*d*) S. Kobayashi and K. Manabe, *Pure Appl. Chem.*, 2000, **72**, 1373–1382; (*e*) F. Fringuelli, O. Piermatti, F. Pizzo and L. Vaccaro, *Eur. J. Org. Chem.*, 2001, **66**, 439–455; (*f*) Various authors, *Acc. Chem. Res.*, 2002, **35**, (9), whole issue; (*g*) H. Shinokubo and K. Oshima, *Synlett*, 2002, 674–686; (*h*) U. M. Lindström, *Chem. Rev.*, 2002, **102**, 2751–2772; (*i*) S. Kobayashi and K. Manabe, *Chem.–Eur. J.*, 2002, **8**, 4095–4102; (*j*) D. Sinou, *Adv. Synth. Catal.*, 2002, **344**, 221–237; (*k*) L. A. Paquette, *Synthesis*, 2003, 765–774; (*l*) F. Fringuelli, O. Piermatti, F. Pizzo and L. Vaccaro, *Curr. Org. Chem.*, 2003, **7**, 1661–1689; (*m*) C. J. Li, *Chem. Rev.*, 2005, **105**, 3095–3165; (*n*) *Organic Reactions in Water*, ed. U. M. Lindström, Blackwell, Oxford, UK, 2007.
4 (*a*) F. Fringuelli, F. Pizzo, O. Piermatti and L. Vaccaro, *J. Org. Chem.*, 1999, **64**, 6094–6096; (*b*) F. Fringuelli, F. Pizzo and L. Vaccaro, *J. Org. Chem.*, 2001, **66**, 3554–3558; (*c*) F. Fringuelli, F. Pizzo and L. Vaccaro, *J. Org. Chem.*, 2001, **66**, 4463–4467; (*d*) F. Fringuelli, F. Pizzo, S. Tortoioli and L. Vaccaro, *Adv. Synth. Catal.*, 2002, **344**, 379–384; (*e*) D. Amantini, F. Fringuelli, F. Pizzo and L. Vaccaro, *Org. Prep. Proced. Int.*, 2002, **34**, 111–147; (*f*) D. Amantini, F. Fringuelli, O. Piermatti, F. Pizzo, S. Tortoioli and L. Vaccaro, *Arkivoc*, 2002, 293–311; (*g*) D. Amantini, F. Fringuelli, F. Pizzo, S. Tortoioli and L. Vaccaro, *Synlett*, 2003, 2292–2296; (*h*) F. Fringuelli, M. Matteucci, O. Piermatti, F. Pizzo and M. G. Burla, *J. Org. Chem.*, 2001, **67**, 4661–4666; (*i*) F. Fringuelli, F. Fioroni, F. Pizzo and L. Vaccaro, *Green Chem.*, 2003, **5**, 425–428; (*j*) F. Fringuelli, F. Pizzo, S. Tortoioli and L. Vaccaro, *Green Chem.*, 2003, **5**, 436–440; (*k*) F. Fringuelli, O. Piermatti and F. Pizzo, *Synthesis*, 2003, 2331–2334; (*l*) F. Fringuelli, F. Pizzo, M. Rucci and L. Vaccaro, *J. Org. Chem.*, 2003, **68**, 7041–7045; (*m*) D. Amantini, F. Fringuelli, O. Piermatti, F. Pizzo and

L. Vaccaro, in *Green Chemistry: Environment Friendly Alternatives*, Narosa Publishing, New Delhi, 2003, 293–311; (*n*) F. Fringuelli, O. Piermatti and F. Pizzo, *J. Chem. Educ.*, 2004, **81**, 874; (*o*) F. Fringuelli, F. Pizzo and L. Vaccaro, *J. Org. Chem.*, 2004, **69**, 2315–2321; (*p*) F. Fringuelli, F. Pizzo, S. Tortoioli and L. Vaccaro, *Org. Lett.*, 2005, **7**, 4411–4414.

5 (*a*) F. Fringuelli, F. Pizzo and L. Vaccaro, *J. Org. Chem.*, 2001, **66**, 4719–4722; (*b*) F. Fringuelli, F. Pizzo and L. Vaccaro, *Tetrahedron Lett.*, 2001, **42**, 1131–1134; (*c*) F. Fringuelli, F. Pizzo, S. Tortoioli and L. Vaccaro, *J. Org. Chem.*, 2003, **68**, 8248–8251.

6 R. Ballini, in *Studies in Natural Products Chemistry*, ed. Atta-ur-Rahman, Elsevier, Amsterdam, 1997, **19**, 117–184.

7 (*a*) D. Seebach, E. W. Colvin, F. Lehr and T. Weller, *Chimia*, 1979, **33**, 1–18; (*b*) G. Rosini and R. Ballini, *Synthesis*, 1988, 833–847; (*c*) G. Rosini, R. Ballini, M. Petrini, E. Marotta and P. Righi, *Org. Prep. Proced. Int.*, 1990, **22**, 707–746; (*d*) N. Ono, *The Nitro Group in Organic Synthesis*, Wiley-VCH, New York, 2001; (*e*) R. Ballini and M. Petrini, *Tetrahedron*, 2004, **60**, 1017–1047.

8 (*a*) *The Chemistry of Amino, Nitroso, Nitro and Related Groups*, ed. S. Patai, Wiley, Chichester, 1996; (*b*) J. P. Adams, *J. Chem. Soc., Perkin Trans. 1*, 2002, 2586–2597.

9 (*a*) G. Rosini, in *Comprehensive Organic Synthesis*; B. M. Trost, ed. Pergamon, Oxford, 1991, vol. 2, 321–340; (*b*) F. A. Luzzio, *Tetrahedron*, 2001, **57**, 915–945.

10 R. Ballini, G. Bosica, D. Fiorini, A. Palmieri and M. Petrini, *Chem. Rev.*, 2005, **105**, 933–971.

11 V. V. Perekalin, E. S. Lipina, V. M. Berestovitaskaya and D. A. Efremov, *Nitroalkenes Conjugated Nitro Compounds*, Wiley, Chichester, 1994.

12 S. E. Denmark and A. Thorarensen, *Chem. Rev.*, 1996, **96**, 137–166.

13 (*a*) N. Kornblum, *Org. React.*, 1962, **12**, 101–156; (*b*) H. Feuer and G. Leston, *Organic Syntheses*, Wiley, New York, 1963, vol. 4, 368.

14 (*a*) G. Rosini, R. Ballini, M. Petrini and P. Sorrenti, *Synthesis*, 1985, 515–517; (*b*) B. P. Bandgar, M. B. Zirange and P. P. Wadgaonkar, *Synlett*, 1996, 149–150.

15 F. Fringuelli, G. Pani, O. Piermatti and F. Pizzo, *Tetrahedron*, 1994, **50**, 11499–11508.

16 R. Ballini and G. Bosica, *J. Org. Chem.*, 1997, **62**, 425–427.

17 R. Ballini, D. Fiorini, M. V. Gil and A. Palmieri, *Tetrahedron*, 2004, **60**, 2799–2804.

18 (*a*) R. Ballini, *Synlett*, 1999, 1009–1018; (*b*) R. Ballini, G. Bosica, D. Fiorini and A. Palmieri, *Tetrahedron*, 2005, **61**, 8971–8993.

19 R. Ballini, L. Barboni and L. Pintucci, *Synlett*, 1997, 1389–1390.

20 (*a*) D. J. Ager, I. Prakash and D. R. Schaad, *Chem. Rev.*, 1996, **96**, 835–876; (*b*) T. E. Gunta and F. Sztaricskai, *Tetrahedron*, 1997, **53**, 7985–7998.

21 M. Rieger, *Cosmet. Toiletries*, 1992, **107**, 85–94.

22 P. Perlmutter, *Conjugate Addition Reactions in Organic Synthesis*, Pergamon, Oxford, 1992.

23 A. Lubineau and J. Augé, *Tetrahedron Lett.*, 1992, **33**, 8073–8074.

24 R. Ballini and G. Bosica, *Tetrahedron Lett.*, 1996, **37**, 8027–8030.

25 N. Ono, A. Kamimura and A. Kaji, *Synthesis*, 1984, 226–227.

26 (*a*) G. P. Pollini, A. Barco and G. DeGiuli, *Synthesis*, 1972, 44–45; (*b*) D. W. Chasar, *Synthesis*, 1982, 841–842; (*c*) R. Andruszkiewicz and R. B. Silverman, *Synthesis*, 1989, 953–955.

27 D. E. Bergbreiter and J. J. Lalonde, *J. Org. Chem.*, 1997, **52**, 1601–1603.

28 B. Jouglet, L. Blanco and G. Rousseau, *Synlett*, 1991, 907–908.

29 R. Ballini and G. Bosica, *Eur. J. Org. Chem.*, 1998, 355–357.

30 M. T. Shipchandler, *Synthesis*, 1979, 666.

31 E. Keller and B. L. Feringa, *Synlett*, 1997, 842–844.

32 (*a*) R. C. Cookson and P. S. Ray, *Tetrahedron Lett.*, 1982, **23**, 3521–3524; (*b*) A. Yurdakul, C. Gurtner, E.-S. Jung, A. Lorenzi-Riatsch, A. Linden, A. Guggisberg, S. Bienz and M. Hesse, *Helv. Chim. Acta*, 1998, **81**, 1373–1392; (*c*) R. Ballini, L. Barboni, G. Bosica and D. Fiorini, *Synthesis*, 2002, 2725–2728.

33 S. Mirando, P. Lopez-Alvarado, G. Giorgi, J. Rodriguez, C. Avendaño and J. C. Menéndez, *Synlett*, 2003, 2159–2162.

34 (*a*) A. Fontana, P. De Maria, G. Siani, M. Pierini, S. Cerritelli and R. Ballini, *Eur. J. Org. Chem.*, 2000, 1641–1646; (*b*) F. Gasparrini, M. Pierini, C. Villani, P. De Maria, A. Fontana and R. Ballini, *J. Org. Chem.*, 2003, **68**, 3173–3177.

35 R. Ballini, D. Fiorini, A. Palmieri and M. Petrini, *Lett. Org. Chem.*, 2004, **1**, 335–339.

36 R. Ballini, L. Barboni, G. Bosica, P. Filippone and S. Peretti, *Tetrahedron*, 2000, **56**, 4095–4099.

37 R. Ballini, L. Barboni and Giovanna Bosica, *J. Org. Chem.*, 2000, **65**, 6261–6263.

38 R. Ballini, L. Barboni and G. Giarlo, *J. Org. Chem.*, 2003, **68**, 9173–9176.

39 (*a*) R. Ballini, D. Fiorini, M. V. Gil, A. Palmieri, E. Román and J. A. Serrano, *Tetrahedron Lett.*, 2003, **44**, 2795–2797; (*b*) E. G. Occhiato, A. Guarna, F. De Sarlo and D. Scarpi, *Tetrahedron: Asymmetry*, 1995, **6**, 2971–2976.

40 (*a*) H. Yoda, M. Mizutani and K. Takabe, *Heterocycles*, 1998, **48**, 679–686; (*b*) E. J. Corey and X.-M. Cheng, *The Logic of Chemical Synthesis*, John Wiley and Sons, New York, 1989; (*c*) Z. G. Hajois, M. P. Wachter, H. M. Werblood and R. E. Adams, *J. Org. Chem.*, 1984, **49**, 2600–2608; (*d*) J. Y. Lee and B. H. Kim, *Tetrahedron*, 1996, **52**, 571–588.

41 R. Ballini and M. Petrini, *Synthesis*, 1986, 1024–1026.

42 (*a*) R. A. Hellison, *Synthesis*, 1973, 397–412; (*b*) T. L. Ho, *Synth. Commun.*, 1974, **4**, 265–287.

43 *Comprehensive Organic Functional Group Transformations*, ed. A. R. Katritzky, O. Meth-Cohn and C. V. Rees, Pergamon Press, Oxford, 1995, vol. 6.

44 Y. Liang, D. Dong, Y. Lu, W. Pan, Y. Chai and Q. Liu, *Synthesis*, 2006, DOI: 10.1055/s-2006-950227.

45 R. Ballini, F. Papa and C. Abate, *Eur. J. Org. Chem.*, 1999, 87–90.

46 G. Giorgi, S. Mirando, P. Lopéz-Alvarado, C. Avendaño, J. Rodriguez and J. C. Menéndez, *Org. Lett.*, 2005, **7**, 2197–2200.

47 (*a*) K.-Y. Zee-Cheng and C.-C. Cheng, *J. Med. Chem.*, 1969, **11**, 1107–1108; (*b*) N. Latif, F. M. Asaad and H. Hosni, *Liebigs Ann. Chem.*, 1987, 495–498; (*c*) A. Ramos, A. Vizoso, A. Edreira, J. Betancourt and M. Decalo, *Mutat. Res.*, 1997, **390**, 233–238.

48 (*a*) A. G. M. Barrett and G. G. Graboski, *Chem. Rev.*, 1986, **86**, 751–762; (*b*) *The Chemistry of Nitro and Nitroso Groups, Part 1 and 2*, ed. S. Patai, Wiley Interscience, New York, 1969/70; (*c*) J. Ji, D. M. Barnes, J. Zhang, S. A. King, S. J. Witterberg and H. E. Morton, *J. Am. Chem. Soc.*, 1999, **121**, 10215–10216; (*d*) D. Seebach, I. M. Lypkalo and R. Dahinden, *Helv. Chim. Acta*, 1999, **82**, 1829–1842; (*e*) N. Ono, *The Nitro Group in Organic Synthesis*, Wiley-VCH, New York, 2001.

49 (*a*) D. Seebach, A. K. Beck, T. Mukhopadhyay and E. Thomas, *Helv. Chim. Acta*, 1982, **65**, 1101–1133; (*b*) A. G. M. Barrett, *Chem. Soc. Rev.*, 1991, **20**, 95–127; (*c*) G. W. Kabalka and R. S. Varma, *Org. Prep. Proced. Int.*, 1987, **19**, 283–328.

50 R. Ballini and G. Bosica, *J. Org. Chem.*, 1997, **62**, 425–427.

51 P. Knochel and D. Seebach, *Synthesis*, 1982, 1017–1018.

52 (*a*) J. Melton and J. E. McMurry, *J. Org. Chem.*, 1975, **49**, 2138–2139; (*b*) M. Miyashita, R. Yamaguchi and A. Yoshikoshi, *Chem. Lett.*, 1982, 1505–1508.

53 (*a*) P. Knochel and D. Seebach, *Tetrahedron Lett.*, 1982, **23**, 3897–3900; (*b*) D. Seebach and P. Knochel, *Helv. Chim. Acta*, 1984, **67**, 261–283.

54 (*a*) G. D. Buckley and C. W. Scaife, *J. Chem. Soc.*, 1947, 1471–1472; (*b*) D. Ranganathan, C. B. Rao, S. Ranganathan, A. K. Mehrotra and R. Iyengar, *J. Org. Chem.*, 1980, **45**, 1185–1189.

55 R. Ballini, R. Castagnagni and M. Petrini, *J. Org. Chem.*, 1992, **57**, 2160–2162.

56 A. K. Saikia, N. C. Barua, R. P. Sharma and A. C. Ghosh, *Synthesis*, 1994, 685–686.

57 (*a*) C. B. Gairaud and G. R. Lappin, *J. Org. Chem.*, 1953, **18**, 1–3; (*b*) S. N. Karmarkar, S. L. Kelkar and M. S. Wadia, *Synthesis*, 1985, 510–512.

58 O. Shales and H. A. Graefe, *J. Am. Chem. Soc.*, 1952, **74**, 4486–4490.

59 D. Amantini, F. Fringuelli, O. Piermatti, F. Pizzo and L. Vaccaro, *Green Chem.*, 2001, **3**, 229–232.

60 (*a*) A. M. El-Naggar, M. H. A. El-Gamal, B. A. H. El-Tawil and F. S. M. Ahmed, *Acta Chim. Acad. Sci. Hung.*, 1976, **89**, 279–284; (*b*) R. S. Mali, S. N. Yeola and B. K. Kulkarni, *Indian J. Chem.*, 1983, **22B**, 352–354; (*c*) R. Raue, H. Harnisch and K. H. Drexhage, *Heterocycles*, 1984, **21**, 167–190.

61 (*a*) G. Brufola, F. Fringuelli, O. Piermatti and F. Pizzo, *Heterocycles*, 1996, **43**, 1257–1266; (*b*) G. D'Ambrosio, F. Fringuelli, F. Pizzo and L. Vaccaro, *Green Chem.*, 2005, **8**, 874–877.

View Online

62 S. S. Jew, H. D. Kim, Y. S. Cho and C. H. Cook, *Chem. Lett.*, 1986, 1747–1748.
63 (*a*) R. Ballini and G. Bosica, *Tetrahedron Lett.*, 1996, **37**, 8027–8030; (*b*) A. R. Martinez and G. Y. Moltrasion Iglesias, *J. Chem. Res. (S)*, 1998, **169**, S853–S859.
64 (*a*) S. E. Denmark and M. Seierstad, *J. Org. Chem.*, 1999, **64**, 1610–1619; (*b*) M. Avalos, R. Babiano, P. Cintas, F. J. Higes, J. L. Jimenez, J. C. Palacios and M. A. Silva, *J. Org. Chem.*, 1999, **64**, 1494–1502; (*c*) D. Monti, P. Gramatica, G. Speranza and P. Manitto, *Tetrahedron Lett.*, 1983, **24**, 417–418; (*d*) R. Ballini and G. Bartoli, *Synthesis*, 1993, 965–967.
65 D. Amantini, F. Fringuelli and F. Pizzo, *J. Org. Chem.*, 2002, **67**, 7238–7243.
66 (*a*) F. Felluga, P. Nitti, G. Pitacco and E. Valentin, *Tetrahedron*, 1989, **45**, 2099–2108; (*b*) S. E. Denmark and B. Herbert, *J. Org. Chem.*, 2000, **65**, 2887–2896; (*c*) S. E. Denmark and J. J. Cottell, *J. Org. Chem.*, 2001, **66**, 4276–4284.
67 A. Papchikhin, P. Agback, J. Plavec and J. Chattopadhyaya, *J. Org. Chem.*, 1993, **58**, 2874–2879.
68 (*a*) Y. Tohda, K. Tani, N. Yamawaki, M. Ariga, N. Nishiwaki, K. Kotani and E. Matsumara, *Bull. Chem. Soc. Jpn.*, 1993, **66**, 1222–1228; (*b*) Y. Tohda, N. Yamawaki, H. Matsui, T. Kawashima, M. Ariga and Y. Mori, *Bull. Chem. Soc. Jpn.*, 1988, **61**, 461–465.
69 G. Y. Kuster, F. Kalmoua, H. W. Scheeren and R. de Gelder, *Chem. Commun.*, 1999, 855–856.
70 F. Fringuelli, M. Matteucci, O. Piermatti, F. Pizzo and M. C. Burla, *J. Org. Chem.*, 2001, **66**, 4661–4667.
71 R. Ballini and G. Bosica, *Synthesis*, 1994, 723–762.
72 D. Amantini, F. Fringuelli, O. Piermatti, F. Pizzo and L. Vaccaro, *J. Org. Chem.*, 2003, **68**, 9263–9268.
73 F. M. da Silva and J. Jones, Jr., *J. Braz. Chem. Soc.*, 2001, **12**, 135–137.
74 A. Kamimura, H. Sasatani, T. Hashimoto, T. Kawai, K. Hori and N. Ono, *J. Org. Chem.*, 1990, **55**, 2437–2442.
75 N. Mase, K. Watanabe, H. Yoda, K. Takabe, F. Tanaka and C. F. Barbas, III, *J. Am. Chem. Soc.*, 2006, **128**, 4966–4967.
76 S. Shirakawa and S. Kobayashi, *Synlett*, 2006, 1410–1412.

Find a SOLUTION
… with books from the RSC

Choose from exciting textbooks, research level books or reference books in a wide range of subject areas, including:

- Biological science
- Food and nutrition
- Materials and nanoscience
- Analytical and environmental sciences
- Organic, inorganic and physical chemistry

Look out for 3 new series coming soon …

- RSC Nanoscience & Nanotechnology Series
- Issues in Toxicology
- RSC Biomolecular Sciences Series
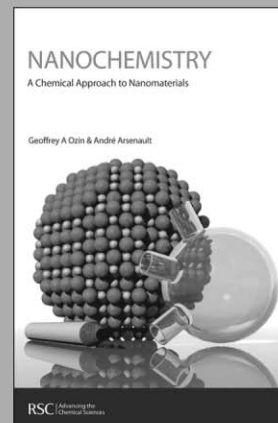
NANOCHEMISTRY
A Chemical Approach to Nanomaterials

Geoffrey A Ozin & André Arsenault

RSC | Advancing the Chemical Sciences

www.rsc.org/books

RSC | Advancing the Chemical Sciences

838 | *Green Chem.*, 2007, **9**, 823–838

This journal is © The Royal Society of Chemistry 2007

Downloaded on 21 November 2010
Published on 23 April 2007 on http://pubs.rsc.org | doi:10.1039/B702334K

The synthesis of diphenolic acid using the periodic mesoporous H₃PW₁₂O₄₀-silica composite catalysed reaction of levulinic acid†

Yihang Guo,[ab] Kexin Li[b] and James H. Clark*[a]

The green water-tolerant acid catalyst, periodic mesoporous H₃PW₁₂O₄₀/SBA-15, has been prepared by a direct sol-gel co-condensation technique. The composite is an efficient and reusable solid catalyst for the condensation of phenol with a biomass-derived platform molecule, levulinic acid, to produce the important molecule diphenolic acid.

Introduction

Condensation of phenol with levulinic acid (LA) to the polymer intermediate diphenolic acid (DPA) is a potentially important application in the light of growing interest in biomass-derived platform molecules.[1,2] Traditional catalysts for the synthesis of DPA are strong Brønsted mineral acids,[3] but they suffer from disadvantages including difficulty in separation and production of large volumes of hazardous waste.[4] In the search for more environmentally acceptable solid acid catalysts, polyoxometalates (POMs) have proved to be effective in this reaction. POMs function in a variety of reactions due to their multifunctionality (strong Brønsted acidity and appropriate redox properties).[5] However, POMs in the bulk form are of low efficiency due to low specific surface areas (1–10 m² g⁻¹), and thus only a limited number of acid sites on the external surface are available for the catalytic reactions, and separation of homogeneous POMs is a problem. Impregnation of POM onto supports by conventional post-synthesis methods gives solid POM catalysts but suffers from several drawbacks like poor control over POM loading, POM leaching, and the loss of homogeneity due to minor changes in the structure.[6] Microporous silica-included Keggin units prepared *via* a direct co-condensation sol-gel technique have been reported to be more active and more stable in catalytic tests (BET surface areas 400–800 m² g⁻¹).[7] However, the narrow pore size (*ca.* 0.6 nm) of this kind of materials has limited their suitability for the conversion of large substrates. Therefore the development of routes to solid POM catalysts with larger pores and surface areas should open up the area of POM catalysis.

Here, we demonstrate, for the first time, a route to generate a series of SBA-15 silica-based Keggin units (H₃PW₁₂O₄₀/SBA-15) by a direct sol-gel co-condensation technique combined with hydrothermal treatment in the presence of non-ionic surfactant P123 (EO₂₀PO₇₀EO₂₀, EO = ethylene oxide, PO = propylene oxide). It is challenging to prepare this kind of material successfully because two problems have to be overcome: (i) avoiding decomposition of the Keggin structure during the processes of simultaneous hydrolysis and condensation of tetraethylorthosilicate (TEOS) with H₃PW₁₂O₄₀ and template removal, as H₃PW₁₂O₄₀ begins to decompose at a pH higher than 1.5 and loses all acidic protons at 465 °C;[8] and (ii) minimizing loss of H₃PW₁₂O₄₀ during the process of template removal by extraction with boiling ethanol. In order to avoid thermal decomposition of the Keggin unit, solvent extraction is the better method to remove the non-ionic surfactant. However, the high solubility of H₃PW₁₂O₄₀ in ethanol may lead to losing most of it from the silica support. Therefore, the preparation method must be designed precisely to ensure immobilization of homogeneous H₃PW₁₂O₄₀ by strong chemical bonding with the mesoporous silica support.

Experimental

In a typical preparation of H₃PW₁₂O₄₀/SBA-15, TEOS/ethanol solution and aqueous H₃PW₁₂O₄₀ (from 0.33 to 1.0 × 10⁻⁴ mol for different loadings) solution were added dropwise into the P123/ethanol solution successively at room temperature with stirring. The molar ratio of P123 : ethanol : TEOS was 1 : 323 : 52. The acidity of the mixture was controlled at pH 1.2 ± 0.2. The clear sol obtained was subjected to hydrothermal treatment at 110 °C for 48 h at a heating ramp of 2 °C min⁻¹. The clear hydrogel formed was dehydrated slowly at 45 °C in a vacuum for 24 to 48 h until a complete gel particulate was formed. The gel particulate was further calcined at 80, 100, and 120 °C, successively, in a vacuum, and then refluxed in boiling ethanol or calcined at 420 °C. The products are represented by H₃PW₁₂O₄₀/SBA-15-C/E-*x*, where C/E refers to the catalyst obtained by calcination/extraction for P123 removal, respectively, and *x* is the H₃PW₁₂O₄₀ loading (wt%) in the composite. For comparative purpose, silica-based H₃PW₁₂O₄₀ with disordered pores (H₃PW₁₂O₄₀/SiO₂-D-*x*) was prepared following the above process in the absence of P123.

The condensation of LA with phenol to produce DPA was carried out in a sealed glass vessel at 100 °C for 8 h. A typical experiment involved a mixture of 0.0136 mol of phenol, 0.0034 mol of LA with 0.05 g of the catalyst. LA and DPA were analyzed simultaneously by an Applied Biosystem liquid chromatography–mass spectrometer equipped with an electrospray ionization source.

Results and discussion

The determined H₃PW₁₂O₄₀ loadings by inductively coupled plasma atomic emission spectrometer (ICP-AES) are as expected
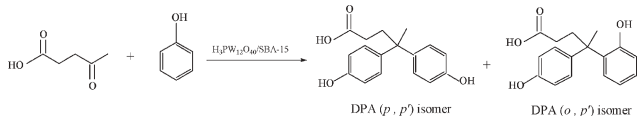
[a]*Green Chemistry Centre, Department of Chemistry, University of York, Heslington, York, UK YO10 5DD. E-mail: jhc1@york.ac.uk; Fax: 44 1904 434550; Tel: 44 1904 432559*
[b]*School of Chemistry, Northeast Normal University, Changchun, 130024, P. R. China. E-mail: guoyh@nenu.edu.cn*
† Electronic supplementary information (ESI) available: Raman spectra (Fig. S1) and XRD patterns (Fig. S2). See DOI: 10.1039/b702739g

Table 1 Surface textural properties and catalytic activity of as-prepared mesoporous $H_3PW_{12}O_{40}$/SBA-15 and reference materials[a]

Catalyst	$2\theta/°$	S_{BET}/m^2 g^{-1}	$D_P{}^b$/nm	Porosity^c	LA conversion (%)	TOF^d	$p,p'/o,p'{}^e$
$H_3PW_{12}O_{40}$/SBA-15-E-4.0	0.95	691.6	7.1	1.20	23.6	6.9	3.6
$H_3PW_{12}O_{40}$/SBA-15-E-14.8	0.92	683.0	7.4	0.95	74.8	46.4	3.0
$H_3PW_{12}O_{40}$/SBA-15-E-17.5	0.90	630.4	8.6	0.91	80.1	51.0	2.8
$H_3PW_{12}O_4$/SBA-15-C-7.5	0.95	753.0	6.0	1.10	19.2	3.5	2.1
$H_3PW_{12}O_4$/SBA-15-C-11.3	0.91	713.2	6.4	0.85	72.3	48.5	3.6
$H_3PW_{12}O_4$/SBA-15-C-15.7	0.96	604.5	6.6	0.75	80.3	53.9	2.9
$H_3PW_{12}O_{40}$/SiO$_2$-D-15.4	—	317.6	1.2	0.34	5.3	0.65	2.8
$H_3PW_{12}O_{40}$	—	5.5	—	—	60.1	1.04	2.9
HCl	—	—	—	—	65.4	0.73	2.2
SBA-15-E	0.99	858.2	5.2	0.71	0	0	—
SBA-15-C	0.96	750.1	5.3	0.51	0	0	—

[a] 0.0034 mol LA, 0.0136 mol phenol, 0.05 g catalyst, 100 °C, 8 h. The retention time for LA, DPA (p,p'), and DPA (o,p') was 1.31, 1.60, and 1.86 min, respectively. [b] Pore diameters are estimated from BJH desorption determination. [c] The porosity is estimated from the pore volume determined using the adsorption branch of the N$_2$ isotherm curve at the $P/P_0 = 0.99$ single point. [d] TOF is based on total molar quantity of the two isomers/molar quantity of active site ($H_3PW_{12}O_{40}$ or HCl). [e] Molar ratio of DPA (p,p') isomer to DPA (o,p') isomer.

(Table 1), implying that the preparation method employed can effectively inhibit the loss of the Keggin unit during the template extraction process. Structure integrity of the Keggin unit is confirmed by Raman scattering studies (Fig. S1 of ESI†). The characteristic Raman scattering peaks for pure $H_3PW_{12}O_{40}$ appear at 1009.5, 993.9 and 912.4 cm^{-1}, respectively, corresponding to stretching vibrations of P–O bonds of the PO$_4$ sites, W=O bonds, and W–O–W bonds of the Keggin unit. After formation of $H_3PW_{12}O_{40}$/SBA-15 composite these three peaks are also observed, with some shifts of the peak positions. The shifts are due to strong interactions between the Keggin unit and the silica support, which interfere with the symmetry of the Keggin unit.

The periodic mesostructure and porosity of as-prepared composites were characterized by X-ray diffraction (XRD), transmission electron microscopy (TEM), and nitrogen sorption determination. The XRD patterns (Fig. S2 of ESI†) of six $H_3PW_{12}O_{40}$/SBA-15 materials show reflection peaks of (100) in the range of 0.90–0.96° (Table 1) and two shoulder peaks of (110) and (200) at *ca.* 1.30 and 1.56°, respectively, indicating the formation of the ordered hexagonal structure of as-prepared composites.[9] The TEM results (Fig. 1) also reveal the well-distributed mesostructure
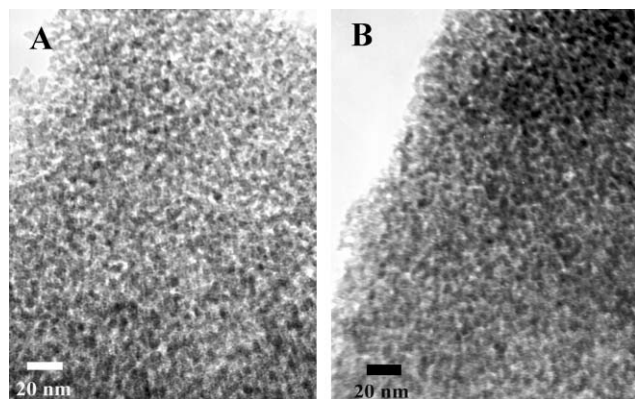
Fig. 1 TEM images of (A) $H_3PW_{12}O_{40}$/SBA-15-C-15.7 and (B) $H_3PW_{12}O_4$/SBA-15-E-17.5.

of the composites. All $H_3PW_{12}O_{40}$/SBA-15 composites showed very high porosity, larger surface area, and larger pore size, even after introduction of the Keggin unit into SBA-15 matrix (Table 1). All of the isotherms are type IV (Fig. 2) showing that the capillary condensation occurs at higher relative pressures ($P/P_0 = 0.45$–0.85), suggesting well-defined mesoporous structures and relatively narrow pore size distributions. In addition, both the extracted and calcined samples result in similar textural properties. Interestingly, the onset of this capillary condensation step occurs at increasing relative pressures with increasing $H_3PW_{12}O_{40}$ loading in the composites. This implies that the average pore size increases with increasing $H_3PW_{12}O_{40}$ loading, which has been evidenced by the result of pore size distribution (Fig. 2). In addition, the uniform pore size distribution suggests homogeneous distribution of the large Keggin unit throughout the sol-gel co-condensed materials. These fascinating textural properties of $H_3PW_{12}O_{40}$/SBA-15 materials are attractive for potential applications in acid-catalysed reactions.

The SBA-15 silica supported $H_3PW_{12}O_{40}$ catalysts were successfully tested in the solventless condensation of LA with phenol to produce DPA, and the results are summarized in Table 1. In the reactions, the two structural isomers, DPA (p,p') and DPA (o,p'), were formed with all the catalysts tested. No other products could be identified by using as-prepared $H_3PW_{12}O_{40}$/SBA-15 materials. Under the same conditions, the TOF is low using $H_3PW_{12}O_{40}$, HCl, or $H_3PW_{12}O_{40}$/SiO$_2$-D-15.4 as the catalyst. However, all six tested $H_3PW_{12}O_{40}$/SBA-15 materials exhibit significantly high activities, and the activities increase with increasing $H_3PW_{12}O_{40}$ loadings. The higher catalytic activity of $H_3PW_{12}O_{40}$/SBA-15 compared to that of $H_3PW_{12}O_{40}$/SiO$_2$-D is due to its special textural properties. The latter is disordered with very small pore size (1.2 nm), which significantly impacts the accessibility and rate of diffusion for the substrates, especially for the DPA synthesis reaction (the size of DPA is large). After the reaction, the catalyst was removed by hot filtration. The catalyst-free reaction liquor was returned to reaction conditions and monitored further, but no further conversion of LA was detected, consistent with a stable heterogeneous catalyst. Furthermore,
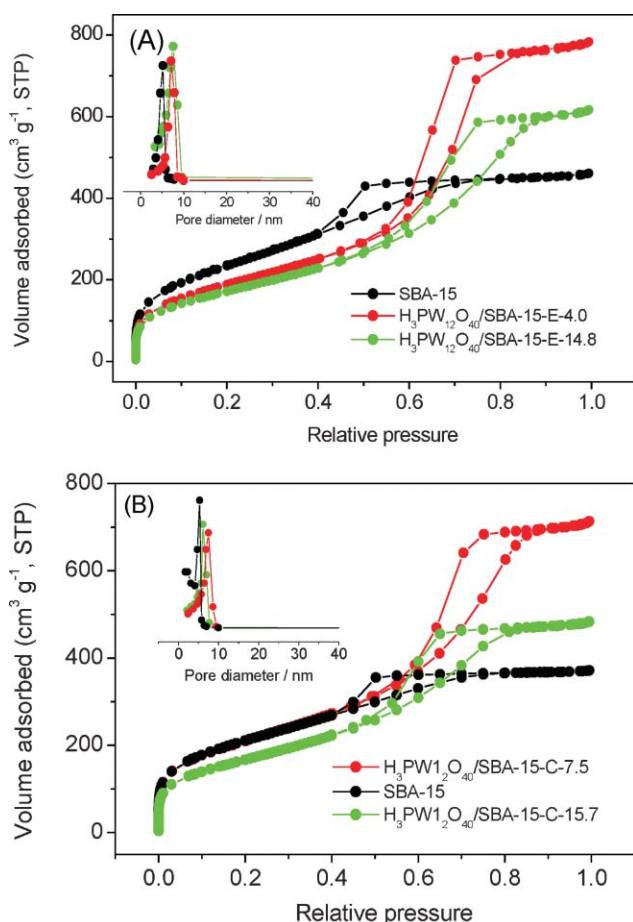
Fig. 2 Nitrogen adsorption–desorption isotherms and pore size distribution profiles (inset) according to BJH desorption dV/dD pore volume of $H_3PW_{12}O_{40}$/SBA-15 materials. P123 was removed by (A) extraction with acidic ethanol and (B) calcination at 400 °C.

analysis of the solution by ICP-AES shows that no significant amount of $H_3PW_{12}O_{40}$ leached into the reaction. However, catalytic activity decreased in the second catalytic cycle due to the strong adsorption of DPA on the $H_3PW_{12}O_{40}$/SBA-15 composite. Calcination of the reused catalysts at 420 °C restored the catalytic activity.

Conclusions

A direct sol-gel co-condensation technique combined with hydrothermal treatment in the presence of a poly(alkylene oxide) triblock copolymer has been demonstrated to prepare a series of ordered mesoporous SBA-15 silica-based $H_3PW_{12}O_{40}$ materials. The materials exhibit unique surface physicochemical properties, including larger BET surface area, higher porosity, larger and well-defined pore size, and evenly dispersed catalytic sites throughout the materials. As-prepared materials are robust and show excellent activity and selectivity in the conversion of one of the top biomass platform molecules, LA, into a valuable polymer intermediate, DPA, compared to other known catalysts, including mineral acid. Importantly, the use of the new acid eases safe handling and simplifies separation allowing reuse of the catalyst after a reactivation step.

Acknowledgements

Notes and references

1 J. J. Bozell, L. Moens, D. C. Elliott, Y. Wang, G. G. Neuenscwander, S. W. Fitzpatrick, R. J. Bilski and J. L. Jarnefeld, *Resour., Conserv. Recycl.*, 2000, **28**, 227–239.
2 Top value added chemicals from biomass: http://www.eere.energy.gov/biomass/products_rd.html.
3 Y. Isoda and M. Azuma, Honshu Chemical Ind., *Jap. Pat.* 08053390, 1996.
4 (*a*) J. H. Clark, *Green Chem.*, 1999, **1**, 1–8; (*b*) J. H. Clark, *Green Chem.*, 2006, **8**, 1–17.
5 M. Misono, *Chem. Commun.*, 2001, **13**, 1141–1152.
6 (*a*) I. V. Kozhevnikov, K. R. Kloetstra, A. Sinnema and H. W. Zandbergen, *J. Mol. Catal. A: Chem.*, 1996, **114**, 287–298; (*b*) Q. Liu, W. Wu, J. Wang, X. Ren and Y. Wang, *Microporous Mesoporous Mater.*, 2004, **76**, 51–60.
7 (*a*) Y. Izumi, M. Ono, M. Kitagawa, M. Yoshida and K. Urabe, *Microporous Mater.*, 1995, **5**, 255–262; (*b*) Y. Guo, Y. Wang, C. Hu and E. Wang, *Chem. Mater.*, 2000, **12**, 3501–3508.
8 I. V. Kozhevnikov, *J. Mol. Catal. A: Chem.*, 2007, DOI: 10.1016/jmolcata.2006.08.072.
9 D. Zhao, Q. Huo, J. Feng, B. F. Chmelka and G. D. Stucky, *J. Am. Chem. Soc.*, 1998, **120**, 6024–6036.

New chitosan/CEG (compressed expanded graphite) composites—preparation and physical properties

M. Krzesińska,*[a] A. Tórz,[b] J. Zachariasz,[a] J. Muszyński,[a] J. Socha[b] and A. Marcinkowski[a]

The new group of high porous, rigid bio-composite materials based on compressed expanded graphite impregnated by a chitosan were prepared and examined by means of adequate physical methods.

Introduction

The increasing demand from consumers and industry for environmentally friendly and renewable polymers explain the great interest for macromolecules as substitutes of synthetic, petroleum-based polymers. The most recent efforts in the development of cleaner sustainable chemistry are being driven by a shift from petrochemical-based feedstocks toward biological materials. Thus, there is a drive to produce raw materials from biofeedstocks, which in turn is stimulating considerable effort in new areas of chemistry and biotechnology. Given these developments, it seems clear that there will be a key role to be played in the development of biopolymers for use as polymeric supports as well as themselves in pure or modified form by utilising their unique, natural properties like high absorption ability, reactivity, optical activity *etc*. These systems are ecologically friendly materials meeting the needs for materials of new generation. The other, rare properties of natural polymers, such as biodegradability, biocompatibility, non-toxicity make them especially attractive for a number of applications.[1]

It is estimated that approximately 4×10^{11} tons of carbohydrates (mono-, di- and polysaccharides) are biosynthesised each by plants and photosynthesising bacteria. The polysaccharides starch, cellulose and chitin are the world's three biggest natural renewable resources for general consumer applications and are still objects of wide scientific interest. Besides starch and cellulose, which have been extensively studied, chitin exhibits a great potential. Chitin and its *N*-deacetylated derivative chitosan represent a family of biopolymers, made up of β-(1,4)-linked *N*-acetyl-D-glucosamine and D-glucosamine subunits (amino polysaccharides).[2,3] Taking into account the unique properties of chitosan, one can indicate some potential advantages of this polymer: (1) presence of different functional groups, (2) easy modification and even possibility to use it without preliminary modification, (3) rather high thermal stability and durability. Thus, chitosan could be considered as a "green polymer" of a variety of current and potential application in analytical chemistry, water treatment,

agriculture, food and feed additives, medical and pharmaceutical materials or biotechnology.[3–5]

Compressed expanded graphite (CEG) blocks produced from expanded graphite (EG) powders by means of compaction are highly porous and present many interesting properties, such as good electrical and thermal conductivities, satisfactory active surface area and mechanical strengths. The overall, attainable porosity of such material is 98.8% (dependent on parameters of the preparation process) including fully accessible meso- and macro-pores. The specific surface of the raw material is about 40 m^2 g^{-1} but may be easily developed by using "classic" activation methods to reach even 1000 m^2 g^{-1}.[6,7] Because of the interlocking of the constitutive particles, the elastic properties of CEG are surprisingly high, considering its ultra-low density.[8] The good mechanical properties of such a highly porous material as CEG are very important because of one of its possible applications as matrices for high surface polymer-based composites.

The purpose of this communication is to present the first attempts of producing a new class of bio-materials prepared from chitosans and CEGs, which should exhibit a sum of desired properties of the components that were studied and reported separately until now. The continuation of the work will be further functionalisation, *e.g. via* cross-linking by various (natural or synthetic) agents or/and subsequent grafting by monomers and/or other compounds (natural or synthetic) to obtain biodegradable as well as environmentally friendly unique materials with useful properties.

Experimental

Materials

CEG cubes were produced using a powder of EG of an apparent density of 11 kg m^{-3} provided by SGL Carbon (Germany). The cubic monolithic samples were prepared using the following procedure: after weighing, portions of EG powder were introduced into a long parallelepiped tube (inner cross-section 4 cm^2), and compressed under the same pressures to produce the set of samples with the same porosity 85%.

Chitosan/CEG composites were prepared by using a "classic" technique of impregnation, as described in the literature.[4] Dry cubes were immersed into two kinds of water–acetic acid solutions (about 2 wt%) of chitosan (medium molecular weight, Sigma–Aldrich, Germany used as received): 1.29 and 0.62 wt%. The procedure was carried out under vacuum over 1 h. The samples were next dried in air at 60 °C until no change in weight was observed. The materials were neutralized by using of 0.1 mol dm^{-3} water solution of NaOH (1 h), and then washed with distilled

[a]*Institute of Coal Chemistry, Polish Academy of Sciences, Sowińskiego 5, Gliwice, PL-44-121, Poland*
[b]*Silesian Technical University of Technology, Department of Analytical and General Chemistry, Marcina Strzody 9, Gliwice, PL-44-100, Poland*

Table 1 Characteristic of the samples

Sample	Treatment		
	Impregnation by solution of chitosan (wt%)	Neutralisation	Cross-linking
CEG 0	0.62 1.29 "Blank test" sample—initial cube of the untreated CEG		
ChiCEG 1	+	+	+
ChiCEG 2	+	+	
ChiCEG 11	+	+	+
ChiCEG 22	+	+	

water to remove the excess alkali. The samples were dried in the same way as described above and the further investigations were carried out.

The cross-linking of representative composites was carried out by using aqueous solution of glutaraldehyde (Sigma–Aldrich, Germany, used without further purification) of 9.375×10^{-3} mol dm^{-3}. The procedure of immersing and drying was the same as in the case of the impregnation process.

Descriptions of all samples prepared are summarized in Table 1.

Methods

Both apparent and true densities were measured to determine the bulk porosity of samples. Apparent density was calculated from volume of a sample and its weight. The true density was measured using a helium gas displacement pycnometer, type 1305 Micromeritics®.

The bulk porosity of samples was calculated using an expression:

$$P(\%) = ((\rho_{\text{true}} - \rho_{\text{app}})/(\rho_{\text{true}})) \times 100 \qquad (1)$$

where P is a bulk porosity, ρ_{true} and ρ_{app} are true and apparent densities of a sample.

Ultrasonic velocity measurements were performed using an ultrasonic tester CT1 (UNIPAN-ULTRASONIC, Poland). A pair of ultrasonic heads (transmitting and receiving) for the longitudinal waves with a frequency of 100 kHz and with a diameter of 15 mm was used for this study. For anisotropy studies, the velocities were measured along the three orthogonal directions of each sample: one perpendicular to the bedding plane of the graphite flakes ($v_\perp$), and two orthogonal within the bedding plane ($v_\parallel^1$ and $v_\parallel^2$). The bedding plane is perpendicular to the direction of compression by which the samples were prepared.

Discussion of results

1. The true density and bulk porosity

Fig. 1 presents results of the true density measurements carried out for reported samples including CEG 0. The true density of CEG was found to be close to the density of pure graphite crystal, equal to 2.2 g cm^{-3}. Filling of pores by chitosan—more loose material decreased the true density of composite. Higher concentration and cross-linking of chitosan improved compactness of the composite matrix. Probably, the neutralisation process causes strong changes only in the superstructure of the deposited polymer independently of the thickness of it's layer, which should be adequate to the
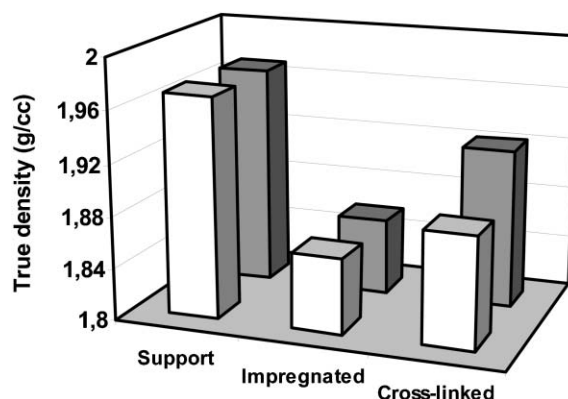
Fig. 1 The true density of initial CEG (support), CEG impregnated with raw chitosan and CEG impregnated with cross-linked chitosan. White and gray columns denote composites characterized by a concentration of 0.62 wt% and 1.29 wt% chotosan, respectively.

concentration of the solution used. The hypothesis (on this step of our studies) may be proven by observing the results of bulk porosity measurements (Fig. 2.), where the composite with less quantity of chitosan covering the walls of the CEG pores exhibits lower porosity. Simultaneously, the cross-linking process increases the density of the samples, compared to the impregnated and neutralized samples, without detectable changes of their porosity. It may be assumed that this is an effect of changes in the free volume of the polymer (by incorporating the glutaraldehyde between polymer chains) that occurs without significant deviations of the film dimensions. Although the bulk porosity of composites was lower than that of initial CEG, the chitosan/CEG composites still kept high porosity, reaching values above 80%.

2. The ultrasonic measurements

The dynamic elastic moduli (which corresponds to the elastic/ mechanical properties of a material) of the samples were estimated by means of measurements of the velocity of the longitudinal ultrasonic wave propagated along three mutually orthogonal directions: one perpendicular to the bedding plane, and two orthogonal within the bedding plane. The results of the experiments are
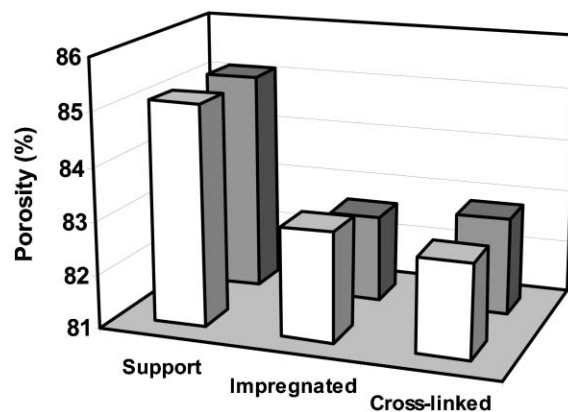
Fig. 2 The bulk porosity of initial CEG (support), CEG impregnated with raw chitosan and CEG impregnated with cross-linked chitosan. White and gray columns denote composites characterized by a concentration of 0.62 wt% and 1.29 wt% chitosan, respectively.
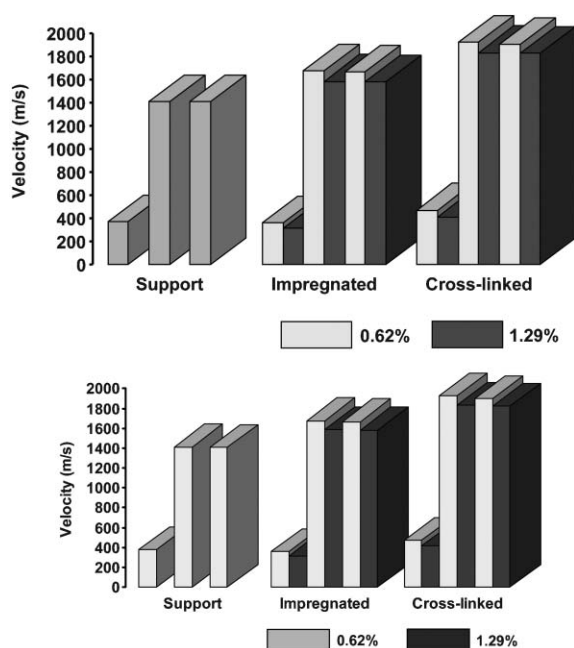
Fig. 3 The ultrasonic velocity measured in the initial CEG (support), CEG impregnated with raw chitosan (impregnated) and CEG impregnated with cross-linked chitosan (cross-linked); low columns denote $v_\perp$, high columns denote $v_\parallel^1$ and $v_\parallel^2$ ($v_\parallel^1 \cong v_\parallel^2$).

summarized in Fig. 3. The same values of $v_\parallel^1$ and $v_\parallel^2$, different than $v_\perp$, denote that chitosan/CEG composites conserve the transverse isotropy of the initial CEG. Addition of chitosan to the CEG support increases stiffness in the direction parallel to the bedding plane, which could be explained by the filling of pores present between planes parallel to the bedding plane. Cross-linking of the same portion of chitosan introduced into the CEG distinctly increases the elastic properties, resulting in the higher stiffness of the composite; the increase of the ultrasonic velocity observed for composite with addition of 0.62 wt% of cross-linked chitosan was 26% for $v_\perp$ and 36% for $v_\parallel$, respectively. The change of the ultrasonic velocity is not so strong in the case of the wave propagation perpendicular to the bedding plane. The elastic

properties measured in the directions parallel to the bedding plane revealed systematic tendency of increasing the stiffness of the composites as follows:

$$ChiCEG11 > ChiCEG22 > CEG\ 0$$
$$ChiCEG1 > ChiCEG2 > CEG\ 0 \quad (2)$$

The observed tendencies may be due to the anisotropy of the graphite support, which is a result of its structure, as well as corresponding to the deposition of the polymer. This proves that the impregnation of expanded graphite shapes by chitosan (and especially cross-linking of the chitosan) can result in homogeneous composites of better mechanical properties compared to initial materials, and which should probably preserve all their specific properties. Similar results were reported by Lekka et al.[5] The results of ref. 5 show the increase in Young's modulus values (Young's modulus is proportional to the ultrasonic velocity) obtained for cancer cells treated with chitosan. The formation of a relatively hard, thick chitosan shell around the soft cell can increase cell stiffness about 4 times in comparison with non-treated cells.

Acknowledgements

Our cordially thanks for Prof. James H. Clark for the inspiration and especial care.

Notes and references

1 J. Clark and D. Macquarrie, *Handbook of Green Chemistry & Technology*, Blackwell Publishing, Oxford, 2002.
2 M. Rinaudo, *Prog. Polym. Sci.*, 2006, **31**, 603.
3 D. J. Macquarrie and J. J. E. Hardy, *Ind. Eng. Chem. Res.*, 2005, **44**, 8499.
4 B. Krajewska, *Sep. Purif. Technol.*, 2005, **41**, 305.
5 M. Lekka, P. Laidler, J. Ignacak, M. Łabędź, J. Lekki, H. Struszczyk, Z. Stachura and A. Z. Hrynkiewicz, *Biochim. Biophys. Acta*, 2001, **1540**, 127.
6 M. Krzesińska and A. I. Lachowski, *Mater. Chem. Phys.*, 2004, **86**, 105.
7 A. Celzard, J. F. Mareche and G. Furdin, *Carbon*, 2002, **40**, 2713.
8 M. Krzesińska, A. Celzard, B. Grzyb and J. F. Marêché, *Mater. Chem. Phys.*, 2006, **97**, 173.

Enhanced selectivity in green catalytic epoxidation using a supported cobalt complex

Rajesh Chakrabarty,[a] Birinchi K. Das*[a] and James H. Clark[b]

A supported reagent made by immobilising a tetrameric cobalt(III) cubane cluster on mesoporous silica catalyses the aerobic oxidation of α-pinene with enhanced epoxidation selectivity compared with other systems.

The use of renewable feedstocks in the production of chemicals is considered as the first step in greening the life cycle of chemical products. In this context, oxidation of α-pinene, which occurs widely in the plant kingdom, may be viewed as an important reaction because oxidation products of α-pinene find use as the starting materials for fragrance, flavour and therapeutic agents, including taxol.

In addition to some cobalt(II) based homogeneous autoxidation catalysts,[1] several heterogeneous catalysts including titanium incorporated mesoporous molecular sieves,[2] metal–Schiff base complexes supported on zeolite[3] and Zn(II)–Al(III) layered double hydroxide (LDH),[4] oxomolybdenum(VI) complexes supported on MCM-41 and MCM-48,[5] polyoxometallate supported materials,[6] transition metal containing AlPOs[7] and others[8] have been studied for the catalytic oxidation of α-pinene. The usefulness of these studies has been hampered by low conversion as well as poor selectivity for the various products formed. Better yield and selectivity have been achieved using sacrificial aldehydes as oxygen acceptors, but this process leads to poor atom economy.[7]

Since cobalt(III) acts as the key intermediate species in Co(II)-catalysed oxidation processes,[9] the direct use of catalytically active Co(III) for such reactions has been considered to be beneficial. For instance, oligomeric oxo-cobalt(III) complexes have been shown to be effective as catalysts for oxidation of hydrocarbons.[10] Vis-à-vis published results on the use of trimeric oxo clusters having a $[Co_3-\mu_3-O)]^{n+}$ core ($n = 0, 1$), the use of tetrameric tetraoxo clusters having cubane-like $[Co_4(\mu_3-O)_4]^{4+}$ at the core is worth exploring. Earlier studies have shown that the cubane cluster, $[Co_4^{III}O_4(O_2CC_6H_5)_4(4-CNpy)_4]$ (I) displays excellent catalytic activity in the epoxidation of α-pinene under homogeneous conditions.[11] In the synthesis of these cobalt(III) species via H_2O_2 oxidation, it has been our observation that it is always the tetramer which can be isolated in high yield from a reaction mixture involving a cobalt(II) salt, a sodium carboxylate, the selected pyridine, along with H_2O_2(aq.) oxidant, added in excess, in methanol.[12,13] This suggests greater thermodynamic stability of the Co(III) tetramers. Recently we have developed a heterogeneous

[a]Department of Chemistry, Gauhati University, Guwahati 781014, India. E-mail: das_bk@rediffmail.com; Fax: +91 361 2570535; Tel: +91 361 2570535
[b]Green Chemistry Centre, Department of Chemistry, University of York, Heslington, York, UK YO10 5DD. E-mail: jhc1@york.ac.uk

catalyst by immobilising a cubane complex of cobalt(III) (vide infra) on organomodified hexagonal mesoporous silica (HMS)[14] support. Herein we report our results on air oxidation of α-pinene catalysed by 'Co(III)-HMS', which has been prepared by supporting an in-situ formed cobalt(III)–cubane complex on HMS containing –$(CH_2)_2CO_2H$ groups as surface modifiers. The use of $Co_4O_4(O_2CR)_4(py)_4$ (R = an alkyl or aryl group, py = pyridine or a substituted pyridine), which has a robust Co_4O_4 cubane core, as a catalyst for air oxidation of hydrocarbon compounds, is being seen as a promising catalytic process in view of the increased catalyst stability.[12]

The HMS functionalized with –$(CH_2)_2CO_2H$ groups was synthesized by the method originally developed by Macquarrie et al.[14] HMS–$(CH_2)_2CN$ was prepared from tetraethylorthosilicate (TEOS) and (2-cyanoethyl)triethoxysilane (CTES) in aqueous ethanol in the presence of n-dodecylamine as the templating agent. It was converted to HMS–$(CH_2)_2CO_2H$ by H_2SO_4 treatment. To prepare the supported reagent, 2 g of HMS–$(CH_2)_2CO_2H$ was suspended in a solution of $Co(OAc)_2\cdot4H_2O$ (0.996 g, 4 mM) in 40 mL of water. Addition of 4-cyanopyridine (0.499 g, 4.8 mM) to the boiling solution followed by oxidation of the resultant mixture with 30% H_2O_2 (v/v, 5 mL, ~50 mM) instantaneously changed the colour of the solid particles from pink to dark olive-green. The resulting olive-green catalyst was filtered after 4 h under reflux, washed with water, methanol and acetone and dried at 110 °C for 12 h. The catalyst so prepared is called Co(III)-HMS (Scheme 1).

N_2 adsorption isotherms of the support material HMS–$(CH_2)_2CO_2H$ and Co(III)–HMS are of similar shape (Type IV),[15] indicating that the porous structure has been maintained after immobilization. While HMS–$(CH_2)_2CO_2H$ shows a BET surface area of 1071 m^2 g^{-1} with a total pore volume of 0.69 mL g^{-1}, the corresponding values for the Co(III)–HMS catalyst are found to be 622 m^2 g^{-1} and 0.60 mL g^{-1}. Moreover, 87% of pores in the supported reagent are found to have diameters in the range 3.2–6.0 nm, making the material sufficiently porous to allow passage of organic molecules of the expected size.
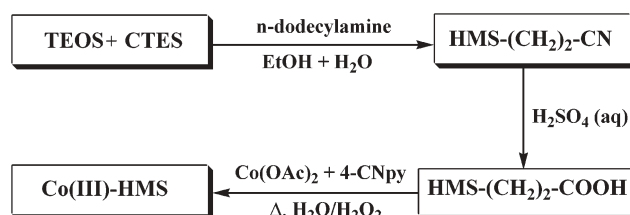
Scheme 1
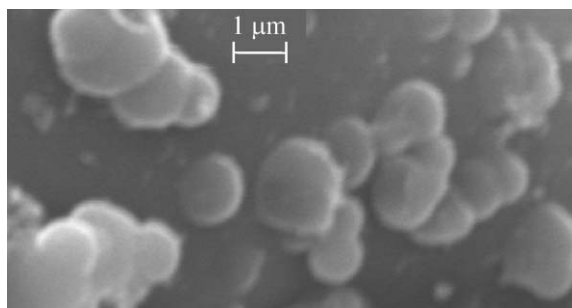
Fig. 1 Scanning electron micrograph of Co(III)-HMS particles.

AAS analysis gives a cobalt loading of 1.39 mmol g^{-1} for Co(III)–HMS. EDAX measurements of the catalyst gives a Co:Si ratio of ∼1:8, which is consistent with the cobalt loading determined by AAS. This study also shows that the cobalt complex is uniformly dispersed in the support. SEM pictures recorded for Co(III)–HMS (Fig. 1) show that the average particle diameters are ∼1 μm or smaller, and that the particles are spherical in shape. The olive green colour of the solid particles of the catalyst is indicative of the presence of a Co(III) complex. In order to ascertain the nature of the complex anchored on the support, we have used the DRIFTS technique. Fig. 2 shows the DRIFTS spectra of the support material and the immobilised catalyst Co(III)–HMS along with the spectrum of the tetrameric cobalt(III) complex [Co$_4^{III}$(μ$_3$-O)$_4$(μ-O$_2$CCH$_3$)$_4$(4-CNpy)$_4$]† (**II**), prepared by following a procedure similar to that for complex **I**, and complex **II** immobilised on HMS–(CH$_2$)$_2$CO$_2$H *via* a ligand exchange reaction.[16] The appearance of a band for the nitrile group (2255 cm^{-1}) and of two strong bands at 1534 and 1415 cm^{-1} corresponding to the v_{asym} and v_{sym} vibrations of bridging –COO$^-$ groups, respectively, is suggestive of the presence of a cobalt(III) complex closely related to **II** in Co(III)–HMS. The striking similarity of the spectra of the Co(III)–HMS and the complex **II** immobilised material (Fig. 2c) leaves no doubt that in Co(III)–HMS we indeed have anchored a tetrameric cobalt(III) complex having a [Co$_4$(μ-O)$_4$]$^{4+}$ core.[13] Immobilization of a related
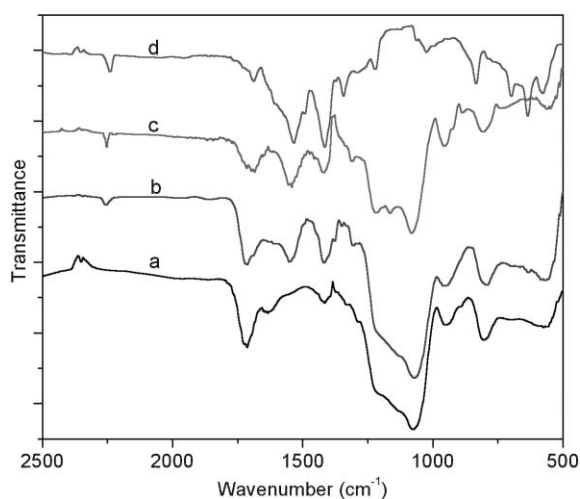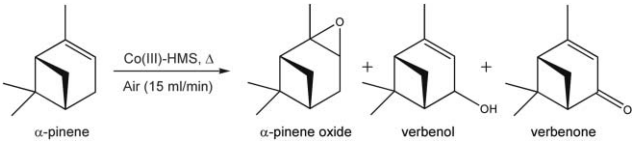
oligonuclear oxo-bridged complex was indicated earlier for a cobalt(III) based catalyst suitable for the oxidation of alkyl-aromatic hydrocarbons.[17]

II
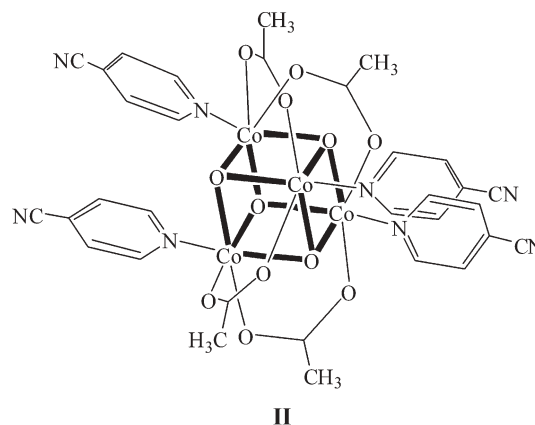
The Co(III) supported material, Co(III)–HMS, was tested as a catalyst in the aerobic oxidation of α-pinene. The catalyst was found to be highly active and selective in the epoxidation of α-pinene to α-pinene oxide with air as the oxidant. Results are summarised in Table 1, and Fig. 3 shows a representative kinetic plot. In a typical reaction, 100 mg (0.09 mol%) of the catalyst was added to the reaction mixture consisting of α-pinene (3.97 mL, 25 mmol) and 40 mL of 1,4-dioxane. An airflow of 15 mL min^{-1} was used. In the absence of solvent, however, even at 60 °C rearrangement of products takes over to give α-campholenic aldehyde and other minor products, which were also observed by other investigators in cobalt(II) catalyzed oxidations.[18] In aceto-nitrile, significant decrease in the reaction rate and product selectivities was observed, with approximately equal amounts of epoxidation and allylic oxidation products. To optimize the reaction temperature air oxidation was performed at 60 °C, 80 °C or 100 °C and the progress of the reaction was monitored by GC. It has been observed that an increase in the reaction temperature accelerates aerobic oxidation of α-pinene. This is in conformity with an earlier report where higher reaction temperatures led to a similar acceleration in the air oxidation of α-pinene.[19] At the lowest temperature of 60 °C, only 6.6% conversion of α-pinene could be observed at the end of 24 h. Prolonging the reaction time did not significantly enhance the conversion and only 10.5% conversion of α-pinene was observed after 48 h. On increasing the temperature to 100 °C, however, conversion rose to 81.5% (entry 3, Table 1) after 24 h. The TOF (h^{-1}) values calculated at the end of 4 h are: 8.87 (entry 3), 37 (entry 4), 16 (entry 5). At reaction temperatures higher than 100 °C, extensive rearrangement of the products was observed. The observed selectivity (61%) for α-pinene oxide at 100 °C (at 81.5% conversion) is rather significant because the yield for the epoxidised product is also reasonably high. The increased selectivity for α-pinene oxide at higher temperatures is likely to be an outcome of the suppression of the allylic oxidation route of α-pinene oxidation.

In contrast to our results, previous reports have shown that selectivities >50% for α-pinene oxide are difficult to achieve.[1] A recently reported[20] Co/SiO$_2$ composite was shown to catalyze α-pinene with molecular oxygen, giving both epoxidation and allylic oxidation products with substrate conversion of around 40% with selectivities for the former and the latter being 24–30%

Fig. 2 DRIFT spectra of: [a] HMS–(CH$_2$)$_2$CO$_2$H; [b] Co(III)–HMS; [c] complex **II** immobilised on HMS–(CH$_2$)$_2$CO$_2$H *via* ligand exchange; [d] complex **II**.

Table 1 Catalytic aerobic oxidation of α-pinene by Co(III)-HMS under atmospheric pressure[a]

Entry	Catalyst (mol%)	Temp./°C	Conv. (%)	Product[b] yield (selectivity) (%)		
				α-Pinene oxide	Verbenol	Verbenone
1	0.09	60	6.6	3.5 (53)	1.1 (17)	2.0 (30)
2	0.09	80	34.2	11.6 (34)	5.4 (16)	7.5 (22)
3	0.09	100	81.5	50.1 (61)	2.9 (4)	16.9 (21)
4	0.005	100	66.0	40.1 (61)	5.8 (9)	13.4 (20)
5	0.02	100	73.0	41.1 (56)	8.0 (11)	9.5 (13)

[a] Reaction conditions: α-pinene, 3.97 mL (25 mmol); 1,4-dioxane, 40 mL; oxidant, air (15 mL min^{-1}); reaction time = 24 h. Conversion and product composition were determined by GC and identified by GC-MS. [b] Minor amounts of rearranged products of α-pinene oxide also formed.
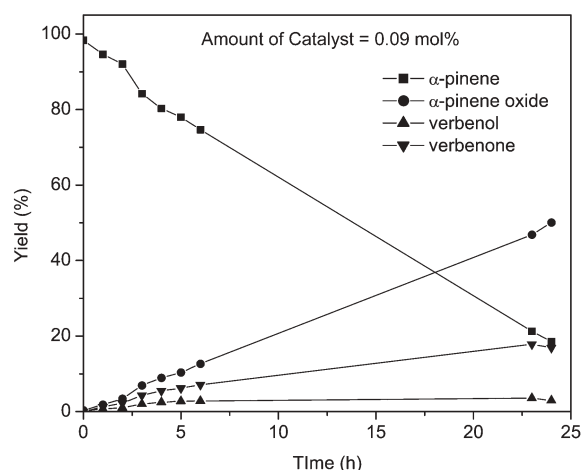
Fig. 3 A plot of data on air oxidation of α-pinene using Co(III)–HMS as catalyst under atmospheric pressure at 100 °C.

and 44–52%, respectively. A higher selectivity of 84% for α-pinene epoxide could be observed by Thomas et al. at 56% conversion in a study on the aerobic oxidation of α-pinene using a microporous Co(III) containing aluminophosphate (CoAlPO-36) catalyst.[7] This reaction, however, required the use of a sacrificial aldehyde co-reactant and 30 bar air pressure. On the other hand, formation of only trace amounts of α-pinene oxide was observed in α-pinene oxidation by TBHP and H$_2$O$_2$ using copper, manganese and palladium based catalysts.[21] Finally, it should be mentioned here that the observed activity and selectivity shown by Co(III)–HMS are comparable to those observed for the homogeneous reaction catalysed by complex **I**.[11] More importantly, the α-pinene conversion as well as epoxide selectivity observed by us using the Co(III) based homogeneous and heterogeneous catalysts stand among the highest reported for the reaction. In essence, our results are significant from a green chemistry point of view because no sacrificial aldehyde, other additives or applied pressure, have been used by us in the aerobic oxidation of α-pinene.

In order to test the true heterogeneity of the catalyst, following the method described by Sheldon et al.,[22] the catalyst was filtered off at the reaction temperature after 1 h and the filtrate was allowed to react further for 24 h at 100 °C to find no substantial conversion of α-pinene. After 3 h (overall reaction time) only 2.5% of α-pinene conversion was observed. The reaction under same conditions with the catalyst showed 15.8% conversion of α-pinene after 3 h. The detected conversion is presumably due to the autoxidation of α-pinene under the reaction conditions used. Our assumption is also supported by the fact that no cobalt could be detected in the filtered reaction mixture. Preliminary studies on recycling the catalyst showed that there was only a marginal drop in catalyst activity, suggesting that the catalyst developed by us may be re-usable.

In summary, we have prepared and characterized a Co(III) based heterogeneous catalyst for the aerobic oxidation of α-pinene and found it to give the best reported combination of activity and selectivity to epoxide under low environmental impact conditions.

Notes and references

† Physicochemical data on complex [Co$_4^{III}$(μ$_3$-O)$_4$(μ-O$_2$CMe)$_4$(4-CNpy)$_4$]: analysis for C$_{32}$H$_{28}$N$_8$O$_{12}$Co$_4$, % calculated: C, 40.35; H, 2.94; N, 11.77, Co, 24.77; found: C, 40.73; H, 3.03; N, 11.92; Co, 24.46 (gravimetric). ^{1}H NMR (270 MHz; D$_2$O; δ, ppm): 8.41 (d, J = 6.3 Hz, 4H), 7.65 (d, J = 6.0 Hz, 4H), 2.05 (s, 12H). UV–visible data: (CH$_2$Cl$_2$, λ$_{max}$): 634 nm (sh), 445 nm (ε = 8017 L mol^{-1} cm^{-1}), 362 nm (sh), 259 (sh). IR data (KBr): ν_{max}/cm^{-1} 3427(w), 3054(w), 3011(w), 2930(w), 2240(m), 1611(m), 1533(s), 1492(m), 1411(s), 1337(m), 1218(m), 1064(m), 1030(w), 830(m), 791(w), 698(m), 634(s), 579(s) and 558(m) [s, strong; m, medium; w, weak].

1 M. K. Lajunen, *J. Mol. Catal. A: Chem.*, 2001, **169**, 33; M. K. Lajunen, T. Manula and A. M. P. Koskinen, *Tetrahedron*, 2000, **56**, 8167; M. J. da Silva, P. Robles-Dutenhefner, L. Menini and E. V. Gusevskaya, *J. Mol. Catal. A: Chem.*, 2003, **201**, 71; M. M. Reddy, T. Punniyamurthy and J. Iqbal, *Tetrahedron Lett.*, 1995, **36**, 159; T.-J. Wang, Y.-Y. Yan, M.-Y. Huang and Y.-Y. Jiang, *React. Funct. Polym.*, 1996, **29**, 145; M. F. T. Gomez and O. A. C. Antunes, *J. Mol. Catal. A: Chem.*, 1997, **121**, 145; R. A. Budnik and J. A. Kochi, *J. Org. Chem.*, 1976, **41**, 1384.

2 Y.-W. Suh, N.-K. Kim, W.-S. Ahn and H.-K. Rhee, *J. Mol. Catal. A: Chem.*, 2003, **198**, 309; M. P. Kapoor, A. Bhaumik, S. Inagaki, K. Kuraoka and T. Yazawa, *J. Mater. Chem.*, 2002, **12**, 3078; F. Chiker, J. P. Nogier, F. Launay and J. L. Bonardet, *Appl. Catal., A: General*, 2003, **243**, 309.

3 T. Joseph, D. P. Sawant, C. S. Gopinath and S. B. Halligudi, *J. Mol. Catal. A: Chem.*, 2002, **184**, 289.

4 S. Bhattacharjee, T. J. Dines and J. A. Anderson, *J. Catal.*, 2004, **225**, 398.

5 C. D. Nunes, M. Pillinger, A. A. Valente, J. Rocha, A. D. Lopes and I. S. Gonçalves, *Eur. J. Inorg. Chem.*, 2003, 3870.

6 T. Sakamoto and C. Pac, *Tetrahedron Lett.*, 2000, **41**, 10009.

7 R. Raja, G. Sankar and J. M. Thomas, *Chem. Commun.*, 1999, 829.

8 N. V. Maksimchuk, M. S. Melgunov, J. Mrowiec-Białoń, A. B. Jarzębski and O. A. Kholdeeva, *J. Catal.*, 2005, **235**, 175.

9 F. A. Chavez and P. K. Mascharak, *Acc. Chem. Res.*, 2000, **33**, 539; F. A. Chavez, C. V. Nguyen, M. M. Olmstead and P. K. Mascharak, *J. Am. Chem. Soc.*, 1998, **120**, 9015.

10 S. A. Chavan, D. Srinivas and P. Ratnasamy, *Chem. Commun.*, 2001, 1124.

11 R. Chakrabarty and B. K. Das, *J. Mol. Catal. A: Chem.*, 2004, **223**, 39.

12 R. Chakrabarty, Ph.D. Thesis, Gauhati University, India, 2006; R. Chakrabarty, D. Kalita and B. K. Das, *Polyhedron*, 2007, **26**, 1239.

13 P. Sarmah, R. Chakrabarty, P. Phukan and B. K. Das, *J. Mol. Catal. A: Chem.*, 2007, **268**, 36.

14 D. J. Macquarrie, *Chem. Commun.*, 1996, 1961; D. J. Macquarrie, D. B. Jackson, J. E. G. Mdoe and J. H. Clark, *New J. Chem.*, 1999, **23**, 539.

15 K. S. W. Sing, D. H. Everett, R. A. W. Haul, L. Moscou, R. A. Pierotti, J. Rouquérol and T. Siemieniewska, *Pure Appl. Chem.*, 1985, **57**, 603; M. Kruk and M. Jaroniec, *Chem. Mater.*, 2001, **13**, 3169.

16 In this method the cobalt(III) cubane complex of choice is reacted with HMS-$(CH_2)_2CO_2H$ under reflux in a polar solvent.

17 B. K. Das and J. H. Clark, *Chem. Commun.*, 2000, 605.

18 G. Rothenberg, Y. Yatziv and Y. Sasson, *Tetrahedron*, 1998, **54**, 593; M. K. Lajunen, M. Myllykoski and J. Asikkala, *J. Mol. Catal. A: Chem.*, 2003, **198**, 223.

19 M. K. Lajunen, T. Manula and A. M. P. Koskinen, *Tetrahedron Lett.*, 1994, **35**, 4461.

20 C.-C. Guo, W.-J. Yang and Y.-L. Mao, *J. Mol. Catal. A: Chem.*, 2005, **226**, 279.

21 B. A. Allal, L. E. Firdoussi, S. Allaoud, A. Karim, Y. Castanet and A. Mortreux, *J. Mol. Catal. A: Chem.*, 2003, **200**, 177.

22 H. E. B. Lempers and R. A. Sheldon, *J. Catal.*, 1998, **175**, 62.

Synthesis of chloroanilines: selective hydrogenation of the nitro in chloronitrobenzenes over zirconia-supported gold catalyst†

Daiping He, Hui Shi, Yu Wu and Bo-Qing Xu*

Selective production of chloroanilines from chloronitrobenzenes without any dechlorination was found feasible by catalytic hydrogenation over zirconia-supported gold catalyst, which uncovers a clean synthetic approach for useful chloroanilines.

Introduction

Chloroanilines (CANs) from chloronitrobenzenes (CNBs) are an important class of industrial intermediates for a variety of specific and fine chemicals, including pharmaceuticals, dyes, herbicides and pesticides.[1] The conventional technology using stoichiometric reducing agents is a tedious process and harmful to the environment. With the increasing interest in human health and environmental protection, environmentally benign preparation of chemicals is attracting increasing attention.[2] It is highly desirable to produce these intermediates by selective reduction of the corresponding chloronitrobenzenes with H_2 using supported metal catalysts (*e.g.*, Pt, Ru, Pd, Ni).[3–5] A severe problem related with the catalytic hydrogenation has been the co-occurrence of the catalytic hydrodechlorination reaction of the substrates, which significantly limits the selectivity to chloroanilines and leads to a lot of waste. Furthermore, hydrogen chloride produced from the hydrodechlorination is also corrosive to the reactor. It remains a big challenge to develop heterogeneous catalysts that would ensure the selective reduction of the nitro groups while leave intact the carbon–chlorine bond in the same molecule. Many efforts have been made to tailor the hydrogenation selectivity of supported metal catalysts toward a specific hydrogenation of the nitro groups in CNBs, *e.g.*, by modifying the active metal with different promoters[3] or a second metal component[4] and by assembling metal-colloids onto suitable oxide nanoparticles[5] or using amorphous structures.[6] Very recent exploratory work identified a few highly selective catalysts, like nanostructured Ru/SnO$_2$ for ortho-CAN (*o*-CAN),[5] and amorphous Ni–P–B for para-CAN (*p*-CAN) synthesis.[6]

Started a couple of decades ago, catalysis by gold continues to show a fascinating future in the field of catalysis.[7] Nanosized Au particles in interaction with a variety of support materials showed special selectivity in catalyzing a number of reactions including CO oxidation,[8] alcohol oxidation,[9] olefin epoxidation,[10] vinyl chloride synthesis,[11] selective hydrogenation of unsaturated hydrocarbons,[12,13] aldehydes and ketones.[14] For the reduction of nitro compounds with H$_2$, Au/TiO$_2$, Au/Fe$_2$O$_3$ and Au/SiO$_2$ catalysts were recently found to be very specific in reducing the nitro group in various compounds containing other functional groups.[15] Unfortunately, none of the CNBs was included in the work. Also, further work would be required to understand the behavior of catalysts in different reaction conditions and their reusability. We have recently shown that zirconia supported gold catalysts are highly selective for the reduction of butadiene to form butenes.[13,16] In the present study, we challenge the synthesis of CANs from CNBs with Au/ZrO$_2$ catalyst. We show that Au nanoparticles on ZrO$_2$ are highly efficient catalysts for the selective hydrogenation of the nitro groups in CNBs without any dechlorination.

Experimental

Preparation of zirconia supported gold catalyst

Zirconia with BET surface area of 123 m^2 g^{-1} was prepared by thermal processing in flowing air (60 ml min^{-1}) of a conventional ZrO(OH)$_2$ hydrogel at 400 °C for 5 h. Detailed preparation of the hydrogel was described previously.[17] Au/ZrO$_2$ catalyst (BET surface area of 87 m^2 g^{-1}) was prepared using HAuCl$_4$ as the gold precursor by deposition–precipitation with urea onto the ZrO$_2$. After drying at 110 °C for 12 h, the sample was calcined at 200 °C for 5 h in flowing air (60 ml min^{-1}). The gold content in the catalyst was 3.8 wt% according to ICP-AES analysis.

General procedure for the catalytic test

Catalytic tests were performed with magnetic stirring in a 25 ml stainless steel autoclave containing 2.0 mmol CNBs in 4.0 ml ethanol (solvent). The catalyst (3.8 wt% Au/ZrO$_2$ powders, particle size 0.09 mm) used in each run of the reaction was 25.0 mg; the overall molar CNB/Au ratio was 415. The reactor was flushed five times with 0.5 MPa H$_2$ before it was pressurized to the desired H$_2$ pressure and placed in an oil bath maintained at the reaction temperature. The reaction was stopped at a selected time by cooling the reactor in an ice-water bath. Analysis of the reaction products was done on an HP4890 GC with an HP-5 capillary column and an FID as detector, using benzene as an internal standard.

Results and discussion

Unless otherwise specified, Au/ZrO$_2$ refers to the as-prepared fresh catalyst sample (*i.e.*, unreduced calcined sample). The particles size of Au particles in this Au/ZrO$_2$ catalyst appeared mainly in the

Innovative Catalysis Program, Key Lab of Organic Optoelectronics & Molecular Engineering, Department of Chemistry, Tsinghua University, Beijing, 100084, China. E-mail: bqxu@mail.tsinghua.edu.cn; Fax: +86-10-6279-2122; Tel: +86-10-6277-2592
† Electronic supplementary information (ESI) available: Fig. S1–S3 and Table S1. See DOI: 10.1039/b618367k

Table 1 Catalytic results of the selective hydrogenation of chloro-nitrobenzenes over Au/ZrO$_2$ catalyst[a]

| Substrate | Time/h | Conv. (%) | Product sel. (%) | | Dechlor. (%) |
			CAN[b]	Others[c]	
p-CNB	1	43	96.6	3.4	0
	5	100	99.4	0.6	0
o-CNB	1	36	98.5	1.5	0
	5	85	99.6	0.4	0
2,5-DCNB	1	28	95.9	4.1	0
	5	81	99.4	0.6	0

[a] Reaction conditions: 25.0 mg catalyst, 2.0 mmol substrate in 4.0 ml ethanol (solvent), 150 °C, 1.0 MPa H$_2$. [b] CAN for substrate p-CNB, o-CNB and 2,5-DCNB refers to p-CAN, o-CAN and 2,5-dichloroaniline (DCAN), respectively. [c] Other products are N-ethyl-chloroaniline or N-ethyl-dichloroaniline (0.2–0.5%), bis-chlorophenyl-diazene or bis-dichlorophenyl-diazene (0.1–3.5%), dichloro-azoxybenzene or tetrachloroazoxybenzene (0–0.6%).

range of 2–5 nm with an average of *ca.* 4.0 nm by TEM measurement [ESI† Fig. S1A]. Table 1 shows the catalytic results of p-CNB, o-CNB and 2,5-dichloronitrobenzene (DCNB) hydrogenation over Au/ZrO$_2$ catalyst at 150 °C, 1.0 MPa H$_2$. Blank tests using p-CNB as the substrate showed no reaction of CNBs in the absence of the catalyst. The conversion of p-CNB over the "pure" ZrO$_2$ support was *ca.* 1% in 1 h and less than 5% in 5 h. For all of the three CNB substrates, the Au/ZrO$_2$ proves to be an active catalyst for the selective hydrogenation of CNBs to the corresponding CANs. The CAN selectivity was higher than 95% when the reaction was carried out for only 1 h, it increased to almost 100% with increasing the reaction time up to 5 h when the substrate conversion became close to 100%. For comparison, our test of nitrobenzene (NB) hydrogenation under the same conditions gave an aniline selectivity of 97% (NB conversion was 95%) in 1 h. Thus, reactivity of the substrate molecule appears sensitive to the position and number of chlorines, *i.e.*, NB > p-CNB > o-CNB > DCNB, which could be due to combined steric and inductive effects of the chlorine substitution.

Special attention was paid to distinguish by-products of the hydrogenation reactions with GC-MS. Any by-product that amounted to 0.03% in the reaction mixture can be unambiguously detected in our method of product analysis. Dichloroazoxybenzene or tetrachloroazoxybenzene (<0.6%), bis-chlorophenyldiazene or bis-dichlorophenyldiazene (<3.5%) and N-ethyl-chloroaniline or N-ethyl-dichloroaniline (<0.5%) were detected as the main by-products in the reaction of CNBs. All of these by-products, except N-ethyl-chloroaniline or N-ethyl-dichloroaniline, can be further hydrogenated to the desired product CANs, which is supported by the observed increase in the selectivity of the desired CANs with increasing the substrate conversion or the reaction time (Table 1). The most significant aspect of the data in Table 1 is that the C–Cl bonds in the substrate molecules were kept intact during the reaction, which indicates that the undesired hydrodechlorination reaction usually observed over other metal catalysts[1,3,4] can be successfully avoided over the Au/ZrO$_2$ catalyst.

H$_2$ pressure has a significant effect on the substrate reactivity and product selectivity (Fig. 1). The conversion of p-CNB and selectivity to p-CAN were seen to increase with the H$_2$ pressure. The conversion of p-CNB and selectivity to p-CAN were 43% and 96.6%, respectively, at 1.0 MPa H$_2$. The conversion increased to
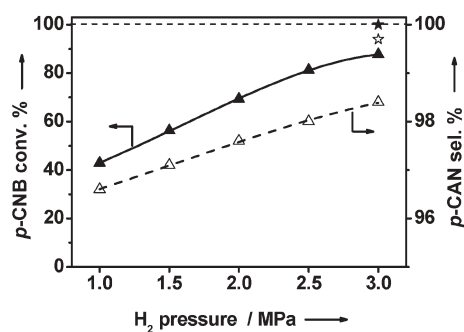
Fig. 1 Effect of H$_2$ pressure on p-CNB conversion (–▲–) and p-CAN selectivity (–△–) in the hydrogenation of p-CNB over Au/ZrO$_2$ catalyst. Other reaction conditions: 25.0 mg Au/ZrO$_2$, 2.0 mmol p-CNB in 4.0 ml ethanol (solvent), 150 °C, 1 h. The star (★, ☆) data were obtained by extending the reaction under 3.0 MPa for 3 hours.

88% and the selectivity reached 98.4% at 3.0 MPa H$_2$. When the reaction was continued for 3 h under 3.0 MPa H$_2$, we observed a complete conversion of p-CNB and a 99.7% selectivity to p-CAN (see the star data in Fig. 1); the only by-product was N-ethyl-(p-chloro)-aniline, a condensation product between p-CAN and ethanol (the solvent). These data demonstrate that the undesired hydrodechlorination can also be avoided over the Au/ZrO$_2$ catalyst even when very high H$_2$ pressure is used for the reaction.

The selective hydrogenation of CNBs also has a broad window (110–230 °C) in the reaction temperature, which is exemplified for the reaction of p-CNB under 1.0 MPa H$_2$ (Fig. 2). The increase in reaction temperature resulted in continuous increase in both p-CNB conversion and the selectivity to p-CAN without formation of any dechlorination product. The highest selectivity to p-CAN (97.5%) was obtained at *ca.* 190 °C. A slight decrease in the p-CAN selectivity was observed with further increasing the reaction temperature up to 230 °C. Still, formation of any dechlorination product was not detected at all, which demonstrates a remarkable feature of the Au/ZrO$_2$ catalyst for successfully avoiding any occurrence of the dechlorination reaction at the highest temperature used (230 °C).

When o-CNB was used as the substrate, the changes of reaction temperature and H$_2$ pressure produced similar effects on the selectivity to o-CAN. Therefore, our catalytic data prove that Au/ZrO$_2$ catalyst has the peculiarity to effect selective reduction of the nitro groups in CNB substrates while at the same time to maintain intact of the C–Cl bonds in the CNBs.
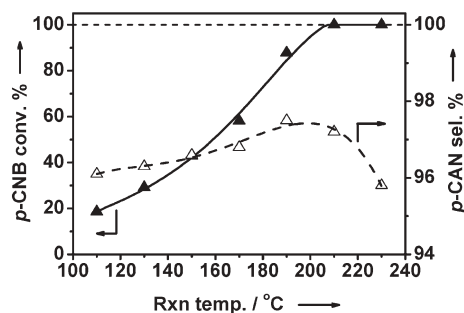
Fig. 2 Effect of temperature on p-CNB conversion (–▲–) and p-CAN selectivity (–△–) in the hydrogenation of p-CNB over Au/ZrO$_2$ catalyst under 1.0 MPa H$_2$. Other reaction conditions are the same as in Fig. 1.

Table 2 Reusability of Au/ZrO$_2$ catalyst for the selective hydrogenation of p-CNB[a]

| Catalyst | Cycle | Conv. (%) | Product sel. (%) | | Dechlor. (%) |
			p-CAN	Others[b]	
Au/ZrO$_2$	1	100	99.4	0.6	0
	2	61	98.9	1.1	0
	3	49	98.7	1.3	0
Au/ZrO$_2$-R	1	100	98.3	1.7	0
	2	89	99.2	0.8	0
	3	86	99.3	0.7	0
	4	84	99.1	0.9	0

[a] Reaction conditions: 25.0 mg catalyst, 2.0 mmol substrate in 4.0 ml ethanol (solvent), 150 °C, 1.0 MPa H$_2$, 5 h. [b] See footnote c in Table 1.

The Au/ZrO$_2$ catalyst was reduced for 2 hours at 200 °C in a flow of 5% H$_2$/Ar. XPS measurements [ESI† Fig. S2] showed that the as-prepared fresh Au/ZrO$_2$ catalyst (unreduced) contained coexisting Au^0 and Au^{1+} at a Au^0/Au^{1+} ratio of *ca.* 7.0, whereas gold in the reduced catalyst (coded as Au/ZrO$_2$-R) was almost 100% in the metallic (Au^0) state. This Au/ZrO$_2$-R catalyst was also tested for the hydrogenation of p-CNB at 150 °C under 1.0 MPa H$_2$. The p-CNB conversion and p-CAN selectivity were 46% and 97.2%, respectively, after 1 hour reaction, which are slightly higher than those over the unreduced Au/ZrO$_2$ catalyst (see the data given in the first row of Table 1), which suggests that the metallic surface Au^0 sites on the Au/ZrO$_2$ catalyst were acting as the catalytic sites in the hydrogenation of CNBs.[18] However, a remarkable difference was observed between the two catalysts when they were compared for reusability in the reactions. For instance, the hydrogenation of p-CNB was performed for 5 h to ensure a complete substrate conversion; the catalyst was then carefully recovered from the reactor by filtration and washing with ethanol. As can be seen in Table 2, the unreduced catalyst Au/ZrO$_2$ showed continued loss of catalytic activity after each recovery. In contrast, the reduced catalyst Au/ZrO$_2$-R exhibited a much better reusability for the reaction. Thus, the reusability of Au/ZrO$_2$ catalyst can be significantly improved with pre-reduction.

A possible reason for the activity decline of the as-prepared fresh Au/ZrO$_2$ catalyst (unreduced) could be a leaching of Au by the reaction liquids. We checked the Au content in the recovered catalyst and found that there was no loss of Au in the recovered catalyst. Another possibility for the activity loss would be aggregation of the Au particles. TEM measurements showed that the average size of Au particles of 7.0 nm in the recovered Au/ZrO$_2$ sample was significantly bigger than that in the as-prepared fresh (un-reacted) Au/ZrO$_2$ catalyst (4.0 nm) [ESI† Fig. S1]. It is known that catalysis by gold is sensitive to the size of Au particle,[7] which could also be the case in this present work. The improved reusability of the prereduced Au/ZrO$_2$-R catalyst (Table 2) would mean that aggregation of the Au particles in this pre-reduced catalyst was not that significant during the reaction [ESI† Fig. S3]. We believe that there is an open chance to further improve the reusability of gold catalyst by optimizing the size distribution of Au particles with the selection of support material and preparation procedure. Also, with a proper search for alternative unreactive solvent (ethanol can also be reductive), it would be possible to achieve with gold catalyst a 100% CAN selectivity at complete CNBs conversion[19] since all of the by-products except N-ethyl-chloroaniline can be further hydrogenated to the desired CANs.

Conclusions

This work shows that Au nanoparticles on ZrO$_2$ are efficient catalysts for the selective reduction of the nitro groups in CNBs with H$_2$ while the C–Cl bonds in the same CNB molecules maintain intact. Proper pre-reduction with hydrogen of the as-prepared fresh Au/ZrO$_2$ catalyst significantly improves the catalyst reusability for the synthesis of CANs from CNBs. Further optimization of gold catalyst with the control of gold particle size distribution and gold-support interaction could develop a practical gold catalyst for a green synthesis of various haloanilines from their corresponding halonitroaromatics.

Notes and references

1 H. U. Blaser, U. Siegrist and H. Steiner, in *Aromatic Nitro Compounds: Fine Chemicals through Heterogeneous Catalysis*, VCH, Weinheim, 2001, p. 389; R. S. Downing, P. J. Kunkeler and H. van Bekkum, *Catal. Today*, 1997, **37**, 121.
2 M. Chatterjee, A. Chatterjee and Y. Ikushima, *Green Chem.*, 2004, **6**, 114; J. P. Mikkola, P. Virtanen and H. Karhu, *Green Chem.*, 2006, **8**, 197; Q. X. Shi, R. W. Lu and K. Jin, *Green Chem.*, 2006, **8**, 868.
3 B. Coq, A. Tijani, R. Dutartre and F. Figuéras, *J. Mol. Catal. A: Chem.*, 1993, **79**, 253.
4 Z. K. Yu, S. J. Liao, Y. Xu, B. Yang and D. R. Yu, *J. Chem. Soc., Chem. Commun.*, 1995, 1155.
5 B. J. Zuo, Y. Wang, Q. L. Wang and J. L. Zhang, *J. Catal.*, 2004, **222**, 493.
6 Y. C. Liu, C. Y. Huang and Y. W. Chen, *Ind. Eng. Chem. Res.*, 2006, **45**, 62.
7 G. C. Bond, C. Louis, D. T. Thompson, *Catalysis by Gold*, Imperial College Press, London, 2006; M. Haruta, *Gold Bull.*, 2004, **37**, 27.
8 M. Haruta, N. Yamada, T. Kobayashi and S. Iijima, *J. Catal.*, 1989, **115**, 301; H. H. Kung, M. C. Kung and C. K. Costello, *J. Catal.*, 2003, **216**, 425.
9 M. Holscher, *Green Chem.*, 2006, **8**, 762; C. H. Christensen, B. Jorgensen, J. Rass-Hansen and K. Egeblad, *Angew. Chem., Int. Ed.*, 2006, **45**, 4648.
10 M. D. Hughes, Y. J. Xu, P. Jenkins and P. McMorn, *Science*, 2005, **437**, 1132.
11 G. J. Hutchings, *Gold Bull.*, 2004, **37**, 3.
12 M. Okumura, T. Akita and M. Haruta, *Catal. Today*, 2002, **74**, 265.
13 X. Zhang, H. Shi and B. Q. Xu, *Angew. Chem., Int. Ed.*, 2005, **44**, 7132.
14 R. Zanella, C. Louis and S. Giorgio, *J. Catal.*, 2004, **223**, 328; A. Arcadi, G. Bianchi and S. Di Giuseppe, *Green Chem.*, 2003, **5**, 64.
15 A. Corma and P. Serna, *Science*, 2006, **313**, 332; Y. Y. Chen, J. S. Qiu and X. K. Wang, *J. Catal.*, 2006, **242**, 227.
16 X. Zhang, H. Shi and B. Q. Xu, *Catal. Today*, 2007, DOI: 10.1016/j.cattod.2007.02.016.
17 S. F. Yin and B. Q. Xu, *ChemPhysChem*, 2003, **4**, 277.
18 We showed previously that the gold cations in the Au/ZrO$_2$ samples containing less than 1.0% Au were Au^{3+} and were highly active for the hydrogenation of 1,3-butadiene.[13,16] The Au^{3+} ions were found not active for the hydrogenation of nitrobenzenes (unpublished data). The presence of Au^{1+} ions in the present 3.8% Au/ZrO$_2$ would suggest that the nature of cationic gold depends on the overall loading of the metal.
19 Toluene was tested as an alternative of the ethanol solvent during the revision of this communication. Indeed, we obtained a 100% p-CAN selectivity at 100% p-CNB conversion over the as-prepared fresh Au/ZrO$_2$ catalyst [ESI† Table S1].

Green synthesis of silver nanoparticles using *Capsicum annuum* L. extract†

Shikuo Li, Yuhua Shen,* Anjian Xie,* Xuerong Yu, Lingguang Qiu, Li Zhang and Qingfeng Zhang

Silver nanoparticles (NPs) were rapidly synthesized by treating silver ions with a *Capsicum annuum* L. extract. The reaction process was simple and convenient to handle, and was monitored using ultraviolet-visible spectroscopy (UV-vis). The effect of *Capsicum annuum* L. proteins on the formation of silver NPs was investigated using X-ray photoemission spectroscopy (XPS), electrochemical measurements, Fourier-transform infrared spectroscopy (FTIR) and differential spectrum techniques. The morphology and crystalline phase of the NPs were determined from transmission electron microscopy (TEM), selected area electron diffraction (SAED) and X-ray diffraction (XRD) spectra. The results indicated that the proteins, which have amine groups, played a reducing and controlling role during the formation of silver NPs in the solutions, and that the secondary structure of the proteins changed after reaction with silver ions. The crystalline phase of the NPs changed from polycrystalline to single crystalline and increased in size with increasing reaction time. A recognition–reduction–limited nucleation and growth model was suggested to explain the possible formation mechanism of silver NPs in *Capsicum annuum* L. extract.

Introduction

Noble metal nanoparticles (NPs) are well known to have important applications in the fields of electronic, magnetic, optoelectronics, and information storage.[1–4] It is now understood that the intrinsic properties of a noble metal NP are determined by its size, shape, composition, crystallinity, and structure (solid or hollow). Silver NPs, as a significant member of the noble metal NPs, are excellent substrates for surface enhanced Raman scattering (SERS)[5] to probe single molecules, and are excellent as catalysts for accelerating some chemical reactions.[6]

A number of approaches are available for the synthesis of silver NPs. For example, silver ions are reduced by chemical,[7] electrochemical,[8] radiation,[9] and photochemical methods,[10] and Langmuir–Blodgett,[11,12] and biological techniques.[13] Among those methods, biological syntheses are not only a good way to fabricate benign nanostructure materials, but also to reduce the use or generation of hazardous substances to human health and the environment. This approach provides a facile and convenient entry to producing multiple inorganic NPs. People have used purified natural materials to prepare noble metal NPs, such as Nadagouda and Varma who used vitamin B2 to synthesize gold and platinum NPs with interesting morphologies.[14] John and co-workers have used vitamin C to prepare gold NPs in molecular gels and liquid crystal systems.[15] And our group has used vitamin E to prepare silver NPs using the Langmuir–Blodgett technique.[11]

Now, there is more and more interest in green synthesis research.

Synthesis using bio-organisms, especially plants that secrete the functional molecules for the reaction, is compatible with the green chemistry principles: the bio-organism is (i) eco-friendly as are (ii) the reducing agent employed, and (iii) the capping agent in the reaction. There are some examples of synthesizing nanomaterials using plants, including the use of live alfalfa to synthesize Au and Ag NPs,[16] the secretions from germinating chickpea seeds to biosynthesize $CaCO_3$ crystals,[17] and the broth of lemongrass and geranium leaves to synthesize Au and Ag NPs.[18,19] *Capsicum annuum* L. is a traditional vegetable in China and northern America, and is largely cultivated in many countries. It is available in supermarkets and is inexpensive. In addition, no toxicity, compared to other reducing agents, makes it an ideal multifunctional agent for the production of nanomaterials. The *Capsicum annuum* L. extract contains a lot of biomolecules, such as proteins/enzymes, polysaccharides, amino acids and vitamins, *et al.*,[20,21] which could be used as reductants to react with silver ions and as scaffolds to direct the formation of silver NPs in solution. To the best of our knowledge, the use of plant extracts at room temperature for the green synthesis of noble metal NPs, such as silver NPs, has not been reported. It is important to study the formation of NPs in *Capsicum annuum* L. extracts for the understanding of the mechanism of biological synthesis and for exploring new green ways to prefabricate nanomaterials.

Results and discussion

The UV-vis spectrum of the *Capsicum annuum* L. extract is shown as an inset in Fig. 1a; the peaks are typical of the absorptions of proteins. The peak at 210 nm was assigned to the strong absorption of peptide bonds in the extract. The absorption at 280 nm indicated the presence of tyrosine, tryptophan, and/or phenylalanine residues in the proteins,

School of Chemistry and Chemical Engineering, Anhui University, Hefei 230039, China. E-mail: s_yuhua@163.com; anjx@163.com; Fax: +86-551-5107342; Tel: +86-551-5108090

† Electronic supplementary information (ESI) available: Details of the extracting process of *Capsicum annuum* L., figures of N1s and O1s core level spectra, and the frequencies and the percentages of the secondary structures of *Capsicum annuum* L. proteins. See DOI: 10.1039/b615357g
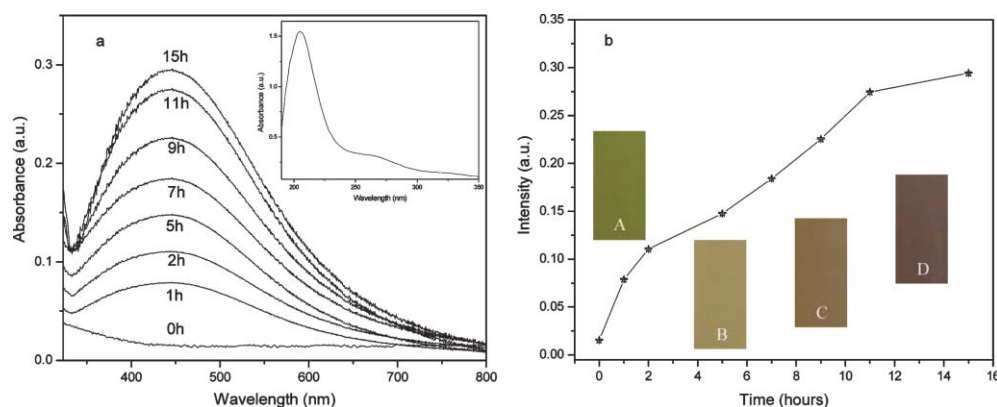
Fig. 1 (a) UV-vis spectra of the solution (I) recorded as a function of time; the inset is the UV-vis spectrum of *Capsicum annuum* L. extract. (b) Plot of the intensity of the surface plasmon resonance at 440 nm against the reaction time; the insets are photos of the solution changes with reaction time (A, B, C and D at 0, 5, 9 and 11 h, respectively).

which are known to interact with silver ions.[22] Fig. 1a displays the UV-vis spectra of solution (I) as a function of reaction time. The strong resonance centered at 440 nm was clearly observed and increased in intensity with time. It might arise from the excitation of longitudinal plasmon vibrations in silver NPs in the solution. The results were in accordance with the report of Naik *et al.*[13] Fig. 1b presents a plot of the plasmon intensity at 440 nm against reaction time. It can be seen easily that the plasmon intensity at the reaction time of 11 h is near to that at 15 h, meaning completion of the reaction. The insets of Fig. 1b present the color changes in the mixture solution

over the reaction time. The extract was light green before reaction with silver ions (A) and changed to pale yellow (B), yellow (C) and dark brown (D) after reaction times of 5, 9 and 11 h, respectively, and then the color did not change any more with reaction time. The characteristic brown color of silver solutions provided a convenient spectroscopic signature to indicate their formation.

Fig. 2 shows typical TEM micrographs of silver NPs synthesized using *Capsicum annuum* L. extract at different reaction times and concentrations of silver ions. Fig. 2a is the TEM graph of silver NPs in solution (I) with a reaction time of
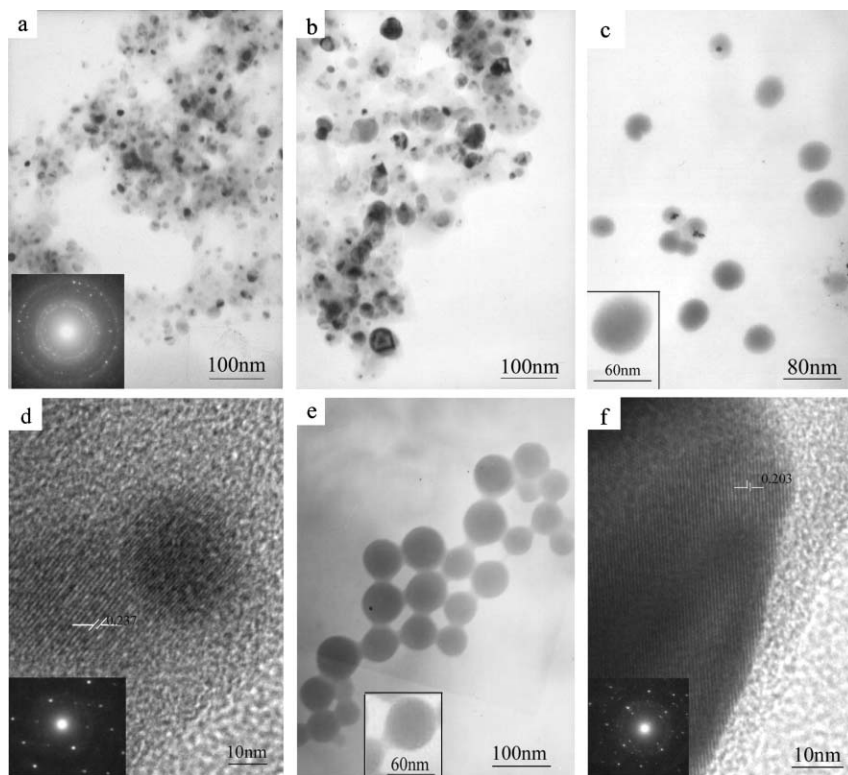
Fig. 2 (a), (b), and (c) TEM images of silver NPs synthesized in solution (I), with reaction times of 5, 9, and 13 h, respectively; (d) HRTEM of the silver NPs of (c); (e) NPs synthesized in solution (II) with a reaction time of 13 h; (f) HRTEM of the silver NPs of (e). In (a), (d) and (f), the insets are the SAED patterns of the silver NPs.

5 h. The morphology of the NPs was spherical with an average size of 10 ± 2 nm. The inset SAED pattern revealed that the diffraction rings from inner to outer, with *d*-spacings of 0.236, 0.2202, 0.141, and 0.121, could be indexed as (111), (200), (220), and (311) reflections, respectively, corresponding to face-centered cubic (fcc) silver. The diffraction rings also suggested the NPs were polycrystalline. When the reaction time increased to 9 h and 13 h, the size of the NPs increased to 25 ± 3 nm (Fig. 2b) and 40 ± 5 nm (Fig. 2c), respectively. It was noticeable that the edges of the particles were lighter than the centers (shown as an inset in Fig. 2c), suggesting that biomolecules, such as proteins in *Capsicum annuum* L. capped the silver NPs. From the HRTEM (Fig. 2d), the thickness of the capping protein was about 3 nm, and the fringe spacing (0.237 nm) was in agreement with the spacing of the [111] lattice. The inset is the SAED pattern of the single particle; the sharp diffraction spots clearly suggest the particle is of single-crystal quality, and the plane could be indexed to the fcc silver. The representative image of silver NPs synthesized in solution (II), with an increased concentration of silver ions, is shown in Fig. 2e. The particle morphology was also spherical, and the sizes were in the range 30 to 70 nm, with an average size of 45 ± 3 nm. The distribution of these particles was very interesting: they were connected to each other and were arranged in a regular manner. The inset is a magnification of part of Fig. 2e. It is clearly seen that proteins are present among the particles and are adhered to their surfaces. An HRTEM image (Fig. 2f) further confirmed that the silver NPs were capped by biomolecules. The thickness of the coating protein (10 nm) was thicker than that found in Fig. 2d (3 nm). The lattice spacing was about 0.203 nm between the [200]

planes, consistent with fcc silver. The SAED pattern indicated that the particle was also single-crystalline phase, with (111), (200), (220), and (311) planes. The above results suggested that the size of the spherical silver NPs increased with reaction time, and the crystalline phase of the particles translated from polycrystalline to single crystalline. However, the morphology and crystalline phase of the silver NPs was not affected by the increase in silver ions.

Fig. 3 displays the XPS spectra of silver (I), produced using *Capsicum annuum* L. extract. The general scan spectrum showed the presence of strong C1s, O1s, N1s and Ag3d core levels (shown in Fig. 3a). The C1s core level could be decomposed into three chemically distinct components that are present in the protein molecules (Fig. 3b). In addition to the C1s peak at 284.8 eV BE (major peak), which corresponds to the carbon atoms within the phenyl rings of tyrosine, tryptophan, and/or phenylalanine residues of the protein, peaks at 286.4 and 288.3 eV BE were observed. The higher BE (binding energy) peak at 288.3 eV was attributed to electron emission from carbons in carbonyl groups (carbonyl carbons of the proteins/enzymes or polysaccharides),[23] the lower peak at 286.4 eV BE was most likely from carbons α to the carbonyl carbons. The N1s (see ESI, Fig. S1a†) could also be resolved into two components, centered at 399.8 and 403.2 eV, and were assigned to neutral amine and protonated amine groups (N$^+$) present in the protein moiety. The O1s core level (see ESI, Fig. S1b†) was broad and centered at 532.1 eV, which was assigned to the carboxylate groups. The Ag3d core level spectrum is shown in Fig. 3c, and is resolved into two spin–orbit components, Ag3d$_{5/2}$ and Ag3d$_{3/2}$, peaks which occur at BEs of 368.0 and 374.0 eV, respectively. There was little
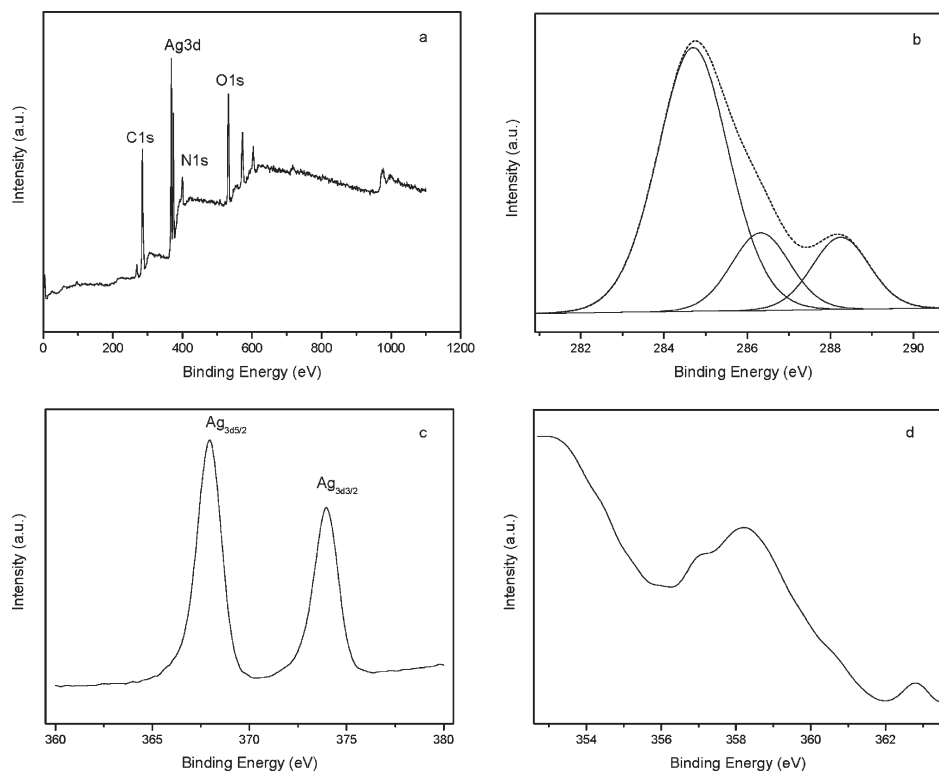
Fig. 3 XPS survey (a), C1s (b), Ag3d (c), and AES (d) core level spectra recorded from silver (I).
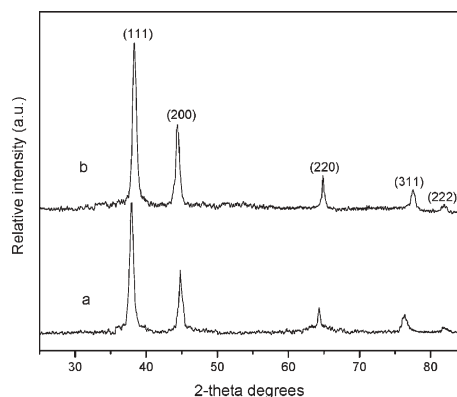
Fig. 4 XRD patterns of silver NPs synthesized by *Capsicum annuum* L. extract: (a) reaction solution (I), and (b) solution (II).

Fig. 5 FTIR spectra of *Capsicum annuum* L. extract (a), solution (I) (b) and solution (II) (c).

difference between the binding energy of Ag and Ag$^+$. The formation of Ag or Ag$^+$ cannot be judged only through the binding energy of Ag$_{3d3/2}$. The Ag$_{3d}$ Auger core level spectrum (AES) was observed at 358.3 eV (shown in Fig. 3d). The summation of binding energy and Auger energy was 726.3 eV, which indicated the formation of Ag.[24] Thus it was concluded from XPS measurements that the silver ions were reduced to the metallic form, and the silver NPs were capped by protein. The results confirmed the hypothesis mentioned in the TEM analysis.

Fig. 4 shows XRD patterns of silver (I) (a), and (II) (b), respectively. The Bragg reflections show that the two samples were in the same space group. The peaks were assigned to diffraction from the (111), (200), (220), (311) and (222) planes of face-centered cubic (fcc) silver, which were in good agreement with reference to the unit cell of the fcc structure (JCPDS File No. 87-0720) with a lattice parameter of a = 4.077 Å. It is worth noting that the relative intensity of the (200) to (111) diffraction peaks in Fig. 4a, b (0.50, 0.54) was higher than the conventional value (0.45). This result indicated that the synthesized silver NPs in our system were enriched in {100} facets, and thus their {100} planes tended to be preferentially oriented parallel to the surface of the supporting substrate.[25] In addition, the intensity ratio of the (200) to (111) peaks of silver (II) (0.54) was higher than for silver (I) (0.50), which suggested that {100} planes were easier to grow in a higher concentration of the silver ion solution by allowing more silver atoms to accumulate onto them. Meanwhile, the size of these particles could be estimated from the Debye–Scherrer equation (eqn (1)) by determining the width of the (111) Bragg reflection.[26]

$$L = \frac{k\lambda}{\beta \cos \theta} \qquad (1)$$

k is the Scherrer constant, λ is the wavelength of the X-ray, β and θ are the half width of the peak and half of the Bragg angle, respectively. Therefore the size (L) of the particles could be easily estimated; the sizes of silver NPs (I) and (II) were about 42.3 and 45.9 nm, respectively. The results were consistent with the TEM results.

Fig. 5 shows the FTIR spectra for *Capsicum annuum* L. extract (a), reaction solution (I) (b), and solution (II) (c). There
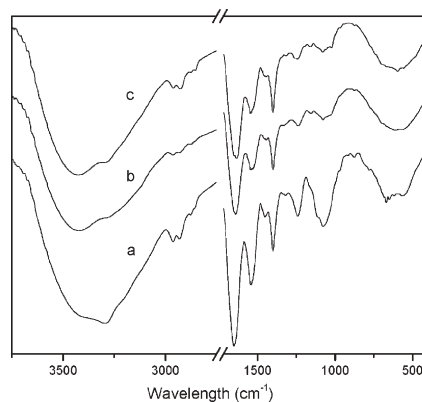
are several characteristic protein bands in Fig. 5a. 1652 cm^{-1} is the stretching vibration of amide I C=O groups in *Capsicum annuum* L. proteins.[27] The peaks at 1542 and 1241 cm^{-1} are the stretching vibration of N–H groups and the bending vibration of C–N groups, amide II and III bands, in the proteins. 671 cm^{-1} is the plane bending vibration of N–H groups in the proteins. 1401 cm^{-1} and 1078 cm^{-1} are the bending vibration of COH groups and the antisymmetric stretching band of C–O–C groups of polysaccharides and/or chlorophyll. The bands at 2962 and 2873 cm^{-1} are characteristic of stretching vibrations of methyl groups. The peak at 3295 cm^{-1} is the characteristic band of hydrogen bonded NH groups. After reaction with silver ions (Fig. 5b and c), the strength of the peak at 3426 cm^{-1} corresponded with that seen for the proteins/enzymes or polysaccharide components, and was assigned to the vibration of –N–N– groups. The absence of the 671 cm^{-1} peak in Fig. 5b and 5c indicated that the reduction of the silver ions was coupled to the oxidation of the amine components. Meanwhile, the intensity of the above mentioned hydrogen bonded NH groups weakened obviously. These changes in the infrared spectra suggested that protein with functional amine groups might act as a reductant. As we know that the *Capsicum annuum* L. extract contains a lot of reductive amino acids and vitamins; they may have participated in the reduction reaction as well. After reaction, the amide I band at 1652 cm^{-1} has broadened, which indicates capping of silver NPs by proteins. A similar phenomenon was also observed by Shankar *et al.*[19] It is known that proteins can bind to gold NPs, either through free amine groups or cysteine residues.[28] A similar mechanism could be operating in the present case, where proteins extracted from *Capsicum annuum* L. coat the silver NPs and stabilize them. Fig. 5c is similar to Fig. 5b, indicating that the reaction that occurred in solution (II) was the same as that in solution (I).

It is known that structure changes in proteins can reveal more detailed information about interactions with silver ions. The secondary structures of *Capsicum annuum* L. proteins before and after reaction with silver ions were studied by second derivative techniques followed by curve fitting[29] (shown in Fig. 6a, b). The bands (see ESI, Table 1†) at 1603–1639 and ∼1691; 1654–1665; 1679–1680; and ∼1645 cm^{-1} were assigned to β-sheet, α-helix, β-turn and random coil of the
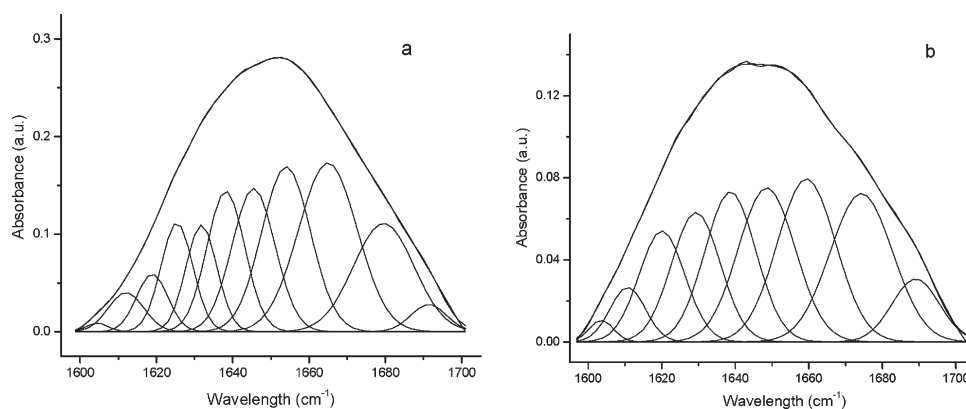
Fig. 6 Second derivative and Gaussian curve fitting of the amide I band of *Capsicum annuum* L. protein (a) and the reaction solution product (I) (b).

proteins, respectively. The β-sheet, α-helix, β-turn and random coil percentages of the proteins were 35.1, 12.8, 39.1 and 13.0%, respectively. After reaction with silver ions, the percentages of β-sheet, β-turn and random coil all increased, while α-helix significantly decreased (see ESI, Table 2†). The results suggested that the reaction of the protein with silver ions makes its conformation disordered.

To explore the mechanism of the reaction, we examined the electrochemical behavior of the extract. Fig. 7a shows the typical cyclic voltammogram (CV) of the *Capsicum annuum* L. extract recorded at a scan rate of 0.02 V s^{-1} in the potential window between −0.70 and 0.90 V. It can be seen clearly from the dashed line in Fig. 7a that there was no redox activity at the Au electrode in pure water in the potential range. However, there appeared to be an oxidation peak (solid line in Fig. 7a) at the potential of about 0.50 V in the *Capsicum annuum* L. extract, which possibly arose from the redox activity of amine residues of the proteins/enzymes in the *Capsicum annuum* L. extract.[30] In general, azo components exhibit several oxidation and reduction peaks, which arise from the cleavage of the azo bonds. But in pure amino acids or protein systems, there are only quasi-irreversible redox peaks present in the potential range.[31] To extract the information from the oxidation peak, differential pulse voltammetry (DPV) was recorded with a pulse width of 0.001 s in the potential window between −0.15 and 0.85 V (shown in Fig. 7b), which obviously displays the oxidation present in the *Capsicum annuum* L. extract. The

appearance of oxidation suggested that the amine residues of proteins/enzymes might contribute to an effective process for obtaining electrons on the Au electrode. The results of CV and DPV illustrated that the reductive materials in the *Capsicum annuum* L. extract could gain electrons and be oxidized in the surrounding of an electric field.

According to the nucleation and growth theory,[32] to form a spherical particle, the overall free energy change (ΔG) must be overcome. ΔG is the sum of the free energy due to the formation of a new volume and the free energy due to the new surface created:

$$\Delta G = -\frac{4}{V}\pi r^3 k_B T \ln(S) + 4\pi r^2 \gamma \qquad (2)$$

where V is the molecular volume of the precipitated species, r is the radius of the nucleus, k_B is the Boltzmann constant, S is the saturation ratio, and γ is the surface free energy per unit surface area, respectively. From eqn (2), it follows that a decrease in surface energy (γ) or an increase in supersaturation (S) is helpful to the formation of silver NPs. In our reaction solutions, the interactions of *Capsicum annuum* L. proteins with silver ions made the concentration of silver ions rich around the negatively charged groups, and the protein adhered to the silver nuclei, leading to a lower surface energy of the crystal lattice. Therefore, the effect of protein recognition could make the reaction occur more easily.
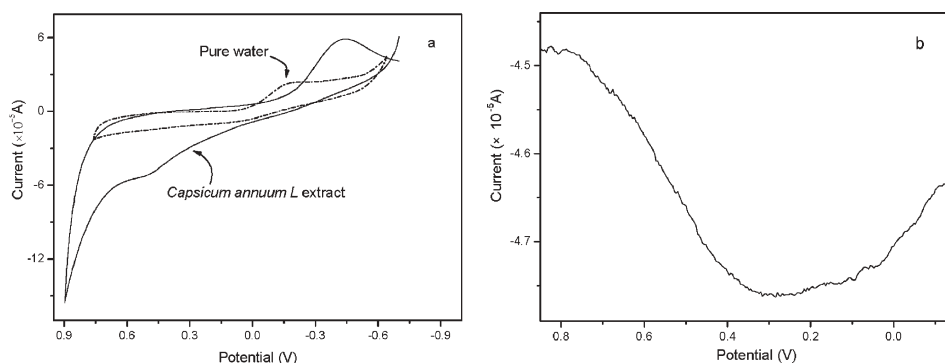
Fig. 7 The CV (a) and DPV (b) of the *Capsicum annuum* L. extract recorded at a scan rate of 0.02 V s^{-1} in the potential window between −0.70 and 0.90 V.
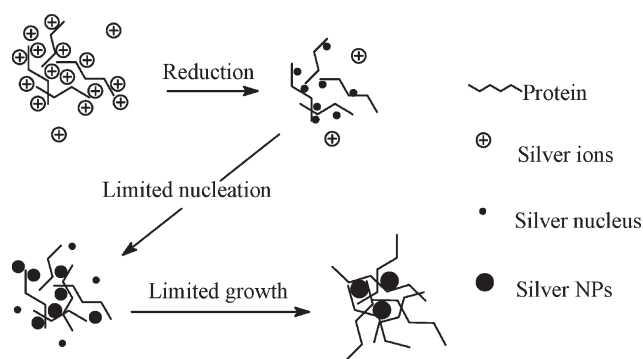
Fig. 8 Schematic representation of the formation process of silver NPs in the reaction solutions.

According to the literature,[32,33] we supposed the model of recognition–reduction–limited nucleation and growth to explain the silver NP formation mechanism in the reaction solutions. The schematic representation is shown in Fig. 8. First, silver ions were trapped on the surface of proteins in the *Capsicum annuum* L. extract *via* electrostatic interactions. This stage was the recognition process. Thereafter, silver ions were reduced by proteins extracted from *Capsicum annuum* L., leading to the changes in the secondary structures of the proteins and formation of silver nuclei, which subsequently grew by further reduction of silver ions and accumulation on these nuclei. The flexible linkage of the proteins and the large numbers of biomolecules ranged in the reaction solutions might have led to the isotropic growth and the formation of the most stable spherical silver NPs. With an increase in aging time, large sized silver NPs formed and the crystalline phase changed from polycrystalline to single crystalline through Ostwald ripening.

Conclusions

A rapid, eco-friendly synthesis process for silver NPs using proteins extracted from *Capsicum annuum* L. has been demonstrated. The reduction of silver ions and stabilization of the silver NPs was thought to occur through the participation of proteins. With increasing reaction time, the size of the silver NPs increased and the crystalline nature of the NPs changed from polycrystalline to single crystalline. Meanwhile the supposed recognition–reduction–limited nucleation and growth model has been used to explain the formation mechanism of silver NPs in *Capsicum annuum* L. extract. Most importantly, the reaction was simple and convenient to handle, and it is believed that it has advantages over other biological syntheses.

Experimental section

Materials and methods

The *Capsicum annuum* L. used in this experiment was fresh and green, and was purchased from the supermarket of Anhui University. Silver nitrate, acetone and anhydrous alcohol were all received from Shanghai Reagent Co., China. The above reagents were of analytical purity and were used without

further purification. Double distilled water was used in this experiment.

Synthesis of silver NPs using *Capsicum annuum* L. extract

Prior to an experiment, the cleaned *Capsicum annuum* L. was put into a juice extractor to extract the juice, which was collected for the subsequent reaction (details shown in ESI†). In a typical experiment, 10 ml of a 0.01 M aqueous $AgNO_3$ solution was added to 50 ml of the above extract. The mixture was called reaction solution (I). During the reaction, part of the solution was taken out for measurements by UV-vis spectroscopy and TEM at different times. The remnants of the reaction mixture were separated by eccentricity of 12 000 rpm, and then washed with double distilled water, acetone and absolute ethanol, several times each, and dried under vacuum at 20 ± 2 °C. The product was called silver (I). When the concentration of $AgNO_3$ was adjusted to 0.1 M (the other experimental parameters were similar to the above-mentioned operation), the formed mixture and solid product were called reaction solution (II) and silver (II) respectively.

Characterization

Cyclic voltammograms and differential pulse voltammetry on the *Capsicum annuum* L. extract were carried out on an Autolab PGSTAT30 (ECO CHEMIE) instrument, using a Au electrode as the working electrode, Pt flag as the counter electrode and Ag/AgCl as the reference electrode, and without adding any electrolyte for this experiment. UV-vis spectra were measured using a TU-1901 model UV-vis double beam spectrophotometer (Beijing Purkinje General Instrument Co., Ltd, China). FTIR spectra were performed and recorded with a Fourier-transform infrared spectrophotometer Nicolet 870 between 4000 and 400 cm^{-1}, with a resolution of 4 cm^{-1}. XPS analysis was carried out on a VG ESCALAB MKII instrument at a pressure greater than 10^{-6} Pa. The general scan C1s, N1s, O1s and Ag3d core level spectra were recorded with un-monochromatized Mg Kα radiation (photon energy = 1253.6 eV). The core level binding energies (BEs) were aligned with respect to the C1s BE of 285.0 eV. XRD was performed on a MAP18XAHF instrument, with the X-ray diffractometer using Cu Kα radiation (λ = 1.5 Å) at a scan rate of 0.05° $2\theta\ s^{-1}$ to determine the crystalline phase. The accelerating voltage and applied current were 35 kV and 20 mA, respectively (MAC Science, Japan). TEM, SAED and HRTEM were performed on JEM model 100SX and 2010 electron microscopes (Japan Electron Co.) and operated at accelerating voltages of 80 and 200 kV, respectively.

All experiments were carried out at room temperature (20 ± 2 °C).

References

1 M. Grätzel, *Nature*, 2001, **414**, 338.
2 M. Okuda, Y. Kobayashi, K. Suzuki, K. Sonoda, T. Kondoh, A. Wagawa, A. Kondo and H. Yoshimura, *Nano Lett.*, 2005, **5**, 991.
3 J. Dai and M. L. Bruening, *Nano Lett.*, 2002, **2**, 497.
4 C. B. Murray, S. Sun, H. Doyle and T. Betley, *MRS Bull.*, 2001, **26**, 985.
5 A. Tao, F. Kim, Y. Sun, Y. Xia and P. Yang, *Nano Lett.*, 2003, **3**, 1229.
6 Y. Shiraishi and N. Toshima, *J. Mol. Catal. A: Chem.*, 1999, **141**, 187.
7 Y. Sun, Y. Yin, B. T. Mayers, T. Herricks and Y. Xia, *Chem. Mater.*, 2002, **14**, 4736.
8 B. Yin, H. Ma, S. Wang and S. Chen, *J. Phys. Chem. B*, 2003, **107**, 8898.
9 N. M. Dimitrijevic, D. M. Bartels, C. D. Jonah, K. Takahashi and T. Rajh, *J. Phys. Chem. B*, 2001, **105**, 954.
10 A. Callegari, D. Tonti and M. Chergui, *Nano Lett.*, 2003, **3**, 1565.
11 L. Zhang, Y. H. Shen, A. J. Xie, S. K. Li, B. K. Jin and Q. F. Zhang, *J. Phys. Chem. B*, 2006, **110**, 6615.
12 A. Swami, P. R. Selvakannan, R. Pasricha and M. Sastry, *J. Phys. Chem. B*, 2004, **108**, 19269.
13 R. R. Naik, S. J. Stringer, G. Agarwal, S. Jones and M. O. Stone, *Nat. Mater.*, 2002, **1**, 169.
14 M. N. Nadagouda and R. S. Varma, *Green Chem.*, 2006, **8**, 516.
15 P. K. Vemula, U. Aslam, V. A. Mallia and G. John, *Chem. Mater.*, 2007, **19**, 138.
16 J. L. Gardea-Torresdey, E. Gomez, J. R. Peralta-Videa, J. G. Parsons, H. Troiani and M. J. Yacaman, *Langmuir*, 2003, **19**, 1357.
17 D. Rautaray, A. Sanyal, A. Bharde, A. Ahmad and M. Sastry, *Cryst. Growth Des.*, 2005, **5**, 399.
18 S. S. Shankar, A. Rai, A. Ahmad and M. Sastry, *Chem. Mater.*, 2005, **17**, 566.
19 S. S. Shankar, A. Ahmad and M. Sastry, *Biotechnol. Prog.*, 2003, **19**, 1627.
20 O. Collera-Zuniga, F. G. Jimenez and R. M. Gordillo, *Food Chem.*, 2005, **90**, 109.
21 B. H. Jagadeesh, T. N. Prabha and K. Srinivasan, *Plant Sci. (Amsterdam, Neth.)*, 2004, **167**, 1263.
22 L. C. Gruen, *Biochim. Biophys. Acta*, 1975, **368**, 270.
23 S. Senapati, A. Ahmad, M. I. Khan, M. Sastry and R. Kumar, *Small*, 2005, **1**, 517.
24 C. D. Wagner, W. M. Riggs, L. E. Davis, J. F. Moulder and G. E. Muilenberg, *Handbook of X-ray Photoelectron Spectroscopy*, Perkin-Elmer Corporation Physical Electronics Division, Eden Prairie, MN, 1979.
25 Y. G. Sun and Y. N. Xia, *Science*, 2002, **298**, 2176.
26 H. Borchert, E. V. Shevchenko, A. Robert, I. Mekis, A. Kornowski, G. Grubel and H. Weller, *Langmuir*, 2005, **21**, 1931.
27 N. Bouropoulos, S. Weiner and L. Addadi, *Chem.–Eur. J.*, 2001, **7**, 1881.
28 A. Gole, C. Dash, V. Ramakrishnan, S. R. Sainkar, A. B. Mandale, M. Rao and M. Sastry, *Langmuir*, 2001, **17**, 1674.
29 A. E. Andreeva and I. R. Karamancheva, *J. Mol. Struct.*, 2001, **565–566**, 177.
30 K. Kashiwagi, K. Uchiyama, F. Kurashima, J. Anzai and T. Osa, *Anal. Sci.*, 1999, **15**, 907.
31 A. Zille, P. Ramalho, T. Tzanow, R. Millward and A. Cavaco-Paulo, *Biotechnol. Prog.*, 2004, **20**, 1588.
32 (*a*) C. Burda, X. Chen, R. Narayanan and M. A. El-Sayed, *Chem. Rev.*, 2005, **105**, 1025; (*b*) X. S. Fang, C. H. Ye, X. S. Peng, Y. H. Wang, Y. C. Wu and L. D. Zhang, *J. Mater. Chem.*, 2003, **13**, 3040.
33 (*a*) J. T. McCann, D. Li and Y. Xia, *J. Mater. Chem.*, 2005, **15**, 735; (*b*) B. Mayers and Y. Xia, *J. Mater. Chem.*, 2002, **12**, 1875; (*c*) U. Jeong, P. H. C. Camargo, Y. H. Lee and Y. Xia, *J. Mater. Chem.*, 2006, **16**, 3893; (*d*) F. Kim, S. Connor, H. Song, T. Kuykendall and P. Yang, *Angew. Chem., Int. Ed.*, 2004, **43**, 3637; (*e*) X. S. Fang, C. H. Ye, L. D. Zhang, J. X. Zhang, J. W. Zhao and P. Yan, *Small*, 2005, **1**, 422; (*f*) X. S. Fang, C. H. Ye, L. D. Zhang, Y. H. Wang and Y. C. Wu, *Adv. Funct. Mater.*, 2005, **15**, 63; (*g*) X. S. Fang and L. D. Zhang, *J. Mater. Sci. Technol.*, 2006, **22**, 1–18; (*h*) C. J. Murphy, A. M. Gole, S. E. Hunyadi and C. J. Orendorff, *Inorg. Chem.*, 2006, **45**, 7544; (*i*) M. Yamamoto, Y. Kashiwagi and M. Nakamoto, *Langmuir*, 2006, **22**, 8581.

Green Chemistry

Cutting-edge research for a greener sustainable future

Aggregation

Activity

RSCPublishing

Enzyme aggregation in ionic liquids studied by dynamic light scattering and small angle neutron scattering

Daniel Sate,[a] Michiel H. A. Janssen,[b] Gill Stephens,[c] Roger A. Sheldon,[b] Kenneth R. Seddon[d] and Jian R. Lu*[a]

Candida antarctica Lipase B (CALB) formed a seemingly homogeneous solution in water, 1-ethyl-3-methylimidazolium dicyanamide ([C$_2$mim][N(CN)$_2$]) or dimethyl sulfoxide (DMSO). However, dynamic light scattering (DLS) and small angle neutron scattering (SANS) demonstrated that the enzyme formed aggregates in the non-aqueous solvents. In aqueous solution, SANS measurements revealed that CALB formed cylindrical nano-structures with a diameter of 5 nm and a length of 4 nm, equivalent to the dimensions of a single CALB molecule. The enzyme also formed cylindrical structures in DMSO but the diameter was 4 nm and the length was 12 nm, indicating that the enzyme had aggregated to form dimers or trimers. In [C$_2$mim][N(CN)$_2$], disc-shaped aggregates were formed, with an average diameter of 49 nm and a length of 3.8 nm, equivalent to the volume of 150 CALB molecules. In all cases, the hydrodynamic diameters measured by DLS matched the long axial lengths of the aggregates determined by SANS, indicating a good consistency between the two techniques. DLS measurements showed that CALB aggregates in [C$_2$mim][EtOSO$_3$] and [C$_2$mim][NO$_3$] had a smaller diameter than in [C$_2$mim][N(CN)$_2$]. In all cases, the aggregation observed in the solvents was associated with loss of enzymatic activity.

1. Introduction

Ionic liquids, sometimes referred to as room-temperature molten salts, are liquids composed entirely of ions.[1,2] Although they have been known for many years, there has been a recent explosion of interest, fuelled by more than a dozen industrial applications, ranging from catalytic synthesis to paint additives, from batteries to gas adsorbers, and from refinery applications to cleaning.[1] The versatility of this class of fluids stems from the ability to change either the anion or the cation, yielding a wide range of organic, inorganic and polymeric compounds with different physical and chemical properties. Moreover, ionic liquids (ILs), unlike many common organic solvents, do not usually exhibit a measurable vapour pressure at room temperature,[3] making them potentially attractive 'green solvent' alternatives in many industrial processes.[4]

The idea of using organic solvents and ionic liquids as a medium for biocatalysis is not a new one, with enzymes being exploited for, amongst other things, asymmetric synthetic transformations in these media, fuelled by the growing demand for enantiopure pharmaceuticals.[1,5,6] The switch from water, the enzyme's natural environment, to alternative solvents is

necessitated by the fact that in an aqueous environment, the range of possible reactions is small, due to issues such as poor substrate solubility, unwanted side reactions and also product hydrolysis. However, while it would appear that enzymes used in organic solvents present a panacea for such problems, this is not necessarily the case. Previous studies suggest that while organic solvents such as tetrahydrofuran and toluene can facilitate enzymatic reactions to varying extents, DMSO and dioxane, for example, cannot; that said, the same is true for many ionic liquids.[5–7] 1,3-Dialkylimidazolium-based ionic liquids such as 1-butyl-3-methylimidazolium hexafluorophosphate, [C$_4$mim][PF$_6$], and 1-butyl-3-methylimidazolium tetrafluoroborate, [C$_4$mim][BF$_4$], have been commonly employed as media for alcoholysis, ammoniolysis and perhydrolysis reactions using enzymes such as the now widely studied *Candida antarctica* Lipase B (CALB),[5–7] while [C$_4$mim]Cl and [C$_4$mim][CH$_3$CO$_2$][8] appear not to support enzyme activity.

From this cursory review, it is clear that no single class of 'solvent' – whether it be ionic liquids or traditional organic solvents – offers a complete solution to problems associated with industrial biocatalytic processes. While certain examples from each class provide suitable conditions for biocatalysis, others adversely affect enzyme function and ultimately product yield. It is hence imperative to identify the factors responsible for these different effects in order to undertake efficient identification of a solvent suitable for a specific task.

A common consensus amongst many authors is that ionic liquids containing a coordinating anion such as chloride, nitrate or lactate, do not permit enzyme activity, but there is a lack of experimental data to support this view. Work by Lau *et al.*[8] and van Rantwijk *et al.*[9] has, however, added some

[a] School of Physics and Astronomy, University of Manchester, Sackville Street, Manchester, UK M60 1QD. E-mail: j.lu@manchester.ac.uk; Tel: +44-161-3063926
[b] Department of Biotechnology, Delft University of Technology, Julianalaan 136, 2628 BL, Delft, the Netherlands
[c] Manchester Interdisciplinary Biocentre, University of Manchester, Sackville Street, Manchester, UK M60 1QD
[d] The QUILL Centre, School of Chemistry and Chemical Engineering, the Queen's University of Belfast, Belfast, Northern Ireland, UK BT9 5AG

credence to the idea that the 'polarity' of a solvent and its subsequent interaction with the enzyme structure are responsible for structural unfolding and deactivation.

In this study, the structure of the enzyme *Candida antarctica* Lipase B was investigated in different solvents using small angle neutron scattering (SANS) and dynamic light scattering (DLS). The aim was to compare any conformational changes in the solvents, and to correlate these with changes in catalytic activity.

2. DLS, SANS and selection of solvents

Dynamic light scattering (DLS) has been used to determine the average size of protein molecules or their aggregates in different solvents. In DLS experiments, particles in solution are illuminated with light of a given wavelength and the intensity fluctuations from the scattered light are measured over a time course between 1 ns and 1 ms. The intensity fluctuations encountered occur due to the random diffusion of particles through the solvent, known as Brownian motion. The change in signal intensity over the time course of an experiment arising from these fluctuations can be principally described through the autocorrelation function, eqn (1),[10]

$$G^{(1)}(\tau) \propto \int_{R_{\min}}^{R_{\max}} N(R)M^2(R)P(q)S(q)\exp\left(-mR^{-1}q^2\tau_{\mathrm{rel}}\right)\mathrm{d}R \quad (1)$$

which contains the distribution of relaxations τ and the scattering amplitudes of the studied components, where m is the proportionality component. $N(R)$ and $M(R)$ denote the number and mass of particles with radius R between the integration limits $R_{\min}$ and $R_{\max}$. $P(q)$ is the 'intraparticle scattering factor', and it arises from the intraparticle interference effects. $S(q)$ is defined as the 'interparticle scattering factor', because it describes the interference effects arising from the particles.[11] The significance of the autocorrelation function is that particles with a larger hydrodynamic radius will diffuse with a lower velocity through the bulk solvent. As a result, the autocorrelation function (which describes how similar the two signals are) will be greater for particles with a larger hydrodynamic radius, *i.e.* the signal from a larger particle will not have altered as much over time as that from a smaller particle.

If the particles studied are small compared to the employed wavelength, the translational diffusion coefficient, D_{o}, can be determined through Laplace inversion of the autocorrelation function. From the diffusion coefficient, the hydrodynamic radius of the scattering particles can be calculated from the Stokes–Einstein equation, eqn (2),[10]

$$R_{\mathrm{h}} = k_{\mathrm{B}}T/6\pi\eta D_{\mathrm{o}} \quad (2)$$

where k_{B} denotes the Boltzmann constant, T the absolute temperature, and η is the viscosity of the solvent in the same temperature. R_{h} is experimentally the measure of the maximal radius of a hydrated object (assuming it rotates along all directions). In the case of a non-spherical object, it approximates to the largest rotational radius. DLS cannot, therefore, provide information about the shape of a particle as measured.

Small angle neutron scattering (SANS) is a well-established technique for investigating both the size and the shape of nanoparticles in solution, with higher resolution and sensitivity. SANS has become a widely used technique in the characterisation of biomacromolecules, and information pertaining to enzyme conformation is examined through the determination of the size and shape of protein molecules under different conditions. An increase in size greater than that found in the crystalline structure of the enzyme is usually attributed to molecular aggregation driven by structural deformation and unfolding.[12,13]

SANS measures the differential scattering cross-section, $(\mathrm{d}\Sigma/\mathrm{d}\Omega)(Q)$, which contains information on the size, shape and interactions between the scattering centres or particles in the sample.[11] A generalised expression for the small angle neutron scattering from any sample is given in eqn (3),

$$\frac{\mathrm{d}\Sigma}{\mathrm{d}\Omega}(Q) = NV_{\mathrm{p}}^2(\Delta\rho)^2 P(Q)S(Q) + B \quad (3)$$

where N is the number concentration of scattering centres, V_{p} is the volume of one scattering centre, $\Delta\rho$ is the contrast, indicating the difference in scattering length density between the scattering object and the surrounding solvent and B is the background signal.

Similarly, $S(Q)$ is the interparticle form factor and $P(Q)$ is the self form factor which changes with the length and radius of the particle. The general form of $P(Q)$ is given by van de Hulst's equation, eqn (4),

$$P(Q) = \frac{1}{V_{\mathrm{p}}^2}\left|\int_0^{V_{\mathrm{p}}} \exp[if(Q\alpha)]\,\mathrm{d}V_{\mathrm{p}}\right|^2 \quad (4)$$

where α is a 'shape parameter' – which may represent a length or radius depending on the geometry of the particle. Analytical expressions exist for most common shapes, for example, cylinder and sphere, and also for more complex structural shapes. Eqn (5) represents the analytical expression for a disc of finite thickness and radius, R_{p},

$$P(Q) = \frac{2}{(QR_{\mathrm{p}})^2}\left[1 - \frac{J_1(2QR_{\mathrm{p}})}{QR_{\mathrm{p}}}\right] \quad (5)$$

where J_1 is a first-order Bessel function. The interparticle form factor $S(Q)$ is modulated by interference effects between radiation scattered by different scattering bodies, for example, several protein molecules in a single solution. As a result, $S(Q)$ is dependent on local order or, likewise, the concentration of the sample. In the context of these experiments, the concentration of particles in solution is so small that $S(Q)$ is close to 1. Large scale suspensions are undesirable for SANS measurements, due to the Q range of detection of the SANS instrument, usually <2000 Å.

Information about the structure of scattering objects is usually obtained by comparing a scattering profile calculated from a presumed geometrical shape with the obtained data, and the process is iterated until an acceptable fit is produced. In data analysis, the isotopic contrast is usually coupled to the scale factor (*sf*), which is related to

the concentration of the aggregates, and can be expressed by eqn (6),

$$sf = B\phi(\rho_p - \rho_w)^2 \qquad (6)$$

where ϕ is the aggregate volume fraction in the form of a water-filled cylindrical object, and is proportional to the enzyme concentration; ρ_p denotes the scattering length density of the water-filled aggregate, and ρ_w denotes that of the solvent; B is the constant relating to the unit of ρ used. In this instance the scale factor is an important parameter to observe, as any changes in concentration will be mirrored by a change in scale factor. The scale factor can also be affected by incomplete dissolution of proteins in the bulk. If the enzyme does not solubilise, large aggregates are formed, and if they are outside of the Q range of the instrument, ϕ is lower than the anticipated value.

The effect of solvents on the signal of small angle neutron scattering and DLS depends on how the solvent interacts with, in this case, the protein. When a solvent shows good solubility with regard to the protein molecule, the average scattering density of the solvated protein becomes closer to that of the pure solvent, *i.e.* we are approaching homogeneity. However, if the solvent causes structural unfolding, this may change the shape of the protein molecule (*e.g.* different diameter and/or length), and it could also result in protein aggregation to form larger scattering objects. Therefore, we used SANS and DLS to detect changes in size and shape of CALB in a range of different solvents which are known to inactivate CALB.

From our previous work (unpublished), it was observed that [C₂mim][N(CN)₂] (Fig. 1) caused almost complete abolition of enzyme activity. It is possible that such a drastic effect on catalysis is due to the ability of the solvent to interact with the protein tertiary structure; such interactions may cause sufficient changes such that the active site is disrupted. Therefore, we studied the effect of [C₂mim][N(CN)₂] on the structure of CALB using both SANS and DLS. We also used DLS to study the structure of CALB in [C₂mim][EtOSO₃] and [C₂mim][NO₃].

Dimethyl sulfoxide (DMSO) was also employed as a solvent in this investigation due to the fact that it is one of the few organic solvents that impart a sufficiently good solubility to proteins,[3–6] but at the cost of low enzyme activity;[14,15] this therefore should provide an interesting comparison between the behaviour of CALB in a polar organic solvent and in an ionic liquid. Water was used as a reference solvent in this study due to the fact that in nature, enzymes are almost exclusively found to exist in an aqueous environment and as a result it would be expected that the enzyme would be in its most active conformation in this medium.
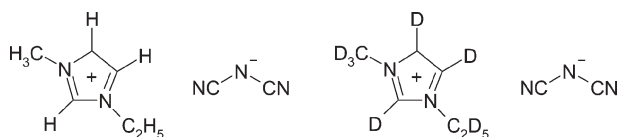
Fig. 1 Cationic structure of hydrogenated [C₂mim][N(CN)₂] (left) and deuterated [C₂mim-*d₁₁*][N(CN)₂] (right).

3. Experimental

(a) Materials

The enzyme used in this study was prepared from a commercial product from Altus Biologics, which contained non-cross-linked CALB enzyme crystals and buffer salts used during crystallisation. In order to remove the unwanted buffer salts, the enzyme was dissolved in water and then centrifuged. The resulting pellet was then diluted in 2 mM potassium phosphate buffer pH 7, and passed through a 10 000 Da filter. The resultant enzyme solution was then added slowly to cold 1,2-dimethoxyethane to precipitate. Once the protein had precipitated, the solution was again centrifuged and the supernatant liquid was then washed with diethyl ether and vacuum dried.

The D₂O and DMSO-*d₆* used were purchased from Sigma and contained 99.8% D. The D₂O was buffered at pH 7, using 2 mM phosphate buffer pH 7. All other deuterated chemicals were obtained from Aldrich, and used as supplied (all containing >99.5% D). Weakly acid aluminium oxide (type 506 C) was obtained from Fluka, and used as supplied. 1-(methyl-*d₃*)imidazole was synthesised according to two literature procedures.[16,17] Alkylation of 1-(methyl-*d₃*)imidazole was performed according to two alternative procedures using either bromoethane-*d₅* or ethyl-*d₅* tosylate as reactants, as described in the chemical syntheses below.

(b) Assessment of CALB activity

Assessment of CALB activity was undertaken using the alcoholysis (transesterification) of ethyl butanoate with butanol in water and the ILs, following the same procedures as described in the literature.[8] The transesterification of ethyl butanoate (0.06 M) with butanol (0.12 M) was carried out in 0.5 cm³ solvent. CALB (15 mg) and 1,3-dimethoxybenzene (internal standard, 0.06 M) were added and the reaction was carried out at 40 °C. The reactions were monitored for 24 h, and samples were taken for chromatographic analysis against time.[8] The initial activity test, following the solution preparation from the free CALB lyophilised powder, showed that the enzyme had a relatively high activity compared to the supplied product specification, and that the enzyme activity had been little affected by the preparatory steps. The activity of CALB in aqueous solution measured in the triacetin hydrolysis assay (2 mM triacetin in 100 mM potassium phosphate pH 7.5, 21 °C) was found to be 10 540 U g⁻¹. If this was defined as 100% active, the relative activity of the enzyme in DMSO and the ionic liquids after 24 h was close to zero. Our CALB activity in DMSO was lower than reported in the literature[11] and was possibly due to the full solubilisation and longer time exposure.

(c) Chemical syntheses

Scheme 1 outlines the main steps involved in the preparation of deuterated 1-ethyl-3-methylimidazolium-*d₁₁* dicyanamide, [C₂mim-*d₁₁*][N(CN)₂], with the synthesis of key intermediates described in the following.

1-(Methyl-*d₃*)imidazole from (methyl-*d₃*)ammonium chloride (see ref. 16). (Methyl-*d₃*)ammonium chloride (5.89 g,
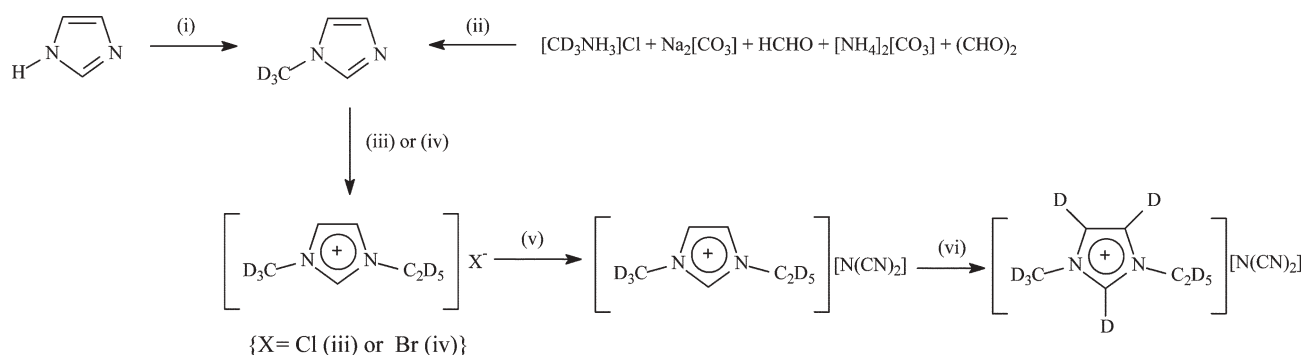
Scheme 1 Synthesis of 1-ethyl-3-methylimidazolium-d_{11} dicyanamide. *Reagents and conditions*: (i) step 1: NaOH, 200 °C, vacuum; step 2: CD$_3$I, −25 °C in ethanenitrile; (ii) aqueous medium, 10 °C; (iii) step 1: C$_2$D$_5$OTs, 0 °C to RT; step 2: anion exchange with Dowex 1X8-200 [Cl$^-$ form]; (iv) C$_2$D$_5$Br, reflux; (v) Ag[N(CN)$_2$] in water; (vi) K$_2$[CO$_3$] in D$_2$O, 100 °C.

83.5 mmol) was dissolved in water (30 cm^3) and stirred at −15 °C. Sodium hydrogencarbonate (7.01 g, 83.5 mmol), methanal (2.51 g, 83.5 mmol), ammonium hydrogencarbonate (6.60 g, 83.5 mmol), and glyoxal (4.85 g, 83.5 mmol) were added. Immediately after the addition of methanal, the mixture started to effervesce. The mixture was then allowed to slowly warm up to room temperature. Water was removed under reduced pressure and 1-(methyl-d_3)imidazole was vacuum distilled using a Kugelrohr apparatus, yielding a clear, water-like liquid (4.31 g, 50.6 mmol, 61%). ^{1}H-NMR (300.2 MHz, DMSO-d_6, TMS): 6.90 (t, 1H), 7.10 (t, 1H), 7.57 (s, 1H).

1-(Methyl-d_3)imidazole from iodomethane-d_3 (see ref. 17). Sodium hydroxide (6.95 g, 0.174 mol) was dissolved in water (25 cm^3) and imidazole (11.83 g, 0.174 mol) was added. The mixture was heated to 100 °C for 30 min and 200 °C for 10 min, the water was removed *in vacuo*, and the white solid (sodium imidazolate) was dried overnight at 100 °C *in vacuo*. Ethanenitrile (74 cm^3) was added to the white dry solid and the mixture was cooled to −25 °C, followed by slow addition of iodomethane-d_3 (25.0 g, 0.173 mol). The mixture was slowly allowed to warm up to room temperature and stirred for three days. The solvent was removed under reduced pressure and 1-(methyl-d_3)imidazole was vacuum distilled from the mixture using a Kugelrohr apparatus, yielding a clear, water-like liquid (7.62 g, 89.5 mmol, 52%). ^{1}H-NMR (300.2 MHz, CDCl$_3$, TMS): 6.88 (s, 1H), 7.04 (s, 1H), 7.42 (s, 1H).

1-(Ethyl-d_5)-3-(methyl-d_3)imidazolium bromide and dicyanamide. Bromoethane-d_5 (1.57 g, 20 mmol) was treated with 1-(methyl-d_3)imidazole (1.17 g, 13.8 mmol) in ethanenitrile (5.0 cm^3) under a dinitrogen atmosphere at 40 °C and protected from light. After four days, the solvent was evaporated *in vacuo* and the viscous ionic liquid was immediately used for metathesis with freshly prepared Ag[N(CN)$_2$]. The latter was prepared by slowly adding an aqueous solution of sodium dicyanamide (2.31 g, 26.0 mmol) to an aqueous solution of silver(I) nitrate (3.40 g, 20.0 mmol) under dinitrogen while stirring; the solid silver dicyanamide was collected by filtration. All the Ag[N(CN)$_2$] was added to the aqueous solution of [C$_2$mim-d_8]Br (38.94 g, 0.204 mol) and stirred overnight. The green-yellow solid (silver bromide and excess silver

dicyanamide) was removed by filtration, and the water was removed by rotary evaporation, yielding a slightly yellow ionic liquid (2.31 g, 12.5 mmol, 90%).

Ethyl-d_5 tosylate, Me-4-C$_6$H$_4$SO$_2$OC$_2$D$_5$. Ethanol-d_6 (10.00 g, 0.192 mol) was reacted with tosyl chloride (36.59 g, 0.192 mol) in dry pyridine and yielded a clear, oil-like liquid after vacuum distillation using a Kugelrohr apparatus (34.49 g, 0.168 mol, 88%). ^{1}H-NMR (300.2 MHz, CDCl$_3$, TMS): 1.59 (3H), 7.35 (d, 2H), 7.79 (dd, 2H).

1-(Ethyl-d_5)-3-(methyl-d_3)imidazolium tosylate, chloride, and dicyanamide. (Methyl-d_3)imidazole (7.62 g, 89.5 mmol) was cooled in an ice bath and ethyl-d_5 tosylate (18.37 g, 89.5 mmol) was added. The temperature was slowly increased to room temperature and the mixture was stirred overnight. Water was added and the mixture was heated to 100 °C for 30 min, after which the volatiles were removed *in vacuo* at 100 °C, yielding a white solid [C$_2$mim-d_8][OTs] (25.51 g, 87.8 mmol). Metathesis to the chloride salt was performed by ion exchange over a Dowex 1X8-200 (Cl$^-$ form) column. The water was evaporated, yielding a slightly yellow, viscous oil, [C$_2$mim-d_8]Cl. ^{1}H-NMR (300.2 MHz, DMSO-d_6, TMS): 7.76 (t, 1H), 7.86 (t, 1H), 9.41 (t, 1H). Metathesis with silver dicyanamide as described above, followed by aluminium oxide column purification using ethanenitrile as an eluent, yielded a clear, water-like ionic liquid (10.49 g, 56.6 mmol, 64%).

1-Ethyl-3-methylimidazolium-d_{11} dicyanamide, [C$_2$mim-d_{11}][N(CN)$_2$] (see ref. 18). [C$_2$mim-d_8][N(CN)$_2$] (11.01 g, 59.4 mmol) was dissolved in D$_2$O (107.16 g, 5.35 mol), anhydrous potassium carbonate (0.42 g, 3.0 mmol) was added, and the mixture was stirred at 100 °C under a dinitrogen atmosphere for one day. D$_2$O was removed by rotary evaporation, the ionic liquid was dissolved in dry ethanenitrile, and the solid potassium carbonate removed by filtration. The solvent was evaporated and the residue dissolved in dry dichloromethane and stored at −20 °C overnight. Residual solid salt was removed by filtration, and the solvent evaporated. The ionic liquid was dried *in vacuo* over phosphorus(V) oxide at 80 °C, yielding a slightly yellow coloured ionic liquid (10.99 g, 58.4 mmol, 98%). ^{1}H-NMR

analysis in D_2O using sodium ethanoate as an internal reference showed little residual hydrogen, with the D content estimated to be over 98%. The H/D exchanges at ring positions 4 and 5 were complete and the residual hydrogen content was well under 2%. The residual water or ion level in the ionic liquid was not checked, but our previous analyses following similar treatments showed that the samples were extremely dry.

The $[C_2mim][N(CN)_2]$ used in the first round of SANS experiments was shown to contain 3757.7 ppm chloride, (0.38%); with the $[C_2mim][N(CN)_2]$ from the second round of experiments containing 0.66% chloride and 0.1% nitrate. The $[C_2mim][N(CN)_2]$ from the final round of SANS experiments had a chloride content of 0.24% and a nitrate content of 0.016%, with a total deuterium content of 99.5%.

In each round of experiments, the CALB solutions were made to a protein concentration of around 1% (weight/volume, w/v%) and stirred for a minimum of 8 h, using a magnetic stirrer in anhydrous conditions to prevent H/D exchange due to adventitious moisture. Prior to SANS measurements, the samples were transferred to pre-cleaned and dried quartz cells.

(d) SANS

SANS measurements were made on the white beam time-of-flight scattering instrument, LOQ, ISIS Facility, Rutherford Appleton Laboratory (RAL), Didcot, Oxford, UK, which has a wavelength range of 2–10 Å. The 64 cm square detector was at a distance of 4.1 m, giving a wave vector (Q) range of 0.006–0.28 Å^{-1}. Samples were contained in 2 mm path fused silica cells. Data were corrected for the wavelength dependence of the incident spectrum, the measured sample transmission, and relative detector efficiencies, prior to subtraction of background from respective D_2O buffers. Absolute scaling was obtained by comparison to the scattering from a partially deuteriated polystyrene standard. To obtain solutions of lower enzyme concentrations – 1, 0.5 and 0.2% (w/v%) – it was necessary to serially dilute the relevant sample with an appropriate solvent. All the SANS data were recorded at 25 °C. The data modelling was performed using the FISH2 fitting program developed by Dr R. K. Heenan at RAL.

(e) DLS

All DLS measurements were made using a commercially available, Malvern Instruments Nano-S machine, and the instrument was fitted with a red laser (633 nm) with a size detection range of 0.6 nm to 6 μm. The detection angle was 173° with respect to the incoming beam. Samples analysed were contained in a 1 cm path length quartz cell and the data were analysed using Malvern Instruments Dispersion Technology Software. The protein refractive index was taken to be 1.45 with an absorbance of 0.001. The viscosity and refractive index of D_2O, $[C_2mim][N(CN)_2]$ and DMSO were taken as: 0.887 mPa s and 1.330; 21.0 mPa s and 1.514; and 21.4 mPa s and 1.479 at 25 °C, respectively. Six measurements were performed on each sample, with an average of ten runs taken for each measurement, each within one minute.

4. Results

(a) Dynamic light scattering

The solution properties of CALB in water, DMSO and $[C_2mim][N(CN)_2]$ were first examined using dynamic light scattering. CALB formed nanoparticles of different sizes in these solvents (Fig. 2). In water, the hydrodynamic diameter of the nanoparticles was centred around 5 nm and was distributed between 3 nm and 7.5 nm. It was a relatively homogeneous size distribution. In DMSO, the mean diameter was 12 nm. However, the size distribution was extremely broad, ranging from 5 nm to 30 nm, indicating that the enzyme had aggregated to form structures with a wide range of sizes. In $[C_2mim][N(CN)_2]$ the average diameter was 50.7 nm, and the size distribution was narrower than in DMSO. Nevertheless, the minimum and maximum diameters were 25 nm and 90 nm, which again indicated the formation of aggregates with various sizes. These results show a clear trend of size increase from water to DMSO and then to $[C_2mim][N(CN)_2]$, with a concomitant increase in the breadth of the size distribution.

Further to this, the hydrodynamic diameters of CALB in two more ionic liquids, $[C_4mim][NO_3]$ and $[C_2mim][EtOSO_3]$ (data not shown), were also analysed using DLS. As was the case with $[C_2mim][N(CN)_2]$, CALB formed particles with a mean diameter of 37.8 nm in $[C_2mim][EtOSO_3]$ and 43.8 nm in $[C_4mim][NO_3]$, both indicating substantial aggregation.

From this set of experiments, it can be concluded that aggregation took place in both the organic solvent, DMSO, and in the ionic liquids, $[C_4mim][NO_3]$, $[C_2mim][EtOSO_3]$ and $[C_2mim][N(CN)_2]$, with the largest enzyme aggregates forming in the ionic liquids. It should be noted that the sizes of the aggregates were extremely variable.

(b) Small angle neutron scattering

SANS measurements were performed initially on CALB dissolved in D_2O, as this solvent would allow us to obtain information on the enzyme in its most active conformation. Fig. 3 shows the scattering intensity (I) plotted as a function of the wave vector (Q), for solutions of varying enzyme concentration in D_2O.
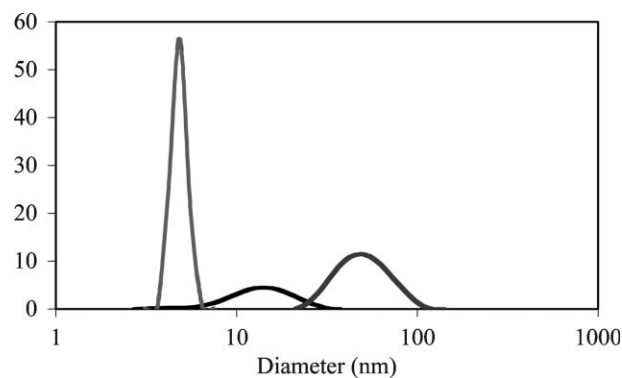
Fig. 2 DLS size distribution in the form of hydrodynamic diameters for aggregates of CALB formed in water (leftmost trace) DMSO (middle trace) and $[C_2mim][N(CN)_2]$ (rightmost trace). The y-axis is shown in relative scattering intensity (arbitrary unit).
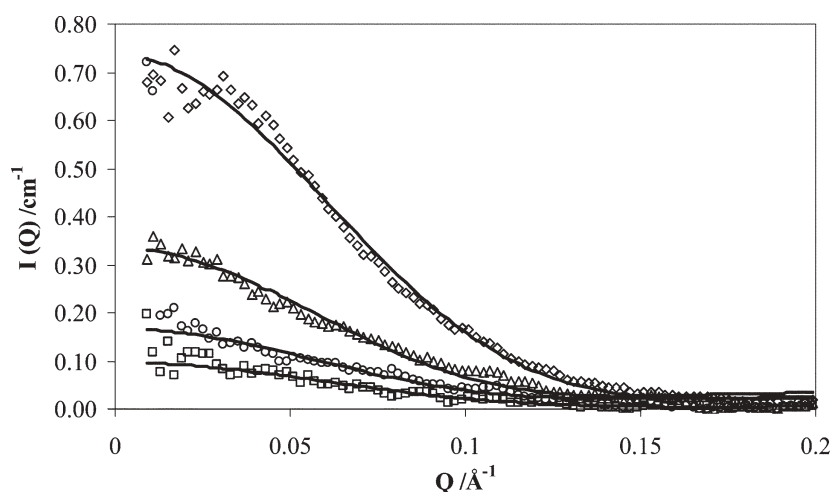
Fig. 3 Small angle neutron scattering intensity (I) plotted as a function of wave vector (Q) for CALB in D_2O at concentrations of 0.2 ($\square$), 0.5 ($\bigcirc$), 1.0 ($\triangle$) and 1.5 w/v% ($\diamond$).

Table 1 Structural parameters obtained from fitting the disc model to the SANS profiles shown in Fig. 3, for different concentrations of CALB dissolved in water

Enzyme conc. (w/v%)	Fitted scale factors	Diameter/nm	Length/nm
1.5	6.48×10^{-6}	5 ± 0.1	4 ± 0.3
1.0	4.32×10^{-6}	5 ± 0.3	4 ± 0.3
0.5	2.16×10^{-6}	5 ± 0.2	4 ± 0.2
0.2	8.64×10^{-7}	5 ± 0.2	4 ± 0.2

The subsequent analysis to the SANS scattering profiles demonstrated a number of salient features. Using the 'disc' model, whereby the diameter of the particle is greater than the length, each scattering intensity profile could be fitted with a length and diameter and the scale factor relating to the concentration of the enzyme. The parameters of the scattering objects present in the bulk solution from the model calculation were a diameter of 5 nm and a length 4 nm. CALB is a globular protein,[14] with approximate dimensions of $3 \times 4 \times 5$ nm. The particle size detected by SANS is in agreement with the crystalline molecular structure, indicating that the enzyme was completely dissolved in the water.

The next feature of the scattering profiles obtained from the data is that as the concentration of protein in solution decreases, so does the scale factor (Table 1). It can thus be seen from Fig. 3 that the scattering intensity profiles are sensitive to changes in enzyme concentration. This observation suggests

that all the enzymes dissolved contributed to the formation of monomers.

It is useful to compare the structural information from SANS with the DLS data as already described. DLS provides information about the size of the molecule along its longest axis, whereas SANS detects not only the size but also the shape of the aggregates. The diameter of 5 nm for the cylindrical structure determined from SANS corresponds extremely well with the hydrodynamic diameter of 4.9 nm determined by DLS. The main parameters obtained from DLS and SANS are listed in Table 2 for comparison.

With the ability of SANS to determine protein size and shape in solution successfully demonstrated, the next step was to study the solution state of CALB in DMSO. As with D_2O, the same four protein concentrations were used in deuterated DMSO and the corresponding SANS scattering profiles are shown in Fig. 4.

The plots of scattering intensity profiles shown in Fig. 4 provide direct evidence that CALB formed aggregates in DMSO, rather than the monomers formed in water. Analysis of the scattering profiles resulted in the fitting of the measured profiles as represented by the continuous lines shown in Fig. 4, this time using a cylindrical model. The main parameters obtained are given in Table 3. The average dimensions of the aggregates were found to be greater than the monomers in D_2O, with a diameter of 4 nm and a length of 12 nm. This would suggest that the enzymes

Table 2 Comparison of aggregate size and shape as detected by DLS (hydrodynamic sphere) and SANS (disc/cylinder) in different solvents. Note that the activity of CALB in aqueous solution was measured in the triacetin hydrolysis assay and taken as 100%, and the relative activities in DMSO and the ionic liquids after 24 h were close to zero. Our CALB activity in DMSO was lower than reported in the literature[13] and was possibly caused by the full solubilisation and longer time exposure (see the Experimental section for more details)

Solvent	DLS (sphere) diameter/nm	SANS (disc or cylinder)		Relative activity (%)
		Diameter/nm	Length/nm	
D_2O	4.9	5	4	100
DMSO	12.5	4	12	0
[C_2mim][EtOSO$_3$]	37.8	—	—	7
[C_2mim][NO$_3$]	43.8	—	—	3
[C_2mim][N(CN)$_2$]	50.7	48.6	3.8	0
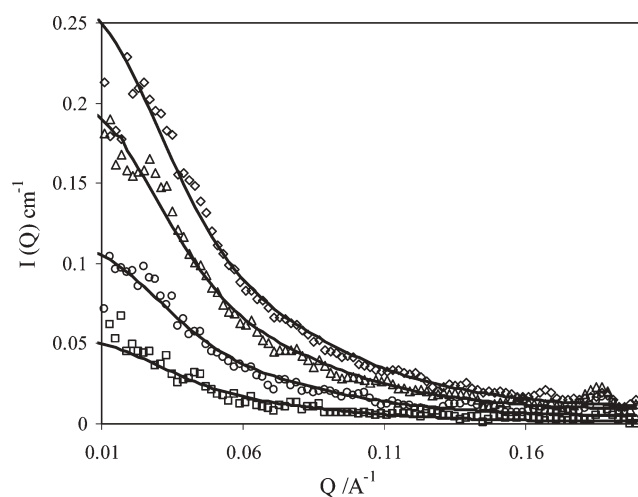
Fig. 4 Small angle neutron scattering intensity (*I*) plotted as a function of wave vector (*Q*) for CALB in deuteriated DMSO at the concentrations of 0.2 (□), 0.5 (○), 1.0 (△) and 1.5 w/v% (◇).

Table 3 Structural parameters obtained from cylinder model fitting to the SANS profiles shown in Fig. 4 for different concentrations of CALB dissolved in DMSO

Enzyme conc. (w/v%)	Fitted scale factors	Diameter/nm	Length/nm
1.5	1.693×10^{-6}	4.0	12
1.0	1.264×10^{-6}	4.0	12
0.5	7.09×10^{-7}	4.0	12
0.2	3.10×10^{-7}	4.0	12

coalesce to form a unit resembling a dimeric or trimeric end-to-end assembly.

As in water, the DLS and SANS data were in agreement within the experimental error. The hydrodynamic diameter measured by DLS (12.5 nm) showed consistency with the length of the aggregate as obtained from the SANS

Table 4 Structural parameters obtained from disc model fitting to the SANS profiles shown in Fig. 5 for different concentrations of CALB in [C$_2$mim][N(CN)$_2$]

Enzyme conc. (w/v%)	Fitted scale factors	Diameter/nm	Length/nm
1.5	2.29×10^{-7}	48.6 ± 0.3	3.8 ± 0.3
1.0	1.53×10^{-7}	48.6 ± 5.2	3.8 ± 0.7
0.5	7.65×10^{-8}	48.6 ± 20	3.8 ± 0.7

measurement. Furthermore, the scale factors obtained from the data analysis are in good proportion to enzyme concentration. However, they are somewhat lower than those from the previous data set, which might suggest that DMSO was not dissolving the protein to the same extent as water – with large particles outside the range of detection.

In the final round of neutron scattering experiments, deuterated ionic liquid {[C$_2$mim-*d*$_{11}$][N(CN)$_2$]} was used as the solvent. Data could only be obtained when the enzyme concentration was 0.5, 1.0 and 1.5 w/v%, since the solution containing 0.2% CALB gave an extremely low signal with too much scatter of the data.

Fig. 5 shows the resultant SANS scattering profiles with the fitted structural parameters given in Table 4. Even without any attempt to fit the data, it can be seen directly from Fig. 5 that the system involves some substantial aggregation because the SANS profiles were shifted to a lower *Q* range. Fitting analysis showed that CALB dissolved in [C$_2$mim-*d*$_{11}$][N(CN)$_2$] formed large, disc-like aggregates, with a diameter of 48.6 nm and length 3.8 nm.

In keeping with the previous sets of data, the scale factors were again directly proportional to the enzyme concentration, which was indicative of structural homogeneity against concentration increase. It is also useful to note that the hydrodynamic diameter determined by DLS of some 50 nm compared well with the SANS diameter of 48.6 nm, again showing a high degree of consistency between the two techniques.
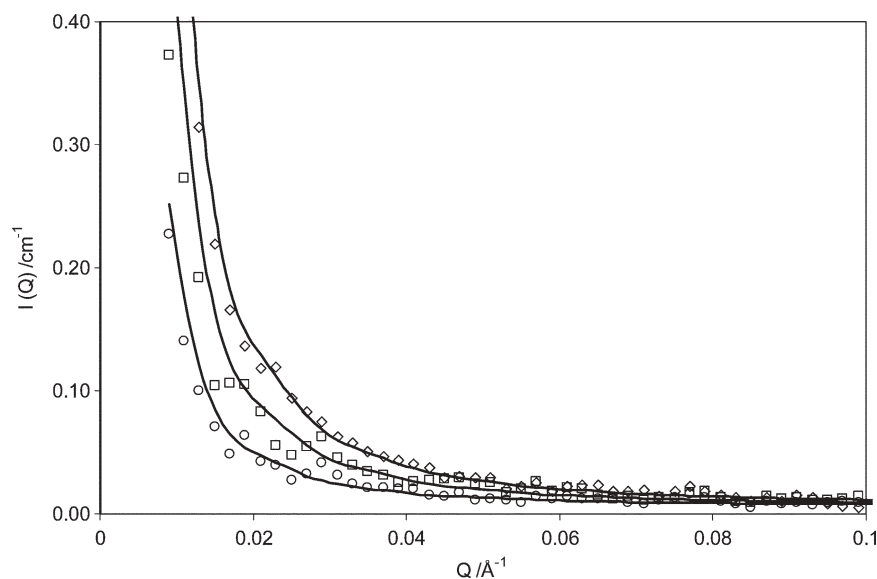
Fig. 5 Small angle neutron scattering intensity (*I*) plotted as a function of wave vector (*Q*) for CALB in ionic liquid [C$_2$mim][N(CN)$_2$] at the concentration of 0.5 (○), 1.0 (△) and 1.5 w/v% (◇).

5. Discussion

Extensive studies over the past few decades have focused on understanding how different aqueous and non-aqueous solvents affect biocatalysis.[1,9,19–21] Although enzyme biocatalysis in ionic liquids has now become attractive, our general understanding of the solubilisation and deactivation of enzymes in these novel solvents is comparatively poor. As deactivation is often associated with structural deformation and aggregation, DLS and SANS have been used in our work to determine the structural features of CALB in ionic liquids. As this was our first scattering study, measurements were also made for CALB in the conventional solvents, water and DMSO.

As expected, no aggregation was detected in water, and the corresponding enzyme activity was found to be the highest. In contrast, CALB in DMSO formed aggregates with a range of size distributions, with the average size corresponding to dimers or trimers. Even this extent of aggregation resulted in complete loss of activity. Others have reported that CALB is active in DMSO,[13] but this difference may be because we incubated the enzyme long enough in DMSO to obtain full solubilisation.

The ionic liquids [C_2mim][EtOSO$_3$], [C_2mim][NO$_3$] and [C_2mim][N(CN)$_2$] all dissolved CALB, but also all caused formation of large aggregates. However, the aggregates in [C_2mim][N(CN)$_2$] were disc-shaped, suggesting 'side-by-side' aggregation, rather than the 'end-to-end' aggregation seen in DMSO. These aggregates were completely inactive, whereas the aggregates in [C_2mim][EtOSO$_3$] or [C_2mim][NO$_3$] retained very low levels of enzymatic activity.

The structure of enzymes in solution depends very strongly on the presence of water molecules in the structured hydration shell surrounding the enzyme molecules.[21] Many non-aqueous solvents[9,22,23] such as ethanol, ethanenitrile, 1,4-dioxane and DMSO can dissolve enzymes to form homogenous solutions, but in doing so they may strip away the hydration shell, causing enzyme denaturation. We might also expect ionic liquids to sequester water associated with the hydration shell, depending on their affinity for water, and this may partly explain the aggregation that we observed using DLS and SANS. However, CALB is known to be active even when completely dehydrated,[24] so it seems more likely that the cations and anions caused aggregation and inactivation by interacting directly with the enzyme molecule, *via* charged groups or by rearrangement of hydrogen bonding.[8,9,23] Indeed, Lau *et al.*[8] found that the secondary structure of CALB changed dramatically from α-helix to β-sheet when dissolved in several ionic liquids (but unfortunately not the ionic liquids studied here).[18] Lau *et al.* suggested that this was due to hydrogen bonding between the enzyme and the ionic liquids in place of the normal intramolecular hydrogen-bonding within the polypeptide backbone. The formation of β-sheets would normally be associated with an increased propensity to aggregate, and we found that the ionic liquids did cause extensive aggregation. The average size of the CALB aggregates increased with the electron density (and hence hydrogen-bonding potential) of the anion, in the order [EtOSO$_3$]$^-$ < [NO$_3$]$^-$ < [N(CN)$_2$]$^-$, and this also corresponded to the decrease in activity. Therefore, we suggest that our structural

studies provide further support for the hypothesis that strongly hydrogen-bonding ionic liquids should be avoided when choosing solvents for biocatalysis.

6. Conclusions

The selection of an appropriate solvent for enzymes in biocatalysis has attracted a great deal of interest from academic and industrial communities. Many studies have already been devoted to relating enzyme activity and stability to the physical properties of a solvent, particularly its hydrophilicity and polarity. However, the variety of enzymes and the range of solvents (including ionic liquids) emerging as potential candidates have meant that it is unrealistic to attempt to give any general rules without any insight into enzyme structure in the solvent and understanding of the possible interactions behind it. Whilst it is well known that enzymes may retain their activities in some media and that their activities may be completely lost in others, it is necessary to unravel their solution structures and the associated interactions. This study demonstrates that it is feasible to determine the structure of enzyme aggregates in different solvents by DLS and SANS.

The results from this work have shown that the three types of solvent caused different degrees of enzyme aggregation and dissolution. The extent of aggregation reflected the deviation from the enzyme's native structural framework, showing a clear correlation between the different activities of the enzyme in different solvents and the underlying interactions at the molecular level. Enzyme aggregation thus reflects the extent of interaction between protein and solvent *via* forces such as hydrogen bonding, and hydrophobic and electrostatic interactions; the effect of such interactions on enzyme activity is vital to gaining an understanding of how to tailor-make a solvent for a particular enzyme-catalysed reaction.

References

1 R. A. Sheldon, *Green Chem.*, 2005, **7**, 267–278; R. A. Sheldon, F. van Rantwijk and R. M. Lau, in *Ionic Liquids as Green Solvents: Progress and Prospects*, ed. R. D. Rogers and K. R. Seddon, ACS Symp. Ser., Vol. 856, American Chemical Society, Washington DC, 2003, pp. 192–205.

2 *Ionic Liquids in Synthesis*, ed. P. Wasserscheid and T. Welton, Wiley-VCH, Weinheim, 2003; A. Stark and K. R. Seddon, in *Kirk-Othmer Encyclopaedia of Chemical Technology*, ed. A. Seidel, John Wiley & Sons, Inc., Hoboken, New Jersey, vol. 26, 2007, pp. 836–920.

3 M. J. Earle, J. M. S. S. Esperanca, M. A. Gilea, J. N. C. Lopes, L. P. N. Rebelo, J. W. Magee, K. R. Seddon and J. A. Widegren, *Nature*, 2006, **439**, 831–834; M. Deetlefs and K. R. Seddon, *Chim. Oggi-Chem. Today*, 2006, **24**, 16–23.

4 *Green Industrial Applications of Ionic Liquids*, ed. R. D. Rogers, K. R. Seddon and S. Volkov, NATO Science Series II: Mathematics, Physics and Chemistry, Kluwer, Dordrecht, vol. 92, 2002; *Ionic Liquids IIIB: Fundamentals, Progress, Challenges, and Opportunities – Transformations and Processes*, ed. R. D. Rogers

and K. R. Seddon, ACS Symp. Ser., American Chemical Society, Washington DC, vol. 902, 2005; *Ionic Liquids IIIA: Fundamentals, Progress, Challenges, and Opportunities – Properties and Structure*, ed. R. D. Rogers and K. R. Seddon, ACS Symp. Ser., American Chemical Society, Washington DC, vol. 901, 2005; *Ionic Liquids as Green Solvents: Progress and Prospects*, ed. R. D. Rogers and K. R. Seddon, ACS Symp. Ser., American Chemical Society, Washington DC, vol. 856, 2003; *Ionic Liquids: Industrial Applications for Green Chemistry*, ed. R. D. Rogers and K. R. Seddon, ACS Symp. Ser., American Chemical Society, Washington DC, vol. 818, 2002; M. J. Earle and K. R. Seddon, *Pure Appl. Chem.*, 2000, **72**, 1391–1398.

5   R. A. Sheldon, G. Stephens and K. R. Seddon, *Green Chem.*, 2004, **6**, G65–G66.

6   R. A. Sheldon, *Chem. Commun.*, 2001, 2399–2407.

7   J. L. Kaar, A. M. Jesionowski, J. A. Berberich, R. Moulton and A. J. Russell, *J. Am. Chem. Soc.*, 2003, **125**, 4125–4131.

8   R. M. Lau, M. J. Sorgedrager, G. Carrea, F. van Rantwijk, F. Secundo and R. A. Sheldon, *Green Chem.*, 2004, **6**, 286–290; R. M. Lau, F. van Rantwijk, K. R. Seddon and R. A. Sheldon, *Org. Lett.*, 2000, **2**, 4189–4191.

9   F. Van Rantwijk, F. Secundo and R. A. Sheldon, *Green Chem.*, 2006, **8**, 282–286.

10 B. G. Vertesse, S. Magazu, A. Mangione, F. Migliardo and A. Brandt, *Macromol. Biosci.*, 2003, **3**, 477–481.

11 S. M. King, in *Modern Techniques for Polymer Characterisation*, ed. R. A. Pethrick and J. V. Dawkins, Wiley, New York, 1999, ch. 7.

12 L. M. Simon, K. László, A. Vértesi, M. Bagi and B. Szajáni, *J. Mol. Catal. B: Enzym.*, 1998, **4**, 41–45.

13 D. I. Svergun, S. Richard, M. H. J. Koch, Z. Sayers, S. Kuprin and G. Zaccai, *Proc. Natl. Acad. Sci. U. S. A.*, 1998, **95**, 2267–2272.

14 C. Follomer, F. V. Pereira, N. P. da Silveira and C. R. Carlini, *Biophys. Chem.*, 2004, **111**, 79–87.

15 R. A. Sheldon, R. M. Lau, M. J. Sorgedrager, F. van Rantwijk and K. R. Seddon, *Green Chem.*, 2002, **4**, 147–151.

16 A. J. Arduengo, F. P. Gentry, P. K. Taverkere and H. E. Simmons, *US Pat.*, 6177575, 2001.

17 M. Begtrup and P. Larsen, *Acta Chem. Scand.*, 1990, **44**, 1050–1057.

18 G. J. Martin, X. Y. Sun, C. Guillou and M. L. Martin, *Tetrahedron*, 1985, **41**, 3285–3296.

19 A. M. Klibanov, *Nature*, 2001, **409**, 241–246.

20 S. Garcia, N. M. T. Lourenco, D. Lousa, A. F. Sequeira, P. Mimoso, J. M. S. Cabral, C. A. M. Afonso and S. Barreiros, *Green Chem.*, 2004, **6**, 466–470.

21 F. Merzel and J. C. Smith, *Proc. Natl. Acad. Sci. U. S. A.*, 2002, **99**, 5378–5383.

22 J. Uppenberg, M. T. Hansen, S. Patkar and T. A. Jones, *Structure*, 1994, **2**, 293–308.

23 R. M. Lau, M. J. Sorgedrager, G. Carrea, F. van Rantwijk, F. Secundo and R. A. Sheldon, *Green Chem.*, 2004, **6**, 483–487.

24 A. T. J. W. de Goede, W. Benckhuijsen, F. van Rantwijk, L. Maat and H. van Bekkum, *Recl. Trav. Chim. Pays-Bas*, 1993, **112**(11), 567–572.

Extraction of glycerol from biodiesel into a eutectic based ionic liquid

Andrew P. Abbott,* Paul M. Cullis, Manda J. Gibson, Robert C. Harris and Emma Raven

A Lewis basic mixture of quaternary ammonium salts with glycerol has been used to extract excess glycerol from biodiesel formed from the reaction of triglycerides with ethanol in the presence of KOH. The effect of the cation on the partition coefficient of glycerol was determined, together with the time taken for the systems to reach equilibrium. Protocols were also investigated for the separation of glycerol from the quaternary ammonium salt mixtures.

Introduction

Biodiesel can be manufactured from a variety of natural product oil feedstocks, for example, sunflower oil, rapeseed oil, rubber seeds, and soy bean oil.[1–8] Its synthesis from a natural product means biodiesel is a carbon-neutral fuel (*i.e.* carbon dioxide generated from its combustion is equal to or less than the carbon dioxide used up by the plants it is derived from) and it produces significantly fewer particulates[1] than conventional diesel fuel with no sulfurous emissions. It can be used pure or blended with mineral diesel in most modern compression-ignition engines.[9]

The manufacturing procedure for biodiesel is much the same, regardless of the feedstock used. The triglyceride oil extracted from the plant is transesterified into alkyl esters (usually methyl or ethyl) using a catalyst such as KOH, NaOH, or a lipase. This yields three moles of ester and one mole of glycerol per mole of triglyceride as shown schematically in Fig. 1.[7]

The liberated fatty acid esters comprise a mixture of C-18 products, such as stearic, linoleic, linolenic, and oleic acid, and C-16 derivatives, such as palmitic acid in varying compositions depending on the source. The glycerol is an unwanted by-product and must be removed before the ester biodiesel can be used as fuel, as the viscosity of the glycerol present in the mixture impedes the high-pressure injection system of a modern diesel engine and may cause damage.
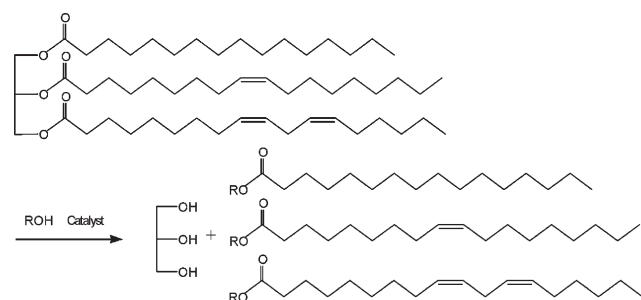
Fig. 1 Transesterification of triglycerides to alkyl esters of fatty acids and glycerol.

Chemistry Department, University of Leicester, Leicester, UK, LE1 7RH. E-mail: Andrew.abbott@le.ac.uk; Fax: +44 116 252 3789

Several methods have been used to remove glycerol from biodiesel and these include adsorption over silica,[10] membrane reactors,[11] and the addition of lime and phosphoric acid.[12] There are numerous problems associated with the costs and complications of operating biodiesel synthesis on an industrial scale.[7] Currently it is cheaper to drill and refine mineral diesel than to grow, extract, transesterify, and purify biodiesel, and methods to improve the economical feasibility of biodiesel production are sought.

The aim of this study is to design a system to separate glycerol and residual ethanol from some ethanol-esterified natural oils. We have previously shown that ionic liquids formed from eutectic mixtures of quaternary ammonium salts and hydrogen bond donors (HBDs) are an effective method of producing inexpensive, non-toxic, and environmentally benign solvent systems.[13,14] These so-called deep eutectic solvents (DESs) are made from quaternary ammonium salts mixed with a small HBD molecule, of which glycerol is one example. These DESs have been shown to have practical use in applications such as electropolishing[15] and metal oxide processing.[16]

The eutectic point (the composition of lowest freezing point and viscosity) of these solvents, that have so far been characterised, tends to occur at either 1 : 1 or 2 : 1 HBD : salt molar ratio.[13,14] The components of the mixture have a high affinity for each other due to the strength of the hydrogen bonding interactions formed. The high affinity of the salt for glycerol should mean that if a Lewis basic mixture of salt and glycerol is mixed with a phase with a low affinity for glycerol, then the former should be able to extract the excess glycerol. The high affinity of the ionic liquids for alcohols should also allow excess ethanol to be extracted from the biodiesel layer.

The aim of this work is to characterise and optimise a eutectic extraction system capable of washing glycerol out of the biodiesel product. Five quaternary ammonium salts were studied and all formed eutectics with glycerol that were miscible with water and immiscible with oils.

Experimental

The alcoholysis of vegetable oils was studied using alkaline catalysts. Potassium hydroxide, 5 g (0.9 mol) was suspended in 1 L of absolute ethanol and shaken until dissolved. 1 g of this solution was mixed with 5 g of oil and shaken in a small

stoppered flask. The flasks were placed in an incubator shaker at 40 °C and 400 rpm for 24 h. After this time, they were allowed to stand for 1 h. Separation of the KOH-catalysed reaction in ethanol did not occur, but separation of the NaOH-catalysed reaction in methanol was observed. The molecular mass of soy bean oil was assumed to be 965.

A larger volume (10 ml oil and 2 ml 0.9 M KOH–ethanol) was produced under the same conditions and this was divided into 1 ml samples and used to test the eutectics and quaternary ammonium salts as extraction media. 1 mole equivalent of each salt was added to the oil samples and heated with agitation, but a lower layer was not seen to form. 1 : 1 eutectics of each quaternary ammonium salt were prepared and added to the solutions in a 1 : 1 salt : oil molar ratio.

For the larger scale experiments 500 g of oil (rapeseed or soy bean) and 150 g of 0.9 mol KOH in absolute ethanol were mixed in an incubator at 40 °C and 400 rpm for 24 h. After this period, a lower layer separated from the rapeseed oil reaction. This was collected and NMR analysis confirmed it to be predominantly glycerol. The soy bean oil reaction did not separate on standing.

The DES used for extraction was made by heating 46 g (0.5 mol) glycerol and 69.8 g (0.5 mol) of choline chloride on a hotplate at 50 °C until a homogenous transparent liquid formed. This was added to the homogeneous oil resulting from the soy bean oil reaction and the separated oil from the rapeseed oil reaction, shaken and allowed to stand for 30 min. Samples of the upper and lower layers were analysed by ^{1}H NMR in 1-butanol and dichloromethane, respectively, and a 10 μl sample of the upper layer was analysed by GC.

Removal of glycerol from a standard solution of ethyl caprate–glycerol was carried out using a standard solution of ethyl caprate–glycerol in a 3 : 1 molar ratio. To this 0.5% v/v solution, ethanol was added to aid miscibility. 10 ml of this solution was mixed with a 1 : 1 glycerol–acetylcholine chloride eutectic and samples were taken from the upper layer and analysed by FT-IR.

Viscosity and freezing point determination of deep eutectic solvents: viscosity was determined using a Brookfield DV-E viscometer according to the standard procedure. The freezing point was taken to be the glass transition temperature or crystallisation temperature as was measured with a Jenway 4071 temperature probe after gradual cooling in ice followed by dry ice–acetone.

The chloride ion concentration was determined using potentiometry with a silver chloride and calomel electrode.

In the cell

$$Hg|Hg_2Cl_2|KCl_{(sat)}||Cl^-_{analyte}\ Cl^-|AgCl|Ag$$

the change in potential with chloride ion concentration was found to follow a Nernstian behaviour.

Results and discussion

Soy bean oil was chosen as the feedstock of study because of its favourable cetane number, and also because it did not separate readily from glycerol at the end of the reaction, and therefore was useful for the principles to be studied. Fig. 2
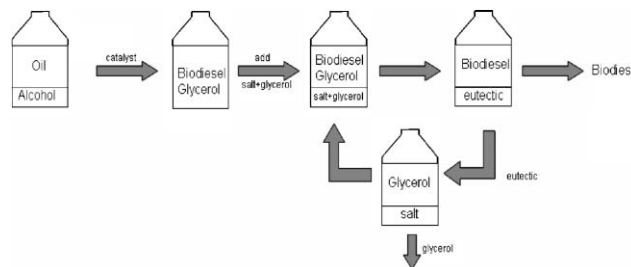
Fig. 2 Schematic diagram for the production of biodiesel and removal of excess glycerol using a sub-eutectic salt : glycerol mixture.

shows a schematic of a process that uses a choline chloride–glycerol mixture to draw out excess glycerol from biodiesel.

It was decided to concentrate on KOH and NaOH as the catalysts as these gave quantitative conversion of the oil to the methyl esters. Enzyme catalysed transesterification was also attempted, but of the fifteen lipases studied only *Candida antarctica* B gave a reasonable yield (38%) after a 24 h period of incubation. These data are comparable to the yields achieved with different oils published by Abigor *et al.*[17]

^{1}H NMR studies of the reaction products were undertaken using the solvent 1-butanol-d_{10}, as this was the only solvent in which glycerol, fatty acid esters, and unreacted soy bean oil were found to dissolve. The spectrum of the potassium hydroxide-catalysed reaction contained the glycerol signal but no discernible glyceride peaks (δ 4.15 and δ 4.3 ppm), which confirmed that the reaction had gone to completion.

Extraction of glycerol using sub-eutectic salt mixtures

Initially, pure quaternary ammonium salts were added to the crude biodiesel, to see if a deep eutectic would spontaneously form *in situ* extracting the glycerol and forming a separate layer. After the reaction was complete, the resulting oil was separated into 1 ml samples and each of these was shaken with a 0.5 mole equivalent of each of the quaternary ammonium salts chosen for the study. Upon shaking and heating, the salts all remained as solids and did not dissolve in the liquid phase, form a separate liquid phase, or effect any noticeable extraction of the glycerol from the biodiesel–glycerol mixture. This is probably due to the enthalpy of formation of the eutectic mixtures, and so an alternative approach was attempted.

Lewis basic mixtures of salt and glycerol (*i.e.* a 1 : 1 molar ratio) were made and heated until they formed homogeneous liquids. These were added to 1 ml samples of biodiesel in such quantity to ensure that the sum contents of both phases was a 1 : 2 salt : glycerol molar ratio. The mixtures were shaken, allowed to separate, and then analysed by ^{1}H NMR against the unwashed biodiesel product. A decrease in the glycerol signals (δ 3.55 and δ 3.45 ppm) in the oil phase was observed in all cases. No significant decrease in glycerol signals was observed when 1 : 2 salt : glycerol eutectics were added to the crude biodiesel in the same way, showing that the mixture is only effective at extracting glycerol when it is Lewis basic. No signal was detected for either ethanol or catalyst left in the biodiesel phase.

These initial results show that mixtures of salt and glycerol below the eutectic point can remove glycerol from crude
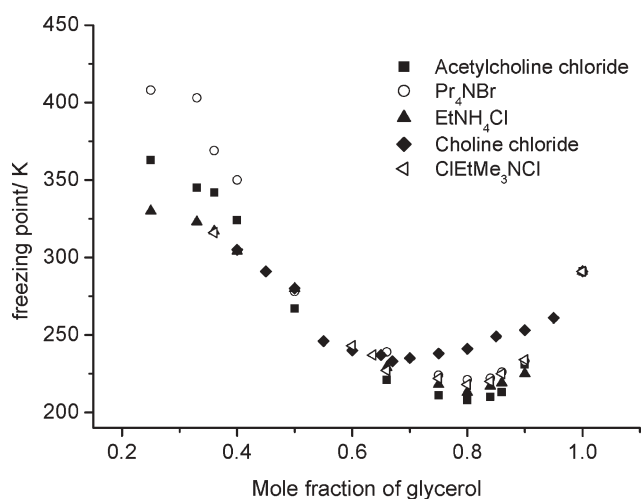
Fig. 3 Phase diagram of eutectics at different glycerol mole fractions.

biodiesel yields and suggests this extraction method to be suitable for more in-depth study.

Comparison of the physical properties of glycerol mixtures

The phase behaviour and viscosity of the salt : glycerol mixtures were characterised to identify which salts could be practically used to extract glycerol from biodiesel. The mixtures should preferably be liquid at ambient temperature and have viscosities that permit physical separation of phases by decantation or filtration. Five quaternary ammonium salts were used, and viscosities and freezing points of the mixtures were measured as a function of glycerol mole fractions in the range 0.35 to 1. The results obtained are shown in Fig. 3 and Fig. 4.

All of the eutectics studied showed their lowest viscosity at the mole fraction of approximately 0.75, whereas the freezing point minima tended to vary slightly depending on the salt. Choline chloride had a minimum freezing point at
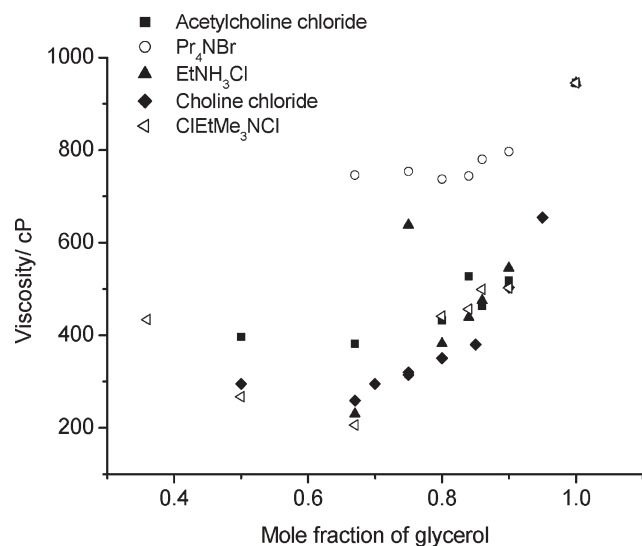
Fig. 4 Viscosity graph for eutectics at different glycerol mole fractions.

approximately 0.7, while the other salts had minima at mole fractions between 0.8 to 0.85. The freezing points at the eutectic point occurred between 210 and 235 K, meaning that all systems could be used effectively at ambient temperatures.

All the salts were also viable with respect to their viscosity. Since mixtures at the eutectic point were not found to be effective at removing glycerol from biodiesel, a Lewis basic mixture was needed. The 1 : 1 ratio of salt : glycerol mixture appeared to be the best compromise between viscosity and melting point and low mole fraction of glycerol. In this way, it is hoped that a 1 : 1 mixture of salt : glycerol could be used to extract one mole of glycerol from an equivalent 3 moles of biodiesel.

Quantification of glycerol extraction

The acetylcholine chloride eutectic was selected to study the extraction of glycerol from biodiesel as a function of time because the acetyl group on the cation and the OH group in glycerol have strong FT-IR resonances at 3330 and 1740–1730 cm^{-1}, respectively. These absorbances can be monitored over time to ascertain the time taken to reach equilibrium. By dividing the absolute intensity of the OH resonance by the absolute intensity of the acetyl resonance for studies of various molar ratios of the eutectic, a calibration curve was produced. A molar equivalent of 1 acetylcholine chloride eutectic to 1 glycerol was then used to wash a 1 ml sample of crude biodiesel. At various times, 10 µl samples of the eutectic layer were taken and analysed by FT-IR. The results are shown in Fig. 5.

This experiment revealed that the eutectic reached glycerol saturation after 10 min. Saturation corresponded to an approximate 1 : 2 molar ratio of acetylcholine chloride : glycerol and >99% removal of glycerol from the ester layer.

Effect of salt and initial composition of washing liquid

A standard mixture of 3 moles of ethyl caprate and 1 mole glycerol, with 5% v/v ethanol to aid miscibility, was mixed with
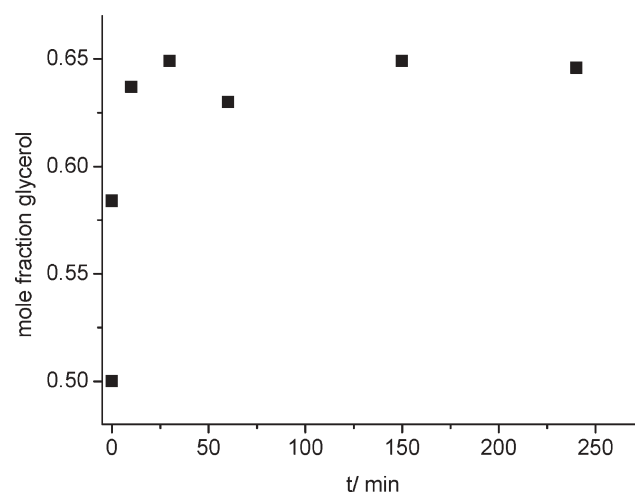
Fig. 5 Glycerol mole fraction in an acetylcholine chloride–glycerol mixture in contact with biodiesel containing glycerol as a function of time.
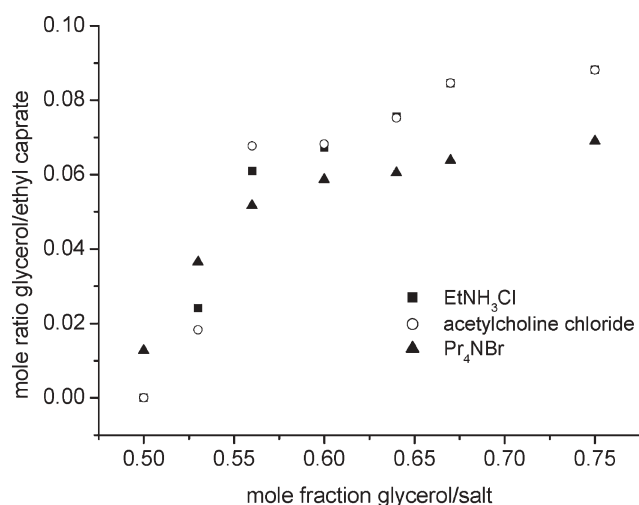
Fig. 6 Mole ratio of glycerol : ethyl caprate remaining in the biodiesel phase after washing with different salt–glycerol mixtures.

a variety of quaternary ammonium salt–glycerol mixtures of different molar ratios to determine their efficacy for glycerol removal. After shaking and warming the vials and allowing them to settle into two layers, the upper (ethyl caprate) layer was assayed by GC. The resulting glycerol–ethyl caprate mole fractions are shown in Fig. 6.

Fig. 6 shows similar profiles for the acetylcholine chloride and EtNH$_3$Cl eutectics. Pr$_4$NBr shows a slightly different profile with a better extraction of glycerol at higher mole fractions but a weaker extraction efficacy at the lower (0.5) mole fraction. From these results, it would appear the ability of the salt to draw glycerol out of the other phase may be dependent on the anion but is unaffected by the cation. The ability of chloride to extract glycerol at the 0.5 mole fraction is likely due to the higher electronegativity of the ion compared to bromide. Conversely, the lower ionic radius of chloride may become more of an issue at higher mole fractions of glycerol, and thus bromide is more effective at extracting glycerol at these mole fractions because its larger ionic radius simply means more moles of glycerol will fit around it spatially.

These results showed that the ability of the eutectics to remove glycerol from a standard system decreased with increasing glycerol concentration. The 1 : 1 molar ratio of glycerol : salt was found to be the most suitable in terms of its extraction ability and its ease of use. The three salts all gave very similar partition coefficients.

Extraction of glycerol from biodiesel into a eutectic solvent

The ideas developed with the ethyl caprate standard were applied to a practical sample of biodiesel produced using KOH, ethanol and soy bean oil. Mixtures of glycerol and salts were prepared in 1 : 1 molar ratios and used to extract 1 ml samples of crude biodiesel. The biodiesel layer was then analysed by GC to calculate the mole fraction of glycerol remaining. The results are shown in Table 1.

A significant decrease was observed in the mole fraction of glycerol remaining in the biodiesel layer after washing with all of the salt–glycerol mixtures. Particularly effective removal

Table 1 Mole fraction of glycerol in the biodiesel layer after washing with 1 : 1 glycerol : salt mixtures

Washing eutectic	$X_{glycerol}$
No wash	0.15
Pr$_4$NBr	0.08
EtNH$_3$Cl	0.00
ClEtMe$_3$NCl	0.00
Choline chloride	0.05
Acetylcholine chloride	0.03

was noted with EtNH$_3$Cl and ClEtMe$_3$NCl, with effectively complete removal of glycerol from the biodiesel. The least effective salt was Pr$_4$NBr, which confirms the earlier result using the standard ethyl caprate system in Fig. 6.

^{1}H NMR of the washed biodiesel and eutectic mixtures showed no traces of cross contamination of the two phases. However, the biodiesel yields showed impurities on the GC trace after washing with Pr$_4$NBr eutectic, thought to result from possible contamination with Pr$_3$N, and likewise after washing with acetylcholine chloride eutectics, the biodiesel layer showed evidence of impurities on the NMR spectrum, corresponding to the signals on the NMR spectra of the free amines of these salts which almost certainly comes from trace impurities in the original quaternary ammonium salts. No evidence of contamination, however, was seen when choline chloride, ClEtMe$_3$NCl, or EtNH$_3$Cl were used in washing solvents. Taking all these factors into account, ClEtMe$_3$NCl and EtNH$_3$Cl appear to be the most suitable quaternary ammonium salts for making eutectics for the extraction of glycerol from biodiesel, as they both remove almost all of it to practical detection limits in this system.

Separation of salt from glycerol mixture

To make the separation of glycerol from biodiesel using this method a viable process, a method of recovering the glycerol and the quaternary ammonium salt from the washing eutectic is necessary. In the system that has been developed here, the glycerol is recovered as a 2 : 1 mixture with a salt. In order to recycle the salt, it must be recovered or reduced to at least a 1 : 1 molar composition and the rest of the glycerol separated.

Possible purification methods include recrystallisation of the choline chloride, either by cooling or by addition of an antisolvent, and distillation of the glycerol. Distillation would be energetically difficult due to the high boiling point of glycerol (182 °C at 20 mm Hg) although vacuum distillation may be ultimately the easiest solution.

On cooling in ice, 1 : 2 mixtures of choline chloride : glycerol and acetylcholine chloride : glycerol both formed needle-like crystals. Filtration and analysis by the electrochemical method, however, showed that only about 4 wt% of the quaternary ammonium chloride could be recovered with either system. Further cooling of the solution in dry ice–acetone mixtures produced a glass-like material with no crystallisation.

Gas expansion of the mixtures was attempted using CO$_2$ at 50 bar as an antisolvent. The gas was soluble in the liquids as evidenced by opalescence of the solution on pressurisation and vigorous degassing on depressurisation, but no precipitation or crystal formation was observed over 24 h under pressure,

Table 2 Yield of biodiesel resulting from the transesterification of 550 g samples of two vegetable oils together with the amount of glycerol remaining after washing with a 1 : 1 glycerol : choline chloride mixture

Oil	Yield of biodiesel/g	Glycerol (wt%)
Soy bean	465	0.06
Rapeseed	471	0.02

and the potentiometric analysis showed the solution to be unchanged.

An alternative approach was attempted by adding a liquid co-solvent to aid the separation of the salt on cooling. 1-Butanol was added to the 1 choline chloride : 2 glycerol mixture, warmed to 50 °C to aid mixing and then cooled in ice. Significantly, more choline chloride formed as a precipitate than just by cooling the eutectic mixture. Analysis of the filtrate showed that 25% of the salt could be recovered by this method. While still unoptimised, the process shows that an anti-solvent could be added to recover the quaternary ammonium salt.

Scaled-up biodiesel synthesis with eutectic solvent extraction

To assess the suitability using salt–glycerol mixtures to purify biodiesel, a larger scale batch procedure was carried out. Both rapeseed and soy bean oil (500 g) were used with 150 g of KOH and ethanol for 24 h. Table 2 shows the yield of biodiesel produced from each experiment together with the amount of glycerol remaining after extraction with a 1 mole equivalent of 1 : 1 choline chloride : glycerol eutectic. After separation, the upper, biodiesel layer was analysed by ^{1}H NMR and GC-MS.

This shows that glycerol can be effectively removed from a biodiesel product on a moderate scale using a eutectic mixture.

Conclusions

Quaternary ammonium salt–glycerol mixture solvents were found to be successful as extraction media for glycerol from biodiesel product mixtures. A 1 : 1 glycerol : salt molar ratio was found to be the most effective for extracting glycerol from the biodiesel product. Of the salts studied, choline chloride, ClEtMe$_3$NCl, and EtNH$_3$Cl showed the best results in terms of effective glycerol removal. Choline chloride was recovered with some success from a 1 : 2 mixture with glycerol by

recrystallisation from 1-butanol, although this process was not optimised.

The process was scaled-up to a 500 ml batch process, with full alcoholysis of the triglyceride starting material and glycerol was successfully extracted by a choline chloride–glycerol washing solvent. Overall, the use of quaternary ammonium salt–glycerol DESs to remove glycerol by-products from the finished biodiesel reaction was found to be successful, but it is hoped further research will reveal a better method for recycling the salt and recovering the glycerol afterwards.

Acknowledgements

References

1 R. L. McCormick, M. S. Graboski, T. L. Alleman and A. M. Herring, *Environ. Sci. Technol.*, 2001, **35**, 1742–1747.
2 W. Du, Y. Xu, D. Liu and J. Zeng, *J. Mol. Catal.*, 2004, **30**, 125–129.
3 D. Pimental and T. W. Patzek, *Nat. Resour. Res.*, 2005, **14**, 65–76.
4 A. S. Ramadhas, S. Muraleedharan and S. Jayaraj, *Renewable Energy*, 2005, **30**, 1789–1800.
5 G. Vicente, M. Martinez, J. Aracil and A. Esteban, *Ind. Eng. Chem. Res.*, 2005, **44**, 5447–5454.
6 H. Fukuda, A. Kondo and H. Noda, *J. Biosci. Bioeng.*, 2001, **92**, 405–416.
7 F. Ma and M. A. Hanna, *Bioresour. Technol.*, 1999, **70**, 1–15.
8 J. van Gerpen, *Fuel Process. Technol.*, 2005, **86**, 1097–1107.
9 C. S. Lee, S. W. Park and S. I. Kwon, *Energy Fuels*, 2005, **19**, 2201–2208.
10 J. C. Yori, S. A. D'Ippolito, C. L. Pieck and C. R. Vera, *Energy Fuels*, 2007, **21**, 347–353.
11 M. A. Dube, A. Y. Tremblay and J. Liu, *Bioresour. Technol.*, 2006, **98**, 639–647.
12 C. W. Chiu, M. A. Dasari, W. R. Sutterlin and G. J. Suppes, *Ind. Eng. Chem. Res.*, 2006, **45**, 791–795.
13 A. P. Abbott, G. Capper, D. L. Davies, R. Rasheed and V. Tambyrajah, *Chem. Commun.*, 2003, 70–71.
14 A. P. Abbott, D. Boothby, G. Capper, D. L. Davies and R. Rasheed, *J. Am. Chem. Soc.*, 2004, **126**, 9142–9147.
15 A. P. Abbott, G. Capper, K. J. McKenzie and K. S. Ryder, *Electrochim. Acta*, 2006, **51**, 4420–4425.
16 A. P. Abbott, G. Capper, D. L. Davies, R. Rasheed and P. Shikotra, *Inorg. Chem.*, 2005, **44**, 6497–6499.
17 R. D. Abigor, P. O. Uadia, T. A. Foglia, M. J. Haas, K. C. Jones, E. Okpefa, J.U. Obibuzor and M. E. Bafor, *Biochem. Soc. Trans.*, 2000, **28**, 979–981.

Effect of ionic liquids on human colon carcinoma HT-29 and CaCo-2 cell lines

Raquel F. M. Frade,[a] Ana Matias,[a] Luis C. Branco,[bc] Carlos A. M. Afonso[c] and Catarina M. M. Duarte*[a]

The toxicity of ionic liquids, involving different classes of cations and different types of anions, was evaluated by a colorimetric assay with 3-(4,5-dimethylthiazolyl-2)-2,5-diphenyltetrazolium bromide (MTT) in two colon carcinoma HT-29 and CaCo-2 cell lines. Confluent CaCo-2 cells can undergo spontaneously an enterocytic differentiation and represent a good *in vitro* model of normal human intestinal epithelium. Ionic liquids are highly promising due to their low vapour pressures, however, toxicity evaluation of these ionic liquids is of great importance to assess the risk of these ionic liquids to humans and the environment.

Introduction

Ionic liquids (ILs) are potential "environmentally friendly" solvents due to their negligible vapour pressures. ILs are usually water-soluble and thus, they can easily enter and accumulate in the environment. As such, it is important to investigate their toxicological properties for further risk assessment of ILs. The numerous number of possible anion–cation combinations facilitates a change in the properties of the solvents; around 10^{12} accessible compounds have been estimated. The main classes of cations are imidazolium (IM), pyridinium, phosphonium and ammonium; IM remaining the most studied, so far.[1] The IM cations have 2 variable residues, one residue is usually either a methyl (MIM) or an ethyl (EIM) group, whereas the other residue is usually an alkyl chain. Regarding the anions, there also exists many possibilities; however, tetrafluoroborate (BF_4^-) and hexafluorophosphate (PF_6^-) have been extensively studied. Experiments with model microorganisms and some mammalian cell cultures have been published and no rule has yet been established between the type of anion and toxicity level, however, they do affect the cytotoxicity.[2–5] In contrast, toxicity seems to be directly correlated to the length of the alkyl chains present in the cation. Toxicity tests using the soil warm *Caenorhabditis elegans* demonstrated that increasing toxicity follows the trend C_4MIM (1-butyl-3-methylimidazolium) < C_8MIM (1-octyl-3-methylimidazolium) < $C_{10}MIM$ (1-decyl-3-imidazolium)[6] and similar results were reported for *Vibrio fischeri*,[4] the green algae *Oocystis submarina*,[7] the diatom *Cyclotella meneghiniana*,[7] an aquatic organism very sensitive to metals and organic compounds, the floating aquatic organism, *Lemna minor*,[8] and

the fast growing terrestrial plant, *Lepidium sativum*;[8] the last two organisms usually employed as models to investigate the hazardous potential of industrial chemicals. Addition of functional groups to the alkyl chains can be used to change the properties of ILs, such as the introduction of polar functional groups, which has already been suggested to reduce the toxicity of ILs.[8] Not many studies have been published about different classes of cations, but there is some evidence that toxicity might increase for ammonium salts when compared with IM, pyridinium or pyrrolidinium.[9]

In this paper we compare toxicological data of several ILs based on MIM (methyl-imidazolium) with different substituent chains, Aliquat® (tri-*n*-octylmethylammonium), P66614 (tri-*n*-hexyl-tetra-*n*-decylphosphonium) and DMG (tetra-*n*-hexyldimethylguanidinium) cations combined with different anions (Table 1). Assays were performed in two human colon carcinoma HT-29 and CaCo-2 cell lines. Confluent CaCo-2 cells are a suitable model to study enterocytic differentiation *in vitro*.[10]

Experimental

Materials

RPMI medium 1640, fetal bovine serum (FBS) and L-glutamine 200 mM (100×) and trypsin-EDTA solution were from GIBCO and the cell proliferation reagent 3-(4,5-dimethylthiazolyl-2)-2,5-diphenyltetrazolium bromide (MTT) was purchased from Sigma.

Ionic liquids

The ILs were generally prepared in this laboratory following reported procedures[11] which involved final washing with water as liquid or as dichloromethane solution, and removal of volatile components under vacuum. They were further purified by dissolving in the appropriate solvent (usually dichloromethane), filtration through a layered activated charcoal–silica column, followed by solvent removal under vacuum and dried overnight at 60–70 °C with stirring and under vacuum (0.1–0.5 mmHg). The purity of the ILs was checked by NMR.

[a]*Nutraceuticals and Delivery Laboratory, ITQB/IBET, Aptd. 12, 2781-901, Oeiras, Portugal. E-mail: rfrade@itqb.unl.pt; amatias@itqb.unl.pt; cduarte@itqb.unl.pt; Fax: +351 21 442 11 61; Tel: +351 21 446 97 27*
[b]*REQUIMTE, Departamento de Química, Faculdade de Ciências e Tecnologia, Universidade Nova de Lisboa, 2829-516, Caparica, Portugal. E-mail: luis_c_branco@yahoo.com*
[c]*Centro de Química Física Molecular, Complexo-1, Instituto Superior Técnico, Av. Rovisco Pais, P-1049-001, Lisboa, Portugal. E-mail: carlosafonso@ist.utl.pt; Fax: +351 21 8419785; Tel: + 351 21 846 4455/7*

Table 1 Schematic representation of the cations and anions

Name (abreviation)	Structure	Name (abreviation)	Structure
Cations		Anions	
1-(2-Hydroxyethyl)-3-methylimidazolium (C$_2$OHMIM)		Tetrafluoroborate	$BF_4^{\ominus}$
1-(2-(2-Methoxyethoxy)ethyl)- 3-methylimidazolium (C$_5$O$_2$MIM)		Hexafluorophosphate	$PF_6^{\ominus}$
Choline		Dicyanoamide (DCA)	NC–N–CN
1-n-Butyl-3-methylimidazolium (C$_4$MIM)		Acesulfame	
1-n-Butyl-2,3-dimethylimidazolium (BDMIM)		Sacharin	
1-n-Octyl-3-methylimidazolium (C$_8$MIM)	n-C$_8$H$_{17}$	Bistrifluoromethane-sulfonimidate (NTf2)	F$_3$CO$_2$S–N–SO$_2$CF$_3$
1-n-Decyl-3-methylimidazolim (C$_{10}$MIM)	n-C$_{10}$H$_{23}$		
Tetra-n-hexyldimethylguanidinium (DMG)	n-C$_6$H$_{13}$, NH, N, n-C$_6$H$_{13}$, n-C$_6$H$_{13}$, n-C$_6$H$_{13}$		
Tri-n-hexyl-n-tetradecylphosphonium (P66614)	n-C$_{14}$H$_{29}$, n-C$_6$H$_{13}$, P, n-C$_6$H$_{13}$, n-C$_6$H$_{13}$		
Tri-n-octylmethylammonium (Aliquat)	n-C$_8$H$_{17}$, N, n-C$_8$H$_{17}$, n-C$_8$H$_{17}$		

For the new ILs, chloride, water and combustion analysis (C, H) were also performed. Aliquat and P66614 cations are commercially available as chloride salts and thus, anion exchange was executed from these materials.

Cell culture

Human colon carcinoma HT-29 (ATTC, USA) and CaCo-2 (ATTC, USA) cells were used in this experimental work. Cells were cultured in 175 cm^2 flasks in RPMI medium 1640, supplemented with 10% FBS and 2 mM L-glutamine at 37 °C in a humidified atmosphere of 5% CO$_2$. The medium was changed when depleted and cells were sub-cultured after reaching confluence. The medium was removed from the flask and the flask rinsed with approximately 4 mL of 1% trypsin–EDTA solution. The same volume of 1% trypsin–EDTA was added to the flask and the flask incubated at 37 °C for 5–10 min. 6 mL of fresh medium was added and the cell suspension was diluted 1 : 3. The flask was supplemented with more medium until a total volume of 35 mL was reached.

Viability cell assay

A colorimetric assay with MTT was used to assess the viability of the cells. HT-29 cells were trypsinised and plated out in 96-well plates with a confluence of 10^5 cells mL^{-1}; each well contained 100 µL of medium. Stock solutions of the ILs were prepared either in 100% absolute ethanol or, in case ethanol did not ensure complete dissolution, 5% (C$_5$O$_2$MIM BF$_4$, C$_2$OHMIM PF$_6$, BMIM PF$_6$ and DMG DCA) or 10% DMSO (C$_5$O$_2$MIM PF$_6$). All the ILs were homogenous in solution and were tested in a concentration range up to 6000 µM.

HT-29 cells were cultured in 0.5% FBS for 24 h and then incubated for 4 h with the ILs in a 5% FBS medium. This length of time was chosen according to the digestion time. After treatment, the medium from the plates was changed with fresh 0.5% FBS medium and the plates returned to the incubator for an additional 24 h period. After this period, 100 µL of the colorimetric reagent MTT (0.5 g L^{-1}) was added to each well and left for 4 h. MTT is reduced to a purple formazan product by mitochondrial reductase enzymes active

in viable cells and therefore the amount of formazan product is proportional to the number of viable cells. Reaction was stopped with 150 μL DMSO in each well and formazan was quantified by measurement of the absorbance at 540 nm in a plate reader.

ILs not toxic for HT-29 cells, in the concentration range studied, were suspected to be not toxic for CaCo-2 cells. This was confirmed by evaluation of CaCo-2 cells viability, previously treated at the highest experimental concentration (6000 μM). The remaining ILs were studied as previously within the same concentration range.

Toxicological assays using CaCo-2 cells were done after reaching confluence and therefore cells were not left in the incubator for 24 h. MTT reagent was added straight after the 4 h incubation period with the ILs.

In all cell assays, each sample was incubated in three different wells and three different measurements were obtained and the average used in the data analysis. The ratio between the absorbance of IL treated cells and the absorbance of solvent treated cells (control) was used to determine the cell viability. This parameter was represented as a function of the base 10 logarithm of the IL concentration (μM). In some cases, viability stands above 1 and this is believed to be due to a mitogenic response at lower doses, since this effect has been verified for some toxic compounds.[12] A mathematical function that best fits to the experimental data was found and the different concentrations used were interpolated to construct the curves presented in the graphs. EC_{50} values represent the concentration at which the IL induced 50% decrease of cells viability and they were derived using the logistic model[4] when applied.

Results and discussion

EC_{50} was determined for ILs that reduced viability more than 50% and whose data points were able to be fitted to the logistic model.[4] When viability just varied slightly within the studied concentration range or, on the contrary, was strongly reduced at low doses of IL, EC_{50} was not possible to achieve.

Imidazolium ionic liquids

To investigate the influence of the substituent chain on the toxicity of the MIM (i) alkyl chain substituents of different lengths and (ii) substituent chains with functional polar groups were subjected to the MTT assay with HT-29 and CaCo-2 cell lines.

HT-29 cell line

Independent of whether the BF_4 or PF_6 anion was used, C_8MIM decreased the cells' viability more than C_4MIM (Fig. 1). However, the decrease was bigger for the PF_6 anion and thus, the effect of the IL is dependent on the type of anion. As expected from the previous results, viability was drastically reduced when C_8MIM BF_4 was changed to $C_{10}MIM$ BF_4 (Fig. 1). Accordingly, HT-29 cells viability decreased considerably with increasing length of the alkyl chain which agrees with previous publications.[4,5]
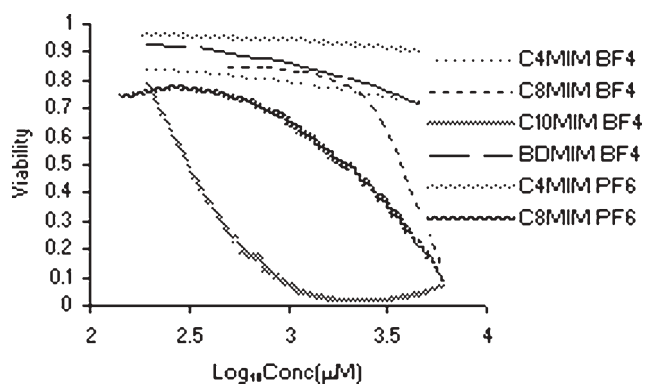
Fig. 1 Experimental toxicity data for MIM ILs with substituent chains of different lengths. The assay was performed on HT-29 cells and samples were incubated for 4 h.
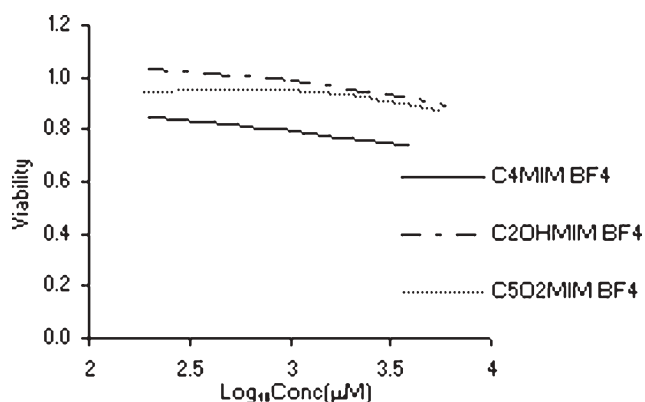
Fig. 2 Experimental toxicity data for MIM BF_4 ILs containing polar substituent groups. The assay was performed on HT-29 cells and samples were incubated for 4 h.

The presence of functional polar groups (C_2OH and C_5OH) in the MIM substituent chain enhanced the cells' viability in the presence of either BF_4 (Fig. 2) or PF_6.

For a better understanding of the effect of the anion on the IL's toxicity, this study was extended to other species. C_4MIM reference cation was used in combination with the anions acesulfame, saccharin, DCA and NTf2. While C_4MIM acesulfame was not toxic, the others induced a slight decrease in the viability (Fig. 3). The C_2OHMIM cation was also studied in combination with acesulfame and saccharin and did not have any effect on the viability which supports the finding that the presence of functional polar groups contributes to diminishing toxicity.

CaCo-2 cell line

Increasing of the toxicity with the length of the alkyl substituent chain on the MIM cations was also observed for this cell line (Fig. 1). The presence of polar groups seems to contribute to a lower toxicity also in this case. The study of C_4MIM with different anions revealed that C_4MIM acesulfame, C_4MIM saccharin, C_4MIM DCA and C_4MIM NTf2 induced negligible toxicity (Fig. 3).
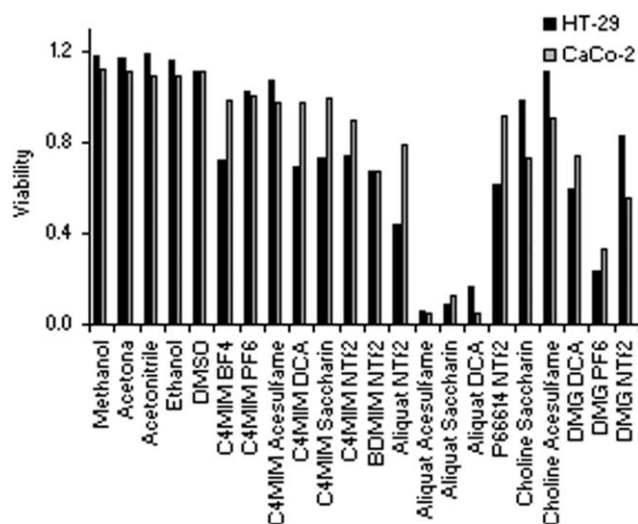
Fig. 3 Comparison of the toxicity of the ILs investigated in both HT-29 and CaCo-2 cells. Cells were treated with a similar concentration ($\cong 6000$ μM) of the different ILs and organic solvents (methanol, acetone, acetonitrile, ethanol and dimethyl sulfoxide (DMSO)) for 4 h.

Aliquat ionic liquids

HT-29 cell line. Some of the anions were tested with other cations including Aliquat (Fig. 3 and 4). Aliquat DCA, Aliquat acesulfame and Aliquat saccharin induced a high toxicity even at low doses; about 80% of cells were not viable when exposed to approximately 100 μM of these ILs (Fig. 4). The viability curve obtained for Aliquat NTf2 suggests this ionic pair is the least toxic within this group because viability did not go below 50% in the studied concentration range (Fig. 4).

CaCo-2 cell line. Similar results were obtained for this cell line. Aliquat DCA, Aliquat acesulfame and Aliquat saccharin reduced drastically the cells' viability, whereas cells incubated with Aliquat NTf2 had their viability just reduced to about 20% for the maximum concentration used (Fig. 3).
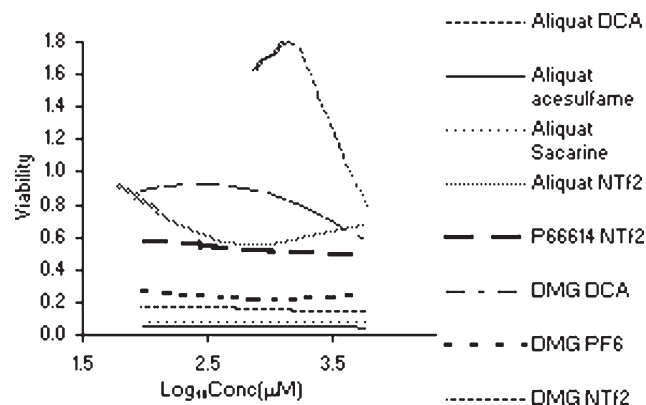
Fig. 4 Toxicity data for Aliquat, DMG and P66614 ILs performed on HT-29 cells. ILs were incubated for 4 h and viability assessed by MTT.

Choline ionic liquids

HT-29 cell line. Choline saccharin and choline acesulfame were not toxic for these cells within the studied concentration range (Fig. 3).

CaCo-2 cell line. Choline acesulfame and choline saccharin seemed to decrease just slightly the CaCo-2 cells' viability (Fig. 3).

Phosphonium and guanidinium ionic liquids

HT-29 cell line. Phosphonium P66614 NTf2 was also studied and compared with C_4MIM NTf2, DMG NTf2 and Aliquat NTf2. P66614 NTf2 is more harmful than C_4MIM NTf2 or DMG NTf2, however, EC_{50} was never attained (Fig. 3). On the contrary, it is a better IL than Aliquat NTf2 (Fig. 3 and 4).

CaCo-2 cell line. P66614 NTf2 was negligibly toxic for CaCo-2 and induced a similar response comparatively with C_4MIM NTf2 and Aliquat NTf2. For this cell line, DMG NTf2 was more toxic (Fig. 3).

Comparison of IL's toxicity with conventional organic solvents

Methanol, acetone, acetonitrile, ethanol and DMSO were the solvents utilized for comparison and the concentration used was equal to the maximum concentration used for ILs. C_4MIM PF_6 and C_4MIM acesulfame did not induce any decrease of viability in both cell lines as the organic solvents tested (Fig. 3). All the other C_4MIM combinations decreased slightly the HT-29 cells' viability whereas BDMIM NTf2 decreased slightly the viability of both cell types (Fig. 3). C_2OHMIM BF_4/PF_6, $C_5OHMIM$ BF_4/PF_6, C_2OHMIM acesulfame and C_2OHMIM saccharine were also inoffensive for both cell lines and therefore do not present any further risk than the experimented organic solvents. Choline saccharin and choline acesulfame seem to decrease to some extent CaCo-2 viability but the toxic effect is not significant. Aliquat ILs were extremely toxic for both cells, with the exception of Aliquat NTf2 that did not affect significantly CaCo-2 viability. Therefore, Aliquat ILs do not present suitable alternatives to conventional solvents (Fig. 3 and 4). Cations P66614 and DMG are not as toxic as Aliquat but are more destructive than commonly used solvents (Fig. 3 and 4).

Conclusions

Two colon carcinoma HT-29 and CaCo-2 cell lines were used to evaluate the toxicity of ILs, involving different classes of cations and different types of anions and the results are summarised in Table 2. In both cells, C_4MIM, C_2OHMIM, C_5OHMIM and cholines were the least toxic cations independently of the anion. Within the studied combinations, C_4MIM PF_6, C_4MIM acesulfame, C_2OHMIM BF_4/PF_6, C_5OHMIM BF_4/PF_6, C_2OHMIM acesulfame and C_2OHMIM saccharine were not toxic and present good alternatives to organic solvents.

Increasing the length of the substituent chain contributed to a significant increasing of MIM toxicity and thus, C_8MIM and

Table 2 Toxicity of ILs in both HT-29 and CaCo-2 cell lines. EC$_{50}$ was not achieved in many cases and as a result was not determined. ILs that at the lowest concentration killed most of the cells are classified in this table as toxic (T) whereas ILs that did not change or induced negligible variations in the viability are represented here as not toxic (NT) within the studied concentration range

	logEC$_{50}$ (µM) HT-29	logEC$_{50}$ (µM) CaCo-2		logEC$_{50}$ (µM) HT-29	logEC$_{50}$ (µM) CaCo-2
Anion PF$_6$			**Anion acesulfame**		
C$_5$O$_2$MIM PF$_6$	NT	NT	C$_2$OHMIM acesulfame	NT	NT
C$_2$OHMIM PF$_6$	NT	NT	C$_4$MIM acesulfame	NT	NT
C$_4$MIM PF$_6$	NT	NT	Choline acesulfame	NT	NT
C$_8$MIM PF$_6$	3.53 ± 0.21	3.19 ± 0.01	Aliquat acesulfame	T	T
DMG PF$_6$	T	T	**Anion saccharin**		
Anion BF$_4$			C$_2$OHMIM saccharin	NT	NT
C$_2$OHMIM BF$_4$	NT	NT	C$_4$MIM saccharin	NT	NT
C$_5$O$_2$MIM BF$_4$	NT	NT	Choline saccharin	NT	NT
BDMIM BF$_4$	>3.78	NT	Aliquat saccharin	T	T
C$_4$MIM BF$_4$	>3.78	>3.48	**Anion DCA**		
C$_8$MIM BF$_4$	3.60 ± 0.21	3.34 ± 0.13	C$_4$MIM DCA	>3.78	NT
C$_{10}$MIM BF$_4$	2.46 ± 0.06	2.78 ± 0.02	DMG DCA	>3.78	NT
Anion NTF2					
C$_4$MIM NTf2	NT	NT			
DMG NTf2	NT	>3.78			
P66614 NTf2	≅3.18	>3.78			

C$_{10}$MIM had a strong toxic effect on the cells. Out of this class, the most toxic ILs were Aliquat acesulfame, Aliquat saccharin, Aliquat DCA and DMG PF$_6$.

The results suggested that the presence of the NTf2 anion decreases the toxicity to a large extent, independently of the cation and for both cell types. If NTf2 is the anion used, toxicity of the cation seems to follow the trend choline/MIM < DMG < phosphonium < Aliquat.

Acknowledgements

References

1 *Ionic Liquids; Industrial Applications for Green Chemistry; ACS Symposium Series 818*, ed. D. Rogers and K. R. Seddon, ACS, Washington DC, 2002; P. Wasserscheid and T. Welton, *Ionic Liquids in Synthesis*, VCH-Wiley, Weinheim, 2002; J. D. Holbrey and K. R. Seddon, *Clean Prod. Process.*, 1999, **1**, 223; T. Welton, *Chem. Rev.*, 1999, **99**, 2071; J. Duppont, R. F. Souza and P. A. Z. Suarez, *Chem. Rev.*, 2002, **102**, 3667.

2 F. Ganske and U. T. Bornscheuer, *Biotechnol. Lett.*, 2006, **28**, 465.

3 S. M. Lee, W. J. Chang, A. R. Choi and Y. M. Koo, *Kor. J. Chem. Eng.*, 2005, **22**, 687–690.

4 J. Ranke, K. Molter, F. Stock, U. Bottin-Weber, J. Poczobutt, J. Hoffmann, B. Ondruschka, J. Filser and B. Jastorff, *Ecotoxicol. Environ. Saf.*, 2003, **58**, 396–404.

5 P. Stepnowski, A. C. Skladanowski, A. Ludwiczak and E. Laczynska, *Hum. Exp. Toxicol.*, 2004, **23**, 513–517.

6 R. P. Swatloski, J. D. Holbrey, S. B. Memon, G. A. Caldwell, K. A. Caldwell and R. D. Rogers, *Chem. Commun.*, 2004, 668–669.

7 A. Latala, P. Stepnowski, M. Nedzi and W. Mrozik, *Aquat. Toxicol.*, 2005, **73**, 91–8.

8 B. Jastorff, K. Molter, P. Behrend, U. Bottin-Weber, J. Filser, A. Heimers, B. Ondruschka, J. Ranke, M. Schaefer, H. Schroder, A. Stark, P. Stepnowski, F. Stock, R. Stormann, S. Stolte, U. Welz-Biermann, S. Ziegert and J. Thoming, *Green Chem.*, 2005, **7**, 362–372.

9 C. Pretti, C. Chiappe, D. Pieraccini, M. Gregori, F. Abramo, G. Monni and L. Intorre, *Green Chem.*, 2006, **8**, 238–240.

10 C. Jumarie and C. Malo, *J. Cell Physiol.*, 1991, **149**, 24–33.

11 Colin F. Poole, *J. Chromatogr., A*, 2004, **1037**, 49–82; Luís C. Branco, João N. Rosa, Joaquim J. Moura Ramos and Carlos A. M. Afonso, *Chem.–Eur. J.*, 2002, **8**, 3671–3677; Nuno M. M. Mateus, Luís C. Branco, Nuno M. T. Lourenço and Carlos A. M. Afonso, *Green Chem.*, 2003, **5**, 347–352.

12 W. C. Dorsey, P. B. Tchounwou and D. Sutton, *Int. J. Environ. Res. Public Health*, 2000, **1**(2), 100–5.

A green process for *O*-heterocyclization of cycloocta-1,5-diene by peroxotungstic species with aqueous H$_2$O$_2$

Ruihua Gao,[a] Wei-Lin Dai,*[a] Yingyi Le,[a] Xinli Yang,[a] Yong Cao,[a] Hexing Li[b] and Kangnian Fan[a]

The hydroxy- and carbonyl-derivatives of 9-oxabicyclo[3.3.1]nonane have been synthesized through an economic and green catalytic reaction between cycloocta-1,5-diene (COD) and aqueous H$_2$O$_2$ with tungstic acid as the catalyst. This process has advantages from the viewpoint of green chemistry, in that the aqueous H$_2$O$_2$ is used as the green oxygen donor, the only by-product of H$_2$O$_2$ is water and the tungstic acid catalyst can also be easily recovered. The excellent yields of the object products (**1** and **2**) (see Scheme 1) are reached easily under mild reaction conditions.

1. Introduction

The γ-butyrolactone structure is a versatile building block in organic synthesis since countless compounds containing this functional group show interesting biological activity.[1–3] For example, 5-hydroxy-γ-decalactone is a potent cytotoxic agent on different tumour cell lines.[4] It is commonly accepted that 9-oxabicyclo[3.3.1]nonane-2,6-dioles (**1**) and 2-hydroxy-9-oxabicyclo[3.3.1]nonane-6-one (**2**) are the major starting material for the synthesis of γ-butyrolactones. Therefore, it is of great significance to develop efficient and accessible approaches to affording these products (**1** and **2**). Classical routes to **1** and **2** employ peroxo acid or permanganate as oxidants. For example, Behr *et al.* obtained a 23.3% yield of **1** by using peracetic acid as the oxidant and cycloocta-1,5-diene (COD) as the raw material.[5] If peracetic acid was replaced by permanganate, a much lower conversion of COD was observed. Moreover, the yield of **1** can reach 70% if performic acid is used, according to Hegemann *et al.*[6] However, the performic acid, as well as peracetic acid and permanganate, is an expensive chemical and leads to a large amount of by-products. Therefore, difficult separation of **1** from the products mixture is inevitable in these routes because of the low conversion and selectivity.

Nowadays, the development of environmental friendly techniques is one of the priority goals of chemical research, and this is especially true in the field of the oxidation of organic compounds, where there is an urgent need to replace wasteful and toxic stoichiometric oxidants with "clean" oxygen donors, such as hydrogen peroxide. As we know, the oxidation of organic substrates with hydrogen peroxide is very attractive and has long been studied. Many useful reactions using hydrogen peroxide as oxidant have been developed, such as the epoxidation of olefins and allylic alcohols,[7–9] olefins to carboxylic acids,[10] oxidation of sulfides to sulfoxides and sulfones[11] and oxidative cleavage of carbon–carbon double bonds to aldehydes.[12–16] It is an effective strategy for the synthesis of these two compounds (**1** + **2**) by the selective oxidation of COD with environmentally benign aqueous H$_2$O$_2$. Thus, no noxious substances are needed and no toxic waste is generated in the reaction. However, to the best of our knowledge, no catalytic process has ever been reported so far in this strategy.

Herein we report a green procedure for the *O*-heterocyclization of COD by catalytic oxidation with aqueous H$_2$O$_2$. *tert*-Butanol is chosen as the solvent because the *tert*-butanol–H$_2$O$_2$ system is stable and safe and has been employed in many oxidation reactions.[16] The reaction is carried out under mild conditions and enjoys good selectivity. Tungstic acid is an inexpensive catalyst and aqueous hydrogen peroxide is a relatively safe and non-polluting oxidant. The tungstic acid catalysts which deposit by adjusting the pH value of the solution to higher than 7 can be easily removed by simple filtration. The products can be easily obtained with high purity through decompressed rectification, due to the big difference in boiling point between the object products and *tert*-butanol. Therefore, the large-scale preparation and industrial manufacture of the hydroxy- or carbonyl-derivatives
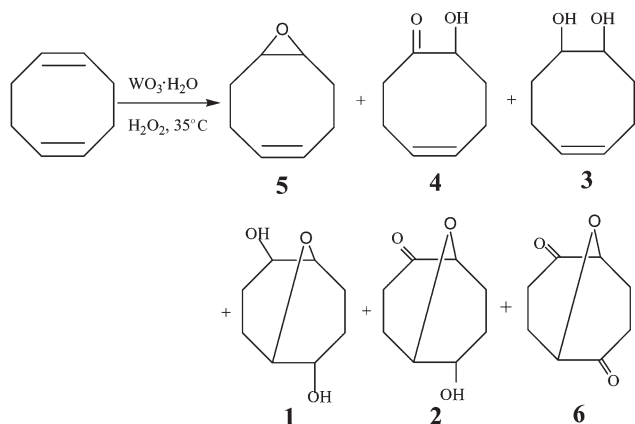
Scheme 1 The oxidation products of COD by H$_2$O$_2$.

[a]*Department of Chemistry and Shanghai Key Laboratory of Molecular Catalysis and Innovative Materials, Fudan University, Shanghai 200433, P. R. China. E-mail: wldai@fudan.edu.cn; Fax: 86-21-65642978*
[b]*Department of Chemistry, Shanghai Normal University, Shanghai 200234, P. R. China. E-mail: Hexing-Li@shnu.edu.cn; Fax: 86-21-64322272*

of 9-oxabicyclo[3.3.1]nonane can be achieved by use of these compounds.

2. Experimental

2.1. Materials

Cycloocta-1,5-diene, 50% aqueous H_2O_2, *tert*-butanol, tungstic acid, 1,4-dioxane, acetonitrile, tetrahydrofuran, methanol, ethanol, n-butanol and iso-propanol were of analytical grade and were used as received.

2.2. Catalyst preparation

The novel catalytic system was prepared by a simple method: the required amount of tungstic acid was added into aqueous H_2O_2 at 60 °C. After 2 h pre-reaction, the mixture was used as the catalytic system.

2.3. Catalytic reaction: COD oxidation

The activity test was performed at 35 °C for a set time ranging from 2 to 24 h with magnetic stirring in a closed 25 mL regular glass reactor using 50% aqueous H_2O_2 as oxygen-donor and *t*-BuOH as the solvent. In a typical experiment, 0.108 g of the $WO_3 \cdot H_2O$ (0.46 mmol) and 1.4 mL of 50 wt% aqueous H_2O_2 (22.5 mmol) were introduced into the regular glass reactor at 60 °C with vigorous stirring. Then, the reaction was started after the addition of 10 mL of *t*-BuOH and 1.06 mL of COD (7.5 mmol) into the mixture and was kept for 2 h or more. The conversion of H_2O_2 was measured by a standard iodimetric titration method. The quantitative analysis of the reaction products was performed by using a GC method and the identification of different products in the reaction mixture was determined by means of GC-MS on HP 6890GC/5973 MS.

3. Results and discussion

3.1. Products of COD oxidation

According to the GC-MS analysis, the products of COD oxidation, as shown in Scheme 1, consist of the two object products **1** and **2** with small amounts of by-products including **3**, **4** and **5** under the present conditions. All the products are the derivatives from the epoxide of C=C bond and the further oxidation of alcoholic moieties into ketones, such as the conversion of **1** into **2** and the conversion of **2** into 9-oxabicyclo[3.3.1]nonane-2,6-dione (**6**), which can be neglected because of the small amount of it present. It is a surprise to find that there are no cleavage products from one or two C=C bonds. Since the two main products, **1** and **2**, can both be oxidized to the same product—γ-butyrolactones—the total yield of these two products is used to determine the catalytic performance of different catalysts.

3.2. Conversion of COD and H_2O_2 and selectivity of various products over the catalyst

The reaction process is indicated in Fig. 1, which shows a typical plot of COD consumption, and the products formation *versus* time under the reaction conditions. It is shown that a complete conversion of COD is achieved and the selectivity to
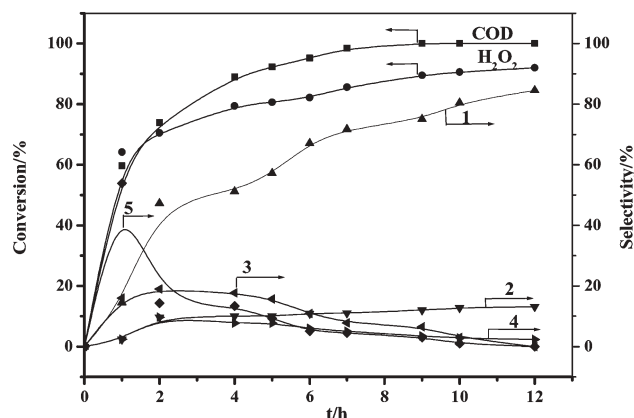
Fig. 1 Conversion of COD and H_2O_2 and selectivity of **1** and **2** over the catalyst (reaction condition: reaction temperature 35 °C, COD 7.5 mmol, H_2O_2 22.5 mmol, catalyst $WO_3 \cdot H_2O$ 0.14 mmol).†

Table 1 Catalytic performances of oxidation of COD over various molar ratios of H_2O_2 to COD[a]

	Conversion (%)		Selectivity (%)		
H_2O_2:COD	COD	H_2O_2	1	2	1 + 2
1:1	71	97	23	1	24
2:1	96	97	67	6	73
2.5:1	98	88	75	11	86
3:1	100	80	79	14	93
4:1	100	80	71	27	98

[a] Reaction condition: reaction temperature 35 °C, H_2O_2 22.5 mmol, catalyst $WO_3 \cdot H_2O$ 0.081 mmol, reaction time 24 h, *t*-BuOH 10 mL.

1 and **2** is satisfactorily high. In particular, the curve of **5** with the highest selectivity in the first period declined *versus* time. At the same time, the tendencies of **3** and **4** are similar to **5**. For the main products of **1** and **2**, the selectivity increases with time. Under this reaction condition, the oxidation of COD to **1** and **2** is a very complex process. Some of these steps are similar to those described in refs. 17 and 18. Therefore, a possible reaction scheme can be described (see footnote†).

3.2. COD oxidation with different amount of H_2O_2

Table 1 shows the performance of the selective oxidation of COD over various molar ratios of H_2O_2 to COD. It can be seen that the conversion of COD rises with the increase in molar ratio of H_2O_2 to COD, as does the selectivity to **1** and **2**. Because H_2O_2 is the oxygen donor, the rate of the reaction and the selectivity of products are due to it. The complete consumption of COD cannot be achieved when the ratio is

† Herein, we assume that the process for this reaction, catalysed by tungstic acid, consists of several steps. COD is first oxidized to its oxides, such as 1,5-epoxycyclooctene (**5**), 1,5 diepoxycyclooctane, *etc.*, then **1** is formed *via* hydrolysis of 1,5-diepoxycyclooctane, accompanied by the formation of a by-product **3**, *via* hydrolysis of **5**. Some of these steps are similar to the study of refs. 17 and 18. The step of **1** being formed from 1,5-diepoxycyclooctane is so fast that the diepoxycyclooctane cannot be tested in our experiments, Following above steps, **4** and **2** are respectively formed *via* deep oxidation of **3** and **1**. Finally, **6** is formed by deeper oxidation of **2**, but the amount of **6** is so small that it can be neglected.

lower than 3:1. The selectivity of **1** rises with the increase of the ratio before 3:1, then it decreases at 4:1. However, the selectivity of **2** rises with the increase of the ratio for all the molar ratios. The result shows that **1** and **2** have different trends of selectivity for various molar ratios of H_2O_2 to COD. Thus, different ratios of H_2O_2 to COD can affect the yield of the object products. At the molar ratio of 4:1, the selectivity of the total products reaches 98%, but considering both good catalytic performance and H_2O_2 utility, the 3:1 ratio of the H_2O_2 to COD is needed.

3.3. Catalytic performance with different amounts of $WO_3 \cdot H_2O$

The reaction results as a function of the amounts of $WO_3 \cdot H_2O$ catalyst used were also investigated, and are listed in Table 2. It was found that conversion of COD in a fixed reaction period ascends with increasing catalyst dosage, the amounts of which are ranging from 0.013 g (0.055 mmol) to 0.108 g (0.46 mmol). When the amounts are higher than 0.108 g, the conversion of COD in 2 h is the same to 100%. It could thus be suggested that the amounts of active species affect the reaction rate. The higher the amount of peroxotungstic acid, the higher the rate of the consecutive reactions. Entries 1–3 in Table 2 indicate that when COD reaches complete conversion, the total selectivity of (**1 + 2**) with the amount of catalyst is almost the same, ranging from 97 to 99%, but the distributions of **1** and **2** are different from each other (the selectivity of **2** ranges from 5 to 17%). Such a phenomenon can also be seen from entries 4 and 5. This indicates that the amount of catalyst not only affects the rate of the reaction but also affects the distribution of **1** and **2**.

3.4. Effect of solvent on COD oxidation

Solvent plays an important role in the selectivity of the reaction, and hence it was decided to investigate the solvent effect. As shown in Table 3, the maximum selectivity of the object products is formed when the solvent is *tert*-butanol, whereas the use of other alcohols results in a low yield compared with *tert*-butanol. It is important to note here that the by-products in solution using linear alcohols are ethers, which derive from the etherification of the hydroxy derivatives with the corresponding alcoholic solvents. This leads to the

Table 2 The effect of the amounts of catalysts over the reaction[a]

Entry	Amount of catalyst/g	COD: catalyst[b]	Time/h	Conversion (%) COD	Conversion (%) H_2O_2	Selectivity (%) 1	Selectivity (%) 2	Selectivity (%) 1 + 2
1	0.324	5.40	2	100	98	94	5	99
2	0.216	8.20	2	100	93	82	17	99
3	0.108	16.3	2	100	96	86	11	97
4	0.059	32.6	2	92	80	50	7	57
5	0.059	32.6	12	100	84	85	13	98
6	0.019	101	12	97	80	65	14	79
7	0.019	101	17	98	85	71	17	88
8	0.013	148	12	86	72	46	11	57
9	0.013	148	17	88	76	56	14	70

[a] Reaction condition: reaction temperature 35 °C; COD: 7.5 mmol; H_2O_2: 22.5 mmol; *t*-BuOH 10 mL. [b] The molar ratio of COD to catalyst (tungstic acid).

Table 3 The effect of the different solvents over the reaction[a]

Solvents	C_{COD} (%)	S_1 (%)	S_2 (%)	S_{1+2} (%)	S_{other} (%)
Methanol	100	42	30	72	28
Ethanol	100	58	26	84	16
n-Butanol	100	78	6	84	16
2-Propanol	100	81	11	92	8
tert-Butanol	100	86	11	97	3
1,4-Dioxane	93	65	29	94	6
Acetonitrile	100	91	5	96	4
Tetrahydrofuran	100	75	22	97	3

[a] Reaction conditions: reaction temperature 35 °C, reaction time 2 h, COD 7.5 mmol, H_2O_2 22.5 mmol, tungstic acid 0.46 mmol, solvent 10 mL.

conclusion that the *tert*-butanol is the best of its kind, the large alkyl structure of which hinders the formation of ethers. Some other water-soluble solvents, such as 1,4-dioxane, acetonitrile and tetrahydrofuran, which have no tendency to give ethers, were also tested (see Table 3) and the conversion of COD and the selectivity of object products were also high. The nature of the oxidation in these solvents is still under investigation.

Independent experiments were carried out to study the effect of the volume of tert-butanol on reaction. Table 4 indicates that there is an optimum volume of tert-butanol at which a maximum amount of (**1 + 2**) is formed. Initially, with a decrease in the volume from 20 to 5 mL, the selectivity of object products increases from almost 88 to 98%. This can be explained by the fact that, for the formation of **1** and **2**, the concentration of active oxidizing species is required. The concentration of active oxidizing species formed depends on the concentration of hydrogen peroxide. At 5 mL, large amount of oxidizing species are formed as compared to the case with high volume of tert-butanol. It is also found that, without the use of desired amount of organic solvents, this reaction cannot be carried out with high efficiency due to the phase splitting between COD and aqueous H_2O_2. Thus, further studies are under way on the search of new catalysts showing good activity and selectivity without the use of any organic solvents.

Here the ammonium tungstate and sodium tungstate also used were compared with tungstic acid. It was found that the performance of ammonium tungstate was similar to that of tungstic acid. However, the sodium tungstate has no activity for this reaction. It was observed that the pH values of the reaction solution were 0.67, 1.82 and 4.83, respectively, for tungstic acid, ammonium tungstate and sodium tungstate. The different pH values hint that the tungsten species are different in those solutions. Lin *et al.*[19] found that the composition of

Table 4 The effect of volumes of *t*-BuOH on the oxidation of COD[a]

Volumes of *t*-BuOH	Conversion (%) COD	Conversion (%) H_2O_2	Selectivity (%) 1	Selectivity (%) 2	Selectivity (%) 1 + 2
5	100	91	78	20	98
10	100	95	86	11	97
15	100	91	83	10	93
20	98	68	80	8	88

[a] Reaction conditions: reaction temperature 35 °C, reaction time 2 h, COD 7.5 mmol, H_2O_2 22.5 mmol, tungstic acid 0.46 mmol.

active tungsten species was affected by the pH value. It can be speculated that the composition of active tungsten species is the inner key to the reaction. However, experiments on the continuous change of the pH value in this reaction by adding alkali were not successful due to the deposition of tungstic species. Detailed work concerning the effect of pH values and the mechanism at molecular level is under way.

4. Conclusions

From this detailed study of *O*-hetero-cyclization of COD by catalytic oxidation with aqueous H_2O_2, the following conclusions can be established. It is possible to oxidize COD to hydroxy- or carbonyl-derivatives of 9-oxabicyclo[3.3.1]nonane at room temperature in the presence of tungstic acid. The reaction rate and selectivity of object products formation are affected by the amount of the tungstic acid and the molar ratio of COD to H_2O_2, as well as the volume ratio of the solvent to reactant. The branched alcohols are recommended as solvents in order to reach good yields of the products. The present method appears to be useful in preparing the hydroxy- or carbonyl-derivatives of 9-oxabicyclo[3.3.1]nonane by oxidation of COD with H_2O_2. It has advantages compared with the other traditional chemical methods. With a high conversion of COD and selectivity of the object products, it is very suitable for the preparation of hydroxy- or carbonyl-derivatives of 9-oxabicyclo[3.3.1]nonane from COD in both the laboratory and industry.

Acknowledgements

References

1 H. M. R. Haffmann and J. Rabe, *Angew. Chem.*, 1985, **97**, 96, (*Angew. Chem., Int. Ed. Engl.*, 1985, **24**, 94).
2 S. M. Kupchan, M. A. Eakin and A. M. Thomas, *J. Med. Chem.*, 1971, **14**, 1147.
3 K. H. Lee, H. Furukawa and E. S. Huang, *J. Med. Chem.*, 1972, **15**, 609.
4 M. J. Rieser, J. F. Kozlowski, K. V. Wood and J. L. McLaughlin, *Tetrahedron Lett.*, 1991, **32**, 1137.
5 S. Behr, K. Hegemann, H. Schimanski, R. Frohlich and G. Haufe, *Eur. J. Org. Chem.*, 2004, **18**, 3884.
6 K. Hegemann, R. Frohlich and G. Haufe, *Eur. J. Org. Chem.*, 2004, **10**, 2181.
7 M. C. Capel-Sanchez, J. M. Campos-Martin and J. L. G. Fierro, *J. Catal.*, 2005, **234**, 488.
8 F. Somma, P. Canton and G. Strukul, *J. Catal.*, 2005, **229**, 490.
9 F. Somma and G. Strukul, *J. Catal.*, 2004, **227**, 344.
10 H. Chen, W. L. Dai, X. L. Yang, R. H. Gao, Y. Cao, H. X. Li and K. N. Fan, *Appl. Catal., A*, 2006, **309**, 62.
11 K. Sato, M. Hyodo, M. Aoki, X. Q. Zheng and R. Noyori, *Tetrahedron*, 2001, **57**, 2469.
12 J. F. Deng, X. H. Xu, H. Y. Chen and A. R. Jiang, *Tetrahedron*, 1992, **48**, 3503.
13 X. H. Xu, H. Y. Chen, J. F. Deng and A. R. Jiang, *Acta Chim. Sin.*, 1993, **51**, 399.
14 W. L. Dai, H. K. Yu, A. R. Jiang and J. F. Deng, *Acta Chim. Sin.*, 1995, **53**, 188.
15 W. L. Dai, X. J. Huang, H. Y. Chen and J. F. Deng, *Indian J. Chem., Sect. B: Org. Chem. Incl. Med. Chem.*, 1997, **36**, 583.
16 X. L. Yang, W. L. Dai, H. Chen, Y. Cao, H. X. Li, H. Y. He and K. N. Fan, *J. Catal.*, 2005, **229**, 259.
17 R. Noyori, M. Aoki and K. Sato, *Chem. Commun.*, 2003, **19**, 1977.
18 P. U. Maheswari, P. de Hoog, R. Hage, P. Gamez and J. Reedijk, *Adv. Synth. Catal.*, 2005, **347**, 1759.
19 H. Q. Lin, H. M. Li, X. Y. Yu, H. S. Zhai, Y. Z. Yuan and H. L. Wan, *Acta Chim. Sin.*, 2004, **62**, 1780.

Supercritical carbon dioxide and poly(ethylene glycol): an environmentally benign biphasic solvent system for aerobic oxidation of styrene

Jin-Quan Wang, Fei Cai, Er Wang and Liang-Nian He*

Aerobic oxidation of styrene catalyzed by $PdCl_2$/CuCl can be smoothly performed in the supercritical carbon dioxide and poly(ethylene glycol) biphasic system. A high conversion of styrene and yield of acetophenone were obtained in the presence of a relatively low catalyst loading. This environmentally benign biphasic catalytic system can be applied to the Wacker oxidation of various alkenes. Furthermore, the $PdCl_2$-mediated oxidation of styrene was preferentially converted into benzaldehyde using a biphasic $scCO_2$/PEG system. The PEG could effectively immobilize and stabilize the catalysts. The present biphasic system could facilitate product separation and catalyst recycling. The effects of the reaction parameters such as solvent and CO_2 pressure were also investigated in detail.

Introduction

Processes involving the oxidation of olefins using air or oxygen are of great importance to industrialized economies because of their role in converting petroleum hydrocarbon feedstocks into industrial organic chemicals. Palladium-catalyzed oxidation of alkenes to methyl ketones has been successfully developed in synthetic organic chemistry as well as in industrial processes. A well-known example is the Wacker process using $CuCl_2$ or CuCl as co-catalyst in acidic aqueous medium under an oxygen atmosphere.[1] However, this catalytic system with high catalyst loading is highly corrosive, and higher alkenes have very poor solubility in water, resulting in low reaction rates and the formation of different types of by-products. To overcome such drawbacks, many efforts have been made, including: (1) the choice of appropriate solvents, such as *N,N*-dimethylformamide,[2] ethanol,[3] acetonitrile,[4] supercritical carbon dioxide ($scCO_2$),[5] poly(ethylene glycol) (PEG),[6] ionic liquids (ILs),[7] $scCO_2$/ILs,[8] *N,N*-dimethylacetamide (DMA);[9] (2) the addition of promoters, like pyridine,[10] hexamethylphosphoramide,[11] calixarenes,[12] bidentate diamine;[13] (3) employing suitable co-catalysts like benzoquinone (BQ),[4,14] ferric chloride,[15] heteropoly acid,[16] iron phthalocyanine;[17] and (4) supporting of Pd(II) catalyst onto polymers.[18] Consequently, the development of a simple, efficient and environmentally friendly method for the selective oxidation of styrene to acetophenone is a desirable research endeavour.[19–21]

PEG is an inexpensive, non-volatile, and environmentally benign solvent, which represents an interesting reaction medium for conventional solvent replacement.[22] $scCO_2$ has attracted much attention as a 'green' replacement for organic solvents, offering economical and environmental benefits due to its favorable physical and chemical properties. Recyclability, ease of solvent removal, and readily tunable

Institute of Elemento-Organic Chemistry, State Key Laboratory of Elemento-Organic Chemistry, Nankai University, Tianjin, 300071, P. R. China. E-mail: heln@nankai.edu.cn; Fax: +86-22-23504216; Tel: +86-22-23509634

solvent parameters make $scCO_2$ a desirable alternative over conventional solvents.[23] In particular, CO_2 appears to be an ideal solvent for use in oxidations. Unlike almost any organic solvent, CO_2 will not be oxidized further, and hence the use of CO_2 as a reaction medium eliminates by-products originating from the solvent. The high miscibility of the gaseous oxidant such as O_2 in $scCO_2$ could eliminate interphase transport limitations.[23]

The biphasic catalysis system using $scCO_2$ as the continuous phase (extracting CO_2-soluble products) and PEG as the stationary catalyst phase (immobilized PEG-soluble catalyst) could offer the possibility of recovering the expensive metal catalyst and running the metal-mediated chemical reactions under continuous flow conditions. Recently, Leitner and co-workers have presented an excellent example for an aerobic oxidation of alcohols catalyzed by PEG-stabilized palladium nanoparticles using a biphasic PEG/$scCO_2$ system.[22f]

Up to now, the Wacker oxidation reaction still suffers from Pd deactivation, high catalyst loading, and a limited substrate scope. In order to circumvent these problems, we introduce a biphasic PEG-300(MW = 300)/$scCO_2$ system to the Wacker reaction as a part of our continuous efforts on utilizing CO_2 as a feedstock or reaction medium.[24] In this work, we would like to present our observation on the Wacker oxidation of styrene catalyzed by $PdCl_2$/CuCl using molecular oxygen in a $scCO_2$/PEG biphasic solvent system, where the present biphasic solvent system can be also successfully applied to the $PdCl_2$-mediated aerobic oxidation of styrene to benzaldehyde (Scheme 1) with efficacious recyclability.

Results and discussion

Currently, Pd-catalysts have been widely used for catalytic oxidation, hydrogenation and C–C coupling reactions in industrial processes, but the application is limited probably due to aggregation and formation of the less active Pd-black. Preventing the deactivation and reducing the catalyst loading is a continuing challenge for chemists in both academia and
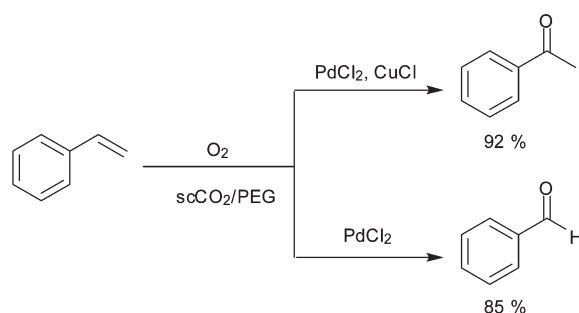
Scheme 1 Aerobic oxidation of styrene in scCO$_2$/PEG.
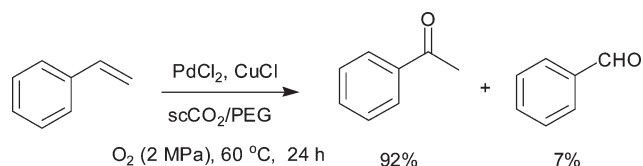
Scheme 2 PdCl$_2$/CuCl-catalyzed Wacker oxidation of styrene to benzaldehyde in scCO$_2$/PEG.

Scheme 3 PdCl$_2$-catalyzed aerobic oxidation of styrene in scCO$_2$/ PEG.

industry. In this context, the biphasic PEG-300/scCO$_2$ catalysis may provide a pathway to address this problem. In our studies, in the PdCl$_2$/CuCl-catalyzed aerobic oxidation of styrene in scCO$_2$/PEG-300 into acetophenone and benzaldehyde, detected by GC–MS as depicted in Scheme 2, no chlorinated product was formed. The results are summarized in Table 1. For the Wacker oxidation, in the absence of any solvent, the reaction did not take place at all (entr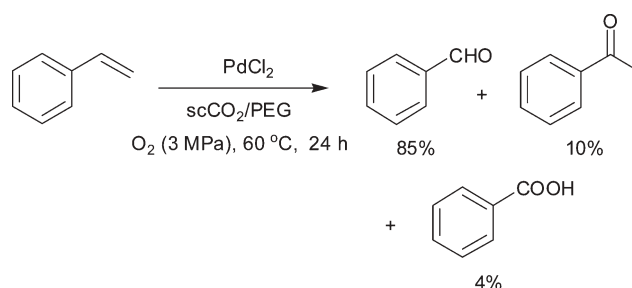y 1, Table 1). In scCO$_2$/ CH$_3$OH, although the conversion of styrene was fair to good, the selectivity to the target molecule acetophenone was poor (entry 8). In pure CO$_2$, the conversion of styrene could reach 100% with 74% yield (entry 2), as previously reported by Jiang et al.[5] However, addition of water had an adverse effect on the catalytic performance (entries 6, 7, and 9).

Notably, the addition of PEG noticeably enhanced the selectivity (entries 10, 11 vs. 2), and the reaction ran quiet well even in pure PEG-300 (entry 4), possibly owing to the unique

properties of PEG including its miscibility with organic substrates and coordination with metal salts and expandability by CO$_2$, accompanied by changes in the physical properties such as viscosity and diffusion rates.[22a,22d,25,26] Furthermore, the oxidation of styrene proceeded smoothly even in a low catalytic amount of 0.6% relative to styrene (entry 10). When CuCl was replaced by CuCl$_2$, the conversion decreased to a great extent, whereas the selectivity towards ketone was still high (entry 14).

It is important to note that the major limitation of the reported Wacker oxidation of styrene is the catalyst deactivation by aggregation and formation of Pd-black, and the high catalyst loading (10%).[7a] Notably, the presence of PEG can stabilize the Pd(0) generated from the catalytic approach,[22f] allowing the catalyst to participate in more catalytic cycles, so the amount of catalyst could be reduced. As a consequence, the best result was obtained in a biphasic scCO$_2$/PEG-300 system (entry 11), in almost 100% conversion and 92% yield of acetophenone. To our knowledge, this is one of the best results to date for aerobic oxidation of styrene to acetophenone.

It is noteworthy that a varying amount of benzaldehyde was formed in the present Wacker reaction process. The PdCl$_2$-catalyzed aerobic oxidation of styrene was found to result in the formation of benzaldehyde, acetophenone and benzoic acid as elaborated in Scheme 3. These results intrigued us for further investigation. The reaction did not occur at all with

Table 1 Aerobic oxidation of styrene in different solvents and catalytic systems[a]

Entry	Solvent	Conversion (%)	Ketone yield[b] (%)	Aldehyde yield (%)
1	None	Trace	—	—
2	scCO$_2$	100	74	22
3[c]	scCO$_2$	Trace	—	—
4	PEG	100	83	11
5[d]	PEG	100	30	35
6[e]	PEG/H$_2$O	100	83	12
7[f]	scCO$_2$/H$_2$O	69	63	4
8[g]	scCO$_2$/CH$_3$OH	100	44	25
9[e]	scCO$_2$/PEG/H$_2$O	53	43	9
10[h]	scCO$_2$/PEG	96	88	7
11	scCO$_2$/PEG	100	92	7
12[i]	scCO$_2$/PEG	Trace	—	—
13[j]	scCO$_2$/PEG	100	10	85
14[k]	scCO$_2$/PEG	69	64	2

[a] Reaction conditions: styrene, 0.3 mL (2.6 mmol); PdCl$_2$, 27 mg (5.8% relative to styrene); CuCl, 200 mg; PEG-300(MW = 300), 2 mL; O$_2$, 3 MPa; total pressure, 16 MPa; temperature, 60 °C; time, 24 h. [b] Determined by GC using an internal standard. Each entry is the average of two tests. [c] PdCl$_2$, 27 mg (5.8%). [d] PdCl$_2$, 27 mg (5.8%); PEG-300, 2 mL. [e] H$_2$O, 1 mL. [f] H$_2$O, 2 mL [g] CH$_3$OH, 2 mL. [h] PdCl$_2$, 3 mg (0.6%). [i] CuCl, 200 mg; PEG-300, 2 mL. [j] PdCl$_2$, 27 mg (5.8%); PEG-300, 2 mL; CO$_2$, 13 MPa. [k] PdCl$_2$, 27 mg (5.8%); CuCl$_2$, 250 mg; PEG-300, 2 mL.

CuCl alone (entry 12), and, also, only traces of benzaldehyde were obtained when PEG-300 was excluded (entry 3). Surprisingly, the catalytic performance in the PdCl₂-mediated oxidation of styrene was significantly improved in the PEG solution with almost complete conversion (entry 5), where the main products were benzaldehyde (30%), acetophenone (35%) and benzoic acid (29%). Further studies showed that benzaldehyde was obtained as a main product with up to 85% yield using a biphasic scCO₂/PEG system (entry 13), with concomitant formation of 10% of acetophenone and a small amount of benzoic acid. Note that the presence of CO_2 could suppress the generation of acetophenone (entry 5 *vs.* 13). Possibly, the favorable physico-chemical properties of scCO₂ in the reaction system could prevent further oxidation from benzaldehyde to benzoic acid. To the best of our knowledge, this is the first example of the PdCl₂-catalyzed aerobic oxidation of styrene to benzaldehyde in high selectivity. In summary, the preferential formation of a methyl ketone such as acetophenone in the PdCl₂/CuCl-catalyzed Wacker oxidation of styrene can be realized by optimizing the reaction parameters like solvents, CO_2 pressure, *etc*. The PdCl₂-catalyzed aerobic oxidation of styrene in a biphasic PEG/scCO₂ system leads to two possible products: benzaldehyde and the Wacker reaction product acetophenone. The selectivity of the reaction can be switched by addition or abdication of the co-catalyst CuCl.
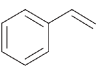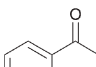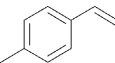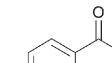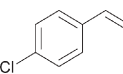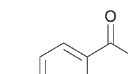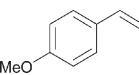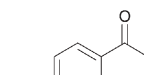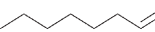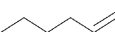
It is well-known that the properties of supercritical fluids are sensitive to pressure, and thus pressure may drastically influence the catalytic activity or the selectivity of the product when a reaction takes place in supercritical conditions. The Wacker oxidation of styrene was chosen as a benchmark reaction to investigate the effect of pressure. The quantitative conversion was approached at 60 °C in the pressure range of 0–20 MPa, suggesting that the total pressure had a negligible effect on the catalytic activity, while CO_2 pressure noticeably affected the selectivity towards acetophenone within 20 MPa (Table 2). As easily seen from Table 2, the favorable pressure was around 16 MPa, at which the selectivity towards acetophenone reached 92% (entry 4, Table 2). The presence of CO_2 is beneficial for improving the selectivity towards the ketone (entry 2 *vs.* 3). Under a total pressure of 9 MPa (entry 3), the selectivity for acetophenone was lower than that at 16 MPa, presumably due to enhancement of the solvent power of CO_2 with increasing pressure. Therefore, less reactant

Table 2 Pressure effect for the Wacker oxidation of styrene[a]

Run	Total pressure/MPa	Conversion[b] (%)	Ketone selectivity[c] (%)
1[d]	16	100	93
2[e]	3	100	83
3	9	100	86
4	16	100	92
5	20	100	90

[a] Reaction conditions: styrene, 0.3 mL (2.6 mmol); PdCl₂, 27 mg (5.8% relative to styrene); CuCl, 200 mg; PEG-300, 2 mL; O₂, 3 MPa; temperature, 60 °C; time, 24 h. [b] Determined by GC using an internal standard. Each entry is the average of two tests. [c] The selectivity is defined as number of moles of the designated product divided by the total number of moles of all the products. [d] O₂, 2 MPa. [e] In the absence of CO_2.

Table 3 Wacker oxidation of olefins in scCO₂/PEG[a]

Substrate	Product	Conversion (%)	Yield (%)
		>99	90
		>99	87
		80	72
		>99	85
		61	58
		>99	99

[a] Reaction conditions: olefin, 2.6 mmol; PdCl₂, 27 mg (5.8% relative to olefin); CuCl, 200 mg; PEG, 2 mL; O₂, 2 MPa; total pressure, 16 MPa; temperature, 60 °C; time, 24 h.

exists in the PEG phase at higher pressure, which significantly prevents the reactant from its isomerization. However, CO_2 with a higher pressure of over 20 MPa might retard the interaction between the substrate and the catalyst, and might cause a low concentration of substrate in the vicinity of the catalyst, thus resulting in a relatively low yield.[24e]

The scope of the substrates was further explored as shown in Table 3 (see Scheme 4). Several terminal olefins were chosen to be tested in the biphasic scCO₂/PEG system for the Wacker oxidation reaction, including four common aromatic olefins as well as two representative aliphatic counterparts. The experimental results display that the catalytic system could be extended to various alkenes. All substrates could be converted to the desired methyl ketone in good to excellent yields and selectivity.

One of the most striking features of this biphasic catalytic system for the PdCl₂-catalyzed aerobic oxidation of styrene into benzaldehyde is the facile separation of the oxidized products from the reaction mixture. The workup[27] of the reactions was performed by extraction either with scCO₂, or with diethyl ether, and the PEG phase which immobilized the
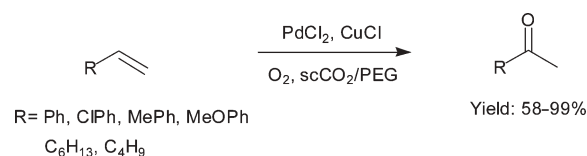
Scheme 4 PdCl₂/CuCl-mediated Wacker oxidation of olefins in scCO₂/PEG.
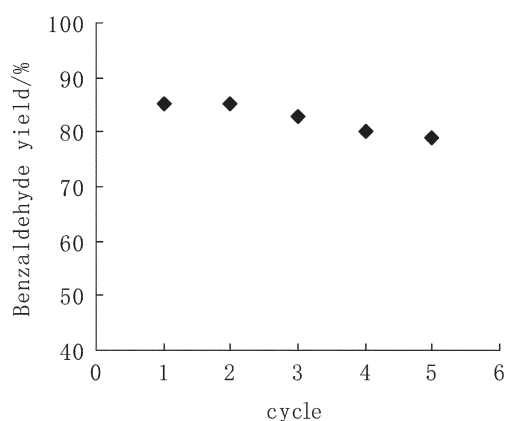
Fig. 1 Catalytic activity of the reused catalyst in scCO$_2$/PEG. Reaction conditions: styrene, 0.3 mL (2.6 mmol); PdCl$_2$, 50 mg; PEG-300, 2 mL; O$_2$, 3 MPa; total pressure, 16 MPa; temperature, 60 °C; time, 24 h.

catalyst was readily reused without further purification or activation. In general, the catalytic activity of the PdCl$_2$ seriously declines,[28] while it is demonstrated in this biphasic system that PdCl$_2$ can be recycled for at least five times without significant loss in activity and the selectivity, as shown in Fig. 1. The yield of product reached over 80% after the fifth recycling process. A noticeable problem in homogeneous Pd-mediated oxidation is catalyst deactivation by aggregation into inactive metallic Pd.[28] The catalyst recycling in our studies suggested that this problem could be addressed by catalyst stabilizing in PEG with a biphasic PEG/scCO$_2$ catalytic system.

In addition, we also tested the leaching of the active ingredient of the catalyst Pd. The content of Pd in the product solution was measured by Atomic Absorption Spectroscopy. The results demonstrated that the Pd leaching was at the level of 0.5 ppm, consistent with experimental results on catalyst recycling, hinting that the biphasic PEG/scCO$_2$ system can enhance the stability of the Pd oxidation catalyst.

The Wacker reaction is usually carried out in aqueous solution. Water plays a key role in dissolving catalysts (PdCl$_2$, CuCl$_2$ and Cu$_2$Cl$_2$), to produce H$_3$O$^+$ and provide nucleophilic species.[29] In this investigation, the Wacker reaction can be successfully performed in a biphasic scCO$_2$/PEG-300 system. The plausible mechanism could be similar to that in alcoholic solvents,[3,5] with the PEG serving as a nucleophilic species to attack the palladium–alkene complex. Mimoun and co-workers have reported that the Pd(II)–OOH species undergoes an oxygen transfer to the terminal alkenes through a five-membered pseudocyclic peroxypalladation mechanism.[30] Takehira *et al.* also proposed the formation of Pd(II)–OOH species from palladium, ethanol, and oxygen.[31] Recently, many groups have reported that the Pd(II)–OOH species was believed to be acting as the key intermediate. Thus, H$_2$O$_2$ was produced in the catalytic cycle.[32] Experimentally, in the course of the Pd-catalyzed oxidation of styrene into benzaldehyde, the peroxide species, being detected by a KI/starch test, possibly facilitates homolytic bond cleavage and formation of benzaldehyde, although the exact mechanism for the cleavage of the double bond of styrene is not clear at the moment.

Conclusions

The PdCl$_2$-catalyzed aerobic oxidation of styrene in a biphasic PEG/scCO$_2$ system leads to two possible products, benzaldehyde and the Wacker reaction product acetophenone. The selectivity of the reaction can be switched by the co-catalyst CuCl, from 92% in favor of acetophenone in the presence of CuCl to 85% favoring benzaldehyde without any co-catalyst. The PEG could effectively immobilize and stabilize the catalysts. The present biphasic scCO$_2$/PEG system could accelerate product separation and catalyst recycling. Moreover, this environmentally benign biphasic catalytic system can be applied to the Wacker oxidation of various alkenes. Notably, another advantage of using a biphasic scCO$_2$/PEG system from an engineering point of view is the possibility of combining reaction and separation in just one integrated process for potential industrial application. The ongoing mechanistic insight to understand this oxidation and to evaluate the process with a broader scope of substrates is currently in progress in our laboratory.

Experimental

Chemical reagents

The olefins and PEG-300 were purchased from J&K CHEMICAL. The solvents prior to use in this study were purified according to the known procedures. The other commercially available reagents were used without further purification.

Typical procedure for aerobic oxidation of styrene in scCO$_2$/PEG†

A mixture consisting of styrene (0.3 mL, 2.6 mmol), PEG-300 (2 mL), PdCl$_2$ (27 mg), and CuCl (200 mg) was placed in a 25 mL autoclave. A certain amount of CO$_2$ and 3 MPa of O$_2$ were successively charged into the autoclave and heated to the reaction temperature. Then the final pressure was adjusted to the desired pressure by introducing the amount of CO$_2$. After reaction, the autoclave was allowed to cool, and then CO$_2$ was vented. The product was slowly separated from the PEG system by extraction. The products were analyzed on a gas chromatograph (Agilent 6890) equipped with a capillary column (HP-5 30 m × 0.25 μm) using a flame ionization detector. The structure and the purity of the products were further identified using GC–MS (HP G 1800A) and GC by comparing the retention times and fragmentation patterns with those of authentic samples. NMR data for some products of the Wacker reaction were as follows:

Benzaldehyde ^{1}H NMR (CDCl$_3$, 400 MHz): δ 7.49 [t, 2H, $^3J_{(H,H)}$ = 7.7 Hz, C$_6$H$_4$], 7.59 [t, 1H, $^3J_{(H,H)}$ = 7.4 Hz, C$_6$H$_4$],

† **Safety warning**: experiments using large amounts of compressed gases, especially molecular oxygen and supercritical fluids, are potentially hazardous and must only be carried out by using the appropriate equipment and under rigorous safety precautions. In particular, oxygen is introduced into the substrate-loaded reactor before CO$_2$ is added. To avoid an explosive regime the following order should be used: substrate > CO$_2$ > oxygen. Moreover, the oxygen content should not exceed 14 vol% when CO$_2$ is used as a reaction medium.

7.84 [d, 2H, $^3J_{(H,H)}$ = 7.9 Hz, C$_6$H$_4$], 9.98 [s, 1H, COH]. ^{13}C {^{1}H} NMR (CDCl$_3$, 100.6 MHz): δ 128.85, 129.58, 134.33, 136.19, 192.28.

Acetophenone ^{1}H NMR (CDCl$_3$, 400 MHz): δ 2.60 [s, 3H, COCH$_3$], 7.46 [t, 2H, $^3J_{(H,H)}$ = 7.7 Hz, C$_6$H$_4$], 7.56 [t, 1H, $^3J_{(H,H)}$ = 7.5 Hz, C$_6$H$_4$], 7.96 [d, 2H, $^3J_{(H,H)}$ = 7.8 Hz, C$_6$H$_4$]. ^{13}C {^{1}H} NMR (CDCl$_3$, 100.6 MHz): δ 26.54, 128.25, 128.51, 133.04, 137.10, 198.06.

p-Methylacetophenone ^{1}H NMR (CDCl$_3$, 400 MHz): δ 2.41 [s, 3H, PhCH$_3$], 2.57 [s, 3H, COCH$_3$], 7.25 [d, 2H, $^3J_{(H,H)}$ = 7.98 Hz, C$_6$H$_4$], 7.85 [d, 2H, $^3J_{(H,H)}$ = 8.14 Hz, C$_6$H$_4$]. ^{13}C {^{1}H} NMR (CDCl$_3$, 100.6 MHz): δ 21.60, 26.49, 128.40, 129.20, 134.71, 143.82, 197.78.

p-Methoxyacetophenone ^{1}H NMR (CDCl$_3$, 400 MHz): δ 2.56 [s, 3H, COCH$_3$], 3.87 [s, 3H, OCH$_3$], 6.93 [d, 2H, $^3J_{(H,H)}$ = 8.88 Hz, C$_6$H$_4$], 7.94 [d, 2H, $^3J_{(H,H)}$ = 8.89 Hz, C$_6$H$_4$]. ^{13}C {^{1}H} NMR (CDCl$_3$, 100.6 MHz): δ 26.27, 55.41, 113.64, 130.54, 163.44, 196.71.

p-Chloroacetophenone ^{1}H NMR (CDCl$_3$, 400 MHz): δ 2.59 [s, 3H, CH$_3$], 7.43 [d, 2H, $^3J_{(H,H)}$ = 8.5 Hz, C$_6$H$_4$], 7.89 [d, 2H, $^3J_{(H,H)}$ = 8.5 Hz, C$_6$H$_4$]. ^{13}C {^{1}H} NMR (CDCl$_3$, 100.6 MHz): δ 26.54, 128.86, 129.70, 135.40, 139.55, 196.80.

Acknowledgements

References

1 J. Tsuji, in *Palladium Reagents and Catalysis*, John Wiley, New York, 1995, pp. 19–30; R. Jira, in *Applied Homogeneous Catalysis with Organometallic Compounds*, ed. B. Cornils and W. A. Herrmann, VCH, Weinheim, 1996, pp. 374–393; E. Monflier and A. Mortreux, in *Aqueous Phase Organometallic Catalysis*, ed. B. Cornils and W. A. Herrmann, VCH, Weinheim, 1997, pp. 513–518.
2 W. H. Clement and C. M. Selwitz, *J. Org. Chem.*, 1964, **29**, 241.
3 W. G. Lloyd and B. J. Luberoff, *J. Org. Chem.*, 1969, **34**, 3949.
4 J. E. Bäckvall, A. K. Awasthi and Z. D. Renko, *J. Am. Chem. Soc.*, 1987, **109**, 4750; J. E. Bäckvall, R. B. Hopkins, H. Grennberg, M. M. Mader and A. K. Awashi, *J. Am. Chem. Soc.*, 1990, **112**, 5160; D. G. Miller and D. D. M. Wayner, *J. Org. Chem.*, 1990, **55**, 2924.
5 H.-F. Jiang, L.-Q. Jia and J.-H. Li, *Green Chem.*, 2000, **2**, 161.
6 A. Haimov and R. Neumann, *Chem. Commun.*, 2002, 876.
7 (*a*) A. Ansare, S. Joyaswal, M. K. Gupta, J. S. Yadav and R. Gree, *Tetrahedron Lett.*, 2005, **46**, 7507; (*b*) V. V. Namboodiri, R. S. Varma, E. S. Demessie and U. R. Pillai, *Green Chem.*, 2002, **4**, 170.
8 Z.-S. Hou, B.-X. Han, L. Gao, T. Jiang, Z.-M. Liu, Y.-H. Chang, X.-G. Zhang and J. He, *New J. Chem.*, 2002, **26**, 1246.
9 T. Mitsudome, T. Umetani, N. Nosaka, K. Mori, T. Mizugaki, K. Ebitani and K. Kaneda, *Angew. Chem., Int. Ed.*, 2006, **45**, 481.
10 T. Nishimura, N. Kakiuchi, T. Onoue, K. Ohe and S. Uemura, *J. Chem. Soc., Perkin Trans. 1*, 2000, 1915.
11 T. Hosokawa and S. I. Murahashi, *J. Synth. Org. Chem., Jpn.*, 1995, **53**, 1009.
12 E. Karakhanov, T. Buchneva, A. Maxinov and M. Zavertyaeva, *J. Mol. Catal.*, 2002, **184**, 11.
13 G. J. T. Brink, I. W. C. E. Arends, G. Papadogianakis and R. A. Sheldon, *Chem. Commun.*, 1998, 2359.
14 Z.-Y. Wang, H.-F. Jiang, C.-R. Qi, Y.-G. Wang, Y.-S. Dong and H.-L. Liu, *Green Chem.*, 2005, **7**, 582.
15 R. Jira and W. Freiesleben, *Organomet. React.*, 1972, **3**, 1.
16 S. F. Davison, B. E. Mann and P. M. Maitlis, *J. Chem. Soc., Dalton Trans.*, 1984, 1223; H. Ogawa, H. Fujinami, K. Taya and S. Teratani, *Bull. Chem. Soc. Jpn.*, 1984, **57**, 1908.
17 H.-M. Li, X.-K. Ye and Y. Wu, *Chin. J. Mol. Catal.*, 1997, **11**, 253.
18 H. M. Tang and D. C. Sherrington, *Polymer*, 1993, **34**, 2821; H. G. Tang and D. C. Sherrington, *J. Catal.*, 1993, **142**, 540; H. G. Tang and D. C. Sherrington, *J. Mol. Catal.*, 1994, **94**, 7; C. G. Jia, F. Y. Jin, H. Q. Pan, M. Y. Huang and Y. Y. Jiang, *Macromol. Chem. Phys.*, 1994, **195**, 751; J. H. Ahn and D. C. Sherrington, *Macromolecules*, 1996, **29**, 4164.
19 J. Tsuji, M. Nagashima and K. Hori, *Chem. Lett.*, 1980, 257.
20 G. Barak and Y. Sasson, *J. Chem. Soc., Chem. Commun.*, 1987, 1266.
21 N. Alandis, I. Rico-Lattes and A. Lattes, *New J. Chem.*, 1994, **18**, 1147.
22 (*a*) J. Chen, S. K. Spear, J. G. Huddleston and R. D. Rogers, *Green Chem.*, 2005, **7**, 64; (*b*) L. Wang, Y.-H. Zhang, L.-F. Liu and Y.-G. Wang, *J. Org. Chem.*, 2006, **71**, 1284; (*c*) J.-H. Li, X.-C. Hu, Y. Liang and Y.-X. Xie, *Tetrahedron*, 2006, **62**, 31; (*d*) D. J. Heldebrant and P. G. Jessop, *J. Am. Chem. Soc.*, 2003, **125**, 5600; (*e*) M. Solinas, J. Y. Jiang, O. Stelzer and W. Leitner, *Angew. Chem., Int. Ed.*, 2005, **44**, 2291; (*f*) Z. S. Hou, N. Theyssen, A. Brindmann and W. Leitner, *Angew. Chem., Int. Ed.*, 2005, **44**, 1346.
23 P. G. Jessop and W. Leitner, *Chemical Synthesis Using Supercritical Fluids*, Wiley-VCH, Weinheim, 1999; P. G. Jessop, T. Ikariya and R. Noyori, *Chem. Rev.*, 1999, **99**, 475; W. Leitner, *Top. Curr. Chem.*, 1999, **206**, 107; *Green Chemistry Using Liquid and Supercritical Carbon Dioxide*, ed. J. M. DeSimone and W. Tumas, Oxford University Press, 2003; G. Muse, M. Wei, B. Subramaniam and D. H. Busch, *Coord. Chem. Rev.*, 2001, **219**–**221**, 789–820; E. J. Beckman, *J. Supercrit. Fluids*, 2004, **28**, 121–191.
24 (*a*) J.-Q. Wang, D.-L. Kong, J.-Y. Chen, F. Cai and L.-N. He, *J. Mol. Catal.*, 2006, **249**, 143; (*b*) Y. Du, J.-Q. Wang, J.-Y. Chen, F. Cai, J.-S. Tian, D.-L. Kong and L.-N. He, *Tetrahedron Lett.*, 2006, **47**, 1271; (*c*) J.-S. Tian, J.-Q. Wang, J.-Y. Chen, J.-G. Fan, F. Cai and L.-N. He, *Appl. Catal., A*, 2006, **301**, 215; (*d*) H. Yasuda, L.-N. He, T. Takahashi and T. Sakakura, *Appl. Catal., A*, 2006, **298**, 177; (*e*) Y. Du, F. Cai, D.-L. Kong and L.-N. He, *Green Chem.*, 2005, **7**, 518; (*f*) Y. Du, D.-L. Kong, H.-Y. Wang, F. Cai, J.-S. Tian, J.-Q. Wang and L.-N. He, *J. Mol. Catal.*, 2005, **241**, 233; (*g*) H. Yasuda, L.-N. He and T. Sakakura, *J. Catal.*, 2005, **233**, 119; (*h*) L.-N. He, H. Yasuda and T. Sakakura, *Green Chem.*, 2003, **5**, 92; (*i*) H. Yasuda, L.-N. He and T. Sakakura, *Stud. Surf. Sci. Catal.*, 2003, **136**, 259; (*j*) H. Yasuda, L.-N. He and T. Sakakura, *J. Catal.*, 2002, **209**, 547; (*k*) J.-C. Choi, L.-N. He and T. Sakakura, *Green Chem.*, 2002, **4**, 230.
25 T. Guadagno and S. G. Kazarian, *J. Phys. Chem. B*, 2004, **108**, 13 995; P. Jessop, D. C. Wyne, S. DeHaai and D. Nakawatase, *Chem. Commun.*, 2000, 693; D. Gourgouillon, H. M. N. T. Avelino, J. M. N. A. Fareleira and M. N. da Ponte, *J. Supercrit. Fluids*, 1998, **13**, 177; Y. W. Kho, D. C. Conrad, R. A. Shick and B. L. Knutson, *Ind. Eng. Chem. Res.*, 2003, **42**, 6511; D. L. Tomasko, H. Li, D. Liu, X. Han, M. J. Wingert, L. J. Lee and K. W. Koelling, *Ind. Eng. Chem. Res.*, 2003, **42**, 6431; J. Sun, L. Wang, S. J. Zhang, Z. X. Li, X. P. Zhang, W. B. Dai and R. Mori, *J. Mol. Catal. A: Chem.*, 2006, **256**, 295.
26 A. M. Scurto and W. Leitner, *Chem. Commun.*, 2006, 3681.
27 (A) The reaction mixture was extracted with scCO$_2$ (200 atm, 50 °C) to afford the corresponding carbonyl compound. The PEG phase containing the metal catalyst was reused without further purification or activation. (B) Extract procedure with diethyl ether: after the addition of diethyl ether (3 × 3 mL) to the resulting mixture upon completion of the reaction, the PEG-300 layer containing the catalyst solidified when cooled to −10 to −20 °C, followed by simple decantation of the ether phase containing the oxidized products allows the catalyst to be recycled. The combined extracts were dried over magnesium sulfate and concentrated *in vacuo* to give the product benzaldehyde. We conducted further oxidation by the addition of successive portions of the olefins to the catalyst–PEG phase followed by stirring under identical reaction conditions.
28 Y. M. A. Yamadas, T. Arakawa, H. Hocke and Y. Uozumi, *Angew. Chem., Int. Ed.*, 2007, **46**, 704; M. M. Konnick,

B. A. Gandhi, I. A. Guzei and S. S. Stahl, *Angew. Chem., Int. Ed.*, 2006, **45**, 2904.

29 J. E. Backvall, B. Akermark and S. O. Ljunggren, *J. Am. Chem. Soc.*, 1979, **101**, 2411.

30 H. Mimoun, R. Charpentier, A. Mitschler, J. Fisher and R. Weiss, *J. Am. Chem. Soc.*, 1980, **102**, 1047; M. Roussel and H. Mimoun, *J. Org. Chem.*, 1980, **45**, 5387; H. Mimoun, *Angew. Chem., Int. Ed. Engl.*, 1982, **21**, 734.

31 K. Takehira, T. Hayakawa and H. Orita, *Chem. Lett.*, 1985, 1835; K. Takehira, T. Hayakawa, H. Orita and M. Shimizu, *J. Mol. Catal.*, 1989, **53**, 15.

32 S. S. Stahl, *Angew. Chem.*, 2004, **116**, 3480; S. S. Stahl, *Angew. Chem., Int. Ed.*, 2004, **43**, 3400; S. S. Stahl, *Science*, 2005, **309**, 1824; C. N. Cornell and M. S. Sigman, *J. Am. Chem. Soc.*, 2005, **127**, 2796; K. M. Gligorich and M. S. Sigman, *Angew. Chem., Int. Ed.*, 2006, **45**, 6612.

Coupling chiral homogeneous biocatalytic reactions with benign heterogeneous separation†

Elizabeth M. Hill,[ad] James M. Broering,[acd] Jason P. Hallett,[ad] Andreas S. Bommarius,[abcd] Charles L. Liotta[abd] and Charles A. Eckert[abd]

We describe a method for sustainable biocatalysis in an organic aqueous tunable solvent (OATS) system in which a hydrophobic substrate is transformed with a homogeneous enzymatic catalyst in a single liquid phase. Subsequent CO_2 addition produces a biphasic mixture where the hydrophobic product partitions preferentially into the organic rich phase for separation while the hydrophilic enzyme catalyst partitions into the aqueous rich phase, where it is recyclable. Greater than 99% enantiomeric excess (ee) is shown for catalyzed hydrolysis of *rac*-1-phenylethyl acetate with *Candida antarctica* lipase B (CAL B) both before and after CO_2-induced separation. Additionally, processing parameters in OATS systems are discussed. This system combines homogeneous enzymatic reactions with a built-in heterogeneous separation for enantiomerically pure products.

Introduction

There is a broadly recognized need for the development of environmentally benign processing techniques and the use of alternative solvents is an active area of investigation.[1,2] We have recently explored enzymatic reactions in organic aqueous tunable solvent (OATS) systems as a sustainable approach which couples homogeneous catalysis with facile product and catalyst separation.[3,4] Enzymatic catalysts are at the forefront of emerging sustainable synthesis and processing techniques, such as those recognized in the United States over the past four years by recipients of the Presidential Green Chemistry Challenge Award.[5] The enormous potential of enzymes for the transformation of synthetic chemicals with high chemo-, regio- and enantioselectivities is well established[3,4,6–8] and useful for the production of single enantiomers of drug precursors or intermediates of increasing importance in the pharmaceutical industry.[6] Additionally, chiral intermediates are also now in high demand for the production of bulk agricultural products.[6,9,10]

Traditional enzymatic reactions are typically limited to aqueous media and consequently also limited to transformations of hydrophilic substrates. In order to broaden the use of biocatalysts to hydrophobic substrates, current research is investigating applications of enzymes in organic solvents[9,11] and ionic liquids.[12–14] To date, such reactions in these solvents are limited mainly to heterogeneous catalysis using immobilized enzymes or dispersed enzyme powders.[15]

OATS systems use homogeneous catalysts which are generally more active and more selective than heterogeneous catalysts;[4] further, they are especially useful for asymmetric synthesis as they almost always result in superior enantiomeric excesses (ee).[16] Homogeneous catalysts avoid limitations such as active-site heterogeneity or mass transport limitations of reactants and products to and from the active site. However, a major barrier is often their expense and/or toxicity; for either reason, they must be separated from the products and if possible, recycled for reuse. OATS can reduce the ecological footprint and cost associated with asymmetric transformations of hydrophobic substrate by:

1. Allowing recycling of both catalyst and solvents;

2. Using highly selective enzymatic catalysts to reduce the production of byproducts requiring downstream purification;

3. Replacing a portion of the volatile organic solvent used in reactions with environmentally and chemically benign water and CO_2, which are both virtually non-toxic, non-flammable, and relatively inert;

4. Applying modest CO_2 pressure as a phase switch for product recovery, in contrast to the massive amounts of organics consumed in conventional liquid–liquid extractions.

Herein, we report the use of OATS for a versatile one-pot enantioselective reaction with a built-in product and catalyst separation. Specific processing challenges with regards to solvent selection and buffer‡ addition for enzyme stability are addressed. Additionally, we compare the OATS process to competing methods for transforming hydrophobic substrates with enzymes.

aSchool of Chemical & Biomolecular Engineering, Georgia Institute of Technology, 311 Ferst Drive, Atlanta, GA, 30332, USA
bSchool of Chemistry & Biochemistry, Georgia Institute of Technology, 311 Ferst Drive, Atlanta, GA, 30332, USA
cParker H. Petit Institute of Bioengineering and Bioscience, Georgia Institute of Technology, 311 Ferst Drive, Atlanta, GA, 30332, USA
dSpecialty Separations Center, Georgia Institute of Technology, 311 Ferst Drive, Atlanta, GA, 30332, USA

† Electronic supplementary information (ESI) available: Additional ternary phase plots of THF and acetonitrile. See DOI: 10.1039/b701409k

‡ Buffer for all solubility tests, kinetic assays, and separation experiments reported refers to a 150 mM monobasic sodium phosphate solution in water titrated to a pH of 7.1. For ternary phase data measurements, buffer is distinguished where appropriate as either a 150 mM monobasic sodium phosphate solution in water titrated to a pH of 7.1 or a 150 mM Hepes solution in water titrated to a pH of 7.01.
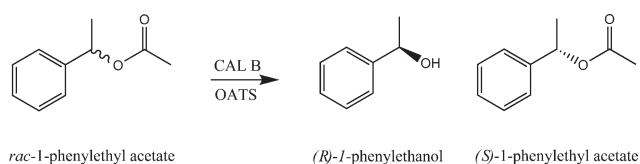
Fig. 1 Kinetic resolution of *rac*-1-phenylethyl acetate to (*R*)-1-phenylethanol with *Candida antarctica* lipase B (CAL B) in an OATS system.

Results and discussion

A homogeneous reaction [Fig. 1] in OATS is coupled with CO_2-induced phase separation as subsequent processing. The enzyme recycling and reactivity in a (1,4)-dioxane OATS mixture has been reported for this catalyst elsewhere.[3] The goal here is to determine the effect of CO_2-induced separation on the overall ee value of the reaction, as well as to examine alternate OATS solvents for effectiveness of biocatalyst reaction and separation.

Acetone, acetonitrile, (1,4)-dioxane, and tetrahydrofuran (THF) were each investigated as OATS solvents. THF showed buffer precipitation even at concentrations as low as 5% by volume and was therefore eliminated from the study. Cloud points (indicating either the substrate or buffer precipitation) were found for organic-aqueous mixtures of acetone, acetonitrile, and (1,4)-dioxane to be at 35%, 50%, and 60% by volume, respectively. Table 1 compares the substrate saturation concentration, rate constant, and ee value of the product for each of these solvents at a fixed volume percent organic solvent. Excellent ee values are observed for all of the solvents studied with this reaction. It is apparent from this table that a (1,4)-dioxane OATS system is best suited for this reaction because of its high saturation concentration as compared to acetonitrile and increased rate constant as compared to acetone.

The 30% (1,4)-dioxane OATS system was tested with subsequent separation as described in the experimental section and compared to a control reaction that did not undergo CO_2-induced separation. The overall ee value of the (*R*)-1-phenylethanol without separation (>99%) is the same as the ee value of the organic and aqueous phases, indicating the CO_2-induced separation has no significant effect on the overall ee value of the product.

Processing considerations

The use of CO_2 as a separating agent for simultaneous biocatalyst recycle and product isolation requires two processing considerations to be understood. First, the solution equilibria of the water–solvent–CO_2 system must be well characterized so that as the product-laden organic phase is removed from the reactor, an accurate make-up stream can be added to maintain the appropriate OATS mixture. This will allow for repeatable separation of successive reaction cycles. Second, the pH of the aqueous phase must be carefully maintained to preserve optimal biocatalyst activity. Addition of CO_2 to aqueous mixtures is known to lower the solution pH due to carbonic acid formation.[17,18] Two commonly used buffers for biocatalytic systems are monobasic sodium phosphate (phosphate buffer) and (2-hydroxyethyl)-1-piperazineethanesulfonic acid (Hepes buffer). Both can adequately buffer against carbonic acid formation seen in water–CO_2 mixtures,[3,19] and the phosphate buffer has been shown to adequately buffer recycled OATS mixtures over six cycles.[3]

The phase equilibria of CO_2 pressurized OATS mixtures is best illustrated on a ternary phase diagram, as shown in Fig. 2. Fig. 2A illustrates a typical diagram for a type 1 ternary made up of two partially immiscible solvents and a solute which is completely miscible in either. The area under the curved line is the two-phase region; outside of this region there exists a single miscible phase. In the absence of solute, the mutual solubilities are given by A and B. As solute is added to the first tie line, the mutual solubilities become C and D, and for the second E and F. At some point enough solute is added to give complete miscibility at a point G called the consolute point. To use such a system for OATS, we seek to use a tie line that gives maximum separation, well below any consolute point.

Ternary phase diagrams at 25 °C are shown for the unbuffered (1,4)-dioxane OATS system (Fig. 2B), a (1,4)-dioxane OATS system with 150 mM phosphate buffer (Fig. 2C), and a (1,4)-dioxane OATS system with 150 mM Hepes buffer (Fig. 2D). As in the example diagram described above (Fig. 2A), these diagrams show the tie lines illustrating type 1 ternary behavior, and one can envision the same phase envelope indicating a two-phase region. For all cases, the two liquid phases can be made purer (relative to the amount of water and dioxane) by the addition of more CO_2 with a resulting increase in pressure.[20] We postulate that the addition of a buffer causes a "salting out" effect of CO_2.[21] Thus, for the buffered cases, the solubility of CO_2 is reduced causing a lower purity of the phases.

While both buffers alter the two-phase region critical to separation in the OATS system, it is clear that the Hepes has a much greater effect. One may better appreciate this effect by comparing the amount of CO_2 pressure required to reach 0.1 mole fraction of water in the organic rich phase (*i.e.* the pressure required to remove 90% of the water from the organic phase). For the unbuffered system only 3.1 MPa is required, however, in the Hepes case the pressure must be raised to 4.4 MPa to achieve a water content of 0.1 mole fraction. The intermediate pressure of 3.7 MPa for the phosphate buffered case illustrates that this effect also occurs for inorganic salts. We surmise that the effect is increased because the organic salt (Hepes buffer) is more soluble in the organic solvent than the inorganic salt (phosphate buffer). (See the ESI for additional ternary plots of THF and acetonitrile).†

Table 1 Comparison of OATS solvents and their effectiveness for the chiral resolution of 1-phenylethyl acetate with *Candida antarctica* lipase B (CAL B)
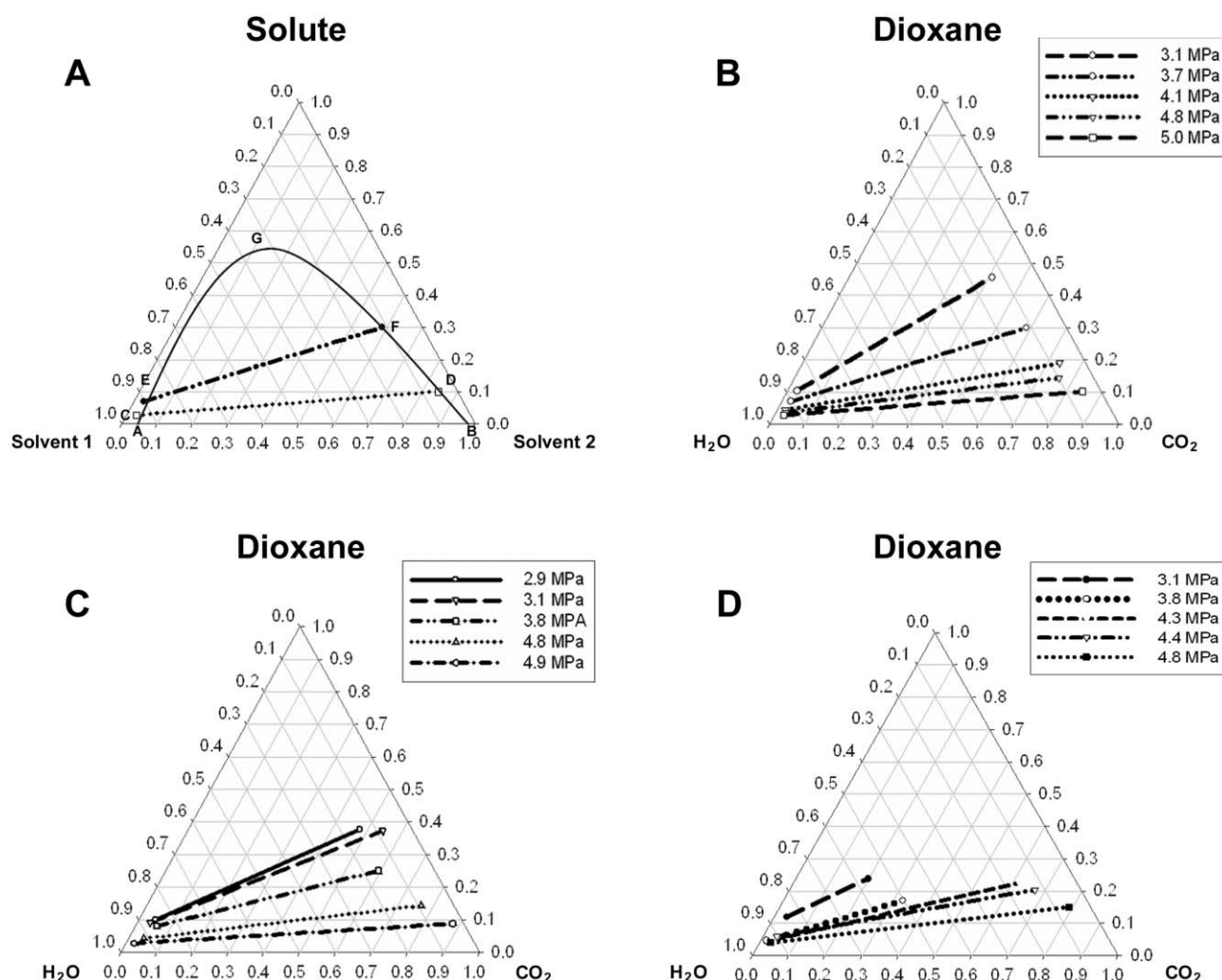
Solvent	% by volume in OATS	Substrate saturation/ mM	Pseudo 1st order rate constant/s^{-1}	Product enantiomeric excess (ee)
Acetone	30	18.1 ± 0.9	0.003 ± 0.001	>99%
Acetonitrile	30	9.1 ± 0.5	0.009 ± 0.001	>99%
(1,4)-Dioxane	30	17.7 ± 0.8	0.014 ± 0.001	>99%

Fig. 2 (A) Model ternary diagram for type 1 behavior. (B) unbuffered (1,4)-dioxane OATS system. (C) (1,4)-dioxane OATS with 150 mM phosphate buffer. (D) (1,4)-dioxane OATS with 150 mM Hepes buffer.

Comparison to alternative techniques

Initial work on enzymatic reactions in organic solvents was originally met with some skepticism as to its practical usefulness;[22] however, research in this area over the past two decades has shown marked success and led to an array of new biocatalytic processing techniques. Among these methods are water-in-oil microemulsion systems and aqueous biphasic catalysis, both of which utilize multiple liquid phases for reaction, and employ either organic solvents or ionic liquids with water. Solid enzyme preparations, for example lyophilized enzymes or enzymes adsorbed on an inert support suspended in an organic solvent or ionic liquid, use a single liquid phase (although, in the presence of a solid catalyst phase) and are therefore most closely related to our own OATS system, which couples monophasic liquid biocatalysis with a biphasic separation.

We compare these three solvent types (pure organic liquids, ionic liquids, and OATS) to better illuminate which of these tools is best suited for a particular application. What is common to all three of these solvent systems is that they allow

enzymatic transformation of hydrophobic substrates not accessible via traditional aqueous media. As mentioned above, the ability to transform such substrates is an extremely desirable asset for the pharmaceutical and agrochemical industries. Organic solvents affect enzymatic performance via three routes:[14]

1. They can strip off the essential water that is associated with the enzyme;

2. They can interact with the enzyme by changing the protein dynamics, conformation, and/or active site;

3. They can interact with the substrates and products by direct reaction.

Medium engineering has also been investigated as a means to influence or even reverse an enzyme's selectivity.[23] However, there is no general paradigm that adequately describes an approach to medium engineering, most likely because multiple factors are involved, among which water content is a critical component.[24–26] One could assume that both ionic liquids and OATS systems might have similar effects on the enzyme; however, the extent would depend greatly on the anion/cation or amount/type of organic cosolvent, respectively.

A clear disadvantage of pure organic solvents is the requirement of the enzyme to be immobilized[9] to achieve high reaction yields. This need for immobilization adds time and effort to already laborious isolation techniques. At present, enzymatic reactions in ionic liquids also require immobilized enzymes, although some research is being conducted to tailor ionic liquids to prevent dissolved enzymes from denaturing.[27]

Ionic liquids are suggested as possible alternative green solvents due to their nonvolatile nature, thermal stability, and ability to be tuned *via* anion/cation selection. This unique ability to be tuned for certain physical and chemical properties, such as polarity, hydrophobicity, viscosity, and solvent miscibility, renders ionic liquids particularly useful for dissolving highly polar substrates such as carbohydrates and amino acids.[28] Conversely, the important issues of toxicity and ecological impact of most ionic liquids are not well known,[2,29] nor are means to effectively recycle the used ionic liquid. For biocatalysis, purification of the ionic liquid is often necessary for good yields,[30] and the practical challenge of developing efficient methods for product isolation from ionic liquids remains. Very volatile products may be evaporated off, products of intermediate volatility have been removed with supercritical CO_2 extraction,[2,31] and ways to isolate nonvolatile products have begun to be addressed through liquid–liquid extraction.[2,28,29]

A major advantage of the OATS system is the inherent sequence of separation and recycling, as illustrated in Fig. 3. Such systems support the dissolution of salt buffers to maintain an adequate pH for completely homogeneous enzymatic catalysis. As in ionic liquids, OATS can be tuned for increased substrate solubility, in this case, through careful selection of the type and amount of organic cosolvent. OATS systems facilitate catalysis of reactions that are unfavorable in water due to solubility constraints, however, they are not appropriate to reduce water-induced side reactions because the miscible mixture requires too high a water content for reaction (generally, around 30–70% water by volume). Additionally, we are in the process of validating the OATS system with more enzymes than the robust CAL B as catalyst. We suggest that this is a promising avenue given the success of mixed aqueous–organic solvents for reaction[11,32] and our ability to also tune our separation with buffer, temperature, and pressure variation.
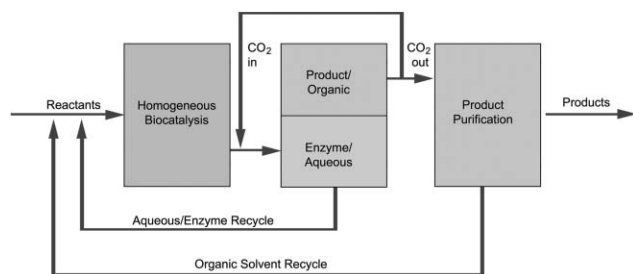
Fig. 3 The OATS system shown above illustrates the facile product recovery with CO_2-induced phase separation as well as the opportunity for both solvents and catalyst recycles.

Conclusions

We show the application of CO_2-switched OATS systems for enantioselective reactions of hydrophobic substrates. The overall ee value of the product is the same before and after OATS separation, at >99%. In OATS systems, a reaction can be run homogeneously in an organic–aqueous miscible mixture, followed by a CO_2-induced phase separation giving a product-containing organic phase and a catalyst-containing aqueous phase at modest pressures. The phase behavior critical to this separation is dramatically affected by the buffer salt Hepes and is mildly altered with the addition of phosphate buffer. Compared to the unbuffered OATS mixtures, both buffers studied require additional CO_2 pressure to achieve "clean" organic and aqueous phases during separation.

As is the case for pure organic solvents and ionic liquids, it is likely that OATS systems can be applied to multiple enzyme types; however, OATS systems are not appropriate for water sensitive reactions. OATS bridges the best of both worlds of catalysis: it offers the increased selectivity, yields, and ee values seen in homogeneous catalysis, while affording the facile separation of heterogeneous catalysis. Furthermore, OATS systems are beneficial because they have a reduced amount of organic solvent in reaction mixtures, and the CO_2-induced separation eliminates the need for large volume solvent extractions for product recovery. In this way, OATS offers a holistic approach to processing by coupling reaction with an inherent separation.

General experimental

Candida antarctica lipase B (SOL-101; $\geqslant 8$ kU mL^{-1}) was a kind gift from Biocatalytics (Pasadena, CA, USA). HPLC grade solvents (99.5%) 1,4-dioxane, acetone, acetonitrile, tetrahydrofuran, and water were purchased from Sigma–Aldrich and were used without further purification. Reagents, used as received, include: *rac*-1-phenylethyl acetate (Acros 99%), *rac*-1-phenylethanol (Acros 98%), (*R*)-1-phenylethanol (Alfa Aesar 99%), (*S*)-1-phenylethanol (Sigma 98%) and CO_2 (Airgas SFC grade). Reaction progress was followed by measuring the 1-phenylethyl acetate and 1-phenylethanol content of samples as compared to calibration standards. Yields were found using an Agilent gas chromatograph (GC-FID model 6890) with a DB17 column (Agilent, Palo Alto, CA, USA). Enantioselectivity was monitored by analytical high performance liquid chromatography (LC) at 245 nm using an Agilent 1100 series LC and a Chiralcel OD-RH (Diacel, Inc., Fort Lee, NJ, USA) with a 0.46 cm I.D. × 15 cm L column set at 35 °C and a flow rate of 0.5 mL min^{-1} (40% acetonitrile–60% water) for 25 minutes. Both *R* and *S* enantiomers were resolved for the purchased racemic mixture; however, the *S* enantiomer was not present in detectable amounts for any of the reaction samples. Therefore, ee is reported as 100% minus the limit of detection, 1%. All samples were immediately mixed 1 : 1 with a mixture of 1 : 1 glacial acetic acid : organic solvent of interest to quench the reaction before either GC or LC analysis.

Solubility tests

The solubility limit for 1-phenylethyl acetate was tested in various OATS systems starting at 10% organic solvent and increasing in increments of 5% until a cloud point was reached. A 5 mL solution of the desired OATS system was prepared. For example, a 30% (1,4)-dioxane OATS system is made by combining 1.5 mL of (1,4)-dioxane with 3.5 mL of buffered water. To this 5 mL solution, 1 mL of 1-phenylethyl acetate was added. The mixture was placed in an oil bath at 25 °C and magnetically stirred for 1 hour. The mixture was then allowed to stand, without agitation, for 10 minutes while it separated into two phases. The top phase was undissolved 1-phenylethyl acetate, and the bottom phase the OATS system saturated with 1-phenylethyl acetate. The bottom phase was sampled and analyzed *via* GC-FID for concentration as compared to a calibration made from standard solutions of 1-phenylethyl acetate.

Kinetic assays

150 mM phosphate buffer (pH 7.1) was mixed with the appropriate amount of solvent and a stock solution of substrate dissolved in organic solvent to yield a final reaction mixture of 6 mL at the desired volume percentage of organic solvent. For example, to make a 15 mM 1-phenylethyl acetate solution in 6 mL of a 30% (1,4)-dioxane OATS system, we mixed 0.45 mL of stock (200 mM) 1-phenylethyl acetate in (1,4)-dioxane, 1.35 mL of pure (1,4)-dioxane, and 4.2 mL of buffered water. 1.75 mL of this reaction mixture was aliquoted to three test tubes for reaction and the remainder 0.75 mL was taken as an initial sample. 0.1 mL of $1/100\times$ enzyme was added to each test tube to initiate the reaction and 0.25 mL was removed periodically for analysis. Each condition was repeated three to five times. Reaction progress was monitored by GC-FID and enantiomeric excess by LC.

Separation experiments

Reactions were carried out in a 50 mL Jurgeson pressure vessel, stirred by a magnetic stir bar. The cell was mounted on a perpendicular rotating shaft so that the cell could be agitated under pressure for more vigorous mixing of the CO_2. Pressure in the cell was measured by a pressure transducer with digital readout (Druck, DPI 260, PDCR 910, GE Infrastructure Sensing, Billerica, MA, USA) which was calibrated against a hydraulic piston pressure gauge (Ruska, GE Infrastructure Sensing, Billerica, MA, USA) to an uncertainty of ±0.1 bar. While pressurized, the cell was kept behind a 1/4″ polycarbonate enclosure as a safety precaution.

All samples taken were quenched with a 1 : 1 mixture of glacial acetic acid : (1,4)-dioxane before further analysis. Reactions were carried out at ambient room temperature (25 °C). 15.92 mL of 150 mM phosphate buffer (pH 7.1) was mixed with 5.117 mL dioxane and 1.706 mL of dioxane containing 200 mM 1-phenylethyl acetate. 2 mL of this mixture was withdrawn as an initial (t = 0) sample, and 1.3 mL of $1/100\times$ enzyme was added to initiate the reaction. The reaction mixture was loaded into the pressure cell and stirred by a magnetic stir bar for 1 hour, after which 0.5 mL

was removed and assayed for conversion by GC-FID and enantiomeric excess by LC, as described in the General Experimental section. The cell was sealed and pressurized with CO_2 to 50 bar. CO_2 was first added through a dip tube at the side of the cell so that it could bubble directly through the liquid phase, thus decreasing the time to reach equilibrium.

While pressurized, the cell was rotated to mix the contents well and aid CO_2 dissolution into the reaction mixture. After several inversions, the cell was turned upright and stirred with the magnetic stir bar to dislodge any organic droplets that may adhere to the cell wall in the aqueous region of the cell. Stirring was then stopped and the phases were allowed to settle. When the cell pressure equilibrated at 50 bar, the CO_2 line was moved to the top port and allowed to continual flow from the supplier's gas cylinder regulated at 50 bar. Once a clear phase boundary was formed, the organic layer was removed by opening the valve on the dip tube and by bubbling the organic layer into a pre-weighed flask containing a known amount of (1,4)-dioxane until the top of the organic layer was just above the dip tube height. The flask was re-weighed to determine the amount organic layer collected and the flask contents were measured by GC-FID and LC to determine the amount of product and reactant in the collected organic layer. After removal of the organic layer, the CO_2 supply line was removed from the cell and the CO_2 was vented to the atmosphere to depressurize. The vessel top was removed and a 0.5 mL sample was taken and measured by GC-FID and LC to determine the amount of product and reactant in the remaining in the aqueous layer.

Ternary phase data measurements

For the unbuffered carbon dioxide–(1,4)-dioxane–water system reported here, a synthetic method of high-pressure vapor–liquid–liquid-equilibria (VLLE) was used, as previously reported.[20] VLLE for the buffered systems was determined by a direct sampling technique. We use a T316 windowed Parr reactor with a Magnadrive impeller for mixing. Pressure in the cell is monitored with a pressure transducer with digital readout (Druck, DPI 260, PDCR 910, GE Infrastructure Sensing, Billerica, MA, USA) calibrated against a hydraulic piston pressure gauge (Ruska, GE Infrastructure Sensing, Billerica, MA, USA) to an uncertainty of ±0.1 bar. Samples are taken *via* a sample loop affixed to a 6-way valve, allowing capture of a fixed sample volume regardless of operating pressure. These samples are depressurized into a dilution solvent and analyzed by GC-FID to determine organic solvent content and Karl Fischer titration to determine water content. For CO_2 content, the 6-way valve on the sample line, instead of being depressurized into the dilution solvent, is diverted to an inverted burette placed in a water bath. The volume of carbon dioxide at STP is determined by the displacement of water in the burette. The sample should not be bubbled through the water as there is an appreciable solubility of carbon dioxide in the water. Without any mixing the rate of dissolution of carbon dioxide into the water is slow enough to be negligible so long as the volume is determined rapidly. The line is flushed with rinse solvent to ensure all the carbon dioxide is in the burette. The sampling is repeated three times

for liquid content and three times for CO_2 content per phase for a given pressure and the results averaged to mitigate error in the sampling procedure. This direct sampling technique was validated by first applying it to an unbuffered system and comparing those results with previous data taken *via* the synthetic method. The buffer concentration was kept below the solubility limit of the gas-free solvent mixture being tested, and we did not observe any salt precipitation upon depressurization.

Acknowledgements

References

1 *Frontiers in Benign Chemical Synthesis and Processes*, ed. P. Anastas and T. WilliamsonUniversity Press, London, 1998.
2 R. A. Sheldon, *Green Chem.*, 2005, **7**, 267–278.
3 J. M. Broering, E. M. Hill, J. P. Hallett, C. L. Liotta, C. A. Eckert and A. S. Bommarius, *Angew. Chem., Int. Ed.*, 2006, **45**, 4670–4673.
4 J. Lu, M. J. Lazzaroni, J. P. Hallett, A. S. Bommarius, C. L. Liotta and C. A. Eckert, *Ind. Eng. Chem. Res.*, 2004, **43**, 1586–1590.
5 Presidential Green Chemistry Challenge Award Winners, http://www.epa.gov/greenchemistry/pubs/pgcc/past.html, accessed December 13th, 2006.
6 R. N. Patel, R. Hanson, A. Goswami, V. Nanduri, A. Banerjee, M.-J. Donovan, S. Goldberg, R. Johnston, D. Brzozowski, T. Tully, J. Howell, D. Cazzulino and R. Ko, *J. Ind. Microbiol. Biotechnol.*, 2003, **30**, 252–259.
7 D. J. Pollard and J. M. Woodley, *Trends Biotechnol.*, 2007, **25**, 66–73.
8 J. Tao, L. Zhao and N. Ran, *Org. Process Res. Dev.*, 2007, **11**, 259–267.
9 C. Giacomo and R. Sergio, *Angew. Chem., Int. Ed.*, 2000, **39**, 2226–2254.
10 G. Paes and M. J. O'Donohue, *J. Biotechnol.*, 2006, **125**, 338–350.
11 A. M. Kilbanov, *Nature*, 2001, **409**, 241–246.
12 R. A. Sheldon, R. M. Lau, M. J. Sorgedrager, F. van Rantwijk and K. R. Seddon, *Green Chem.*, 2002, **4**, 147–157.
13 F. van Rantwijk, F. Secundo and R. A. Sheldon, *Green Chem.*, 2006, **8**, 282–286.
14 Z. Yang and W. Pan, *Enzyme Microb. Technol.*, 2005, **37**, 19–28.
15 P. J. Halling, *Philos. Trans. R. Soc. London, Ser. B*, 2004, **359**, 1287–1296.
16 G. R. Castro and T. Knubovets, *Crit. Rev. Biotechnol.*, 2003, **23**, 195–231.
17 K. L. Toews, R. M. Shroll, C. M. Wai and N. G. Smart, *Anal. Chem.*, 1995, **67**, 4040–4043.
18 K. N. West, C. Wheeler, J. P. McCarney, K. N. Griffith, D. Bush, C. L. Liotta and C. A. Eckert, *J. Phys. Chem. A*, 2001, **105**, 3947–3948.
19 J. D. Holmes, K. J. Ziegler, M. Audriani, T. C. J. Lee, P. A. Bhargava, D. C. Steytler and K. P. Johnston, *J. Phys. Chem. B*, 1999, **103**, 5703–5711.
20 M. J. Lazzaroni, D. Bush, R. Jones, J. P. Hallett, C. L. Liotta and C. A. Eckert, *Fluid Phase Equilib.*, 2004, **224**, 143–154.
21 A. Perez-Salado Kamps, M. Jodecke, J. Xia, M. Vogt and G. Maurer, *Ind. Eng. Chem. Res.*, 2006, **45**, 1505–1515.
22 G. Carrea and S. Riva, *Angew. Chem., Int. Ed.*, 2000, **39**, 2226–2254.
23 Y. Hirose, K. Kariya, J. Sasaki, Y. Kurono, H. Ebike and K. Achiwa, *Tetrahedron Lett.*, 1992, **33**, 7157–7160.
24 H. L. Goderis, G. Ampe, M. P. Feyten, B. L. Fouwe, W. M. Guffens, S. M. Van Cauwenbergh and P. P. Tobback, *Biotechnol. Bioeng.*, 1987, **30**, 258–266.
25 P. J. Halling, *Enzyme Microb. Technol.*, 1984, **6**, 513–514.
26 P. J. Halling, *Enzyme Microb. Technol.*, 1994, **16**, 178–206.
27 H. Zhao, L. Jackson, Z. Song and O. Olubajo, *Tetrahedron: Asymmetry*, 2006, **17**, 2491–2498.
28 R. A. Sheldon, *Green Chem.*, 2004, **7**, 267–278.
29 J. F. Brennecke and E. J. Maginn, *AIChE J.*, 2001, **47**, 2384–2389.
30 S. Park and R. J. Kazlauskas, *J. Org. Chem.*, 2001, **66**, 8395–8401.
31 J. F. Brennecke, L. A. Blanchard, J. L. Anthony, Z. Y. Gu, I. Zarra andD. T. Leighton, in *Clean Solvents ACS Symposium Series*, American Chemical Society, Washington, DC, 2002, pp. 82–96.
32 S. Torres and G. R. Castro, *Food Technol. Biotechnol.*, 2004, **42**, 271–277.

Preparation of crosslinked chitosan/poly(vinyl alcohol) blend beads with high mechanical strength

Mingxian Li, Shaoling Cheng and Husheng Yan*

Crosslinked chitosan beads reported in the literature have the disadvantage of high water content and thus low mechanical strength. In this paper, a chitosan/poly(vinyl alcohol) (PVA) blend aqueous solution was first suspended in toluene–chlorobenzene to form droplets. Some of the water was then distilled out as an azeotrope with the aromatic hydrocarbons to reduce the water content of the suspension droplets. Glutaraldehyde was finally added to the suspension to result in the crosslinked chitosan/PVA beads with low water content and high mechanical strength. It was found that glutaraldehyde reacted with PVA to form crosslinkage at acidic conditions (pH 1 and 2). The H^+ ions act as both protection agents of amino groups of chitosan by forming salts and catalyst for the formation of acetal between aldehyde groups and hydroxyl groups of PVA. At pH 4 and 5, glutaraldehyde reacted with chitosan to form Schiff's base crosslinkage. Crosslinked chitosan/PVA beads with micron size were also prepared by the distillation method using very dilute initial polymer concentration and high stirring speed.

Introduction

Today, there is a growing interest in developing natural, renewable and low-cost alternatives to synthetic polymers. These materials are abundant and environmentally friendly. Chitosan is a derivative from *N*-deacetylation of chitin, the major component of the shells of crustacean organisms and the second most abundant naturally occurring biopolymer next to cellulose. Chitin and chitosan have biological and chemical properties such as non-toxicity, biocompatibility, high chemical reactivity, chirality, chelation and adsorption properties.[1–6] The presence of amine groups makes chitosan unique among biopolymers, for example, its cationic behavior in acidic solutions and its affinity for heavy metal ions.[2–4] Ion exchangers or adsorbents can be made in large scale and low cost from chitosan. These chitosan exchangers or adsorbents have potential applications in enzyme immobilization,[7,8] base catalysis,[9] protein separation and purification,[10,11] sorption of precious metal ions for recovery or as catalysts after reduction,[12–15] wastewater treatment to remove heavy metal ions[2,16–20] and acidic dyes.[4,21–23]

Chitosan beads have been used in sorption columns. The use of chitosan beads as an adsorbent also provides the potential for regeneration after adsorption and reuse of the beads in subsequent adsorption operations. The production of chitosan hydrogel beads involves dissolution of chitosan in an acetic acid solution followed by a precipitation process of injecting the chitosan solution in droplets into a dilute sodium hydroxide solution.[24] However, the hydrogel beads have the disadvantage of poor chemical resistance and mechanical strength. This disadvantage significantly reduces the recycle life of the chitosan beads. To improve these properties,

crosslinking of chitosan beads with glutaraldehyde, epichlorohydrin or ethylene glycol glycidyl ether has been commonly used.[5,12,25,26] These crosslinked chitosan beads are still highly swollen in water. The water content of these wet crosslinked chitosan beads is usually more than 90%. Thus, the mechanical strength of the wet beads is still quite poor. The poor mechanical strength of these chitosan beads has significantly limited their practical applications. In addition, these crosslinking processes have been performed by the reaction of the amino functional groups of chitosan with these crosslinkers. As a consequence, the chemical property of the amino functional groups has changed upon crosslinking. In this paper we developed a method to prepare crosslinked chitosan beads with low water contents, high mechanical strength and unchanged amino functional groups.

Experimental

Materials

Chitosan (deacetylation degree $\geqslant 90\%$) was purchased from Jinan Haidebei Marine Bioengineering Co., Ltd (Jinan, China). Poly(vinyl alcohol) (PVA, degree of polymerization is 1700, degree of hydrolysis is 88%) was obtained from Tianjin Hecheng Science & Technology Co., Ltd (Tianjin, China). Glutaraldehyde and Span-80 (sorbitane monooleate) were provided by Tianjin Damao Chemical Reagent Co. (Tianjin, China). Toluene, chlorobenzene and acetic acid were from Tianjin No. 6 Chemical Reagent Co. (Tianjin, China). All other materials used were of analytical reagent grade from commercial sources.

Preparation of crosslinked chitosan/PVA blend beads

Chitosan solution (4.0%, w/w) was prepared by dissolving 4.2 g of chitosan into 100 g of dilute acetic acid (2% w/w). PVA solution (12.5%, w/w) was prepared by dissolving 14.3 g of

Key Laboratory of Functional Polymer Materials, Ministry of Education; Institute of Polymer Chemistry, Nankai University, Tianjin, 30071, China

PVA in 100 ml of water. Crosslinked chitosan/PVA blend beads were prepared by suspending acidic chitosan/PVA blend solution in toluene–chlorobenzene containing Span-80. Then the system's temperature was raised gradually to distil out a certain amount of water as an azeotrope with the aromatic hydrocarbons to reduce the water content of the suspension droplets, and then glutaraldehyde was added to finish the crosslinking. The following is an example of the preparation. A mixture of 17.2 g of chitosan solution (4.0%, w/w) and 2.8 g of PVA solution (12.5%, w/w) was heated to 70 °C and stirred at this temperature for 12 h, followed by another 12 h stirring at room temperature. A homogeneous polymer gel blend solution with 2/1 (w/w) ratio of chitosan to PVA was obtained. The pH value of the blend solution was adjusted to pH 2 by adding concentrated HCl ($\sim$0.7 ml). The resulting blended solution ($\sim$18.45 g) was suspended in 100 ml of toluene–chlorobenzene (1/3, v/v) containing 1.5 g of Span-80 in a 250 ml three-neck round-bottom flask with stirring speed of 230 rpm. The temperature of the system was raised to 90 °C and 13.1 ml of water as an azeotrope with toluene was distilled out slowly through a Barrett distilling receiver. The system was cooled to room temperature. A 0.33 g of 50% glutaraldehyde solution was added to the flask and the stirring continued at room temperature for 8 h. The resulting beads were filtered off, washed several times with acetone, suspended in 4% NaOH aqueous solution for 8 h, and then rinsed thoroughly with water until neutral pH.

Determination of gelation time caused by crosslinking

In each of five 50 ml beakers, 10 g of chitosan/PVA blend solution prepared as above was placed. The pH value of the blend solution was 5. The pH values of beakers 1–4 were adjusted to 1, 2, 3 and 4, respectively, by adding concentrated HCl. A certain amount of water was added to each of the beakers 2–5 to maintain the final solution volume in each of the beakers equal to that of beaker 1. Each of the solutions was agitated on a magnetic stirrer with the same stirring speed. Then 0.17 g of 50% glutaraldehyde solution was added and the time was set as 0. The gelation time was defined as the time needed for the magnetic bar to stop stirring as the viscosity increased.

Mechanical strength determination

Mechanical strength of the beads was determined by a self-made instrument. A glass syringe tube was vertically fixed, and a hard plastic plate was horizontally placed in the bottom of the tube. A chitosan/PVA bead with diameter of $\sim$1 mm was placed on the center of the plate. The piston of the syringe was inserted into the tube until the end of the piston touched the bead. Increasing weights were added gradually on the top

end of the piston until the bead broke. The minimum broken weight was defined as broken weight.

Water content measurements

Wet chitosan/PVA beads ($\sim$0.5 g) were dried in an oven at 105 °C for 2 h. The water content of the beads was defined as:

$$\text{water content} = (W_{\text{wet}} - W_{\text{dry}})/W_{\text{wet}}$$

where W_{wet}, W_{dry} are the weights of the wet and dry beads, respectively.

Results and discussion

In order to enhance the mechanical strength of crosslinked chitosan beads, chitosan/PVA solution was first suspended in an organic phase (toluene–chlorobenzene) to form aqueous phase droplets. Then part of the water in the droplets was distilled out as an azeotrope with the aromatic hydrocarbons to reduce the water content of the droplets. Finally crosslinker glutaraldehyde was added to the suspension to finish the crosslinking. The resulting crosslinked chitosan beads possessed low water content and thus high mechanical strength. In order to keep the amino groups of chitosan unchanged after crosslinking, chitosan/PVA solution with the amino groups protected by HCl as salts was used. The crosslinking process was tested by determining gelation time caused by crosslinking, as shown in Table 1. It can be seen that gelation time increases when pH values increase from 1 to 3. However, gelation time dramatically decreases when pH values increase to 4 and 5. The pK_a of chitosan amino groups depends on the degree of deacetylation and its degree of neutralization as well as the ionic strength.[27] With the degree of deacetylation of chitosan and the crosslinking conditions used in these experiments, the pK_a was estimated to be 5.5. The protonation degree of the amino groups was calculated based on the pK_a value and listed in Table 1. It can be seen that the amino groups were almost completely protonated at pH 1 and 2 and thus shielded from the reaction with glutaraldehyde. In these cases, glutaraldehyde must mainly react with the hydroxyl groups of PVA to form crosslinkage, as shown in Fig. 1b. It is well known that the reaction of aldehyde with hydroxyl groups is catalyzed by acid. Therefore gelation time decreased with decreasing pH. At pH 4 and 5, 3.1% and 24% of the amino groups, respectively, were free from protonation. As amino groups are much more reactive with aldehyde than hydroxyl groups and the acidic catalytic activities for acetal crosslinkage formation are much weaker at pH 4 and 5 than those at pH 1 and 2, crosslinker glutaraldehyde should mainly react with amino groups of chitosan to form Schiff's base

Table 1 Gelation time of chitosan/PVA crosslinked with glutaraldehyde at different pH values

4% Chitosan/g	12.5% PVA/g	50% Glutaraldehyde/g	pH	Amine protonation (%)	Gelation time/min
8.6	1.4	0.17	1.0	100	6.90
8.6	1.4	0.17	2.0	99.97	9.78
8.6	1.4	0.17	3.0	99.7	21.4
8.6	1.4	0.17	4.0	96.9	1.15
8.6	1.4	0.17	5.0	76.0	0.80
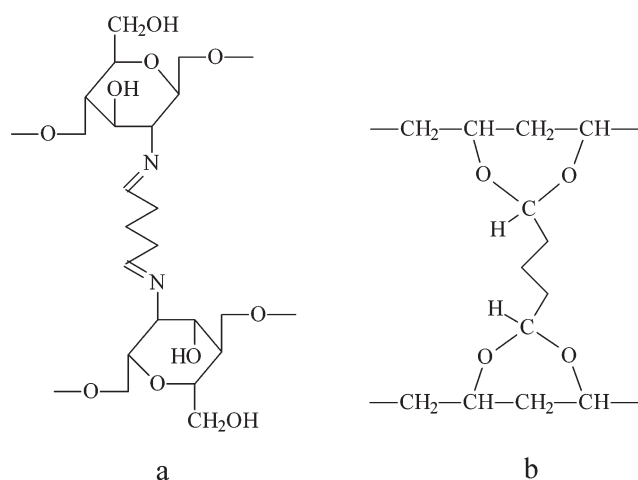
Fig. 1 Schematic representation of (a) PVA and (b) chitosan crosslinked with glutaraldehyde.
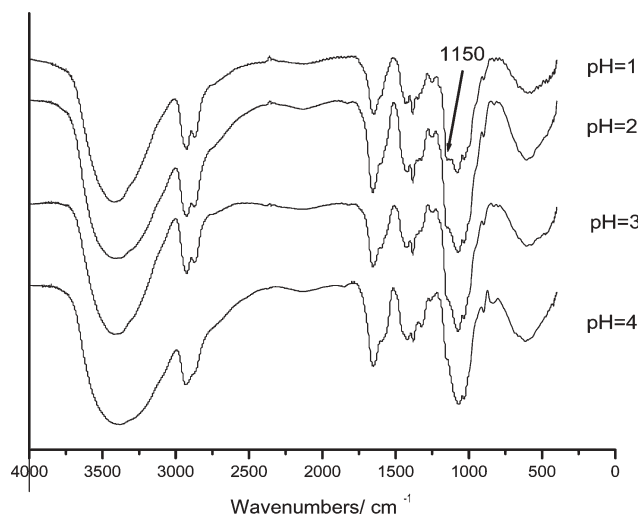
Fig. 2 IR spectra of crosslinked chitosan/PVA beads prepared at pH 1–4.

crosslinkage at pH 4 and 5, as shown in Fig. 1a, which is supported by the much shorter gelation times. At pH 3, the gelation time was longest because of the much fewer free amino groups as compared to pH 4 and 5, and weaker acidic catalytic activity as compared to pH 1 and 2. Thus, both of the crosslinkages may exist in the beads prepared at pH 3. These suppositions were also supported by IR spectra of the crosslinked chitosan/PVA beads (Fig. 2). In the cases of pH 1–3, a peak at 1150 cm^{-1}, which is the characteristic peak of acetal, appeared and the strength of the peak increased with decreasing pH value. The broader peak at 3380 cm^{-1} of crosslinked beads prepared at pH 4 in comparison with those ($\sim$3420 cm^{-1}) of the beads prepared at pH 1–3 should be caused by hydrogen bonding between the adjacent hydroxyl groups in the PVA chains, indicating most of the crosslinkages were formed between the amino groups of chitosan but not hydroxyl groups of PVA and glutaraldehye at pH 4.

Table 2 shows the crosslinking conditions and the properties of the resulting polymer beads. At pH 2, the broken weight increased from 9.5 g to 123 g when polymer concentration increased from 5.2% to 19.6% after distillation. The strength of the beads increased markedly accompanying the water content of the beads decreasing after distillation. Similar results were obtained at pH 1. When the pH value increased from 1 to 4, the strength decreased and the water content also decreased slightly when the other conditions were the same (comparing entries 9, 5, 10 and 11). These results may be caused by the different ratio of the two crosslinkages. The broken weight was roughly negatively correlated with the water content of the beads crosslinked at the same pH.

The beads obtained at pH 1 were opaque while the beads obtained at pH 2 or over were transparent. The opaque beads seem to have pores within them. Fig. 3 shows the SEM images of the beads obtained at pH 1 (the sample of entry 9 in Table 2) and pH 3 (the sample of entry 10 in Table 2). Fig. 3a and b indicate that phase separation occurred during the crosslinking at pH 1.

Fig. 4 shows the effect of crosslinking degree on the mechanical strength of the beads. When the mole ratio of the hydroxyl groups of PVA to glutaraldehyde is 4/1, the crosslinking degree is defined as 100%. It can be seen that the mechanical strength of the beads has a maximum value at a crosslinking degree of 40%. The beads with a higher crosslinking degree were hard, rigid and brittle, while the beads with a lower crosslinking degree were soft and flexible. This may be caused by the flexibility of the unreacted PVA chains.

Table 2 Preparation conditions and properties of crosslinked chitosan/PVA beads

Entry	Chitosan/PVA[a] (w/w)	Distilled water/ml	Polymer conc. after distillation (wt%)	pH	Broken weight[b]/g	H$_2$O content of beads (wt%)
1	2/1	0	5.2	2	9.5 $\pm$ 0.8	93.6
2	2/1	7	9.3	2	13.5 $\pm$ 3.9	74.3
3	2/1	9	11.3	2	14.4 $\pm$ 3.3	76.2
4	2/1	11	14.3	2	44.3 $\pm$ 7.4	72.6
5	2/1	13	19.6	2	123 $\pm$ 13	73.3
6	2/1	0	5.2	1	42.5 $\pm$ 6.6	83.9
7	2/1	7	9.3	1	58.5 $\pm$ 7.0	83.6
8	2/1	9	11.3	1	106 $\pm$ 11	80.5
9	2/1	11	14.3	1	141 $\pm$ 4	75.1
10	2/1	13	19.6	3	83.6 $\pm$ 8.5	72.7
11	2/1	13	19.6	4	27.7 $\pm$ 5.3	71.9

[a] Weight concentration ratio of chitosan to PVA. The initial volume of the polymer solution was 18.5 ml and the initial total polymer concentration was 5.2%. The mole ratio of hydroxyl groups of PVA to glutaraldehyde was 5/1 (80% crosslinking degree). [b] Mean values with standard deviations of ten trials.
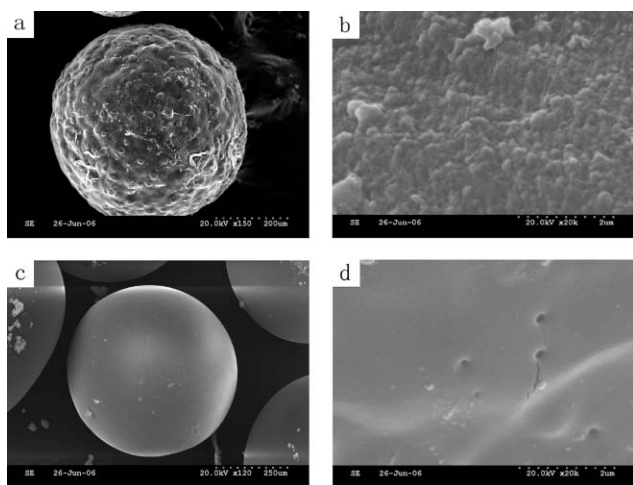
Fig. 3 SEM images of the chitosan/PVA beads prepared at pH 1 (a,b) and pH 3 (c,d).
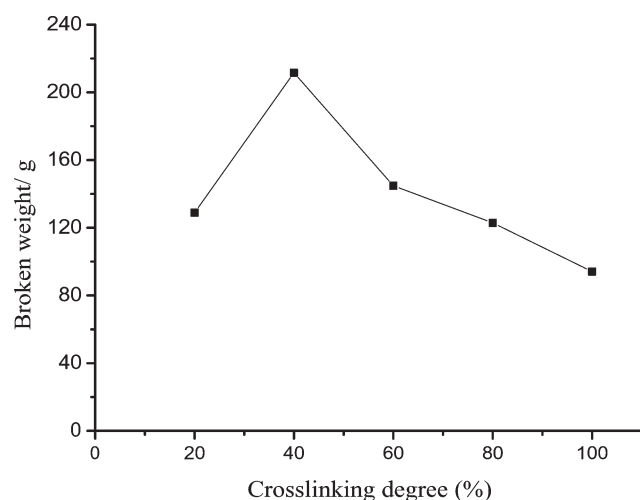
Fig. 4 The effect of crosslinking degree on mechanical strength (the conditions were the same as those of entry 5 in Table 2 except for crosslinking degrees, which were indicated in this figure).

Fig. 5 shows the effect of chitosan/PVA ratio on the mechanical strength with other conditions being the same. It can be seen that the mechanical strength increased with chitosan content decreasing. One of the possible reasons is that PVA chains are flexible and chitosan chains are rigid. When the ratio of chitosan/PVA increased, the beads became more brittle. Thus, PVA in the beads not only acts as the crosslinking matrix but also enhances the mechanical strength of the beads.

Preparation of micron-sized crosslinked chitosan beads with high mechanical strength is difficult using the methods reported in literature.[5,12,25,26] This is because the formation of micron-sized droplets of chitosan solution in the suspension requires a very dilute chitosan solution, due to the high viscosity of chitosan aqueous solution. The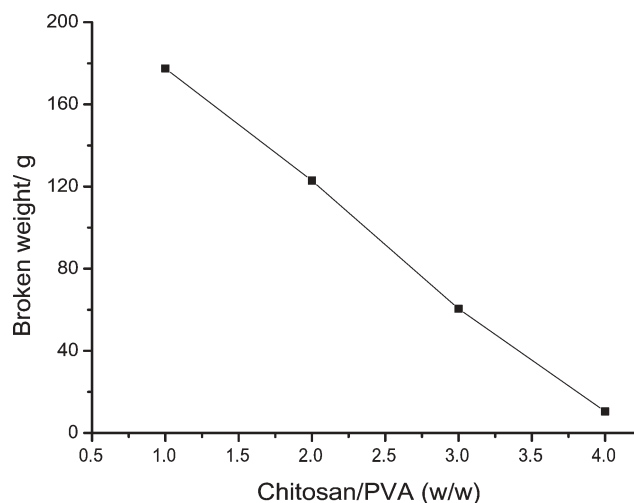 mechanical strength of micron beads prepared by crosslinking these micron-sized droplets with low concentrations of the polymer would be very poor. Microbeads of crosslinked chitosan/PVA, as shown in Fig. 6, were prepared by our method using very dilute initial polymer concentration and high stirring speed. As

Fig. 5 The effect of chitosan/PVA ratio on the mechanical strength (pH 2, the crosslinking degree was 80 mol% and the polymer concentration was 19.6 wt%).

the viscosity of this dilute polymer solution was very low, the small size suspension droplets were obtained. Then most of the water was removed by distillation, and thus the size of the droplets further decreased. The polymer concentration increased dramatically in the droplets after the distillation, and thus the mechanical strength of the resulting beads after crosslinking with glutaraldehyde should be good. Although the mechanical strength of the crosslinked microbeads was not determined because of their small size, the mechanical strength should be close to that of bigger beads with the same polymer concentration of the droplet after distillation.

Conclusions

Due to low saturation concentration of aqueous chitosan solution, crosslinked chitosan/PVA blend beads with low
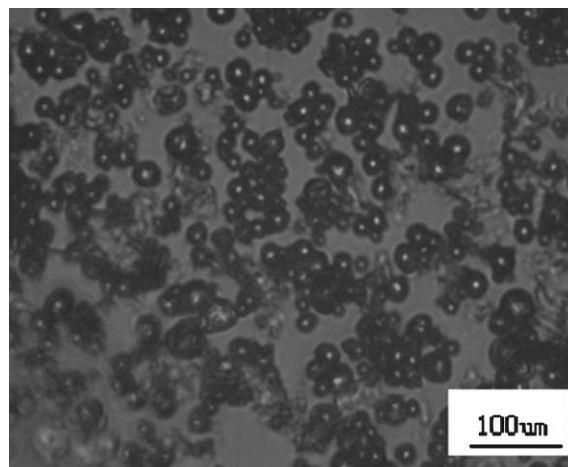
Fig. 6 Optical microscopy image of the crosslinked chitosan/PVA beads (initial concentrations of chitosan and PVA were 0.48% and 0.24%, respectively. Final polymer concentration of the droplets after distillation was ∼19%, pH 2, crosslinking degree was 80%, stirring speed was 450 rpm).

water content, and thus high mechanical strength, were prepared by suspension of aqueous chitosan/PVA blend solution in an organic medium (toluene–chlorobenzene), distillation of some of the water in the suspension droplets as an azeotrope with the aromatic hydrocarbons to increase the polymer concentration of the droplets and finally cross-linking PVA within the droplets in acidic condition (pH 1 and 2) by glutaraldehyde. The crosslinking of PVA with glutaraldehyde was catalyzed by acid. As the amino groups of chitosan should be much more reactive with aldehyde than the hydroxyl groups of PVA, the acidic condition also prevents the reaction of the amino groups of chitosan with glutaraldehyde by protonating them, and thus the amino groups remain unchanged upon crosslinking. If very dilute initial polymer concentration was used, very small size suspension droplets were obtained at high stirring speed because of the low viscosity of the dilute polymer solution. After distillation, most of the water in the droplets was removed, and thus the size of the droplets became smaller. Crosslinked chitosan/PVA microbeads were obtained upon crosslinking the droplets with glutaraldehyde. At pH 4 and 5, glutaraldehyde reacted with amino groups of chitosan rather than hydroxyl groups of PVA to form Schiff's base crosslinkage in the beads.

Acknowledgements

References

1 K. Kurita, *Progr. Polym. Sci.*, 2001, **26**, 1921–1917.
2 G. Crini, *Progr. Polym. Sci.*, 2005, **30**, 38–70.
3 E. Guibal, *Progr. Polym. Sci.*, 2005, **30**, 71–109.
4 G. Crini, *Bioresour. Technol.*, 2006, **97**, 1061–1085.
5 E. B. Denkbas and M. Odabasi, *J. Appl. Polym. Sci.*, 2000, **76**, 1637–1642.
6 P. A. Felse and T. Panda, *Bioprocess Eng.*, 1999, **20**, 505–512.
7 B. Krajewska, *Enzyme Microb. Technol.*, 2004, **35**, 126–139.
8 R. S. Juang, F. C. Wu and R. L. Tseng, *Adv. Environ. Res.*, 2002, **6**, 171–177.
9 K. R. Reddy, K. Rajgopal, C. U. Maheswari and M. L. Kantam, *New J. Chem.*, 2006, **30**, 1549–1552.
10 X. F. Zeng and E. Ruckenstein, *J. Membr. Sci.*, 1998, **148**, 195–206.
11 X. F. Zeng and E. Ruckenstein, *Ind. Eng. Chem. Res.*, 1998, **37**, 159–165.
12 M. Ruiz, A. M. Sastre and E. Guibal, *React. Funct. Polym.*, 2000, **45**, 155–173.
13 T. Vincent and E. Guibal, *Ind. Eng. Chem. Res.*, 2002, **41**, 5158–5164.
14 P. Chassary, T. Vincent, J. S. Marcano, L. E. Macaskie and E. Guibal, *Hydrometallurgy*, 2005, **76**, 131–147.
15 R. K. Katarina, T. Takayanagi, M. Oshima and S. Motomizu, *Anal. Chim. Acta*, 2006, **558**, 246–253.
16 L. Jin and R. Bai, *Langmuir*, 2002, **18**, 9765–9770.
17 T. N. C. Dantas, A. A. D. Neto, M. C. P. A. Moura, E. L. B. Neto and E. P. Telemaco, *Langmuir*, 2001, **17**, 4256–4260.
18 V. M. Boddu, K. Abburi, J. L. Talbott and E. D. Smith, *Environ. Sci. Technol.*, 2003, **37**, 4449–4456.
19 N. Li and R. Bai, *Ind. Eng. Chem. Res.*, 2005, **44**, 6692–6700.
20 N. Li, R. Bai and C. Liu, *Langmuir*, 2005, **21**, 11780–11787.
21 M. S. Chiou and G. S. Chuang, *Chemosphere*, 2006, **62**, 731–740.
22 M. S. Chiou, P. Y. Ho and H. Y. Li, *Dyes Pigments*, 2004, **60**, 69–84.
23 Y. C. Wong, Y. S. Szeto, W. H. Cheung and G. McKay, *Process Biochem.*, 2004, **39**, 693–702.
24 G. L. Rorrer, T. Y. Hsien and J. D. Way, *Ind. Eng. Chem. Res.*, 1993, **32**, 2170–2178.
25 W. S. W. Ngah, C. S. Endud and R. Mayanar, *React. Funct. Polym.*, 2002, **50**, 181–190.
26 T. Y. Hsien and G. L. Rorrer, *Ind. Eng. Chem. Res.*, 1997, **36**, 3631–3638.
27 P. Sorlier, A. Denuziere, C. Viton and A. Domard, *Biomacromolecules*, 2001, **2**, 765–772.

Sustainable from the very beginning: rational design of molecules by life cycle engineering as an important approach for green pharmacy and green chemistry

Klaus Kümmerer

Chemicals are a part of modern life. Products are the main emissions of the chemical and pharmaceutical industries. This makes it difficult to hold them back efficiently. Very often they do not become degraded or fully broken down to water, carbon dioxide and inorganic salts. Often, unknown transformation products are formed in the environment. Therefore, according to the principles of green chemistry, the functionality of a chemical should not only include the properties of a chemical necessary for its application, but also easy and fast degradability after its use. Taking into account the full life cycle of chemicals will lead to a different understanding of the functionality necessary for a chemical. In the present discussion, improvement of synthesis and renewable feedstock are very prominent, whereas the environmental properties of the molecules are somewhat underestimated. To stimulate the discussion about the future role of degradable chemicals several examples are presented to underline the feasibility and the economic potential of this approach, called benign by design.
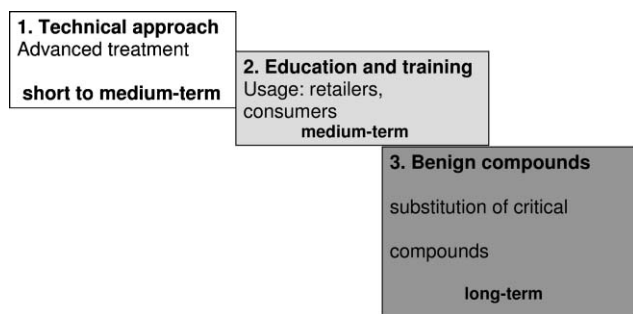
The problem—persistent chemicals

Chemicals are a part of modern life and are present in all spheres of human life. They are used as pharmaceuticals, pesticides, detergents, fertilizers, dyes, paints, finish, preservatives, food additives among others. They contribute to our well being, high life expectancy and economic prosperity. If they are constituents and ingredients of consumer or household products and other open applications they are often emitted into the environment by non-point sources. Very often they do not become degraded, *i.e.* they are not, or are only incompletely, broken down to water, carbon dioxide and inorganic salts. Unknown transformation products can result from such biological and chemical processes such as hydrolysis, redox-reactions or photolysis. These unknown chemical entities can remain in the environment and can also be toxic for humans and environmental organisms. In this case, the situation may be worse as we usually have much less knowledge about the dead end transformation products with regards to their fate, and their effects on the environment than on the parent compounds. Even if there is some degree of degradation, the parent compounds will nevertheless be present at constant levels in the environment if the input rate is higher than their rate of degradation or mineralization. This can be called second order persistency or pseudo persistency. Persistency is one of the most important criteria in the environmental assessment of chemicals.[1–4] A long half life of chemicals in the environment results in a wide range for the chemicals. That is,

they will be present in big compartments for a long time.[2] For chemicals and transformation products with such properties, it is not possible to carry out a risk assessment. The bigger the scales involved, the more uncertainty increases and the more possible effects cannot be tested in lab trials. Polychlorinated biphenyls (PCBs) is a classical example of persistent pollutants. PCBs were synthesized for the first time in 1877, and already in 1899 severe health problems (chloracne) associated with the handling of PCBs were reported. Throughout the years the poisoning of rice oil by these compounds and their neurotoxic effects as well as carcinogenicity has been described in detail. Despite this knowledge, it took until 1999 to ban PCBs fully within the EU—100 years after the first reports of its severe toxicity.[3] This example demonstrates that it is not only the time scales of the chemicals themselves and the environmental processes impacted by them but also the time scales of economical and political systems which have important effects. In addition, the use of persistent chemicals is often associated with high costs in the long run—at least for the general public. In the Stockholm convention, a half life of more than 50 days in water is set as a criterion for POPs. Recent research showed chemicals that are less persistent and have higher polarity than PCBs are distributed globally too, and can also accumulate in humans.[4] A statistical correlation between the persistency of chemicals and the prevalence of chemicals present in the environment which can initiate cancer has been only recently reported.[5] It should be mentioned that chemicals which are of high interest for green chemistry are not necessarily themselves in line with the principles of green chemistry. An example is ionic liquids. Ionic liquids help chemists to contribute to sustainable chemistry because they offer an opportunity to reduce waste which is formed during the synthesis of chemicals. However, they are not biodegradable and they can be toxic for environmental organisms.[6]

Applied Environmental Research Section, Institute of Environmental Medicine and Hospital Epidemiology, University Hospital, Breisacherstraße 115b, 79106 Freiburg, Germany. E-mail: Klaus.Kuemmerer@uniklinik-freiburg.de; Fax: +49-761-270-8213; Tel: +49-761-270-8235

1. Technical approach
Advanced treatment

short to medium-term

2. Education and training
Usage: retailers, consumers
medium-term

3. Benign compounds

substitution of critical

compounds

long-term

Fig. 1 Strategies to reduce the input of chemicals into the environment (www.start-project.de).

In general, three different approaches for preventing the input of chemicals into the environment are possible. These are depicted in Fig. 1. In the meantime, we have learned that the main emission of chemical and pharmaceutical industries is their products. If the chemicals themselves are the products, *e.g.* detergents, pesticides, dyes, paints, flame retardants, pharmaceuticals, personal care products, and others, these very often end up in the environment in the long term. Therefore, an important task is to focus not only on the optimization of the chemical synthesis of a molecule and its use but also to include the molecules themselves. Therefore, "chemical products should be designed so that at the end of their function they do not persist in the environment and break down into innocuous products". [1] Product design as an important part of green chemistry was addressed more detailed in 2002. [7]

The conventional wisdom assumes that a chemical needs to be stable to be successful in the market and the idea described above is in itself a contradiction. The approach of designing chemicals according to both the requirements of application *and* the environment, *i.e.* along their whole life cycle, is quite ambitious. It is at the core of chemistry and pharmacy. In this article, examples of chemicals satisfying the benign-by-design approach are given to move forward the discussion about the feasibility and the range of this approach. For this purpose, historical examples are outlined. A focus is on pharmaceuticals. For them the barriers are much higher than for other chemicals. Beside the requirements to be fulfilled by other chemicals, they have to be of low or even no human toxicity. If it is possible to design benign pharmaceuticals it should be possible for other chemicals too.

General approaches for the prevention and reduction of the input of chemicals into the environment

The traditional short-to-medium term approach for the prevention and reduction of the input of chemicals into the environment within and after their use is containment. This is not possible for chemicals used in every day life. In such cases, treatment of emissions *e.g.* effluent treatment, air treatment, or waste treatment is applied ("end of the pipe technology", strategy 1 in Fig. 1). The shortcomings of this approach are clear: it is difficult, if not impossible, to apply such an approach if the entry of the chemicals into the environment is by non-point sources. Furthermore, very often not all trace compounds are fully removed by such treatment.

More than a decade ago, it was learned that treatment of emissions is often not satisfying and is itself creating new problems. For example, stable transformation products are often formed by end of the pipe treatment. Sometimes, *e.g.* if oxidation techniques are applied, mutagenic transformation products result. Sorption onto powdered charcoal and other so called "advanced" treatment removes some additional compounds, but not all. In any case, such an advanced treatment results in further energy demand and may create new waste to be treated. Furthermore, end of the pipe treatment creates additional costs. End of the pipe treatment can be seen as an opportunity to gain time in order to develop more sustainable approaches, but again this approach creates its own problems. It is a non-sustainable approach. Furthermore, a certain type of technology tends to persist once installed on a large scale. That is, if a big investment has been directed to one type of problem solution (*e.g.* advanced waste water treatment) this technology has a tendency to persist for a long time even if the problems have changed, the technology has advanced or they are no longer adequate for a certain problem.

Containment at the source and responsible care as well as product stewardship (medium-term strategy 2 in Fig. 1) have been created and implemented within a number of industries. This approach contributes to the reduction of emissions there. In the case of chemicals used in open systems, this approach also has its limitations and is not always very efficient. Therefore, other approaches should be considered too. In the following section, the third approach depicted in Fig. 1 will be discussed in more detailed because it is the one which must become a part of green chemistry, not only by enabling chemistry to contribute to sustainability but to make chemistry itself more sustainable.

Structure and properties—at the core of chemistry

One of the principles of green chemistry is the design of environmentally friendly products. This includes the design of environmentally friendly chemicals and pharmaceuticals (long-term strategy 3 in Fig. 1). One possibility to implement such an approach is to design chemicals in such a way that they are readily degradable after their use. This means that the functionality of a chemical consists of more than simply the properties required for successful applications. Functionality in a broader and sustainable sense would also include the ready and complete degradability of a molecule after its use, for example in traditional sewage treatment. Starting from this assumption, it is necessary to include properties necessary for both successful applications on the one hand, as well as after application on the other hand, at the time when new chemical entities are created. A life cycle engineering of chemicals is needed. The conventional wisdom assumes that a chemical needs to be stable to be successful in the market and the idea described above is by itself a contradiction. A closer look reveals that this is not necessarily the case.

The approach of designing chemicals according to both the requirements of application *and* the environment, *i.e.* along their whole life cycle, looks like a totally new approach. Instead, it is at the core of chemistry and pharmacy. Chemistry and the chemist's language are about the relation of the

structure of a chemical and its properties, *e.g.* its reactivity. Even a small change in the structure of a chemical may have tremendous effects on its properties. Benzene is (after metabolic activation) a carcinogen. It is only slowly biodegradable. Simply the insertion of an oxygen atom into a carbon hydrogen bond results in a new compound, phenol with very different properties which are significant for its use and its fate in the environment. In contrast to benzene, phenol is readily aerobically biodegradable, not carcinogenic and active against bacteria. Therefore, it has long been used as a disinfectant. This fundamental connection between structure and properties can be used for the approach of benign by design. It allows the theoretical design of molecules and the assessment of their properties before they are even synthesised.

In the case of molecules of a more complex structure than benzene and phenol, human expertise is limited. Therefore, within the last decades computer based systems have been developed. These so called expert systems assist human experts with the handling and application of this complex type of knowledge.[8–10]

This approach is currently widely in use within pharmaceutical industries and to some extent also in chemical industries.[8,10] It will be of increasing importance within REACH for the assessment of chemicals and is already applied broadly for this latter purpose by the U.S. EPA.[9] Modern pharmaceutical synthesis and drug discovery uses this understanding by applying general rules, such as Lipinsky's rule of five (log P from 1 to 5, molecular weight from 100 to 500, number of H-donors from 0 to 5, number of H-acceptors from 0 to 9, number of rotatable bonds less than 10) and computer-based structure activity relationships.[10] Starting from a lead structure, the desirable activity of a molecule is improved by systematic variation of its chemical structure. At the same time, unwanted properties such as mutagenicity are reduced. The successful candidates are more active and at the same time exhibit less side effects than the original chemical. To have as little side effects as possible means that the inherent safety of the chemicals has been improved and the total functionality of the molecule has been improved as well. A new understanding would be to regard low biodegradability after use as an unwanted side effect also.

In the meantime, there is broad knowledge available as to how certain functionalities govern the properties of a given pharmaceutical lead structure.[10] This is demonstrated in Fig. 2 for the lead structure of the quinolones which are used as antibiotics. The carboxyl function is indispensable for the binding to the target (gyrase) and can therefore not be modified. R_1 controls pharmacokinetics and efficacy. Whether "X" is nitrogen or oxygen impacts the activity, R_7 controls the activity spectrum and is also related to pharmacokinetics. The given example for R_7 enables activity against gram-negative bacteria. Introduction of the fluorine atom resulting in the modern group of fluoroquinolones increases activity. This also seems to be responsible for the increased photosensitivity of patients treated with fluoroquinolones.

This is understandable in terms of the change of the electronic properties of the benzene ring due to the high electronegativity of fluorine. The resulting increase in the energy gap between the highest occupied molecular orbital
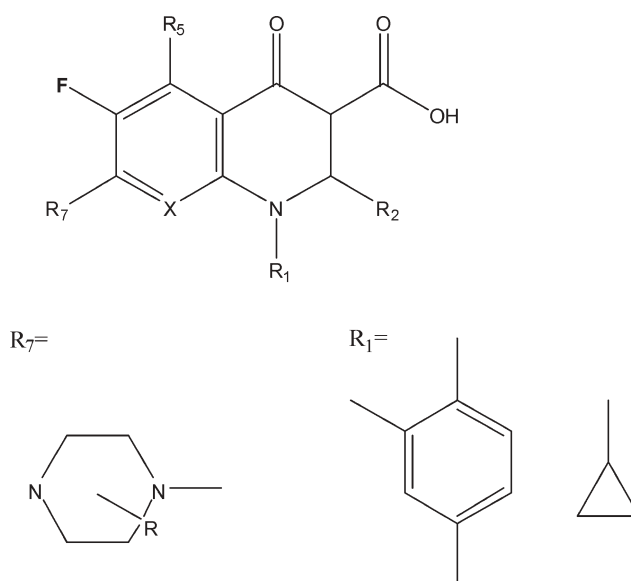

Fig. 2 Structure activity relationships of quinolones

(HOMO) and the lowest unoccupied molecular orbital (LUMO) leads to absorption of radiation with higher energy. A higher energy transfer into the skin of a treated patient is the consequence. At the same time the C–F-bond contributes to the low biodegradability of the fluoroquinolones for the same reason. The C–F-bond is very stable.[11] Due to the fluorine atom attached to the aromatic ring system it is poor in electrons and therefore can also not easily be oxidized by aerobic bacteria and/or radiation of lower energy. Furthermore, by the introduction of the fluorine atom, an important position for hydroxylation as a first step of the biodegradation of aromatics is blocked. As both vicinal positions are not aromatic hydrogen atoms, the formation of a dihydrol is not possible. Both electronic and steric factors contribute to the low biodegradability of fluoroquinolones such as ciprofloxacin.

To put such an approach into the context of green and sustainable chemistry, it is necessary to challenge the paradigm of the stability of chemicals as an indispensable property for their application. Normally, we speak of the stability of a chemical without mentioning the context of a certain environment. We assume that the stability of a chemical is an intrinsic property of a chemical. However, it is the result of the interaction of a molecule with its environment. Stereochemistry and electronic properties of a molecule on the one hand and the constraints set by its environment on the other hand govern the interaction. Therefore, the reactivity of a molecule, *i.e.* the kinetics and thermodynamics, depend on both the properties of the molecule *and* its environment. This is one of the basic principles of chemistry: change the conditions, *e.g.* temperature or moisture, and a molecule may then react in a different way or with a different velocity.

Within the life cycle of a chemical the conditions offered by its environment can often vary. Access of light, pH-value or redox-potential varies with the environment. Additionally, bacterial diversity and differing bacterial density are found in different compartments. Therefore, the metabolic diversity of

bacteria and the potential and pathways for the breakdown of molecules are different. For example, the conditions of a pharmaceutical on the shelf (*e.g.* pure and dry, exclusion of light, room temperature) are different from the ones in the human body (moisture, higher temperature, certain more or less specific enzymes, low pH in the stomach, anaerobic conditions and bacteria in the gut and the intestine) from those in sewage (often high pH, aerobic conditions and bacteria at a different density with enzymes of different type, substrate and activity) and again from those in surface water (neutral pH, low bacterial density, access of light) and sediments (oxygen rich and anoxic conditions, different pH, different matrix for sorption). If we are aware of those facets that are of significance for the "stability" of a chemical, this knowledge can then be used to design chemicals not only for optimised performance during their application but also within the further stages of their life cycle. The same holds for the degradation of molecules as a special type of reaction. From another point of view, stability and degradability are a question of velocity, *i.e.* the relation of the time scales of the different reaction pathways. The challenge is to design a molecule in such a way that its lifetime is sufficient for its use but short enough under environmental conditions.

It also has to be noted that some chemicals are used because of their low stability, such as monomers or pro-drugs such as the anti-neoplastic compounds ifosfamide or cyclophosphamide, which are activated in the human body in order to exert their desired effects.[12] A fully stable chemical would often not be of any use in most cases, because it would not undergo any interaction or reaction with its environment, which is often the prerequisite of its application. At the least, bioactive chemicals such as pesticides, disinfectants and pharmaceuticals have to have a certain amount of reactivity within their range of application. If they do not they would not be bioactive and therefore would be worthless for their intended use. They exert their reactivity within a special environment, *e.g.* within the human body, where they are activated in a specific manner. Other examples of reactive chemicals are coatings.

From the past to the future

The future basis of our designing and handling of chemicals has to abandon the control-oriented end of the pipe approach of the past. This attitude assumes complete knowledge and controllability. Because of the success of emission reduction, the products themselves are now the main emissions of the chemical and pharmaceutical industries. Therefore, an additional focus on the improvement of the chemicals themselves is necessary. Not only for environmental reasons, but also because of economical considerations, it will be necessary in the future to take sustainability into account when a chemical is first developed and designed. That means that, as a very first step, easy degradability after use or application is taken into account even before a chemical's synthesis. Such an approach is not completely new. For example, it is quite common during the development of pharmaceuticals with respect to unwanted side effects.

Compounds with few or no side effects or low toxicity can be called inherently safe.[10] Such chemicals need only little or no special safety measures or special knowledge by a user or applicant. A more holistic understanding of this concept means that chemicals should not only have the lowest possible impact on humans handling and ingesting such compounds but also on the environment. If there is no exposure of the environment to such compounds, no effects have to be considered. This means a different understanding of the functionality of a chemical. It includes its manufacturing and use, as well as its fate after use. Such chemicals are benign by design. For such chemicals a life cycle assessment and optimization is performed according to the specific conditions present at the different life stages before its synthesis and introduction into the market. These include:
•raw materials
•synthesis
•production
•use
•fate after use

Such an approach requires the chemist doing synthesis to have a different understanding. This is because the chemist has to think interdisciplinarily and take into consideration the world outside his laboratory. He is not only a craftsman who assembles molecules, but is also an architect who designs them. This includes accounting for not only the functionalities of a molecule that are necessary for its application but also those which are important throughout its entire life cycle. This is the part of sustainability which is specific for chemistry and is at the core of this new understanding of chemistry. It includes the sustainable use of resources as well as improved efficiency and efficacy. However, it is more than that. Through this approach the criteria of sustainability are applied to chemistry itself, and this requires interdisciplinary thinking.

At first glance, it does not seem very likely that the outlined approach (strategy 3 in Fig. 1) is feasible, nor that it can contribute much to the goals of green and sustainable chemistry. However, looking into chemical literature under the special focus of stability as described above shows that there are quite a lot of examples that demonstrate the feasibility of the approach. Pharmaceuticals are the molecules which present the biggest challenge because they should be very bioactive in terms of desired activity and at the same time inactive in terms of unwanted side effects. Therefore, examples from this area have been chosen to demonstrate the feasibility of the approach.

5-Fluorouracil is one of the important cytostatic agents which has been in medical use for long time. It acts as an anti-metabolite by replacing the natural compound uracil which is a basic constituent of RNA and DNA. A small change in the chemicals' structure, replacement of one hydrogen atom in uracil by a fluorine atom, makes it highly active as an anti-metabolite. The carbon–fluorine bond is well known for its chemical stability.[11] Therefore, 5-flurouracil (Fig. 3) is not readily biodegradable.[13] The negative effect of fluorine on the biodegradability of organic compounds is also found for the structurally similar compounds gemcitabine and cytarabine (Fig. 3), which also act as anti-metabolites and are used as cytostatic agents. Gemcitabine and cytarabine have been developed in order to improve pharmaceutical properties. They illustrate that improved pharmaceutical properties can
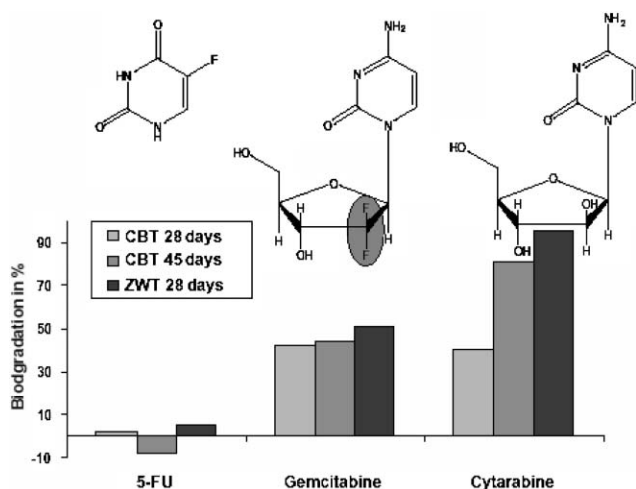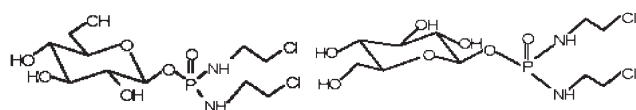
Fig. 3 Different biodegradability and elimination of structurally related anti-metabolites in the closed bottle test (CBT) and in the Zahn-Wellens test (ZWT)[13]

Fig. 5 Modification of the chemical structure of ifosfamide to improve sorption in the bowel by keeping the active principle (bold bonds) to ß-D-Glc-IPM (INN = glufosfamid) also resulted in improved biodegradability under environmental conditions.[14,15]

also result in improved environmental performance. A more detailed analysis of their biodegradability shows that the improved biodegradability of cytarabine as compared to gemcitabine is not only due to the sugar moiety without fluorine atoms but that the cytosine moiety has also been degraded.[13]
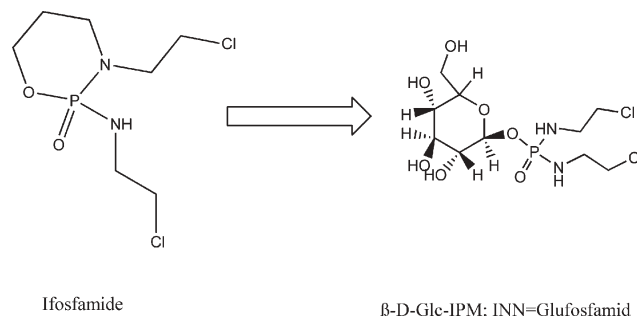
Another example is the cytostatic agent gluphosphamide (ß-D-glucosylisophosphoramidmustard: ß-D-Glc-IPM; Fig. 4). In this case the stereochemistry is of importance, not only for the molecule's activity but also for its biodegradability. Gluphosphamide was developed from ifosfamide, which is one of the classical alkylating cytostatic agents.

The goal of the structural change was to improve its pharmacological properties, such as uptake in the bowel, in order to reduce undesired side-effects. For this purpose, the active moiety (Fig. 5) was kept while the other part of the molecule was modified. ß-D-Glc-IPM is now under clinical trial phase III. However, it has been found that the ß-D-Glc-IPM not only has the desired pharmacological properties,[14] but it is also much more biodegradable than ifosfamide, which is not biodegradable, as are most other cytostatic agents studied to date.

In contrast to ß-D-Glc-IPM the ß-L isomer is neither pharmacologically active nor biodegradable.[14,15] The lack of biodegradability of the ß-L isomer is quite understandable. In the human body, as in nature, the vast amount of enzymes catalyzing reactions of sugars is for ß-D isomers, as most naturally occurring sugars and derivatives are based on ß-D

isomers. It should be emphasised that chemicals of natural origin are often better biodegradable than synthetic ones, but not in general. The uniqueness of a structure and its synthesis and metabolic pathways it fits in may also be of importance.

The different conditions along the life cycle of a chemical

ß-D-Glc-IPM can serve as an illustrative example of which benefits can be gained if the whole life-cycle of a molecule is taken into account. One may ask why ß-D-Glc-IPM is a promising pharmaceutical that is now under clinical trial phase III despite its good biodegradability, *i.e.* "instability" under environmental conditions. Enzymes modifying and degrading sugars are present in the human body too. A closer look shows that there are significant differences within the human body and the environment.

•Compound related:

◦The concentration of the compound is much lower in the environment than in the human body. This affects biodegradation and photodegradation.

•Environment/application related:

◦The presence of other organic material is higher in the gut than in most environmental compartments. This can affect the (bio)availability and solubility of the compound.

◦Parameters such as pH and redox conditions are of importance for non-biotic degradation by hydrolysis, oxidation and reduction.

◦Access of light is not possible in the human body and can be prevented by storage in brown glass on the shelf. In surface water and top soil the access of light (including high energy radiation such as UV light, which is of the utmost importance for photodegradation of organic compounds) is much more extensive than in rooms or in sewage treatment, in soil or sediments. Other organic material such as humic acids is present in environmental waters and may

Fig. 4 Left: glucosylisophosphoramidmustard (ß-D-Glc-IPM; INN = Glufosfamid). Right: ß-L-glucosylisophosphoramidmustard (ß-L-Glc-IPM).

serve as transmitters of light energy for indirect photolysis (type II photolysis).

∘Moisture is low when stored as a powder on the shelf. Therefore, hydrolysis is very slow.

•Microbiology related:

∘The diversity and prevalence of bacteria and enzymes is quite different between the bowel and the environment because of differing conditions. Furthermore, fungi are present the environment and normally not in the human body.

∘In the bowel the ambient temperature is body temperature, which is preferred by thermophilic bacteria. The temperature is lower in sewage treatment and the aquatic environment where mesophilic bacteria are present.

∘In the bowel nutrient rich conditions are found by bacteria, whereas in the environment we have some food rich compartments such as sewage treatment and compartments with a shortage of nutrients (e.g. surface water).

∘In the bowels the conditions are anaerobic. In most environmental compartments aerobic conditions are found. This again selects different bacteria in differing densities with different metabolic capacities and activities.

∘Moisture is low when stored as a powder on the shelf preventing bacterial growth.

∘Redox conditions and pH are additional parameters that are different in the human body and the environment. pH is far below 7 in the stomach, whereas it is mostly above 7 in sewage.

Because of these different conditions, the potential for degradation of chemicals is different at different life stages of a chemical. If the different conditions and dependencies along the life cycle of a molecule are taken into account, stability during the application phase and degradability thereafter are not necessarily in opposition. This knowledge can be used to design chemicals according to the properties of a molecule within the different phases of its life cycle. That means a chemical's structure and its expected environment at each stage need to be looked at as a unit. In other words, the full functionality of a molecule includes the properties necessary for good performance within all life stages of a molecule—not only during the application. This holds not only for its fate after application but also all the other principles of green chemistry such as the preference for renewable resources, as well as aspects of synthesis such as waste minimization and atomic economy.

Examples demonstrating the feasibility

Linear alkylbenzenesulfonates (LAS) are among the most widely used chemicals. Several million metric tons are used as
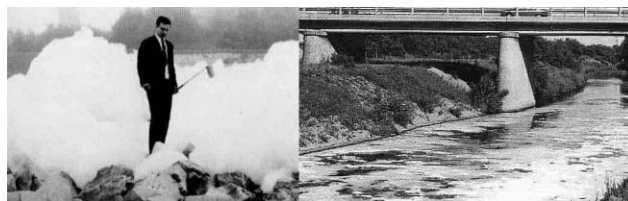

Fig. 6 Foaming in sewage treatment and on rivers in the 1950s caused by non-biodegradable TPS (with permission from the Archives of the Henkel Company, Düsseldorf).

laundry detergents per year worldwide. Its predecessor was tetrapropylene sulfonate (TPS) which was introduced into the market in the 1950s. Its biodegradability was low and resulted in strong foaming during sewage treatment and in rivers (Fig. 6).

As this effect was clearly visible for everyone the authorities took action and announced a special regulation which would soon come into effect. After this announcement the detergent industries started to work on a more biodegradable detergent. LAS were introduced into the market as a substitute for TPS before the new regulation came into force (Fig. 7). In Germany the so called *Detergentiengesetz* came into force in 1961 and was the first environmental regulation in this country. The alkyl chain of LAS is not branched. It is derived from naturally occurring lipids. This is the reason for its biodegradability: the biodegradation pathway starts with a ß-oxidation at its end. Then C_2-units are removed stepwise. This is just the reversal of the natural pathway of its synthesis, the acetyl-CoA-mechanism. Because of the branching and C_3-units this pathway is blocked in TPS. Another interesting detail is that LAS is more toxic to aquatic organisms than TPS but because of the good biodegradability of the latter during sewage treatment this has not prohibited its broad introduction into the market.[16]

EDDS (Fig. 8) is another example of a chemical that has been introduced into the market because of its good biodegradability compared with that of its predecessor ethylenediamine tetra acetate (EDTA).[7,17] EDTA has long
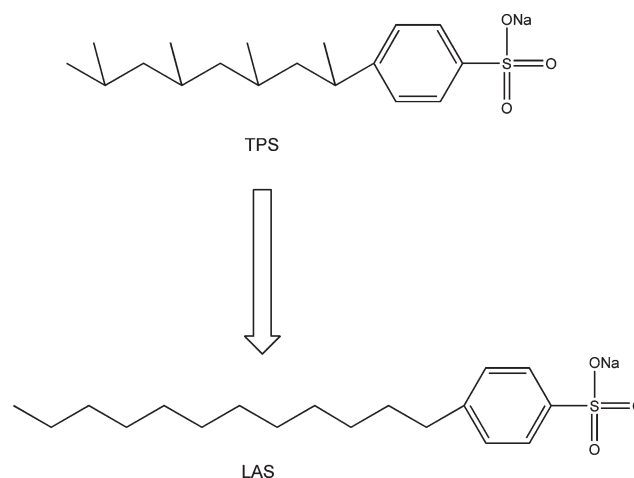
Fig. 7 Change of chemical structure of TPS aimed at improved biodegradability: LAS
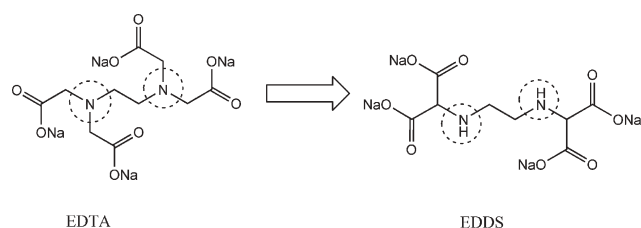
Fig. 8 Improvement of biodegradability and application range by structural change of complexing agents: [S,S]-EDDS is readily biodegradable whereas EDTA is not[17]

been in use as a complexing agent. Due to its heavy use and its low biodegradability it has been and still is frequently found in the environment, especially in sediments, where it remobilizes heavy metals. EDTA contains two tertiary nitrogen atoms. These are known to impede biodegradability. Moving the acetyl groups attached directly to the nitrogen atoms to carbon atoms results in secondary nitrogen atoms which are less constraining. The resulting new compound N,N′-ethylenediamine disuccinic acid (EDDS, IUPAC name: 2-[2-(1,2-dicarboxyethylamino)ethylamino]butanedioic acid)) differs by the type of the amino groups and the [S,S] isomer is much more biodegradable. [S,S]-EDDS is a derivative of aspartic acid, a naturally occurring amino acid. [S,S]-EDDS also works well as a complexing agent and for some applications is even an improved complexing agent. The secondary nitrogen atoms can function as additional binding sites. Interestingly, the stereo-isomeric [R,R]-EDDS is not biodegradable.

The targeted introduction of photochemical deactivation after use of an antibiotically active compound has been only recently described.[18] An impressive example of the improvement of specificity, efficacy and environmental properties combined with economical success is the history of the pesticides. Dichlordiphenyl trichlorethan (DDT) and other chlororganic chemicals such as γ-hexachlorocyclohexane and the bicyclical chlordiens such as aldrin and dieldrin are very persistent and are part of the dirty dozen mentioned in the Stockholm convention. After some time the more easily biodegradable organic phosphorous esters were developed (e.g. parathion). The more specific pyrethroids belong to the following generation of pesticides. Their lead structure is photo-sensitive and they are by far less toxic against humans. Carbamates are accessible to hydrolysis. The latest examples are the spinosoides (e.g. Spinosad™) and the acyl ureas (e.g. Hexoflumuron™). Spinosad for example has been awarded with the Green Chemistry Award because of the combination of its activity to targeted pests and a better environmental and toxicological profile than most synthetic insect control agents.[19]

Rational design: life cycle engineering by molecular design

The correlation of structure and properties is at the core of chemistry and chemical language. This allows for a better design of chemicals. For photochemical degradation, important substructures are already known (chromophores), as well as for hydrolysis (e.g. ester groups) and biodegradation.[7]

Biodegradation of organic chemicals is impeded by fluorine atoms.[11] This is demonstrated by the examples of chloro-fluorohydrocarbons (CFCs), fluorinated hydrocarbons (FCs), and only recently the ubiquitous presence of perfluorinated octanesulfonates (PFOS) in the environment.[4] For molecules that contain different functional groups, empirical knowledge about desired properties and degradability is necessary but often not sufficient to assess their properties. Chemical structure is not the only important criteria for a chemical's biodegradability. Size matters too. The bigger a molecule, the lower its biodegradability. If a molecule is too big it cannot be transported into the cell of a degrading bacterium and/or is not accessible for enzymes. In this respect, it will be of interest to have more biodegradability data of ionic liquids with long alkyl chains and the biodegradability of nano-particles. They offer advantageous new properties. However, their size may prevent their biodegradation in the environment.

For a more systematic approach (quantitative) structure activity relationships ((Q)SARs, here used in a broader sense: also including structure property relationships (SPRs) and other relationships) are an invaluable help for the directed design of new chemical entities.[6–10,20] Recently, expert systems have become available to predict the properties of molecules using (Q)SARs. With some of these computer based systems it is even possible to enlarge the knowledge space. Their application allows at least an orientation in the right direction. For example, when a lead structure for a pharmaceutical has been found, variations of this structure are screened by such in silico systems in order to find the most promising candidates in terms of activity with the lowest amount of unwanted side effects. This results in the saving of costs, time and animal trials. In environmental science, such approaches have been used to date exclusively in a retrospective manner for the assessment of already existing chemicals. The design of pharmaceuticals by application of such computer methods has been only recently reported.[10] These systems also allow including good biodegradability as a property of possibly successful candidates. Considering the functionalities of molecules over their entire life cycle brings into the foreground the application of such methods for the design of new chemicals and to include good degradability such as hydrolysis, photolysis, biodegradation and other elimination pathways such as sorption onto particulate matter and bioaccumulation in organisms under environmental conditions. They can be combined with systems that allow the prediction of metabolites. By doing this, the metabolites of biotransformation in the human body or the transformation products in the environment can be included before a molecule is even synthesized, i.e. a pre-production risk assessment and ranking would be possible.

The potential—politics and economics

The approach described here is not a new one. The examples presented, however, show that the approach is feasible. It is a sustainable one whose application is not limited to the so-called developed countries but can be used everywhere—in contrast to technique based treatment, i.e. end of the pipe technologies such as waste water treatment which in the long

run are not sustainable and which have their own limitations. In the declaration of Rio within agenda 21 adopted in Rio de Janeiro in 1992, it was stated that it is important to intensify the research for the development of safe substitutes for long living chemicals (Agenda 21, # 19.21).[21]

By 1994, a commission of the German parliament developed perspectives for the sustainable handling of chemicals.[22] The principle of the environmentally benign design of chemicals for sustainable development was emphasized. The European Parliament and the European Commission expressed within the 6th Environmental Program that chemicals should be produced and used within one generation only in such a way that results in no negative impact on the environment.[23] This is underlined with the introduction of the new European legislation for chemicals. One of the main ideas of REACH[8] is to minimize the impact of chemicals on humans and the environment along their whole life cycle. Chemicals and pharmaceuticals that are benign by design contribute to this goal. The German expert panel that advises the federal government on environmental issues expects that in the medium and long term the market for environmental friendly substitutes and new products will increase.[24] The activities of the U.S. EPA in green chemistry which have a focus on the synthesis processes are well known. The biggest potential within sustainable chemistry is expected to come from computer supported methods.[25]

The ways in which how chemistry itself can be made more sustainable and how it can contribute to sustainable development in general are clear, we only have to apply them. Appropriate assessment methods are necessary and have been described already elsewhere in detail.
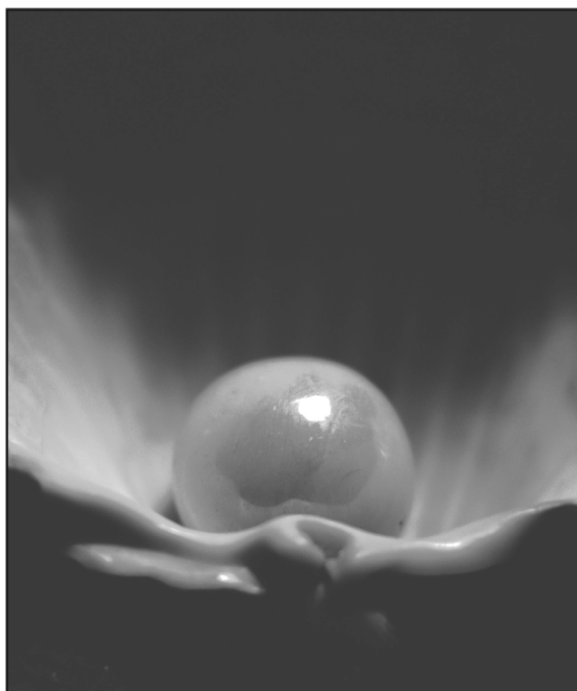
Acknowledgements

References

1 P. T. Anastas and J. C. Warner, *Green Chemistry. Theory and Practice.* Oxford University Press, Oxford, New York, 1998, p. 51.
2 M. Scheringer and M. J. Dunn, *Persistence and Spatial Range of Environmental Chemicals.* Wiley VCH, Weinheim, 2002; K. Kümmerer, *Time & Society*, 1996, **5**, 219–235; J. Cairns, Jr. and D. I. Mount, *Environ. Sci. Technol.*, 1990, **24**, 154–161; S. Böschen, D. Lenoir and M. Scheringer, *Naturwissenschaften*, 2003, **90**, 93–102.
3 EU-EPA, *Late Lessons from Early Warnings*, Report No. 28, EU-Environmental Protection Agency, Kopenhagen, 2001.
4 K. Ballschmiter, R. Hackenberg, W. M. Jarman and R. Looser, *Environ. Sci. Pollut. Res. Int.*, 2002, **9**, 274–288; A. M. Calafat, L. L. Needhama, Z. Kuklenyika, J. A. Reidya, J. S. Tullya, M. Aguilar-Villalobosb and L. P. Naeher, *Chemosphere*, 2006, **63**, 490–496; R. Kallenborn, *Ecotoxicol. Environ. Saf.*, 2006, **63**, 100–107; F. Wania, *Environ. Sci. Technol.*, 2006, **40**, 569–577; C. A. de Wit, M. Alaee and D. C. Muir, *Chemosphere*, 2006, **64**, 209–233.
5 N. Pollack, A. R. Cunningham and H. S. Rosenkranz, *Mut. Res. Fundament. Mol. Mech. Mut.*, 2003, **528**, 81–91.
6 C. Pretti, C. Chiappe, D. Pieraccini, M. Gregori, F. Abramo, G. Monni and L. Intorre, *Green Chem.*, 2006, **8**, 238; J. Ranke, K. Molter, F. Stock, U. Bottin-Weber, J. Poczobutt, J. Hoffmann, B. Ondruschka, J. Filser and B. Jastorff, *Ecotoxicol. Environ. Saf.*, 2004, **58**, 396–404; A. Latala, P. Stepnowski, M. Nedzi and W. Mrozik, *Aquat. Toxicol.*, 2005, **73**, 91–98; B. Jastorff, K. Mölter, P. Behrend, U. Bottin-Weber, J. Filser, A. Heimers, B. Ondruschka, J. Ranke, M. Schaefer, H. Schröder, A. Stark, P. Stepnowski, F. Stock, R. Störmann, S. Stolte, U. Welz-Biermann, S. Ziegert and J. Thöming, *Green Chem.*, 2005, **7**, 362.
7 P. G. Rieger, H. M. Meier, M. Gerle, U. Vogt, T. Groth and H. J. Knackmuss, *J. Biotechnol.*, 2002, **94**, 101–123; M. Eissen, J. O. Metzger, E. Schmidt and U. Schneidewind, *Angew. Chem., Int. Ed.*, 2002, **41**, 414–436.
8 E. Rorije, F. Germa, B. Philipp, B. Schink and D. B. Beimbron, *SAR QSAR Environ. Res.*, 2002, **13**, 199–204, http://ec.europa.eu/environment/chemicals/reach/reach_intro.htm, accessed 12 February 2007.
9 R. S. Boethling and D. Mackay, *Handbook of property estimation Methods for Chemicals – Environmental and Health Sciences*, Lewis Publisher, Boca Raton, 2000; *Quantitative Structure-Activity Relationships in Environmental Sciences-VII*, ed. F. Chen and G. Schüürmann, SETAC Press Pensacola, 1997; J. C. Dearden, *SAR QSAR Environ. Res.*, 1996, **5**, 17–26; *QSARs in the Assessment of the Environmental Fate and Effects of Chemicals*, Technical Report No. 74, ECETOC, Brussels, June 1998; ECVAM, http://ecvam.jrc.cec.eu.int/index.htm, 1997; EPA, http://www.epa.gov/oppt/exposure/docs/episuitedl.htm, 2001.
10 *Modern Methods of Drug Discovery*, ed. A. Hillisch, and R. Hilgenfeld, Birkhäuser, Basel, 2003; B. Jastorff, R. Störmann and U. Wölcke, *Struktur-Wirkungsdenken in der Chemie – eine Chance für mehr Nachhaltigkeit*, Universitätsverlag Aschenbeck und Isensee, Bremen and Oldenburg, 2003; C. A. Lipinski, F. Lombardo, B. W. Dominy and P. J. Feeney, *Adv. Drug Delivery Rev.*, 1997, **23**, 3–25; S. Sahli, B. Stump, T. Welti, D. Blum-Kaelin, J. D. Aebi, C. Oefner, J. H. Bohm and F. Diederich, *ChemBioChem*, 2004, **5**, 996.
11 *Biodegradation and Persistence*, ed. B. Beek, Springer, Berlin Heidelberg New York, 2002.
12 J. Boos, U. Weslau, J. Ritter, G. Blaschke and G. Schellong, *Cancer Chemother. Pharmacol.*, 1991, **28**, 455–460; V. Gilard, M. C. Malet Martino, M. De Forni, U. Niemeyer, J. C. Ader and R. Martino, *Cancer Chemother. Pharmacol.*, 1993, **31**, 387–394.
13 K. Kümmerer and A. Al-Ahmad, *Acta Hydrochim. Hydrobiol.*, 1997, **25**, 166–17.
14 J. Engel, T. Klenner, U. Niemeyer, G. Peter, J. Pohl, M. Schüßler, H. Schupke, A. Voss and M. Wiessler, *Drugs Future*, 2000, **25**, 791; K. Kümmerer, T. Steger-Hartmann and M. Meyer, *Water Res.*, 1997, **31**, 2705–2710.
15 K. Kümmerer, A. Al-Ahmad, B. Bertram and M. Wießler, *Chemosphere*, 2000, **40**, 767–773.
16 J. L. G. De Almeida, M. Defaux, Y. B. Taarit and C. Nacchache, *J. Am. Oil Chem. Soc.*, 1994, **71**, 675–694; R. Schröder, Henkel Company, personal communication, 2006; P. Schöberl, *Tenside Surfactants Deterg.*, 1989, **26**, 86–94.
17 N. Dixon, *Case Study: Biodegradable Alternatives to Chemicals - Octel's experience in the chelant market*, Vortag auf der Tagung 2nd Annual EU Sustainable Chemicals Management, Brüssel 13–14 October 2004, (http://www.euconferences.com/chemicalsmanagement04/day2presenta-tions.htm).
18 W. Lee, L. Zhi-Hong, S. Vakulenko and S. Mobashery, *J. Med. Chem.*, 2000, **43**, 128–132.
19 O. López, J. G. Fernández-Bolaños and M. V. Gil, *Green Chem.*, 2005, **7**, 431–442.
20 M. Alexander, *Biodegradation and Bioremedation*, Academic Press. San Diego, 1994; E. Fasani, A. Profumo and A. Albini, *Photochem. Photobiol.*, 1998, **68**, 666–674; S. B. Haderlein, T. B. Hofstetter and R. P. Schwarzenbach, in *Biodegradation of Nitroaromatic Compounds and Explosives*, ed. J. C. Spain, J. B. Huighes and H. J. Knackmuss, CRC Press, Boca Raton, 2000; J. Damborsky, *SAR QSAR Environ. Res.*, 1996, **5**, 27–36; S. Dimitrov, R. Breton, D. Macdonald, J. D. Walker and O. Mekenyan, *SAR QSAR Environ. Res.*, 2002, **13**, 445–415; G. Klopman, R. Saiakhov and M. H. Tu, *Pure Appl. Chem.*, 1998, **70**, 1385–1394; H. Loonen,

F. Lindgren, B. Hansen, W. Karcher, J. Niemela, K. Hiromatsu, M. Takasuki, W. Pejenenburg, E. Rorije and J. Struijs, *Envrion. Toxicol. Chem.*, 1999, **18**, 1763–1768; A. Sedykh, R. Saiakhov and G. Klopman, *Chemosphere*, 2001, **45**, 971–981.

21 http://www.unep.org/Documents.ultilingual/Default.asp?DocumentID=78&ArticleID=1163.

22 Enquête-Kommission ''Schutz des Menschen und der Umwelt ''Hg., *Die Industriegesellschaft gestalten. Perspektiven für einen nachhaltigen Umgang mit Stoff- und Materialströmen.* Economica, Bonn, 1994.

23 EU-Parlament und EU-Kommission, *Beschluss Nr. 1600/2002/EG des Europäischen Parlaments und des Rates vom 22. Juli 2002 über das sechste Umweltaktionsprogramm der Europäischen Gemeinschaft, 10.9.2002*, Amtsblatt der Europäischen Gemeinschaften, L 242/1–15, 2002.

24 SRU Der Rat von Sachverständigen für Umweltfragen. *Zur Wirtschaftsverträglichkeit der Reform der Europäischen Chemikalienpolitik.* Stellungnahme Nr. 4, Juli, S. 29, Ziffer 38, 2003.

25 C. Tsoka, W. R. Johns, P. Linke and A. Kokossis, *Green Chem.*, 2004, **6**, 401–404.

Achieving great heights

Chem Soc Rev

Chemical Society Reviews

www.rsc.org/chemsocrev   Volume 36 | Number 1 | January 2007 | Pages 1 – 124

ISSN 0306-0012

RSCPublishing

CRITICAL REVIEW
Sourav Saha and J. Fraser Stoddart
Photo-driven molecular devices

TUTORIAL REVIEW
Heinz Berke
The invention of blue and purple pigments in ancient times

0306-0012(2007)36:1;1-G

- Highly cited, succinct and reader friendly reviews

- Topics of international, multidisciplinary and social interest

- 12 monthly issues

- Impact factor: **13.747**

2501D773

RSCPublishing

www.rsc.org/chemsocrev

Registered Charity Number 207890

View Online

03030516 new

Journal of Environmental Monitoring

Comprehensive, high quality coverage of multidisciplinary, international research relating to the measurement, pathways, impact and management of contaminants in all environments.

- Dedicated to the analytical measurement of environmental pollution
- Assessing exposure and associated health risks
- Fast times to publication
- Impact factor: 1.578
- High visibility - cited in MEDLINE

Journal of Environmental Monitoring
Cutting-Edge Research on Environmental Processes & Impacts

www.rsc.org/jem

RSC Publishing   www.rsc.org/jem

SCI- Società Chimica Italiana
GIC-Gruppo Interdivisionale di Catalisi
Divisione di Chimica Industriale

VIII International Symposium on Catalysis
Applied to Fine Chemicals

CAFC-8

16-20 September 2007
Verbania-Pallanza (Italy)

Verbania is situated in a beautiful location on the shore of Lago Maggiore in the Italian Alps and is easily accessible by train (Milano-Genève and Milano-Zürich way) and by plane (50 km away from Malpensa airport)

Main Topics

- **Benign oxidations**
- **Catalysis for C-C bond formation**
- **Enantioselective catalysis**
- **Enzymatic and chemo-enzymatic processes**

Invited lecturers

Walter Cabri (Sigma Tau, Italy) **Vittorio Farina** (Johnson & Johnson, Belgium) **Kiyotomi Kaneda** (Osaka University, Japan) **José A. Mayoral** (Saragoza University, Spain) **Franco Sannicolò** (Milan University, Italy) **Jonathan M. J. Williams** (Bath University, UK)

Registration fees	Before 31/05/07	After 31/05/07
Participants	*400 €*	*550 €*
Students	*200 €*	*350 €*
Accompanying person	*100 €*	*150 €*

Deadline for abstract submission   **15 March 2007**

Selected papers will be published in a special issue of Catalysis Today

Contacts: **Web-site:**

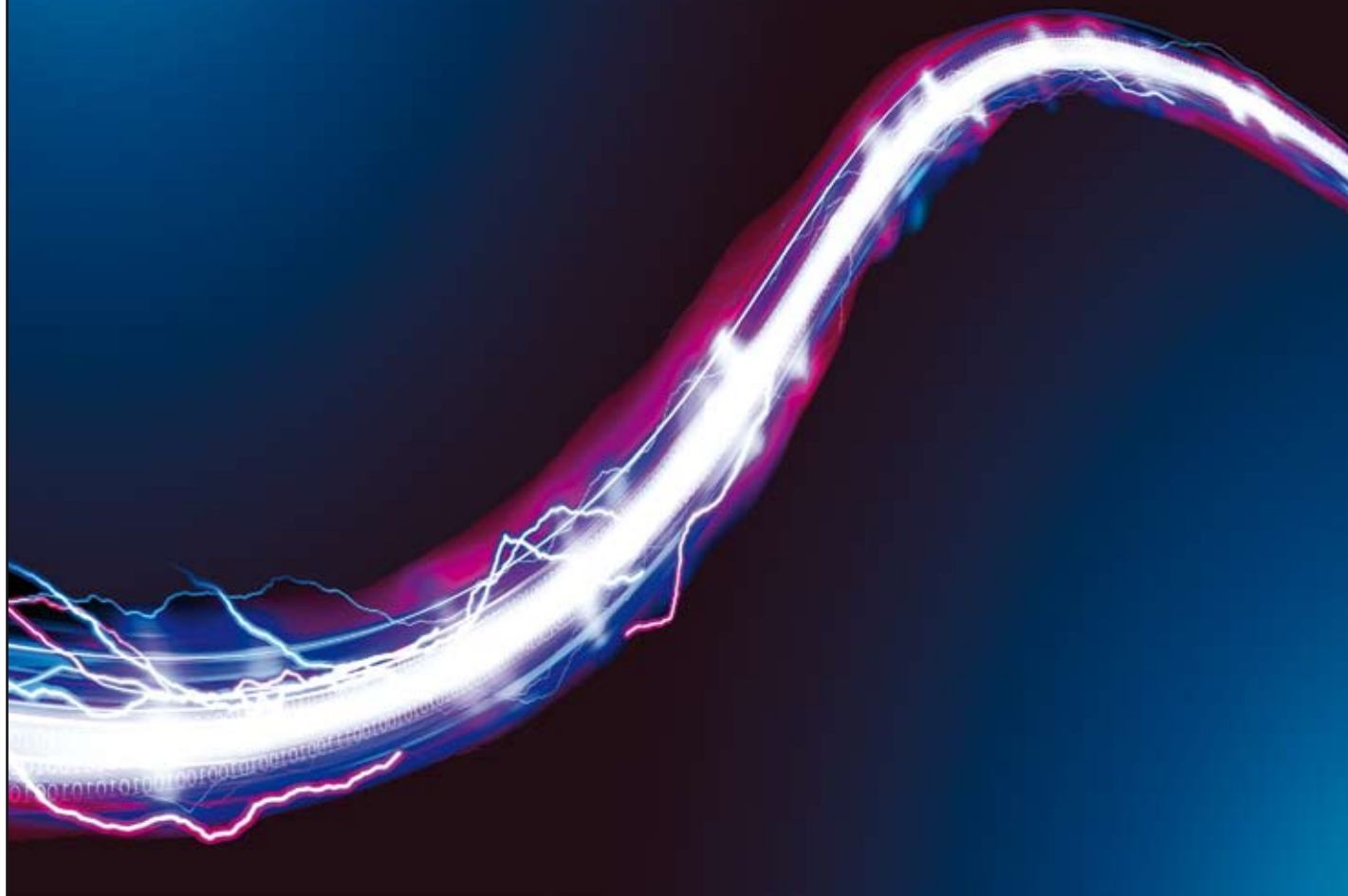n.ravasio@istm.cnr.it or angelo.vaccari@unibo.it   http://www.sci-gic.it/?Cafc8

Hotel Castagnola -Via al Collegio 16 - 28922 Verbania-Pallanza (Italy)

RSC Journals Archive

Over 160 years of essential chemistry at your fingertips

Featuring almost 1.4 million pages of ground-breaking chemical science in a single archive, the **RSC Journals Archive** gives you instant access to **over 238,000 original articles** published by the Royal Society of Chemistry (and its forerunner Societies) between 1841-2004.

The RSC Journals Archive gives a supreme history of top title journals including: *ChemComm, Dalton Transactions, Organic & Biomolecular Chemistry* and *PCCP (Physical Chemistry Chemical Physics)*.

As well as a complete set of journals with multi-access availability, the RSC Journals Archive comes in a variety of purchase options and available discounts.

For more information please contact **sales@rsc.org**

20060760

RSCPublishing

www.rsc.org/archive

Registered Charity Number 207890